Adaptive Control of Systems with Quantization and Time Delays

Siri Marte Schlanbusch

UiA University of Agder

Doctoral Dissertations at the University of Agder 413

Siri Marte Schlanbusch

Adaptive Control of Systems with Quantization and Time Delays

Doctoral Dissertation for the degree *Philosophiae Doctor (PhD)* at
the Faculty of Engineering and Science, Specialisation in Mechatronics

University of Agder
Faculty of Engineering and Science
2023

Doctoral Dissertations at the University of Agder 413
ISSN: 1504-9272
ISBN: 978-82-8427-128-6

Printed by MAKE!Graphics
Kristiansand

Preface

This thesis is submitted in partial fulfillment of the requirements for the degree of Philosophiae Doctor (PhD) at the University of Agder. The thesis presents research results relating to control of nonlinear systems with quantization, uncertainty and input delay, and includes published papers. The work presented, has been carried out in the period between October 2019 and February 2023 at the Department of Engineering Sciences, University of Agder, Norway. During this time, Professor Jing Zhou from the Department of Engineering Sciences at the University of Agder has been the main supervisor and Professor Miroslav Krstić from the Department of Mechanical and Aerospace Engineering at the University of California, San Diego, has been the co-supervisor. The project has received funding by the Ministry of Education in Norway.

First of all I would like to thank my supervisor Professor Jing Zhou for her guidance and support during my research, for introducing me to the field of adaptive control, and for giving me the opportunity to spend more than three years specializing in the field of control theory. To my co-supervisor Professor Miroslav Krstić, thank you for introducing me to the exciting field of delayed systems.

I would also like to thank Professor Ole Morten Aamo, which I visited for six weeks during the autumn of 2021 at NTNU. Thank you for your cooperation and for answering all my elementary questions and your patience with me. During the visit, I was warmly welcomed by the other PhDs and staff at NTNU, which I also would like to thank.

A huge thanks to all my colleagues at UiA, especially to Assistant Professor Morten Ottestad for encouraging me to start on this journey and always keeping an open door for a discussion, to PhD coordinator Emma Horneman for providing all the answers to any administrative issues, and to the great PhD students in Mechatronics that I have gotten to know, who have contributed to a fun and memorable time here at UiA.

Although the Covid situation has been challenging for several reasons, sharing a home-office with my husband Rune also had its benefits. With nowhere to escape, I could bother him with all my questions, and get all the answers I needed. Not only has he contributed to my work, but together with our two kids, William and

Martine, I have received both their patient and constant support. For that I am forever grateful. Also the support from my family both in Grimstad and in Narvik has been significant, and I want to thank all of them for their support and interest throughout these years.

Siri Marte Schlanbusch
Grimstad, Norway
February 2023

Abstract

This thesis addresses problems relating to tracking control of nonlinear systems in the presence of quantization and time delays. Motivated by the importance in areas such as networked control systems (NCSs) and digital systems, where the use of a communication network in NCS introduces several constraints to the control system, such as the occurrence of quantization and time delays. Quantization and time delays are of both practical and theoretical importance, and the study of systems where these issues arises is thus of great importance. If the system also has parameters that vary or are uncertain, this will make the control problem more complicated. Adaptive control is one tool to handle such system uncertainty.

In this thesis, adaptive backstepping control schemes are proposed to handle uncertainties in the system, and to reduce the effects of quantization. Different control problems are considered where quantization is introduced in the control loop, either at the input, the state or both the input and the state. The quantization introduces difficulties in the controller design and stability analysis due to the limited information and nonlinear characteristics, such as discontinuous phenomena. In the thesis, it is analytically shown how the choice of quantization level affects the tracking performance, and how the stability of the closed-loop system equilibrium can be achieved by choosing proper design parameters. In addition, a predictor feedback control scheme is proposed to compensate for a time delay in the system, where the inputs are quantized at the same time. Experiments on a 2-degrees of freedom (DOF) helicopter system demonstrate the different developed control schemes.

Sammendrag

Denne avhandlingen tar for seg problemer knyttet til regulering av ulineære systemer utsatt for kvantisering og tidsforsinkelser. Arbeidet er motivert av områder som nettverksbaserte systemer (NCS) og digitale systemer, der bruken av et kommunikasjonsnettverk i NCS introduserer flere begrensninger for kontrollsystemet, for eksempel forekomsten av kvantisering og tidsforsinkelser. Kvantisering og tidsforsinkelser har både praktisk og teoretisk betydning, og studiet av systemer hvor disse problemstillingene oppstår er derfor av stor betydning. Dersom systemet i tillegg har parametere som varierer eller er usikre, vil dette gjøre reguleringsproblemet vanskeligere. Adaptiv regulering er ett verktøy for å håndtere slike usikkerheter i systemet.

I avhandlingen er adaptive backstepping reguleringer foreslått for å håndtere usikkerhet i systemer, og for å redusere effektene av kvantisering. Ulike problemer er vurdert, der kvantisering introduseres i reguleringssløyfen, enten ved inngangen, systemtilstanden eller både ved inngangen og systemtilstanden. Kvantisering introduserer vanskeligheter i design av regulator og stabilitetsanalysen på grunn av begrenset informasjon og ulineære egenskaper, for eksempel diskontinuerlige fenomener. I avhandlingen er det analytisk vist hvordan valg av kvantiseringsnivå påvirker reguleringsytelsen, og hvordan stabiliteten til likevektspunktet i den lukkede sløyfen kan oppnås ved å velge riktige designparametere. I tillegg foreslås en prediktorregulering for å kompensere for en tidsforsinkelse i systemet, som samtidig er utsatt for kvantisert. Eksperimenter på et helikoptersystem med to frihetsgrader demonstrerer de forskjellige regulatorene som er utviklet.

Publications

Included Works

The following listed papers are included as a part of this thesis. They have been published in peer-reviewed conference proceedings and journals. The included versions in this dissertation differ only in formatting compared to the original published versions.

Paper A S. M. Schlanbusch and J. Zhou, "Adaptive backstepping control of a 2-DOF helicopter system with uniform quantized inputs," in *IECON 2020 The 46th Annual Conference of the IEEE Industrial Electronics Society*, 2020, pp. 88–94, doi: 10.1109/IECON43393.2020.9254497. [1]

Paper B S. M. Schlanbusch, J. Zhou and R. Schlanbusch, "Adaptive backstepping attitude control of a rigid body with state quantization," in *Proceedings of 60th IEEE Conference on Decision and Control*, 2021, pp. 372–377, doi: 10.1109/CDC45484.2021.9683579. [2]

Paper C S. M. Schlanbusch, J. Zhou and R. Schlanbusch, "Adaptive attitude control of a rigid body with input and output quantization," *IEEE Transactions on Industrial Electronics*, vol. 69, no. 8, pp. 8296–8305, 2022, doi: 10.1109/TIE.2021.3105999. [3]

Paper D S. M. Schlanbusch and J. Zhou, "Adaptive backstepping control of a 2-DOF helicopter system in the presence of quantization," in *9th International Conference on Control, Mechatronics and Automation*, 2021, pp. 110–115, doi: 10.1109/ICCMA54375.2021.9646184. [4]

Paper E S. M. Schlanbusch, O. M. Aamo and J. Zhou, "Attitude control of a 2-DOF helicopter system with input quantization and delay," in *IECON 2022 The 48th Annual Conference of the IEEE Industrial Electronics Society*, 2022, doi: 10.1109/IECON49645.2022.9968994. [5]

Paper F S. M. Schlanbusch and J. Zhou, "Adaptive quantized control of uncertain nonlinear rigid body systems," *Systems & Control Letters*, vol. 175, 2023, 105513, doi: 10.1016/j.sysconle.2023.105513. [6]

Additional Contributions

In addition to the papers included in this thesis, the author has also contributed to the following paper as part of the research done in the Top Research Center Mechatronics.

Paper G J. Zhou and S. M. Schlanbusch, "Adaptive quantized control of offshore underactuated cranes with uncertainty," in *Proceedings of the IEEE 17th International Conference on Control & Automation*, 2022, pp. 297–302, doi: 10.1109/ICCA54724.2022.9831937. [7]

Contents

List of Figures

List of Tables

List of Abbreviations

AUV Autonomous underwater vehicle. 3–6, 144, 166

DLR German Aerospace Center. xvii, 3

DOF Degrees of freedom. vii, 8–11, 19, 22, 37, 49–51, 72, 82, 93, 94, 107, 114, 121–123, 143, 144, 147, 165, 166, 183

FBD Free body diagram. 51

FSA Finite spectrum assignment. 7

KD Kinetic diagram. 51

MIMO Multiple-input multiple-output. 5, 6, 19, 36, 50, 51, 66, 72, 81, 91, 94, 95, 107, 122, 123, 135, 144, 147, 165–167, 183

MRAC Model reference adaptive control. 25

NCS Networked control system. vii, ix, 1, 2, 4, 5, 7, 37, 49, 121, 143

ODE Ordinary differential equation. 7, 30, 33, 36, 149

PDE Partial differential equation. xvii, 31, 33, 34, 36, 149

ROTEX Robot technology experiment. xvii, 3

SISO Single-input single-output. 6, 50, 72, 95, 166

UAV Unmanned aerial vehicle. 4, 5, 72, 93, 94, 122, 143

USV Unmanned surface vehicle. 3, 4

Chapter 1

Introduction

This chapter introduces the motivation behind the work presented in this thesis, gives a short introduction into control of systems with quantization and time delays, and also a description of the main contributions of the thesis. Lastly, an outline of the thesis is provided.

1.1 Motivation

Control of systems with quantization and time delays has received a lot of attention in recent years due to its importance in areas such as networked and digital systems. A networked control system (NCS) is a control system where the information between sensors, actuators and controllers is shared through a digital communication network, e.g. the Internet, an Ethernet or a Fieldbus [8–10]. The use of a communication network can provide communication between system components that are physically separated, and where the signals sent between the components, such as control inputs and feedback signals, are shared as information packages over the network. The use of NCS has several benefits, where e.g. the complexity of wiring can be reduced since some of the wiring in the installation may be avoided, there is a large flexibility since it will be easy to add new components to the system, maintenance is easy, and cost can be reduced. This makes control over networks attractive to many industrial companies, for instance to apply remote control systems or for factory automation. The range of applications is numerous, as this can be used both in the air, on the ground and in the water.

However, the use of NCS also has some disadvantages. For conventional control systems, the data exchange between the system components are lossless, while the use of a network introduces communication constraints to the control system. For instance are the data transmitted as digital signals rather than continuous signals, and the signals need to be sampled and quantized before sent through the network. The network also induces time delays, and some of the data packets might be missing

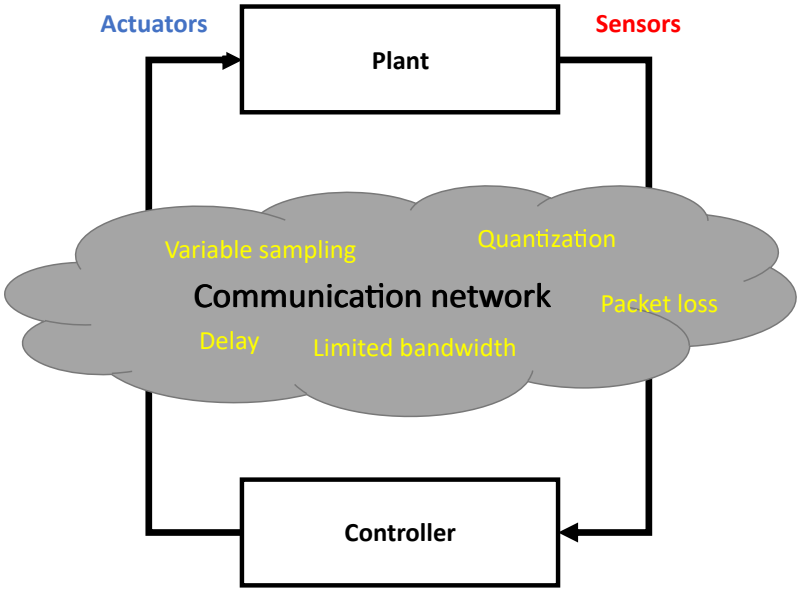

Figure 1.1: Different issues induced by the network.

during transmission. As seen from a control perspective, the main difference between conventional control theory and control over a network, is the occurrence of these imperfections caused by the communication network. These issues can cause poor performance or even destabilize the control system. Some main challenges caused by including a communication network are highlighted in yellow in Figure 1.1 and may include (but are not limited to):

- **Network-induced delays**. This can be *computational delays* in system components because of limited processing speed or capacity of digital devices, that are usually small and negligible, *network access delays* in networked queues since data are sent through a network as packets with waiting time before transmitted, or *transmission delays* in the communication network [8]. Time delays are common in NCS, and there can be delays when signals are sent from a sensor to a controller and from a controller to an actuator through the network, and network characteristics as topology and routing schemes will influence how large the delays are [11]. The delays may have different characteristics such as random, constant or time-varying, depending on application and communication network, and delays will usually degrade performance of the system. For instance will a constant delay occur in NCSs when the controller reads data periodically, and a time-varying delay will occur if the controller and actuator are event-driven. When data loss occurs during a transmission, the delay problem is even worse.

- **Quantization.** Since signals are coded via analog-to-digital converters before sent through a communication network, a quantizer is introduced for the

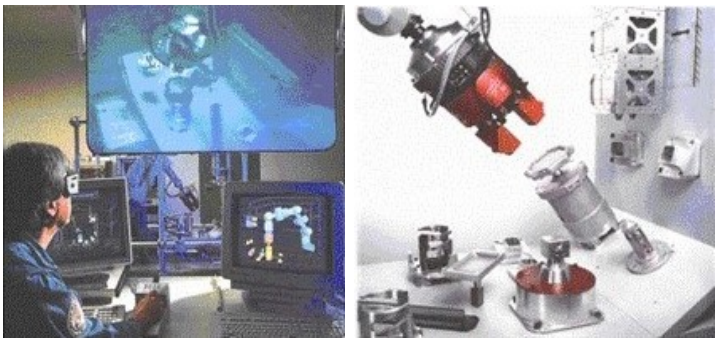

Figure 1.2: The first remotely controlled robot in space, ROTEX. Reproduced with courtesy to German Aerospace Center (DLR) [1].

discontinuous mapping from a continuous-time analog signal to a discrete-time digital signal. This results in quantization errors that are nonlinear. Quantization can also be useful since it can reduce loads on the network and limit bandwidth requirements.

- Other issues such as sampling of signals, data packet dropouts, security and limited bandwidth.

The use of computer networks for transmitting information is seen in for instance telerobotics, where robots are remotely controlled and where there is a physical separation between the human operator and the robot. The research in teleoperation emerged with concern to safety and operations in challenging and hazardous environments. The use of a communication network allows remote control from anywhere. On the local site, there is a human operator with connection to the system through e.g. monitors, joysticks or keyboards. On the remote site there is the robot with sensors, that can manipulate its environment [12]. The first remotely controlled robot in space was the robot technology experiment (ROTEX), where the robot was onboard a space shuttle and flew with the German Spacelab Mission D2 in 1993, see Figure 1.2. It was demonstrated that the robot could be remotely controlled from ground by local sensor feedback, where the human operator on ground received visual feedback and sent feedforward control commands to the robot. For teleoperation of a robot in space from ground, the main problem to handle is the time-delayed transmission links that induce delays for the signal sent from ground to space and vice versa. For the ROTEX, there was a round-trip delay of 5-7 sec.

Communication networks are also used in motor vehicles, where sensors and actuators typically are locally distributed in the vehicle, and sensor data including control signals are transmitted over the communication network [13].

The range of maritime activities are enormous, including different vehicles such as autonomous underwater vehicles (AUVs), unmanned surface vehicles (USVs),

[1] `https://www.dlr.de/rm/en/desktopdefault.aspx/tabid-3827/5969_read-8744/`

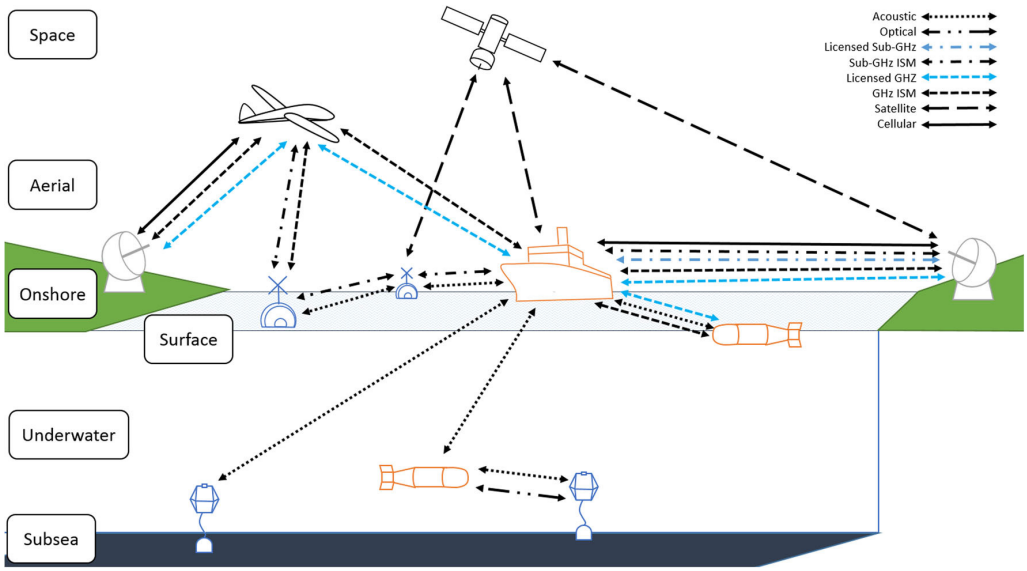

Figure 1.3: Communication and network for marine vessels [14].

manned vessels and so on, and infrastructure such as oil platforms, offshore wind farms, and fish farms. In maritime scenarios, the use of satellite systems or other long-range and low-bit rate communication systems is widespread. E.g., AUVs require an underwater wireless communication system, for instance an acoustic modem for communication. Figure 1.3 illustrates coordinated control and operation of networks of underwater, aerial and surface vehicles. The use and complexity of such networks have been rapidly increasing over the last decade, where the use of unmanned aerial vehicles (UAVs) and USVs also are used for extending communication links [14].

These are some examples related to control over networks, which motivate research into problems where quantization and time delays are in the control loop. Quantization and time delays are not only seen in NCSs. For instance is quantization also used in signal processing, digital control and simulation, and time delays are ubiquitous in practical systems. Some examples where delays are present are in traffic flow, where there is a delay in the drivers reaction time in road traffic [15], in drilling systems, where there is a delay in the flow-rate to manage bottom-hole pressure [16], and in 3D-printing [17]. Both quantization and time delays are of practical importance, since the appearance of these issues may result in poor performance or even cause instabilities for the system. They are also of theoretical importance, because both issues introduce several mathematical challenges, where quantization is nonlinear and with a discontinuous characteristic that causes discrete phenomena to appear, and time delays are infinite-dimensional. This makes analysis of systems with quantization and delays of great importance. Many systems also have parameters that vary or are uncertain, and this will make the control problem more complicated. The appearance of uncertainties, quantized signals and time delays in systems is the

main motivation for the research carried out in this project.

1.2 Control of Systems with Quantization

Quantized control has gained increasing interest during the past decades due to the use of information technology in the development of modern engineering applications, such as digital control systems and NCSs. A quantizer maps a continuous signal into a set of discrete values and introduces nonlinear errors that need to be handled. Quantization is not only inevitable owing to the widespread use of digital processors, but also useful due to the advantage of reducing occupation rate of transmission bandwidth in the communication of signals, see e.g. [18].

The quantized feedback stabilization problem for linear systems where the dynamics are precisely known, has been considered in [18–22]. In [18], it was shown that a logarithmic quantizer is the coarsest one to stabilize a single input linear system, where the number of control values is finite. This work was extended in [20] to consider stabilization of multiple input linear systems.

Stabilization of nonlinear systems in presence of quantization has been investigated in [23–27]. The main result in [18] was further extended to single input nonlinear systems in [23], and for nonlinear uncertain systems in [24–26], where two different adaptive approaches were used in [24, 25], while a robust approach was considered in [26]. If there are uncertainties to the system, the quantization problem becomes more challenging. Since exact system parameters often are unknown for real systems, adaptive control is a useful approach to deal with such uncertainties, where an online estimation of the parameters can be provided. The work in [25], where a backstepping-based adaptive control scheme was presented, was further developed in [27] for the same stabilization problem to consider a hysteresis quantizer, that compared to a logarithmic quantizer has additional quantization levels to avoid chattering. Tracking control in the presence of input quantization has been considered in [28–31] for uncertain nonlinear systems, in [32] for a group of UAVs with unknown parameters, and in [33] for under-actuated AUVs. The developed methods in [23–33] all focused on the input quantization problem, while the controllers were designed by continuous measurements of the state feedback.

Control of uncertain systems with state or output quantization has been studied in [34–36] using robust or adaptive approaches. In [34], an adaptive controller was developed for uncertain linear systems with quantized outputs. In [35], a robust controller for a linear multiple-input multiple-output (MIMO) uncertain system was designed with quantized output measurements. In [36], the stabilization problem for uncertain nonlinear systems with quantized states was investigated, where an adaptive backstepping-based control algorithm was designed.

Although research on quantized control has received much attention in recent years, most work focuses on either input or output quantization. In practice, the control signals sent to the actuators and the signals sent from sensors to the control module need to be quantized before transmitted due to the use of digital processors and considering the accuracy of sensors. Also, for remotely controlled systems, the control signals and sensor measurements are shared via a common digital network where the bandwidth might be limited and it is natural to suppose that both input and output signals are quantized. Some work that considered both input and state quantization are [37–42]. In [37], the quantization effects on remotely controlled single-input single-output (SISO) linear systems were studied, where the stabilization problem was transformed into a robust control problem. Sliding mode controllers were developed in [38, 39] for trajectory tracking in the presence of both input and state quantization, of AUVs in [38], and of mechanical systems in [39]. Neural-network based adaptive tracking controllers in presence of quantization were designed in [40] for uncertain nonholonomic mobile robots, and in [41] for uncertain MIMO nonlinear systems. An adaptive backstepping-based control scheme was developed for a class of uncertain nonlinear systems in [42].

The above references do not address problems which takes input quantization or/and state quantization into account for attitude tracking of rigid body systems with uncertainty. In this thesis, we present solutions to these kind of problems, where backstepping is a design tool. Input quantization is first introduced in the control loop, where the main challenge is that only the quantized inputs can be applied to the system. The quantization directly affects the tracking performance and also introduces extra terms to be handled in the stability analysis. The effects of state quantization are then studied, where the main challenge is that the controller can only use the quantized states. This introduces some difficulties, first in the design of a controller since the quantized states are non-differentiable, and also to analyze the resulting closed-loop control system, since several residual terms appear that need to be dominated. By continuous measurements of the states, the derivative of a virtual controller is used in the design of the controller, however when the states are quantized this is not possible since the virtual controller then is discontinuous. Several problems are also studied where both the inputs and the states are quantized. Challenges related to both input and state quantization are then assessed simultaneously.

1.3 Control of Systems with Time Delays

Time delays are a common phenomenon in practical applications, that impact both the stability and the performance of systems. Some examples where delays appear

are NCS, traffic flow, automotive engines and chemical processes. For instance, in NCS there can be delays when signals are sent from sensor to controller and from controller to actuator through the network, and network characteristics such as topology and routing schemes will influence how large the delays are [11]. Data loss may also occur during transmission, increasing the problem of delays. Nilsson gives a nice overview of different delays in NCS and how to model these in his thesis related to real-time control systems with delays [43]. For remote controlled system over a network, the size of the time delay will depend on both distance and velocity of signals [44], and delays are also the main problem in teleoperation control [45]. Not only are delays of practical importance, but also theoretically, because of its nature of being infinite-dimensional, and thus introducing several mathematical challenges.

When the delay is too large to be ignored in the control loop, a natural decision is to try to compensate for the delay. One of the first tools for handling delays was the Smith predictor, introduced in 1959 to compensate for constant input delays in control systems for linear stable systems [46]. Since then, several modifications of the Smith predictor have been proposed to compensate for input delays, removing limitations of the original version. This was extended to e.g. linear unstable plants in [47–49]. The finite spectrum assignment (FSA) technique was introduced in 1979 by Manitius and Olbrot [47], removing the limitation of open-loop stability. In 1982, Artstein [49] introduced a similar approach under the name *reduction method*, where the stabilization problem for linear systems with delays was reduced to the stabilization problem of a delay-free (reduced) problem [17]. In [50], the two approaches (FSA and model reduction) are presented, and several other modifications of the Smith predictor are presented in [51]. These control design approaches go under the name of predictor feedback.

Several predictor based approaches have been proposed to compensate for input delays for linear systems in [16, 48, 49, 52–55]. Krstić introduced the first predictor feedback design for nonlinear systems in [56], where several others have followed since [17, 57–66]. An infinite-dimensional backstepping transformation was introduced in the control design in [67], which makes it possible to show stability using a Lyapunov functional for the entire closed-loop system consisting of the ODE plant and the infinite-dimensional subsystem of the input delay. In [62], a predictor feedback control design for multi-input nonlinear systems with distinct delays for the input channels was developed.

Controllers belonging to the class of predictor techniques may suffer for being sensitive to parameter uncertainty and to delay mismatch, and if there is an error between model and plant, this can cause instabilities [68, 69]. For a real control system, uncertainties are unavoidable. In [16, 53, 55, 61, 65, 66], adaptive control strategies were developed for estimating an unknown delay, and for compensating

the delay by predictor feedback. In [16, 53, 55] they also considered uncertain plant parameters.

In [70], the attitude stabilization of a quadrotor with a known input delay was considered, where a predictor feedback controller was developed to compensate for the delay. Compared to the stabilization problem, the problem of tracking a time-varying reference signal with time is more challenging. Unless knowing the reference signal in advance, and by sending the reference signal to the controller the delayed-time units ahead, it is not possible to track the desired signal perfectly in presence of a delay. In [53], a predictor feedback controller was developed for trajectory tracking where both input delay and parameters were unknown. In [63, 64], a high-DOF robot manipulator for tracking a desired trajectory in a pick-and-place task was studied compensating input delays in the system, and [65, 66] studied the same problem but where the delay was unknown. The tracking control problem of nonlinear networked and quantized control systems with delays was studied in [71], with focus on sufficient conditions to guarantee the tracking performance, where a trade-off between the maximally allowable transmission interval and the maximally allowable delay was derived.

Only [71] in the above literature considers the problem of simultaneous issues caused by time delays and quantization. However, the derived controller is not predictor-based, and does not aim to compensate for the delay effect. In this thesis, we study the effect of the simultaneous issues caused by input quantization and delay for an attitude control problem, where the delay is compensated for by predictor feedback. This constitutes the main challenge.

1.4 Thesis Contributions

The main contributions of the thesis are summarized as follows:

1. Development of an adaptive controller for a helicopter system with input quantization and uncertainties. Transient and tracking performance of the adaptive system are analyzed and it is further investigated how the inclusion of input quantization affects the system performance. It follows that the stability properties of the equilibrium are directly related to the choice of quantization parameters. The developed controller is tested on a 2-DOF helicopter system.

2. Development of an adaptive backstepping based control scheme for rigid body systems with state quantization and unknown parameters. A new approach to stability analysis is proposed, where the effects of the state quantization are shown to provide practical stabililty. The stability of the closed-loop system

and the transient performance of the tracking error are achieved with given conditions. The developed controller is experimentally tested on a real system.

3. Development of adaptive controllers for rigid body systems where both the inputs and the states/outputs are quantized to reduce the communication burden. All closed-loop signals are ensured uniformly bounded. It is shown that the tracking errors converge to a compact set, and the relation between tracking errors and quantization parameters is given. The developed controllers are tested on a real system.

4. Development of a predictor feedback controller for attitude tracking control of a nonlinear system with delay and quantization in the inputs simultaneously. It is investigated how the inclusion of both input quantization and time delays affects the control design and the stability analysis. The developed controller is tested on a real system.

This thesis is based on the papers listed below.

Paper A – Adaptive Backstepping Control of a 2-DOF Helicopter System with Uniform Quantized Inputs [1]

In this paper, an adaptive backstepping control scheme for a 2-DOF helicopter system with input quantization is proposed. The control objective is to track reference signals for pitch and yaw angles in the presence of both input quantization and uncertain system parameters. Only the quantized inputs can be applied to the helicopter system, and the quantization introduces nonlinear characteristics to be handled in the stability analysis. Based on the analysis, it is shown that the designer can tune the design parameters in an explicit way to obtain the required closed-loop behavior, and that tracking is achieved. The tracking error signals converge towards a compact set that is directly related to the values of the quantization parameters.

Paper B – Adaptive Backstepping Attitude Control of a Rigid Body with State Quantization [2]

The research is focused on adaptive backstepping control of rigid bodies for attitude tracking, where the attitude is represented by quaternions. Furthermore, some of the system parameters are uncertain, and the states are quantized by a uniform quantizer. The quantizer satisfies a bounded condition, and so the quantization error is bounded. Based on the stability analysis, it is shown that by choosing gains and quantization parameters to satisfy some given condition, we can ensure the boundedness of all the closed-loop signals. Also tracking is achieved, where the tracking error is directly related to the

chosen quantization values. The proposed control scheme is illustrated with experiments on a helicopter system.

Paper C – Adaptive Attitude Control of a Rigid Body with Input and Output Quantization [3]

In this paper, an adaptive backstepping control scheme is developed for attitude tracking using quaternions, where both the outputs and the inputs are quantized. Challenges related to both input and output quantization are incorporated into the analysis, where by choosing gains and quantization parameters to satisfy some given condition, the boundedness of all the closed-loop signals can be ensured. It is analytically shown how the choice of quantization levels affects the tracking performance, where higher quantization levels increase the tracking error. Experiments on a helicopter system illustrate the proposed scheme. It is shown that it is possible to reduce the communication burden over the network by including quantization, where a suitable quantization level must be chosen, depending on the performance requirements for the application.

Paper D – Adaptive Backstepping Control of a 2-DOF Helicopter System in the Presence of Quantization [4]

In this paper, the attitude tracking control problem is investigated for a 2-DOF helicopter system, where the system parameters are uncertain. In addition, both the inputs and the states are quantized by a uniform quantizer. An adaptive controller is developed using the backstepping technique, where tracking of a given reference signal is achieved, with bounded tracking errors that are directly related to the values of the quantization parameters. Experiments on a 2-DOF helicopter system illustrate the proposed control scheme.

Paper E – Attitude Control of a 2-DOF Helicopter System with Input Quantization and Delay [5]

This paper investigates the effect of two simultaneous network-induced constraints for attitude tracking of a helicopter system. A predictor feedback controller is developed to compensate a known, constant time delay in the communication, where the inputs are quantized before transmitted over the network. The same time delay is assumed induced for all input channels. The input delay is compensated for by the predictor feedback control law, and the effect of quantization is analytically shown to be related to the tracking error, where a higher quantization level increases the error. Simulations and

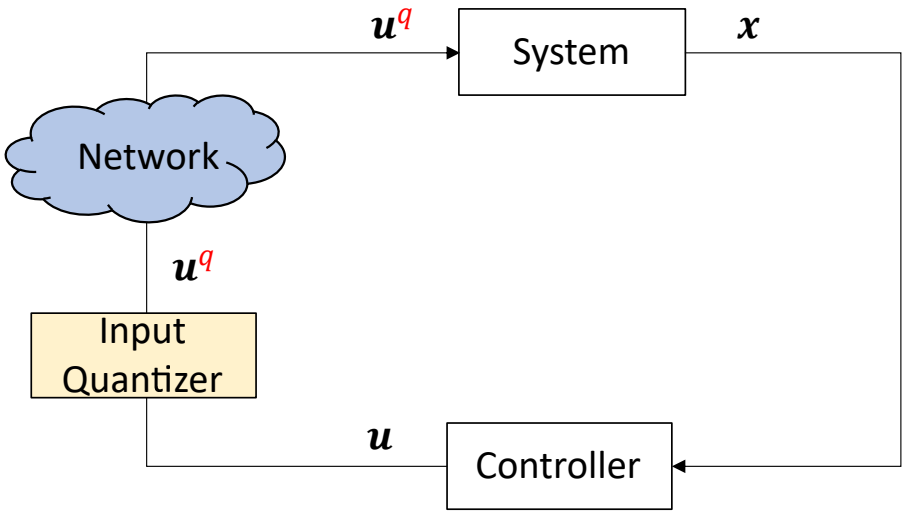

Figure 1.4: System with input quantization.

experiments are carried out to illustrate the proposed control scheme.

Paper F – Adaptive Quantized Control of Uncertain Nonlinear Rigid Body Systems [6]

This paper focuses on the attitude tracking control problem for uncertain nonlinear rigid body systems, where both the inputs and the states are quantized. A class of quantizers that satisfies a sector bounded property is considered, where the quantization error increases as a function of the input to the quantizer, and is not bounded directly. An adaptive controller is designed, and the effect of quantization is analyzed for the closed-loop stability. Inclusion of quantization introduces several terms that need to be dominated, which is shown in the analysis. The tracking errors are shown to converge towards a compact set containing the origin, and the choice of quantization parameters directly affects the size of this set. The problem of unwinding is also addressed, and is avoided by the designed controller. Experiments on a helicopter system illustrates the proposed control scheme, where a logarithmic quantizer is considered.

Here is an overview of how the work in each paper is related. Paper A is an extension of the previous work in [72] related to adaptive backstepping control of a 2-DOF helicopter that was based on the Master thesis [73]. A control structure as shown in Figure 1.4 was considered, where the main contribution was including quantization for the inputs and see how that affected control design and stability analysis. The main challenge is that only the quantized inputs can be applied to the helicopter system, and the quantization introduces extra terms to be handled in the stability analysis.

In Paper B, a control structure as shown in Figure 1.5 was considered. Compared

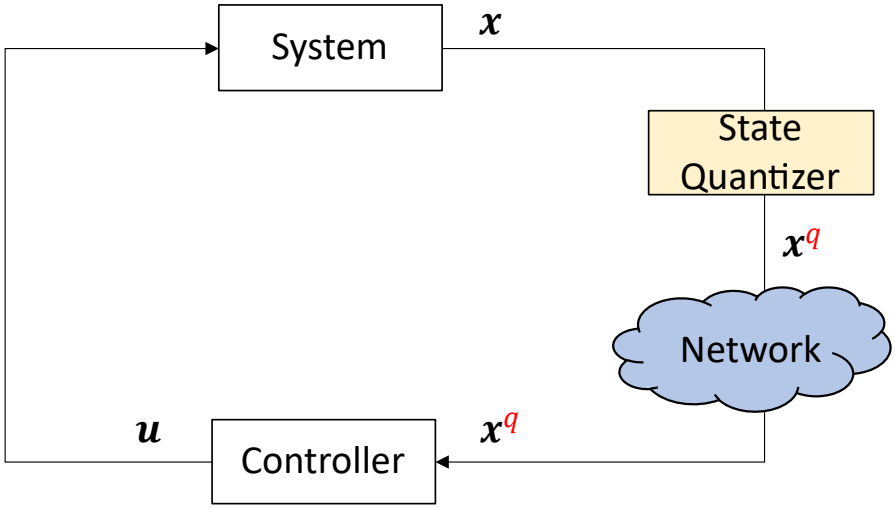

Figure 1.5: System with state quantization.

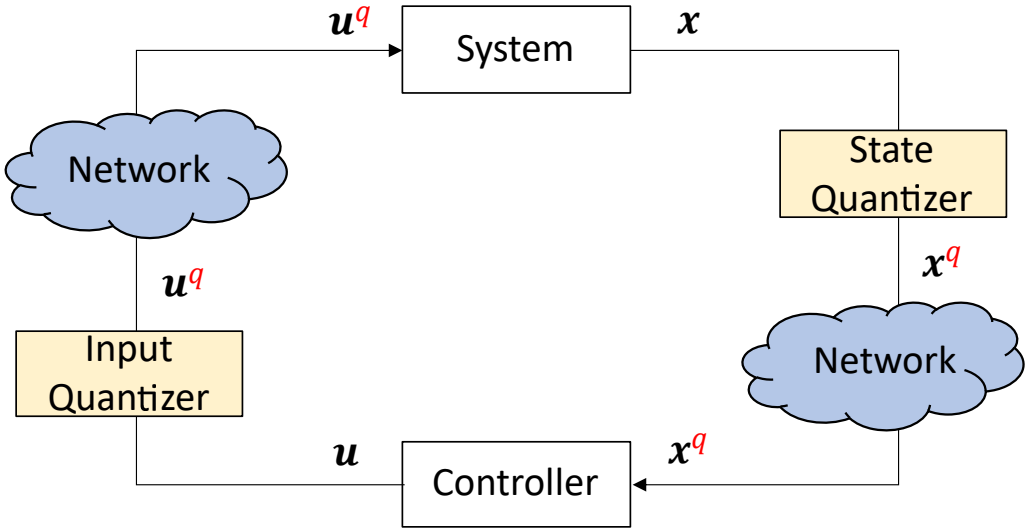

Figure 1.6: System with input and state quantization.

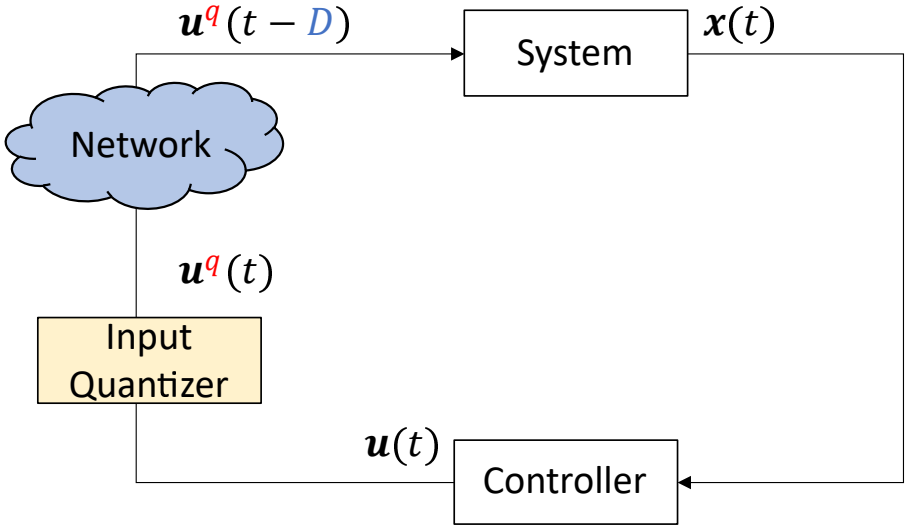

Figure 1.7: System with input quantization and delay.

to Paper A, a general rigid body system was now investigated, where the states were quantized instead of the inputs. The main contribution is to include state quantization, where the attitude and angular velocity are quantized and sent to the controller, to see how this affects the control design and stability analysis. At the same time some of the system parameters are uncertain. The main challenge is that the controller can only use the quantized states, which introduces some difficulties for analyzing the resulting closed-loop control system, since then several residual terms appear that need to be handled and also the quantized states are non-differentiable.

Papers C, D and F all have a control structure as shown in Figure 1.6. Paper C extends the results in Paper B by including both input and output quantization for a rigid body system. Paper D extends the results from Paper A by also including state quantization for the helicopter system, and Paper F extends the result in Paper C to consider a more general quantizer, where the quantization error is not bounded by a constant but depends on the input to the quantizer. The main contribution for these papers are the inclusion of both input and state quantization, where challenges related to both input and state quantization are incorporated into the analysis. Having a sector bounded quantizer as in Paper F, the analysis becomes more challenging.

Lastly, a control structure as given in Figure 1.7 was considered in Paper E. The main contribution of this paper is dealing with the simultaneous issues caused by quantization and delay, where the main challenge is how to compensate for the input delay in the presence of quantization.

1.5 Outline

The rest of this thesis is divided into four main chapters, followed by the appended papers containing the research. Since the main focus in this thesis relates to control of system with quantization, a brief description of the different quantizers that have been considered in this work are presented in Chapter 2. Next, Chapter 3 describes two different models for the dynamics of rigid body systems that have been used, and Chapter 4 presents the control designs, where adaptive backstepping control is considered for systems where there is uncertainty to the system parameters, and predictor feedback control is considered where there is a delay in the control structure. Lastly, Chapter 5 gives some concluding remarks.

Chapter 2

Quantizers

Quantization is the process of mapping a continuous signal into a set of discrete signals by approximating the amplitude of the input signal to the nearest level of a predefined set of discrete signals. It is a memoryless nonlinearity, where the output of the quantization is determined by its input at that instance of time [74]. Quantization is often used in practical applications due to the use of digital processors, but it has also been shown effective in reducing occupation rate of transmission bandwidth in the communication of signals [18].

A device or function that converts a sampled signal into a quantized signal is called a quantizer, e.g. an analog-to-digital converter. There are several different quantizers, such as uniform, logarithmic and hysteresis quantizers, that all have in common that they are piecewise functions, but have different properties. The difference between the input signal to the quantizer and the quantized signal is the quantization error. For the class of quantizers satisfying a sector bounded property, this error can be expressed as

$$|Q(y) - y| = |d| \leq \delta|y| + y_{\min}, \tag{2.1}$$

where y is a signal that is quantized by a quantizer $Q(\cdot)$, d is the quantization error, and where $0 \leq \delta < 1$ and $y_{\min} > 0$ are quantization parameters. If $\delta = 0$, the quantization error will only depend on $y_{\min}$, and so the quantization error is bounded by a constant. When $0 < \delta < 1$, the quantization error also depends on the input to the quantizer. Most practical quantizers satisfy the property in (2.1) and belong to the class of sector bounded quantizers. Three different quantizers have been considered in this thesis, and will be further described.

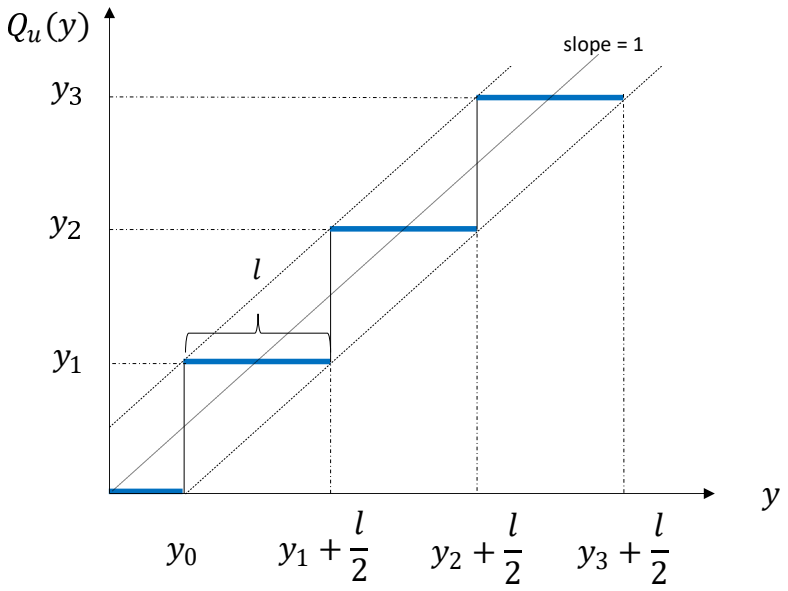

Figure 2.1: Map of the uniform quantizer $Q_u(y)$ for $y > 0$.

2.1 Uniform Quantizer

A uniform quantizer can be described as [75]

$$Q_u(y) = \begin{cases} y_i \operatorname{sgn}(y), & y_i - \frac{l}{2} < |y| \leq y_i + \frac{l}{2} \\ 0, & |y| \leq y_0 \end{cases}, \tag{2.2}$$

where $y_0 > 0$ determines the size of the dead-zone for $Q_u(y)$, and $y_1 = y_0 + \frac{l}{2}$, $y_i = y_{i-1} + l$ with $i = 2, 3, \ldots, l$ is the length of the quantization interval and $\operatorname{sgn}(\cdot)$ is the sign function. The uniform quantization $Q_u(y)$ is in the set $U = \{0, \pm y_i\}$, and a map of the uniform quantizer (2.2) for $y > 0$ is shown in Fig. 2.1. The quantization error of a uniform quantizer satisfies (2.1) with $\delta = 0$ and $y_{\min} = \max\{y_0, l/2\}$, and so the quantization error is bounded by a positive constant.

The uniform quantizer has equal quantization levels and is optimal for uniformly distributed signals, and is the most commonly used quantizer for digital signal processing. Some applications where the use of uniform quantization can be found, is in marine vehicles control [76], wheeled mobile robot control [77], and aircraft wing system control [78].

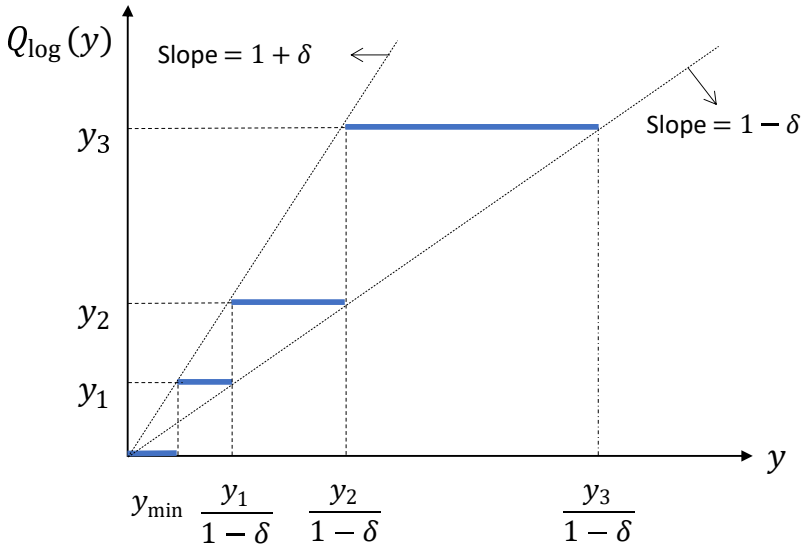

Figure 2.2: Map of the logarithmic quantizer $Q_{\log}(y)$ for $y > 0$.

2.2 Logarithmic Quantizer

A logarithmic quantizer can be expressed as [75]

$$Q_{\log}(y) = \begin{cases} y_i \operatorname{sgn}(y), & \frac{y_i}{1+\delta} < |y| \leq \frac{y_i}{1-\delta} \\ 0, & |y| \leq y_{\min} \end{cases}, \tag{2.3}$$

where $y_{\min} = \frac{y_0}{1+\delta}$ determines the size of the dead-zone for $Q_{\log}(y)$, $0 < \delta < 1$, $y_0 > 0$, $y_i = \rho^{(1-i)} y_0$, with $i = 1, 2, \ldots$, and parameter $\rho = \frac{1-\delta}{1+\delta}$. The parameter ρ can be regarded as a measure of the quantization density, where smaller values of ρ implies that the quantizer is coarser. The quantized signal $Q_{\log}(y)$ is in the set $U = \{0, \pm y_i\}$ and satisfies the property in (2.1) with $0 < \delta < 1$. A map of the logarithmic quantizer (2.3) for $y > 0$ is shown in Fig. 2.2.

The logarithmic quantizer has unequal quantization levels, and is useful where the signals are more concentrated near the equilibrium or have higher resolution around the equilibrium, e.g. for speech signal compression, image processing, etc. For this kind of quantizer, the quantization error depends on the input to the quantizer, and can not be ensured bounded automatically.

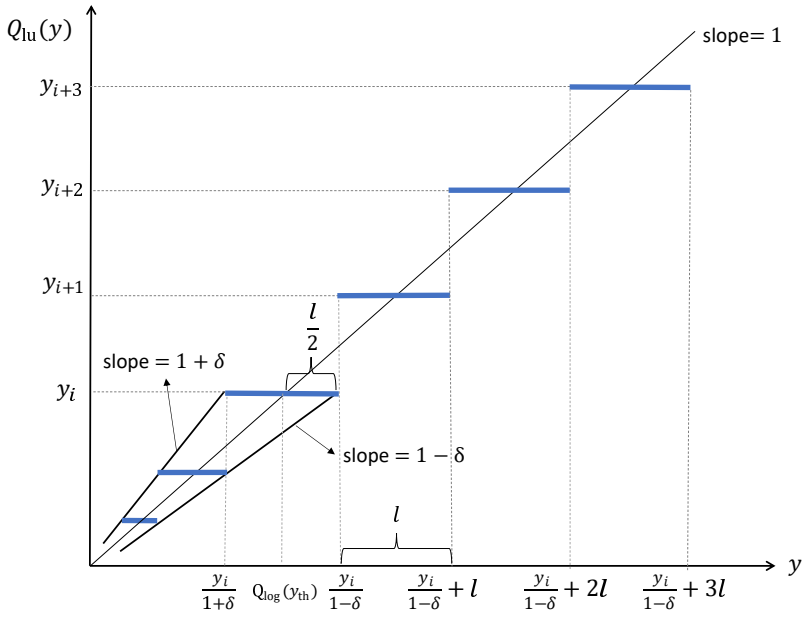

Figure 2.3: Map of the logarithmic-uniform quantizer $Q_{\text{lu}}(y)$ for $y > 0$.

2.3 Logarithmic-Uniform Quantizer

A logarithmic-uniform quantizer combines a uniform quantizer and a logarithmic quantizer and is defined as [28, 79]

$$Q_{\text{lu}}(y) = \begin{cases} Q_u(y), & |y| > y_{\text{th}} \\ Q_{\log}(y) & |y| \leq y_{\text{th}} \end{cases}, \tag{2.4}$$

where y_{th} is a positive constant specified by designer denoting the threshold to switch between the logarithmic and the uniform quantizer. The uniform quantizer, $Q_u(\cdot)$, is defined in (2.2) and the logarithmic quantizer, $Q_{\log}(\cdot)$, is defined in (2.3). The quantizer $Q_{\text{lu}}(y)$ takes advantage of a logarithmic quantizer having high resolution close to the origin, switching to a uniform quantizer for higher values. The length of the quantization interval for the uniform quantizer is defined based on the quantized value of the threshold value, given as $l = 2\delta Q_{\log}(y_{\text{th}}) \left(\frac{1}{1-\delta}\right)$. Then the quantization error satisfies (2.1) with $\delta = 0$ and $y_{\min} = \frac{l}{2}$ for any value of y. A map of the logarithmic-uniform quantizer (2.4) for $y > 0$ is shown in Figure 2.3, where $Q_{\log}(y_{\text{th}}) = y_i$.

Chapter 3

Modelling

The first step in control design is to have a mathematical model of the system, where this model is an approximate representation of the real system. Various methods exist for deriving the equations of motion for rigid body systems, and two commonly used methods are by a Newton-Euler formulation that is based on Newton's law and Euler's rotation dynamics, or by formulating the Lagrangian of the system, and derive the Lagrange's equation of the system. For mechanical systems, the two methods are equivalent, although derived in different ways [80].

The minimum number of coordinates required to describe the motion of a system having n degrees of freedom, is n. A rigid body with six degrees of freedom, would need a minimum of six coordinates to describe the position (three coordinates) and the orientation (three coordinates), with time derivative corresponding to the translational and rotational motion. In this thesis, we are only concerned with the orientation, also called the attitude, and the rotational motion of a rigid body. When analyzing the motion of a rigid body, it is convenient to define two or more coordinate frames, since the motion of the system is seen relative to another frame, often a fixed/inertial frame. A rigid body system that has been considered throughout the project is the 2-DOF helicopter system from Quanser, shown in Figure 3.1. This is a two-rotor laboratory equipment for flight control-based experiments. With a horizontally positioned main thruster and a vertically positioned tail thruster, which resembles a helicopter with two propellers driven by two DC motors. The helicopter is a MIMO system with 2-DOF, and can rotate around two axes. The body-fixed reference frame b is shown in Figure 3.1a, and an inertial frame i is considered to coincide with the body-fixed frame for the orientation shown in the figure. Experiments have been conducted on the helicopter to demonstrate the different control designs.

The following notations are used further in Chapter 3 and 4. Vectors are denoted by small bold letters and matrices with capitalized bold letters. The symbol $\boldsymbol{\omega}_{b,a}^{c}$ denotes angular velocity of frame a relative to frame b, expressed in frame c; $\boldsymbol{R}_{a}^{b}$ is

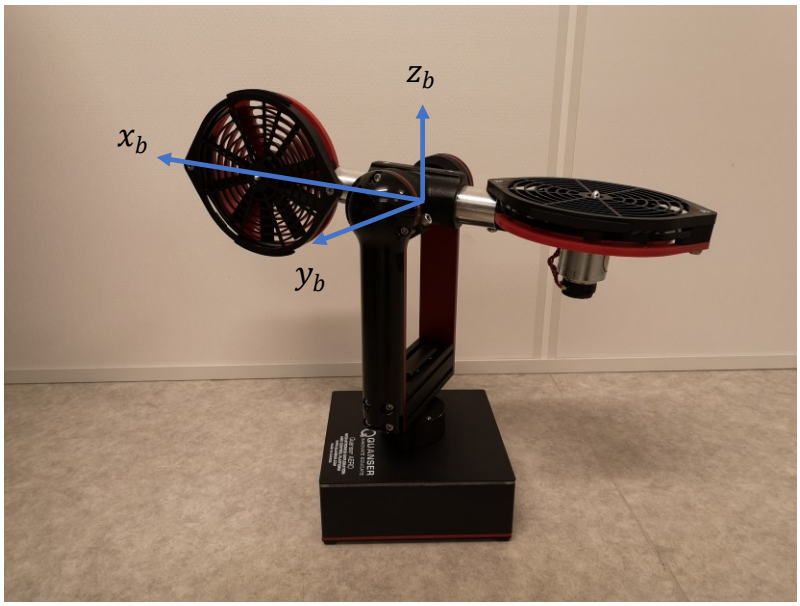

(a) Body fixed coordinate frame.

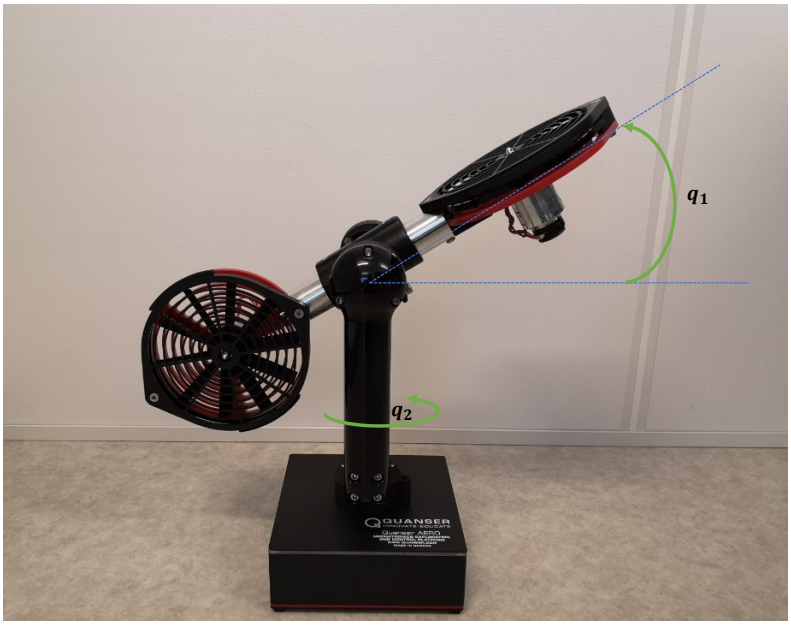

(b) Generalized coordinates, where q_1 is equal the pitch angle and q_2 is equal the yaw angle.

Figure 3.1: Quanser Aero helicopter system.

the rotation matrix from frame a to frame b; the cross product operator $\times$ between two vectors $\boldsymbol{a}$ and $\boldsymbol{b}$ is written as $\boldsymbol{S}(\boldsymbol{a})\boldsymbol{b}$ where $\boldsymbol{S}$ is skew-symmetric; $\lambda_{\max}(\cdot)$ and $\lambda_{\min}(\cdot)$ denotes the maximum and minimum eigenvalue of the matrix $(\cdot)$; the partial derivative $\frac{\partial}{\partial a}u(a,b)$ is expressed as $u_a(a,b)$.

3.1 Equations of Motion based on Newton-Euler Formulation

The attitude of a rigid body can be represented by e.g. Euler angles in [1, 38], (modified) Rodrigues parameters, rotation matrices in [81, 82] or quaternions in [83–85], where each representation has different properties. Any three-parameter representations have some kind of singularity, where e.g. Euler angles (roll-pitch-yaw) have kinematic singularities since it is not possible to describe the angular velocity for all angles, and with the potential problem of gimbal lock. Practical applications are often represented by unit quaternions, since this is a nonsingular parameterization.

The orientation of a rigid body in frame b, relative to an inertial frame i, is here described by a unit quaternion, $\boldsymbol{q} = [\eta, \varepsilon_1, \varepsilon_2, \varepsilon_3]^\top = [\eta, \boldsymbol{\varepsilon}^\top]^\top \in \mathbb{S}^3 = \{\boldsymbol{x} \in \mathbb{R}^4 : \boldsymbol{x}^\top\boldsymbol{x} = 1\}$, that is a complex number, where $\eta = \cos(\upsilon/2) \in \mathbb{R}$ is the real part and $\boldsymbol{\varepsilon} = \boldsymbol{k}\sin(\upsilon/2) \in \mathbb{R}^3$ is the imaginary part, where υ is the Euler angle and $\boldsymbol{k}$ is the Euler axis, and $\mathbb{S}^3$ is the non-Euclidean three-sphere. Considering a fully actuated rigid body, the equations of motion for the attitude dynamics are defined as

$$\dot{\boldsymbol{q}} = \boldsymbol{T}(\boldsymbol{q})\boldsymbol{\omega}, \tag{3.1}$$

$$\boldsymbol{J}\dot{\boldsymbol{\omega}} = -\boldsymbol{S}(\boldsymbol{\omega})(\boldsymbol{J}\boldsymbol{\omega}) + \boldsymbol{\tau}_d + \boldsymbol{B}\boldsymbol{u}, \tag{3.2}$$

where the angular velocity $\boldsymbol{\omega}_{i,b}^b = \boldsymbol{\omega} \in \mathbb{R}^3$, the inertia matrix $\boldsymbol{J} \in \mathbb{R}^{3\times3}$ is positive definite and invertible, the vector $\boldsymbol{\tau}_d \in \mathbb{R}^3$ is the total disturbance torque, the control allocation matrix $\boldsymbol{B} \in \mathbb{R}^{3\times3}$, the control input $\boldsymbol{u} \in \mathbb{R}^3$, and where

$$\boldsymbol{T}(\boldsymbol{q}) = \frac{1}{2}\begin{bmatrix} -\boldsymbol{\varepsilon}^\top \\ \eta\boldsymbol{I} + \boldsymbol{S}(\boldsymbol{\varepsilon}) \end{bmatrix} \in \mathbb{R}^{4\times3}, \tag{3.3}$$

and the matrix $\boldsymbol{S}(\cdot)$ is the skew-symmetric matrix given by

$$\boldsymbol{S}(\boldsymbol{\varepsilon}) = \begin{bmatrix} 0 & -\varepsilon_3 & \varepsilon_2 \\ \varepsilon_3 & 0 & -\varepsilon_1 \\ -\varepsilon_2 & \varepsilon_1 & 0 \end{bmatrix}. \tag{3.4}$$

The orientation between two frames can be described by a rotation matrix given as

$$\boldsymbol{R}(\boldsymbol{q}) = \boldsymbol{I} + 2\eta\boldsymbol{S}(\boldsymbol{\varepsilon}) + 2\boldsymbol{S}^2(\boldsymbol{\varepsilon}), \tag{3.5}$$

and the rotation matrix $\boldsymbol{R} \in SO(3)$ that is a special orthogonal group of order 3, and has the property

$$SO(3) = \{\boldsymbol{R} \in \mathbb{R}^{3\times 3} : \boldsymbol{R}^\top \boldsymbol{R} = \boldsymbol{I}, \det(\boldsymbol{R}) = 1\}. \tag{3.6}$$

The time derivative of a rotation matrix can be expressed as [80]

$$\dot{\boldsymbol{R}}_b^a = \boldsymbol{R}_b^a \boldsymbol{S}(\boldsymbol{\omega}_{a,b}^b) = \boldsymbol{S}(\boldsymbol{\omega}_{a,b}^a)\boldsymbol{R}_b^a. \tag{3.7}$$

In Papers B, C and F, the equations of motion are derived by this method.

3.2 Equations of Motion based on the Lagrangian Approach

Another method for deriving the equations of motion is by following the Lagrangian approach [12, 86], where the Lagrangian L for a rigid body system is given by

$$L = T - V, \tag{3.8}$$

where T is the total kinetic energy of the system and V is the total potential energy of the system, and thus the Lagrangian mechanics describe the system dynamics in terms of energy. Then the Lagrange equations for an n-DOF system can be stated as

$$\frac{d}{dt}\left(\frac{\partial L}{\partial \dot{q}_j}\right) - \frac{\partial L}{\partial q_j} = Q_j, \quad j = 1, \ldots, n, \tag{3.9}$$

for each generalized coordinate q_j, and where Q_j is the generalized force corresponding to the generalized coordinate q_j. This formula is valid in any reference frame (inertial or body frame) as long as generalized coordinates are used [87].

For the 2-DOF helicopter system, the generalized coordinates in the inertial frame are q_1, that is equal to the pitch angle θ, and q_2, that is equal to the yaw angle ψ, and where Q_j represent the external forces and damping corresponding to these angles. The generalized coordinates are shown in Figure 3.1b. The total kinetic and potential energy is

$$T = \frac{1}{2}I_p\dot{q}_1{}^2 + \frac{1}{2}I_y\dot{q}_2{}^2 + \frac{1}{2}mr^2(\sin^2 q_1\dot{q}_2{}^2 + \dot{q}_1{}^2), \tag{3.10}$$

$$V = mgr(1 - \cos q_1), \tag{3.11}$$

where the potential energy is the energy due to gravity, and where I_p and I_y are the moments of inertia of q_1 and q_2 respectively, m is the mass of the helicopter, r is the distance between the center of mass and the origin of the body-fixed frame, and g is the gravitational acceleration. The generalized forces are

$$Q_1 = K_{pp}V_p + K_{py}V_y - D_{Vp}\dot{q}_1, \tag{3.12}$$
$$Q_2 = K_{yy}V_y + K_{yp}V_p - D_{Vy}\dot{q}_2, \tag{3.13}$$

where V_p and V_y are the voltages applied to the main and tail motors, the constants K_{pp} and K_{yy} are the torque thrust gains from the main and the tail motors, K_{py} is the cross-torque thrust gain acting on pitch from the tail motor, K_{yp} is the cross-torque thrust gain acting on yaw from the main motor, and D_{Vp} and D_{Vy} are damping constants.

Then the equations of motion can be derived by taking the partial derivative of (3.10) and (3.11) as described in (3.9), expressed in matrix form as

$$\boldsymbol{M}(\boldsymbol{q})\ddot{\boldsymbol{q}} + \boldsymbol{C}(\boldsymbol{q}, \dot{\boldsymbol{q}})\dot{\boldsymbol{q}} + \boldsymbol{D}\dot{\boldsymbol{q}} + \boldsymbol{g}(\boldsymbol{q}) = \boldsymbol{\tau}, \tag{3.14}$$

where

$$\boldsymbol{M}(\boldsymbol{q}) = \begin{bmatrix} I_p + mr^2 & 0 \\ 0 & I_y + mr^2 \sin^2 q_1 \end{bmatrix}, \tag{3.15}$$
$$\boldsymbol{C}(\boldsymbol{q}, \dot{\boldsymbol{q}}) = \begin{bmatrix} 0 & -mr^2 \sin q_1 \cos q_1 \dot{q}_2 \\ mr^2 \sin q_1 \cos q_1 \dot{q}_2 & mr^2 \sin q_1 \cos q_1 \dot{q}_1 \end{bmatrix}, \tag{3.16}$$
$$\boldsymbol{g}(\boldsymbol{q}) = \begin{bmatrix} mgr \sin q_1 & 0 \end{bmatrix}^\top, \quad \boldsymbol{q} = \begin{bmatrix} q_1 & q_2 \end{bmatrix}^\top, \tag{3.17}$$
$$\boldsymbol{D} = \begin{bmatrix} D_{Vp} & 0 \\ 0 & D_{Vy} \end{bmatrix}, \tag{3.18}$$

where $\boldsymbol{q} \in \mathbb{R}^2$ are the generalized coordinates, $\boldsymbol{M}(\boldsymbol{q}) \in \mathbb{R}^{2\times 2}$ is a symmetric positive definite inertia matrix, $\boldsymbol{C}(\boldsymbol{q}, \dot{\boldsymbol{q}}) \in \mathbb{R}^{2\times 2}$ is a matrix of Coriolis and centrifugal terms, $\boldsymbol{D} \in \mathbb{R}^{2\times 2}$ is a positive definite matrix of damping terms, $\boldsymbol{g}(\boldsymbol{q}) \in \mathbb{R}^2$ is a vector of gravitational loading, and $\boldsymbol{\tau} \in \mathbb{R}^2$ are the generalized external forces associated with $\boldsymbol{q}$, that is

$$\boldsymbol{\tau} = \begin{bmatrix} K_{pp} & K_{py} \\ K_{yp} & K_{yy} \end{bmatrix} \begin{bmatrix} V_p \\ V_y \end{bmatrix}. \tag{3.19}$$

Defining $\boldsymbol{x} = [\boldsymbol{q}^\top, \dot{\boldsymbol{q}}^\top]^\top = [\boldsymbol{x}_1^\top, \boldsymbol{x}_2^\top]^\top \in \mathbb{R}^4$, the system can be written in state

space form as

$$\dot{\boldsymbol{x}} = f(\boldsymbol{x}, \boldsymbol{\tau}), \tag{3.20}$$

where

$$\dot{\boldsymbol{x}}_1 = \boldsymbol{x}_2, \tag{3.21}$$

$$\dot{\boldsymbol{x}}_2 = \boldsymbol{M}(\boldsymbol{x}_1)^{-1} \left(\boldsymbol{\tau} - \boldsymbol{C}(\boldsymbol{x})\boldsymbol{x}_2 - \boldsymbol{D}\boldsymbol{x}_2 - \boldsymbol{g}(\boldsymbol{x}_1) \right). \tag{3.22}$$

The dynamics of mechanical systems such as rigid robot manipulators [66, 88], cranes [89], marine vessels [87] and aerial vehicles [4, 90] are often derived based on the Euler-Lagrange equations, and in Papers A, D and E, the model is derived by this method.

Chapter 4

Control Design

The main requirement for all control systems is stability. One of the concepts used in control theory is Lyapunov stability, where stability of equilibrium points is studied. To determine stability of equilibrium points, a Lyapunov function is used, that often is taken as the total energy of the system. By examining the derivative of this function along the trajectories of the system, one can determine the stability of the equilibrium point. This is thoroughly described in the book Nonlinear Systems by Khalil [74].

A dynamic system to be controlled often has some form of uncertainty to it, and adaptive control has proven to be a well suited tool to control uncertain systems. Adaptive control has been the subject of research since the 1950's, with several related books and papers, so it has a long and rich history. This is a control design method where the controller is continuously changing to maintain the performance of the dynamic system when the system has parameters that vary (for instance mass of an aircraft, that is changing during flight because of fuel consumption) or has parameters that are uncertain. Some of the adaptive control methods proposed are model reference adaptive control (MRAC), adaptive pole placement control, and adaptive backstepping, see e.g. [91, 92]. The main controller design procedure used in this thesis for systems with uncertainties is based on adaptive backstepping, that is a recursive Lyapunov-based design method.

Backstepping is a nonlinear control design method developed in the 1990's, that has become an effective control design tool for control problems related to nonlinear systems. For the class of strict feedback systems, this is a recursive design, stepping back towards the control input. By viewing the nonlinear system as a cascade of subsystems, where the input to the first subsystem comes from the output of the second subsystem and so on, the idea is to use the output of a subsystem as a control variable for the previous subsystem. Then an ideal input for a subsystem can be designed as virtual control laws for the intermediate control. At each step, a control Lyapunov function is chosen, and an intermediate control is designed. This

procedure continuous until the actual control input appears and is designed. For a known nonlinear system (assuming there are no uncertainties), backstepping can transform the system into a linear system in a set of new coordinates, just as feedback linearization. However, one of the advantage of backstepping, is that it can avoid cancellation of nonlinearities that can be useful in the closed loop [92].

An adaptive backstepping controller is designed with a combination of a control law together with an estimate of the unknown parameters that is adjusted when the system is operating, and with the design of virtual control for the intermediate control based on backstepping. The control law is continuously adapted to the new parameter estimated, hence it is an adaptive control law. The uncertainties are considered as unknown constants. The concept of adaptive backstepping control is introduced in Section 4.1 for an uncertain mechanical system.

When there are input delays in a system, the development of predictor-based control laws are often considered, where the delay is compensated, and the system behaves as if there is no delay after a finite time. Predictor feedback design is introduced in Section 4.2 for both linear and nonlinear systems.

4.1 Adaptive Backstepping Control

To introduce the adaptive backstepping control design procedure, lets consider a second order mechanical system

$$\dot{\boldsymbol{x}}_1 = \boldsymbol{x}_2, \tag{4.1}$$

$$\dot{\boldsymbol{x}}_2 = \boldsymbol{u} + \boldsymbol{\Phi}(\boldsymbol{x}_1, \boldsymbol{x}_2)^\top \boldsymbol{\theta}, \tag{4.2}$$

where $\boldsymbol{x}_1 \in \mathbb{R}^n, \boldsymbol{x}_2 \in \mathbb{R}^n$ are the system states, $\boldsymbol{u} \in \mathbb{R}^n$ is the control input vector, $\boldsymbol{\Phi} \in \mathbb{R}^{m \times n}$ are known smooth nonlinear functions of the system states and $\boldsymbol{\theta} \in \mathbb{R}^m$ is a vector of unknown constants. The control objective is to design a control law for $\boldsymbol{u}$ to force $\boldsymbol{x}_1$ to track a reference signal $\boldsymbol{x}_r(t)$, by combining an estimator for the uncertain parameters that are adjusted during operation. The reference signal and the first and second order derivatives are assumed to be piecewise continuous and bounded. By the backstepping procedure [92], a controller is designed recursively by considering some of the system states as virtual controls, for the intermediate control.

Step 1. First, an error variable is introduced as

$$\boldsymbol{z}_1 = \boldsymbol{x}_1 - \boldsymbol{x}_r. \tag{4.3}$$

This is the tracking error that we want to drive towards zero. The derivative of (4.3) is

$$\dot{\boldsymbol{z}}_1 = \boldsymbol{x}_2 - \dot{\boldsymbol{x}}_r, \tag{4.4}$$

and in the first step, a virtual controller $\boldsymbol{\alpha}$ is to be determined. Viewing $(\boldsymbol{x}_2 - \dot{\boldsymbol{x}}_r)$ as a control variable, we introduce the change of coordinates

$$\boldsymbol{z}_2 = \boldsymbol{x}_2 - \dot{\boldsymbol{x}}_r - \boldsymbol{\alpha}, \tag{4.5}$$

as the difference between the virtual controller and the control variable, and so Eq. (4.4) can be described by

$$\dot{\boldsymbol{z}}_1 = \boldsymbol{z}_2 + \boldsymbol{\alpha}, \tag{4.6}$$

in terms of the new variable. Consider a control Lyapunov function

$$V_1 = \frac{1}{2}\boldsymbol{z}_1^\top \boldsymbol{z}_1, \tag{4.7}$$

where the derivative of V_1 along the solutions of the error system is

$$\dot{V}_1 = \boldsymbol{z}_1^\top (\boldsymbol{z}_2 + \boldsymbol{\alpha}). \tag{4.8}$$

The virtual controller is then designed as a stabilizing function for the system, e.g. by choosing $\boldsymbol{\alpha} = -c_1 \boldsymbol{z}_1$, where c_1 is a positive constant. If $\boldsymbol{z}_2 = 0$, then $\dot{V}_1 = -c_1 \boldsymbol{z}_1^\top \boldsymbol{z}_1$ and $\boldsymbol{z}_1$ will converge towards zero asymptotically.

Step 2. Taking the derivative of $\boldsymbol{z}_2$ in (4.5) yields

$$\begin{aligned} \dot{\boldsymbol{z}}_2 &= \boldsymbol{u} + \boldsymbol{\Phi}^\top \boldsymbol{\theta} - \ddot{\boldsymbol{x}}_r - \dot{\boldsymbol{\alpha}} \\ &= \boldsymbol{u} + \boldsymbol{\Phi}^\top \boldsymbol{\theta} - \ddot{\boldsymbol{x}}_r - \frac{\partial \boldsymbol{\alpha}}{\partial \boldsymbol{x}_1}\boldsymbol{x}_2 - \frac{\partial \boldsymbol{\alpha}}{\partial \boldsymbol{x}_r}\dot{\boldsymbol{x}}_r. \end{aligned} \tag{4.9}$$

In this step, the control input appears, that we want to design such that the error system $\boldsymbol{z} = [\boldsymbol{z}_1^\top, \boldsymbol{z}_2^\top]^\top$ converges towards zero. Since $\boldsymbol{\theta}$ is unknown, a certainty equivalence principle will be used when designing the control input, in which $\boldsymbol{\theta}$ is replaced by an estimate $\hat{\boldsymbol{\theta}}$. A control Lyapunov function is chosen for the system including the parameter estimation error as

$$V_2 = V_1 + \frac{1}{2}\boldsymbol{z}_2^\top \boldsymbol{z}_2 + \frac{1}{2}\tilde{\boldsymbol{\theta}}^\top \boldsymbol{\Gamma}^{-1} \tilde{\boldsymbol{\theta}}, \tag{4.10}$$

where $\tilde{\boldsymbol{\theta}} = \boldsymbol{\theta} - \hat{\boldsymbol{\theta}}$ is the estimation error, and $\boldsymbol{\Gamma} \in \mathbb{R}^{m \times m}$ is a positive definite matrix.

The derivative of (4.10) along the solution of the error system gives

$$\dot{V}_2 = -c_1 \boldsymbol{z}_1^\top \boldsymbol{z}_1 + \boldsymbol{z}_2^\top \left(\boldsymbol{z}_1 + \boldsymbol{u} + \boldsymbol{\Phi}^\top \boldsymbol{\theta} - \ddot{\boldsymbol{x}}_r - \frac{\partial \boldsymbol{\alpha}}{\partial \boldsymbol{x}_1} \boldsymbol{x}_2 - \frac{\partial \boldsymbol{\alpha}}{\partial \boldsymbol{x}_r} \dot{\boldsymbol{x}}_r \right) - \tilde{\boldsymbol{\theta}}^\top \boldsymbol{\Gamma}^{-1} \dot{\hat{\boldsymbol{\theta}}}. \quad (4.11)$$

We want to design $\boldsymbol{u}$ and a parameter update law for the estimate to guarantee that the derivative of V_2 is nonpositive. Choosing

$$\boldsymbol{u} = -\boldsymbol{z}_1 - c_2 \boldsymbol{z}_2 - \boldsymbol{\Phi}^\top \hat{\boldsymbol{\theta}} + \ddot{\boldsymbol{x}}_r + \frac{\partial \boldsymbol{\alpha}}{\partial \boldsymbol{x}_1} \boldsymbol{x}_2 + \frac{\partial \boldsymbol{\alpha}}{\partial \boldsymbol{x}_r} \dot{\boldsymbol{x}}_r, \quad (4.12)$$

where c_2 is a positive constant, and by including (4.12) in (4.11) we get

$$\dot{V}_2 = -c_1 \boldsymbol{z}_1^\top \boldsymbol{z}_1 - c_2 \boldsymbol{z}_2^\top \boldsymbol{z}_2 - \tilde{\boldsymbol{\theta}}^\top \boldsymbol{\Gamma}^{-1} (\dot{\hat{\boldsymbol{\theta}}} - \boldsymbol{\Gamma} \boldsymbol{\Phi} \boldsymbol{z}_2). \quad (4.13)$$

We then choose the update law

$$\dot{\hat{\boldsymbol{\theta}}} = \boldsymbol{\Gamma} \boldsymbol{\Phi} \boldsymbol{z}_2, \quad (4.14)$$

resulting in

$$\dot{V}_2 = -c_1 \boldsymbol{z}_1^\top \boldsymbol{z}_1 - c_2 \boldsymbol{z}_2^\top \boldsymbol{z}_2 \leq 0. \quad (4.15)$$

Then, by (4.10) and (4.15), we conclude that V_2, $\boldsymbol{z}$ and $\tilde{\boldsymbol{\theta}}$ are bounded. Since the reference signal (and first and second order derivative) is bounded, it follows that all signals in the closed-loop system are bounded. Then, an argument using LaSalle-Yoshizawa theorem [92, Theorem 2.1] proves that $\boldsymbol{z} \to 0$ as $t \to \infty$, and tracking is achieved.

Adaptive backstepping achieves the goal of tracking (and stabilization), and this is a direct consequence of the recursive design procedure where a Lyapunov function is constructed for the entire system including the estimated parameters.

If the inputs are quantized before applied to the uncertain mechanical system, we have

$$\dot{\boldsymbol{x}}_1 = \boldsymbol{x}_2, \quad (4.16)$$

$$\dot{\boldsymbol{x}}_2 = Q(\boldsymbol{u}) + \boldsymbol{\Phi}(\boldsymbol{x}_1, \boldsymbol{x}_2)^\top \boldsymbol{\theta}, \quad (4.17)$$

where $Q(\cdot)$ is a quantizer, e.g. one of the quantizers introduced in Chapter 2. The change of coordinates (4.3) and (4.5) and Step 1 will be the same as when the inputs are continuous, but in Step 2, the quantized inputs appear. If the control input $\boldsymbol{u}$ and the update law for the estimate $\hat{\boldsymbol{\theta}}$ are designed as without quantization, we can

analyze how quantization affects the stability. This will depend on what kind of quantizer is considered. This problem is addressed in Paper A, where a uniform quantizer is considered for the inputs.

If the states are quantized before sent to the controller, the states $\boldsymbol{x}_1, \boldsymbol{x}_2$ are no longer available for the control design. The mechanical system is still represented by (4.1)–(4.2). We then need to redefine the error variables $\boldsymbol{z}_1, \boldsymbol{z}_2$, the virtual controller $\boldsymbol{\alpha}$, and the nonlinear functions $\boldsymbol{\Phi}$, such that the control law $\boldsymbol{u}$ and parameter update law $\dot{\hat{\boldsymbol{\theta}}}$ are designed by using only the quantized values of the states, since these are available, i.e. $\boldsymbol{u} = f(Q(\boldsymbol{x}_1), Q(\boldsymbol{x}_2))$ and $\dot{\hat{\boldsymbol{\theta}}} = g(Q(\boldsymbol{x}_1), Q(\boldsymbol{x}_2))$. Since the quantized states then are used in the design of the virtual controller $\boldsymbol{\alpha}$, the derivative of the virtual controller is discontinuous and can not be used in the design of the controller, contrary to when the states are not quantized in (4.12). This problem is addressed in Paper B, where the effects of state quantization are analyzed by considering a uniform quantizer for the states.

When both the inputs and the states are quantized, the controller and the update law are designed by the quantized states, i.e $\boldsymbol{u} = f(Q(\boldsymbol{x}_1), Q(\boldsymbol{x}_2))$ and $\dot{\hat{\boldsymbol{\theta}}} = g(Q(\boldsymbol{x}_1), Q(\boldsymbol{x}_2))$, before the input is quantized so that the system receives $Q(\boldsymbol{u})$ and is described by (4.16)–(4.17). The analysis becomes more involved, since both the effects of input and state quantization need to be considered. This problem is addressed in Papers C and D for uniform quantizers, while a more general quantizer is considered in Paper F, making the analysis more difficult.

4.2 Predictor Feedback Design

If a delay in the control loop affects the performance because of its size, a natural decision is to try to compensate the delay. By making a prediction of the future state, the same performance as a delay free system can ideally be achieved after a finite time. For remote controlled mechanical systems, a long, slowly time-varying communication delay, that is often considered constant, is likely to appear [66].

4.2.1 Predictor Feedback Design for Linear Systems with Input Delay

We will here introduce the basic idea of predictor feedback design, starting by considering a linear system with long input delay given as [17, 50, 57]

$$\dot{\boldsymbol{x}}(t) = \boldsymbol{A}\boldsymbol{x}(t) + \boldsymbol{B}u(t - D), \tag{4.18}$$

where $\boldsymbol{x} \in \mathbb{R}^n$, $(\boldsymbol{A}, \boldsymbol{B})$ is a controllable pair, $t \geq 0$, $D > 0$ is the constant delay that is arbitrarily long, and $u(t-D) \in \mathbb{R}$ is the delayed input signal. For the delay-free system, i.e. when $D = 0$, a stabilizing control law for (4.18) is given by

$$u(t) = \boldsymbol{K}\boldsymbol{x}(t), \tag{4.19}$$

where $\boldsymbol{K}$ is chosen such that the matrix $(\boldsymbol{A}+\boldsymbol{B}\boldsymbol{K})$ is Hurwitz. For the system (4.18) with delay, we then have a desire to have the control input such that $u(t-D) = \boldsymbol{K}\boldsymbol{x}(t)$, which alternatively is written as $u(t) = \boldsymbol{K}\boldsymbol{x}(t+D)$. The main idea behind predictor feedback is to make a prediction of the future value of the state

$$\boldsymbol{p}(t) = \boldsymbol{x}(t+D), \tag{4.20}$$

and then replace $\boldsymbol{x}(t)$ in the nominal design (4.19), by the predicted value $\boldsymbol{p}(t)$, such that the delayed input $u(t-D) = \boldsymbol{K}\boldsymbol{x}(t)$, as wanted. By performing a change of variables $t = \theta + D$ in (4.18), we have

$$\frac{d\boldsymbol{x}(\theta+D)}{d\theta} = \boldsymbol{A}\boldsymbol{x}(\theta+D) + \boldsymbol{B}u(\theta), \quad \forall t - D \leq \theta \leq t, \tag{4.21}$$

and by defining the signal

$$\boldsymbol{p}(\theta) = \boldsymbol{x}(\theta+D), \quad \forall t - D \leq \theta \leq t, \tag{4.22}$$

and then solving the ODE for $\boldsymbol{p}(\theta)$ with respect to θ, with the initial condition $\boldsymbol{p}(t-D) = \boldsymbol{x}(t)$, i.e the initial condition is given as the current state, we get

$$\boldsymbol{p}(\theta) = e^{\boldsymbol{A}(\theta-t+D)}\boldsymbol{x}(t) + \int_{t-D}^{\theta} e^{\boldsymbol{A}(\theta-\sigma)}\boldsymbol{B}u(\sigma)d\sigma, \quad \forall t - D \leq \theta \leq t, \tag{4.23}$$

and so the predictor signal is defined as

$$\boldsymbol{p}(t) = \boldsymbol{x}(t+D) = e^{\boldsymbol{A}D}\boldsymbol{x}(t) + \int_{t-D}^{t} e^{\boldsymbol{A}(t-\theta)}\boldsymbol{B}u(\theta)d\theta, \quad \forall t \geq 0, \tag{4.24}$$

which is implementable, involving the history of $u(\theta)$ for all $t - D \leq \theta \leq t$. Then the feedback law is

$$u(t) = \boldsymbol{K}\boldsymbol{p}(t) = \boldsymbol{K}\left(e^{\boldsymbol{A}D}\boldsymbol{x}(t) + \int_{t-D}^{t} e^{\boldsymbol{A}(t-\theta)}\boldsymbol{B}u(\theta)d\theta\right), \quad \forall t \geq 0, \tag{4.25}$$

which is infinite-dimensional, since it contains the distributed delay term involving past controls, i.e. the integral term $\int_{t-D}^{t} e^{\boldsymbol{A}(t-\theta)}\boldsymbol{B}u(\theta)d\theta$. This results in a delay-

compensated closed-loop system

$$\dot{\boldsymbol{x}}(t) = (\boldsymbol{A} + \boldsymbol{B}\boldsymbol{K})\,\boldsymbol{x}(t), \quad \forall t \geq D, \tag{4.26}$$

after the control reaches the system at $t = D$. For $t \in [0, D]$, the system state is given as

$$\boldsymbol{x}(t) = e^{\boldsymbol{A}t}\boldsymbol{x}(0) + \int_0^t e^{\boldsymbol{A}(t-\theta)}\boldsymbol{B}u(\theta - D)d\theta, \quad \forall t \in [0, D]. \tag{4.27}$$

The controller (4.25) is the same as was derived by Artstein [49] under the reduction method. By taking the derivative of the predictor state $\boldsymbol{p}(t)$ in (4.24), we get

$$\dot{\boldsymbol{p}}(t) = \boldsymbol{A}\boldsymbol{p}(t) + \boldsymbol{B}u(t), \quad \forall t \geq 0, \tag{4.28}$$

which reduces into a delay-free system, with the resulting feedback law as given in (4.25).

To analyze the stability of the closed-loop system consisting of the plant (4.18) and the control law (4.25), an infinite-dimensional backstepping transformation is introduced for the actuator state. The reason for including this transformation, is to be able to construct a Lyapunov functional for the entire system in new coordinates, which is less complicated than in the original coordinates. The transformation can be described with a PDE notation, or represented in standard delay notation [17]. We describe the transformation with a standard delay notation for the linear system.

The transformation for the actuator state is given as

$$w(\theta) = u(\theta) - \boldsymbol{K}\boldsymbol{p}(\theta), \quad \forall t - D \leq \theta \leq t, \tag{4.29}$$

and maps the closed-loop system consisting of the plant (4.18) and the control law (4.25) into the target system

$$\dot{\boldsymbol{x}}(t) = (\boldsymbol{A} + \boldsymbol{B}\boldsymbol{K})\boldsymbol{x}(t) + \boldsymbol{B}w(t - D), \tag{4.30}$$

$$w(t) = 0, \quad \forall t \geq 0. \tag{4.31}$$

This can be shown from the fact that $u(t) = \boldsymbol{K}\boldsymbol{p}(t)$ and $\boldsymbol{p}(t - D) = \boldsymbol{x}(t)$. For this choice of target system, $w(t - D)$ becomes zero in finite time, and then the system behaves as if there was no delay in the system.

Then a Lyapunov functional for the target system can be chosen as

$$V(t) = \boldsymbol{x}(t)^\top \boldsymbol{F}\boldsymbol{x}(t) + b\int_{t-D}^t e^{\theta+D-t}w(\theta)^2 d\theta, \tag{4.32}$$

where the matrix $\boldsymbol{F} = \boldsymbol{F}^\top > 0$, and has the property

$$(\boldsymbol{A} + \boldsymbol{B}\boldsymbol{K})^\top \boldsymbol{F} + \boldsymbol{F}(\boldsymbol{A} + \boldsymbol{B}\boldsymbol{K}) = -\boldsymbol{Q}, \tag{4.33}$$

where the matrix $\boldsymbol{Q} = \boldsymbol{Q}^\top > 0$. Taking the time derivative of (4.32) along solutions of the target system (4.30)–(4.31) we get

$$\begin{aligned}
\dot{V}(t) &= -\boldsymbol{x}(t)^\top \boldsymbol{Q}\boldsymbol{x}(t) + 2\boldsymbol{x}(t)^\top \boldsymbol{F}\boldsymbol{B}w(t-D) - bw(t-D)^2 - b\int_{t-D}^{t} e^{\theta+D-t}w(\theta)^2 d\theta \\
&\leq -\frac{1}{2}\lambda_{\min}(\boldsymbol{Q})\|\boldsymbol{x}(t)\|^2 + \left(\frac{2\|\boldsymbol{F}\boldsymbol{B}\|^2}{\lambda_{\min}(\boldsymbol{Q})} - b\right) w(t-D)^2 - b\int_{t-D}^{t} e^{\theta+D-t}w(\theta)^2 d\theta \\
&\leq -\frac{1}{2}\lambda_{\min}(\boldsymbol{Q})\|\boldsymbol{x}(t)\|^2 - b\int_{t-D}^{t} e^{\theta+D-t}w(\theta)^2 d\theta \\
&\leq -\min\left\{\frac{\lambda_{\min}(\boldsymbol{Q})}{2\lambda_{\max}(\boldsymbol{F})}, 1\right\} V(t)
\end{aligned} \tag{4.34}$$

where Young's inequality is used, and by choosing $b \geq \frac{2\|\boldsymbol{F}\boldsymbol{B}\|^2}{\lambda_{\min}(\boldsymbol{Q})}$. From (4.32) and (4.34) stability in the $(\boldsymbol{x}, w)$ variables can be established, where the origin of the target system (4.30)–(4.31) is exponentially stable. To ensure the stability of the closed-loop system (4.18), (4.25), we need to show that the transformation (4.29) is invertible. The inverse backstepping transformation is given as

$$u(\theta) = w(\theta) + \boldsymbol{K}\boldsymbol{\pi}(\theta), \quad \forall t - D \leq \theta \leq t, \tag{4.35}$$

where

$$\boldsymbol{\pi}(\theta) = e^{(\boldsymbol{A}+\boldsymbol{B}\boldsymbol{K})(\theta-t+D)}\boldsymbol{x}(t) + \int_{t-D}^{\theta} e^{(\boldsymbol{A}+\boldsymbol{B}\boldsymbol{K})(\theta-s)}\boldsymbol{B}w(s)ds, \quad \forall t - D \leq \theta \leq t. \tag{4.36}$$

Then stability of the target systems equilibrium point implies stability of the equilibrium point for the closed-loop system (4.18), (4.25).

4.2.2 Predictor Feedback Design for Nonlinear Systems with Input Delay

We here present a nonlinear version of the predictor feedback design. For nonlinear systems, the problem of a finite escape phenomenon must also be considered. If the input delay is large, the control signal may not reach the system before its states escape to infinity. The class of forward complete systems do not exhibit finite escape, where for every initial condition and every bounded input signal the corresponding solution is defined for all times. Most mechanical and electromechanical systems satisfy the property of forward completeness [58], and this property is assumed ensured in the following example. The design of the predictor feedback follows the

procedure in [17].

Considering a nonlinear system with constant long input delay,

$$\dot{\boldsymbol{z}} = h\left(\boldsymbol{z}(t), \tau(t-D)\right), \tag{4.37}$$

where $\boldsymbol{z} \in \mathbb{R}^n$ is the state, $t \geq t_0 \geq 0$, $\tau \in \mathbb{R}$ is the input to the system, and $D > 0$. The design is based on a nominal control law for the delay free system, i.e. when $D = 0$, and so we assume there exists a function κ for the delay-free system

$$\tau(t) = \kappa(t, \boldsymbol{z}(t)), \tag{4.38}$$

that ensures stability of the system in closed-loop. Then a control law for the system (4.37) is

$$\tau(t) = \kappa(t + D, \boldsymbol{p}(t)), \tag{4.39}$$

where

$$\boldsymbol{p}(t) = \boldsymbol{z}(t) + \int_t^{t+D} h\left(\boldsymbol{z}(s), \tau(s-D)\right) ds, \tag{4.40}$$

that is a prediction of the future state $\boldsymbol{p}(t) = \boldsymbol{z}(t+D)$, where by a change of time we have

$$\begin{aligned} \boldsymbol{p}(t) &= \boldsymbol{z}(t) + \int_{t-D}^{t} h\left(\boldsymbol{z}(a+D), \tau(a)\right) da \\ &= \boldsymbol{z}(t) + \int_{t-D}^{t} h\left(\boldsymbol{p}(a), \tau(a)\right) da, \end{aligned} \tag{4.41}$$

that is implementable by current values of the state $\boldsymbol{z}(t)$ and past values of the input $\tau(a)$ and predicted values $\boldsymbol{p}(a)$ for all $t - D \leq a \leq t$, and is given implicitly. Then, the control law (4.39) will compensate the delay, where the delayed input is $\tau(t-D) = \kappa(t, \boldsymbol{p}(t-D)) = \kappa(t, \boldsymbol{z}(t))$. Initial condition for the predictor is given as

$$\boldsymbol{p}(\theta) = \boldsymbol{z}(t_0) + \int_{t_0-D}^{\theta} h(\boldsymbol{p}(s), \tau(s)) ds, \quad \forall \theta \in [t_0 - D, t_0], \tag{4.42}$$

where t_0 is the initial time.

The system (4.37) can equivalently be modeled by a cascade of ODE-PDE [62]

$$\dot{\boldsymbol{z}}(t) = h(\boldsymbol{z}(t), u(0,t)), \tag{4.43}$$

$$u_t(x,t) = u_x(x,t), \quad \forall x \in [0, D], \tag{4.44}$$

$$u(D,t) = \tau(t), \tag{4.45}$$

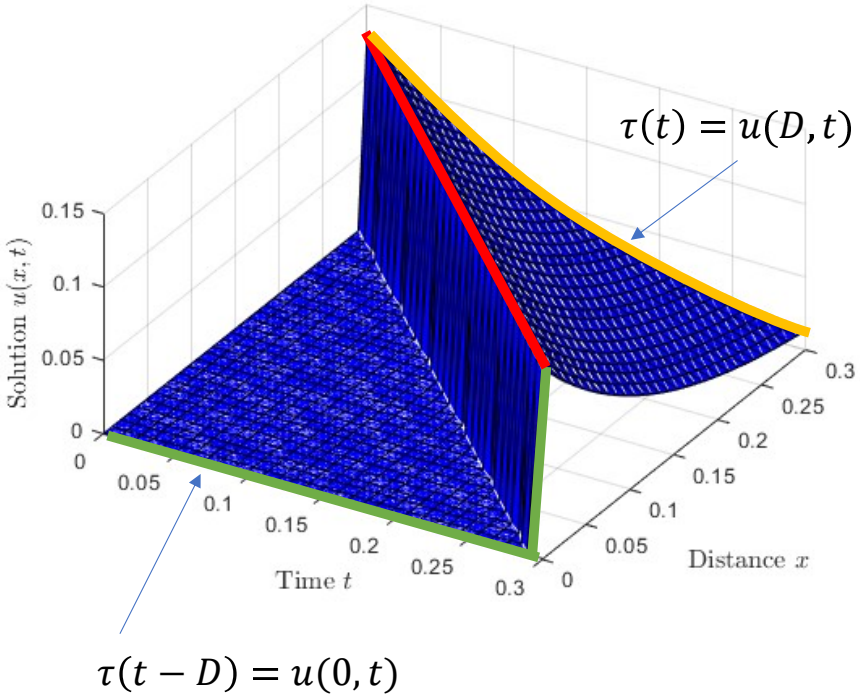

Figure 4.1: Illustration of the transport PDE.

where the actuator state is modeled by a transport PDE and where the solution to (4.44)–(4.45) is given by $u(x,t) = \tau(t+x-D)$ for all $x \in [0,D]$. This can be considered as a boundary control problem, since the PDE is driven by the input $\tau(t)$ at its boundary. An illustration of this is shown in Figure 4.1 for a delay $D = 0.3$, where the red line shows the input $\tau(t=0)$, that reached the system after D-time units, and with initial values for the input $u(x,t_0) = 0$ for all $x \in [0,D]$.

To analyze the stability of the closed-loop system consisting of the plant (4.37) and the control law (4.39), an infinite-dimensional backstepping transformation is introduced for the actuator state. We describe the transformation with a PDE notation this time.

The transformation for the actuator state is given as

$$w(x,t) = u(x,t) - \kappa(t+x, \boldsymbol{p}_1(x,t)), \tag{4.46}$$

where the predictor state in (4.42) equivalently can be represented with a PDE notation given as

$$\boldsymbol{p}_1(x,t) = \boldsymbol{z}(t) + \int_0^x h\left(\boldsymbol{p}_1(y,t), u(y,t)\right) dy, \quad \forall x \in [0,D], \tag{4.47}$$

and where $\boldsymbol{p}_1(D,t) = \boldsymbol{p}(t)$. The control law (4.39) is given as

$$\tau(t) = \kappa(t+D, \boldsymbol{p}_1(D,t)), \tag{4.48}$$

and together with the transformation (4.46), this transforms the system (4.43)–(4.45) into the target system

$$\dot{\boldsymbol{z}}(t) = h(\boldsymbol{z}(t), \kappa(t, \boldsymbol{z}(t)) + w(0,t)), \tag{4.49}$$

$$w_t(x,t) = w_x(x,t), \quad \forall x \in [0, D], \tag{4.50}$$

$$w(D,t) = 0. \tag{4.51}$$

For this choice of target system, $w(x,t)$ becomes zero in finite time (after D time units), and the system behaves as if there was no delay in the system. Then, a Lyapunov functional for the target system can e.g. be selected as

$$V(t) = \frac{1}{2}\boldsymbol{z}(t)^\top \boldsymbol{z}(t) + \frac{k}{2}\int_0^D e^x w(x,t)^2 dx, \tag{4.52}$$

where k is a positive constant. Taking a time derivative of (4.52) along solutions of the target system (4.49)–(4.51) we have

$$\dot{V}(t) = \boldsymbol{z}(t)^\top h(\boldsymbol{z}(t), \kappa(t, \boldsymbol{z}(t)) + \boldsymbol{z}(t)^\top w(0,t) + k\int_0^D e^x w(x,t) w_t(x,t) dx. \tag{4.53}$$

We here assume exponential stability of the origin for the delay-free system such that the term $\boldsymbol{z}(t)^\top h(\boldsymbol{z}(t), \kappa(t, \boldsymbol{z}(t)) \leq -a\boldsymbol{z}(t)^\top \boldsymbol{z}(t)$, for some $a > 0$, by the choice of control law for the delay-free system. Then by using Young's inequality and integration by parts, one obtains

$$\begin{aligned}
\dot{V}(t) &\leq -a\boldsymbol{z}(t)^\top \boldsymbol{z}(t) + \boldsymbol{z}(t)^\top w(0,t) + k\int_0^D e^x w(x,t) w_x(x,t) dx \\
&\leq -\frac{a}{2}\boldsymbol{z}(t)^\top \boldsymbol{z}(t) + \frac{1}{2a} w(0,t)^2 - \frac{k}{2} w(0,t)^2 - \frac{k}{2}\int_0^D e^x w(x,t)^2 dx \\
&\leq -\frac{a}{2}\boldsymbol{z}(t)^\top \boldsymbol{z}(t) + \left(\frac{1}{2a} - \frac{k}{2}\right) w(0,t)^2 - \frac{k}{2}\int_0^D e^x w(x,t)^2 dx \\
&\leq -\min\{a, 1\} V(t),
\end{aligned} \tag{4.54}$$

by choosing $k \geq \frac{1}{a}$. This shows the stability of the target system equilibrium point. To ensure the stability of the closed-loop system (4.37), (4.39), we need to show that the transformation (4.46) is invertible. The inverse backstepping transformation is given as

$$u(x,t) = w(x,t) + \kappa(t + x, \boldsymbol{\pi}_1(x,t)), \tag{4.55}$$

where

$$\boldsymbol{\pi}_1(x,t) = \boldsymbol{z}(t) + \int_0^x h\left(\boldsymbol{\pi}_1(y,t), \kappa(t + y, \boldsymbol{\pi}_1(y,t)) + w(y,t)\right) dy, \quad \forall x \in [0, D]. \tag{4.56}$$

A nonlinear system in presence of both input delay and quantization can be described as

$$\dot{\boldsymbol{z}} = h\left(\boldsymbol{z}(t), Q(\tau(t-D))\right), \tag{4.57}$$

or equivalently by a cascade of ODE-PDE

$$\dot{\boldsymbol{z}}(t) = h(\boldsymbol{z}(t), u(0,t)), \tag{4.58}$$

$$u_t(x,t) = u_x(x,t), \quad \forall x \in [0, D] \tag{4.59}$$

$$u(D,t) = Q(\tau(t)), \tag{4.60}$$

where $Q(\cdot)$ is a quantizer. If the control input $\tau(t)$ is designed as without quantization given in (4.39) and (4.41), we can analyze how quantization affects the stability. This problem is addressed in Paper E for a nonlinear MIMO system, where the inputs are quantized by a uniform quantizer.

Chapter 5

Conclusions and Future Work

5.1 Conclusions

The work presented in this thesis focuses on the attitude tracking control problem for rigid body systems, where quantization, uncertainty and delay are present in the control loop. The work is motivated by the increased interest for wireless communication, remote controlled systems and other NCS, where the control loops are closed through a communication network. Since signals are required to be quantized before transmitted over the network, the network induces delays, and the network bandwidth might be limited, we need to consider these imperfections in the control loop. Furthermore, uncertainties often appear in systems. For instance, the delays might be uncertain, or system parameters are unknown, and so we also need to develop control schemes that can handle such uncertainties that are present.

We have considered both a helicopter system with 2-DOF, and a more general rigid body system where the attitude is represented by quaternions. Adaptive control schemes have been developed by using the backstepping technique, to handle uncertainties in the system. Quantization has been introduced in the control loop, either at the input (Paper A), the state (Paper B) or both input and state (Papers C, D and F). Compared to the tracking control problem of an uncertain nonlinear system, the introduction of quantization in the control loop changes the stability condition of the equilibria, since we can not guarantee asymptotic stability anymore. Instead, the error state is ensured ultimately bounded by a positive constant, that depends on the quantization parameters and controller gains. Also tracking is achieved, with a bounded error that is directly related to the quantization parameters. For the general rigid body system with state or both input and state quantization (Papers B, C and F), the controller gains and quantization parameters must be chosen to satisfy some given conditions to ensure the stability property of the equilibrium.

We have also focused our attention to a class of sector bounded quantizers,

which introduces quantization errors that are linearly dependent on the inputs to the quantizers. This problem was addressed in Paper F. Compared to Paper C where a bounded type of quantizer was considered, the controller is first designed to take advantage of a skew-symmetric property to guarantee the stability. Then, the relations between the quantized signals and the continuous signals are established as functions of the error states, and based on this the stability of the closed-loop equilibrium can be achieved by proper choices of design parameters.

In the last part of the project, the attention has been paid to time delays. A predictor feedback controller was developed to handle arbitrarily large input delays for a nonlinear system, where the inputs also were quantized before transmitted to the helicopter system (Paper E). The delay was then compensated for by the predictor feedback, and tracking achieved with a bounded error proportional to the choice of quantization parameters.

By including quantization in the control loop, the communication burden over a network can be reduced, with the expense of reducing the tracking performance. Then some suitable quantization parameters should be chosen to guarantee the performance requirement for the application. The relationship between quantization level and performance is analytically derived in Papers A–F.

5.2 Future Work

All papers except Paper E include uncertainties to the system, and adaptive controllers were developed for this reason. The problem of compensating delays for nonlinear systems with uncertainties are nontrivial, and is an interesting problem to investigate further. Some attention has been paid to this problem, however without any results yet, and has thus not been presented in this thesis. When the predictor feedback controller was tested on the real helicopter system, it was noted that by increasing the delay, the tracking errors increased. One of the reasons for this increase is probably because the model is not perfect. The error might be reduced if one can take uncertainty in the model into account. This is considered as a possible future direction.

Most of the work that considers some of the network-induced imperfections only considers one at the time. The problem of addressing more than one of the imperfections in the control loop is also a future path for research. For instance the problem of having an uncertain delay while at the same time the signals are quantized.

Bibliography

[1] S. M. Schlanbusch and J. Zhou, "Adaptive backstepping control of a 2-DOF helicopter system with uniform quantized inputs," in *IECON 2020 The 46th Annual Conference of the IEEE Industrial Electronics Society*, 2020, pp. 88–94.

[2] S. M. Schlanbusch, J. Zhou, and R. Schlanbusch, "Adaptive backstepping attitude control of a rigid body with state quantization," in *Proceedings of 60th IEEE Conference on Decision and Control*, 2021, pp. 372–377.

[3] ——, "Adaptive attitude control of a rigid body with input and output quantization," *IEEE Transactions on Industrial Electronics*, vol. 69, no. 8, pp. 8296–8305, 2022.

[4] S. M. Schlanbusch and J. Zhou, "Adaptive backstepping control of a 2-DOF helicopter system in the presence of quantization," in *9th International Conference on Control, Mechatronics and Automation*, 2021, pp. 110–115.

[5] S. M. Schlanbusch, O. M. Aamo, and J. Zhou, "Attitude control of a 2-DOF helicopter system with input quantization and delay," in *IECON 2022 The 48th Annual Conference of the IEEE Industrial Electronics Society*, 2022.

[6] S. M. Schlanbusch and J. Zhou, "Adaptive quantized control of uncertain nonlinear rigid body systems," *Systems & Control Letters*, vol. 175, 2023, 105513.

[7] J. Zhou and S. M. Schlanbusch, "Adaptive quantized control of offshore underactuated cranes with uncertainty," in *Proceedings of the IEEE 17th International Conference on Control & Automation*. IEEE, 2022, pp. 297–302.

[8] X. Ge, F. Yang, and Q.-L. Han, "Distributed networked control systems: A brief overview," *Information Sciences*, vol. 380, pp. 117–131, 2017.

[9] X.-M. Zhang, Q.-L. Han, X. Ge, D. Ding, L. Ding, D. Yue, and C. Peng, "Networked control systems: A survey of trends and techniques," *IEEE/CAA Journal of Automatica Sinica*, vol. 7, no. 1, pp. 1–17, 2020.

[10] D. Zhang, P. Shi, Q.-G. Wang, and L. Yu, "Analysis and synthesis of networked control systems: A survey of recent advances and challenges," *ISA Transactions 66*, pp. 376–392, 2017.

[11] F.-Y. Wang and D. Liu, Eds., *Networked Control Systems - Theory and Applications*. Springer, 2008.

[12] B. Siciliano and O. Khatib, Eds., *Springer Handbook of Robotics*. Springer International Publishing, 2016.

[13] K. Reif, K. Schmidt, F. Gesele, S. Reichelt, M. Saeger, and N. Seidler, "Networked control systems in motor vehicles," *ATZelektronik worldwide*, vol. 3, no. 4, pp. 18–23, 2008.

[14] A. Zolich, D. Palma, K. Kansanen, K. Fjørtoft, J. Sousa, K. H. Johansson, Y. Jiang, H. Dong, and T. A. Johansen, "Survey on communication and networks for autonomous marine systems," *Journal of Intelligent & Robotic Systems*, vol. 95, pp. 789–813, 2019.

[15] E. Fridman, *Introduction to Time-Delay Systems*. Springer International Publishing, 2014.

[16] J. Zhou and M. Krstić, "Adaptive predictor control for stabilizing pressure in a managed pressure drilling system under time-delay," *Journal of Process Control*, vol. 40, pp. 106–118, 2016.

[17] N. Bekiaris-Liberis and M. Krstić, *Nonlinear control under nonconstant delays*. SIAM, 2013.

[18] N. Elia and S. K. Mitter, "Stabilization of linear systems with limited information," *IEEE Transactions on Automatic Control*, vol. 46, no. 9, pp. 1384–1400, 2001.

[19] R. W. Brockett and D. Liberzon, "Quantized feedback stabilization of linear systems," *IEEE Transactions on Automatic Control*, vol. 45, no. 7, pp. 1279–1289, 2000.

[20] C.-Y. Kao and S. R. Venkatesh, "Stabilization of linear systems with limited information multiple input case," in *Proceedings of the 2002 American Control Conference (IEEE Cat. No.CH37301)*. IEEE, 2002.

[21] E. Fridman and M. Dambrine, "Control under quantization, saturation and delay: An LMI approach," *Automatica*, vol. 45, no. 10, pp. 2258–2264, 2009.

[22] M. Fu and L. Xie, "The sector bound approach to quantized feedback control," *IEEE Transactions on Automatic Control*, vol. 50, no. 11, pp. 1698–1711, 2005.

[23] J. Liu and N. Elia, "Quantized feedback stabilization of non-linear affine systems," *International Journal of Control*, vol. 77, no. 3, pp. 239–249, fe 2004.

[24] T. Hayakawa, H. Ishii, and K. Tsumaru, "Adaptive quantized control for nonlinear uncertain systems," *Systems & Control Letters*, vol. 58, no. 9, pp. 625–632, 2009.

[25] J. Zhou and C. Wen, "Adaptive backstepping control of uncertain nonlinear systems with input quantization," in *IEEE Conference on Decision and Control*, 2013, pp. 5571–5576.

[26] C. D. Persis, "Robust stabilization of nonlinear systems by quantized and ternary control," *Systems & Control Letters*, vol. 58, no. 8, pp. 602–608, 2009.

[27] J. Zhou, C. Wen, and G. Yang, "Adaptive backstepping stabilization of nonlinear uncertain systems with quantized input signal," in *IEEE Transactions on Automatic Control*, vol. 59, no. 2, 2014, pp. 460–464.

[28] L. Xing, C. Wen, Y. Zhu, H. Su, and Z. Liu, "Output feedback control for uncertain nonlinear systems with input quantization," *Automatica*, vol. 65, pp. 191–202, 2015.

[29] J. Zhou and W. Wang, "Adaptive control of quantized uncertain nonlinear systems," *IFAC PapersOnLine*, vol. 50, no. 1, pp. 10 425–10 430, 2017.

[30] Y. Li and G. Yang, "Adaptive asymptotic tracking control of uncertain nonlinear systems with input quantization and actuator faults," *Automatica*, vol. 72, pp. 177–185, 2016.

[31] L. Xing, C. Wen, H. Su, Z. Liu, and J. Cai, "Robust control for a class of uncertain nonlinear systems with input quantization," *International journal of robust and nonlinear control*, vol. 26, no. 8, pp. 1585–1596, 2015.

[32] Y. Wang, L. He, and C. Huang, "Adaptive time-varying formation tracking control of unmanned aerial vehicles with quantized input," *ISA Transactions*, vol. 85, pp. 76–83, 2019.

[33] B. Huang, B. Zhou, S. Zhang, and C. Zhu, "Adaptive prescribed performance tracking control for underactuated autonomous underwater vehicles with input quantization," *Ocean Engineering*, vol. 221, 2021.

[34] A. Selivanov, A. Fradkov, and D. Liberzon, "Adaptive control of passifiable linear systems with quantized measurements and bounded disturbances," *Systems and Control Letters*, vol. 88, pp. 62–67, 2016.

[35] A. Margun, I. Furtat, and A. Kremlev, "Robust control of twin rotor MIMO system with quantized output," *IFAC-PapersOnLine*, vol. 50, no. 1, pp. 4849–4854, 2017.

[36] J. Zhou, C. Wen, W. Wang, and F. Yang, "Adaptive backstepping control of nonlinear uncertain systems with quantized states," *IEEE Transactions on Automatic Control*, vol. 64, no. 11, pp. 4756–4763, 2019.

[37] D. F. Coutinho, M. Fu, and C. E. de Souza, "Input and output quantized feedback linear systems," *IEEE Transactions on Automatic Control*, vol. 55, no. 3, pp. 761–766, 2010.

[38] Y. Yan and S. Yu, "Sliding mode tracking control of autonomous underwater vehicles with the effect of quantization," *Ocean Engineering*, vol. 151, pp. 322–328, 2018.

[39] Y. Yan, S. Yu, and C. Sun, "Quantization-based event-triggered sliding mode tracking control of mechanical systems," *Information Sciences*, vol. 523, pp. 296–306, 2020.

[40] S. J. Yoo and B. S. Park, "Quantized-states-based adaptive control against unknown slippage effects of uncertain mobile robots with input and state quantization," *Nonlinear Analysis: Hybrid Systems*, vol. 42, pp. 1–17, 2021, article 101077.

[41] B. M. Kim and S. J. Yoo, "Approximation-based quantized state feedback tracking of uncertain input-saturated MIMO nonlinear systems with application to 2-DOF helicopter," *Mathematics*, vol. 9, no. 9, 2021.

[42] W. Wang, J. Zhou, C. Wen, and J. Long, "Adaptive backstepping control of uncertain nonlinear systems with input and state quantization," *IEEE Transactions on Automatic Control*, 2021.

[43] J. Nilsson, "Real-time control systems with delays," Ph.D. dissertation, Lund University, 1998.

[44] J. E. Normey-Rico and E. F. Camacho, *Control of Dead-time Processes*. Springer, 2007.

[45] J. Cui, S. Tosunoglu, R. Roberts, C. Moore, and D. W. Repperger, "A review of teleoperation system control," in *Proceedings of the Florida Conference on Recent Advances in Robotics*, 2003.

[46] O. J. M. Smith, "A controller to overcome dead time," *ISA Journal*, vol. 6, no. 2, pp. 28–33, 1959.

[47] A. Manitius and A. Olbrot, "Finite spectrum assignment problem for systems with delays," *IEEE Transactions on Automatic Control*, vol. 24, no. 4, pp. 541–552, 1979.

[48] W. Kwon and A. Pearson, "Feedback stabilization of linear systems with delayed control," *IEEE Transactions on Automatic Control*, vol. 25, no. 2, pp. 266–269, 1980.

[49] Z. Artstein, "Linear systems with delayed controls: A reduction," *IEEE Transactions on Automatic Control*, vol. 27, no. 4, pp. 869–879, 1982.

[50] D. Bresch-Pietri, "Robust control of variable time-delay systems. theoretical contributions and applications to engine control," Ph.D. dissertation, Mines, ParisTech, 2012.

[51] Z. J. Palmor, *in The Control Handbook*, 1996, ch. 10.8 Time-delay compensation - Smith predictor and its modifications, pp. 224–237.

[52] M. Krstić and D. Bresch-Pietri, "Delay-adaptive full-state predictor feedback for systems with unknown long actuator delay," in *In American Control Conference*, 2009.

[53] D. Bresch-Pietri and M. Krstić, "Adaptive trajectory tracking despite unknown input delay and plant parameters," *Automatica*, vol. 45, no. 9, pp. 2074–2081, 2009.

[54] M. Krstić, "Lyapunov stability of linear predictor feedback for time-varying input delay," *IEEE Transactions on Automatic Control*, vol. 55, no. 2, pp. 554–559, 2010.

[55] Y. Zhu, M. Krstić, and H. Su, "Adaptive global stabilization of uncertain multi-input linear time-delay systems by PDE full-state feedback," *Automatica*, vol. 96, pp. 270–279, 2018.

[56] M. Krstić, "On compensating long actuator delays in nonlinear control," in *American Control Conference*. IEEE, 2008.

[57] ——, *Delay Compensation for Nonlinear, Adaptive, and PDE Systems*. Birkhäuser Boston, 2009.

[58] ——, "Input delay compensation for forward complete and strict-feedforward nonlinear systems," *IEEE Transactions on Automatic Control*, vol. 55, no. 2, pp. 287–303, 2010.

[59] M. Krstić and N. Bekiaris-Liberis, "Control of nonlinear delay systems: a tutorial," in *51st IEEE Conference on Decision and Control*, 2012, pp. 5200–5214.

[60] D. Bresch-Pietri and M. Krstić, "Backstepping transformation of input delay nonlinear systems," *arXiv:1305.5305*, 2013.

[61] ——, "Delay-adaptive control for nonlinear systems," *IEEE Transactions on Automatic Control*, vol. 59, no. 5, pp. 1203–1218, 2014.

[62] N. Bekiaris-Liberis and M. Krstić, "Predictor-feedback stabilization of multi-input nonlinear systems," *IEEE Transactions on Automatic Control*, vol. 62, no. 2, pp. 516–531, 2017.

[63] M. Bagheri, P. Naseradinmousavi, and M. Krstić, "Feedback linearization based predictor for time delay control of a high-DOF robot manipulator," *Automatica*, vol. 108, 2019.

[64] ——, "Time delay control of a high-DOF robot manipulator through feedback linearization based predictor," in *Proceedings of the ASME 2019, Dynamic Systems and Control Conference*, 2019.

[65] A. Bertino, P. Naseradinmousavi, and M. Krstić, "Experimental and analytical delay-adaptive control of a 7-DOF robot manipulator," in *American Control Conference*. IEEE, 2021.

[66] A. Bertino, P. Naseradinmousavi, and M. Krstic, "Delay-adaptive control of a 7-DOF robot manipulator: Design and experiments," *IEEE Transactions on Control Systems Technology*, pp. 1–16, 2022.

[67] M. Krstić and A. Smyshlyaev, "Backstepping boundary control for first-order hyperbolic PDEs and application to systems with actuator and sensor delays," *Systems & Control Letters*, vol. 57, no. 9, pp. 750–758, 2008.

[68] A. Bahill, "A simple adaptive smith-predictor for controlling time-delay systems: A tutorial," *IEEE Control Systems Magazine*, vol. 3, no. 2, pp. 16–22, 1983.

[69] J.-P. Richard, "Time-delay systems: an overview of some recent advances and open problems," *Automatica*, vol. 39, no. 10, pp. 1667–1694, 2003.

[70] M. Sharma and I. Kar, "Attitude stabilization of quadrotor with input time delay," *IFAC-PapersOnLine*, vol. 53, no. 2, pp. 9360–9365, 2020.

[71] W. Ren and J. Xiong, "Tracking control of nonlinear networked and quantized control systems with communication delays," *IEEE Transactions on Automatic Control*, vol. 65, no. 8, pp. 3685–3692, 2020.

[72] S. M. Schlanbusch and J. Zhou, "Adaptive backstepping control of a 2-dof helicopter," in *Proceedings of the IEEE 7th International Conference on Control, Mechatronics and Automation*, 2019, pp. 210–215.

[73] S. M. Schlanbusch, "Adaptive backstepping control of quanser 2dof helicopter - theory and experiments," Master's thesis, University of Agder, 2019.

[74] H. K. Khalil, *Nonlinear Systems, third edition*. Pearson Education International Inc., 2002.

[75] J. Zhou, C. Wen, and W. Wang, "Adaptive control of uncertain nonlinear systems with quantized input signal," *Automatica*, vol. 95, pp. 152–162, 2018.

[76] L.-Y. Hao, Y. Yu, T.-S. Li, and H. Li, "Quantized output-feedback control for unmanned marine vehicles with thruster faults via sliding-mode technique," *IEEE Transactions on Cybernetics*, vol. 52, no. 9, pp. 9363–9376, 2022.

[77] C.-Y. Tsai and K.-T. Song, "Visual tracking control of a wheeled mobile robot with system model and velocity quantization robustness," *IEEE Transactions on Control Systems Technology*, vol. 17, no. 3, pp. 520–527, 2009.

[78] S. Gao and J. Liu, "Adaptive neural network vibration control of a flexible aircraft wing system with input signal quantization," *Aerospace Science and Technology*, vol. 96, 2020, 105593.

[79] J. Zhou, L. Xing, and C. Wen, *Adaptive Control of Dynamic Systems with Uncertainty and Quantization*. CRC Press, 2021.

[80] O. Egeland and J. T. Gravdahl, *Modeling and Simulation for Automatic Control*. Marine Cybernetics AS, 2003.

[81] N. A. Chaturvedi, A. K. Sanyal, and N. H. McClamroch, "Rigid-body attitude control," *IEEE Control Systems Magazine*, vol. 31, no. 3, pp. 30–51, 2011.

[82] T. Lee, "Robust adaptive attitude tracking on SO(3) with an application to a quadrotor UAV," *IEEE Transactions on Control Systems Technology*, vol. 21, no. 5, pp. 1924–1930, 2013.

[83] A. Benallegue, Y. Chitour, and A. Tayebi, "Adaptive attitude tracking control of rigid body systems with unknown inertia and gyro-bias," *IEEE Transactions on Automatic Control*, vol. 63, no. 11, pp. 3986–3993, 2018.

[84] T. S. Andersen and R. Kristiansen, "Adaptive backstepping control for a fully-actuated rigid-body in a dual-quaternion framework," in *2019 IEEE 58th Conference on Decision and Control (CDC)*, 2019.

[85] C. G. Mayhew, R. G. Sanfelice, and A. R. Teel, "Quaternion-based hybrid control for robust global attitude tracking," *IEEE Transactions on Automatic Control*, vol. 56, no. 11, pp. 2555–2566, 2011.

[86] S. S. Rao, *Mechanical Vibrations*. Pearson Education, 2011.

[87] T. I. Fossen, *Marine Control Systems: Guidance, Navigation, and Control of Ships, Rigs and Underwater Vehicles*. Trondheim, Norway: Marine Cybernetics AS, 2002.

[88] R. Ortega and M. Spong, "Adaptive motion control of rigid robots: a tutorial," in *Proceedings of the 27th IEEE Conference on Decision and Control*, 1988.

[89] Y. Fang, B. Ma, P. Wang, and X. Zhang, "A motion planning-based adaptive control method for an underactuated crane system," *IEEE Transactions on Control Systems Technology*, 2011.

[90] S. Martini, S. Sonmez, A. Rizzo, M. Stefanovic, M. J. Rutherford, and K. P. Valavanis, "Euler-lagrange modeling and control of quadrotor UAV with aerodynamic compensation," in *2022 International Conference on Unmanned Aircraft Systems*. IEEE, 2022, pp. 369–377.

[91] S. Sastry and M. Bodson, *Adaptive Control: Stability, Convergence and Rubustness*. Prentice-Hall, Inc., 1989.

[92] M. Krstić, I. Kanellakopoulos, and P. Kokotović, *Nonlinear and Adaptive Control Design*. John Wiley & Sons, Inc., 1995.

Paper A

Adaptive Backstepping Control of a 2-DOF Helicopter System with Uniform Quantized Inputs

Siri Marte Schlanbusch and Jing Zhou

This paper has been published as:

S. M. Schlanbusch and J. Zhou, "Adaptive backstepping control of a 2-DOF helicopter system with uniform quantized inputs," in *IECON 2020 The 46th Annual Conference of the IEEE Industrial Electronics Society*, 2020, pp. 88–94, doi: 10.1109/IECON43393.2020.9254497.

Adaptive Backstepping Control of a 2-DOF Helicopter System with Uniform Quantized Inputs

Siri Marte Schlanbusch and Jing Zhou

Department of Engineering Sciences
University of Agder
4879 Grimstad, Norway

Abstract

This paper proposes a new adaptive controller for a 2-Degree of Freedom (DOF) helicopter system in the presence of input quantization. The inputs are quantized by uniform quantizers. A nonlinear mathematical model is derived for the 2-DOF helicopter system based on Euler-Lagrange equations, where the system parameters and the control coefficients are uncertain. A new adaptive control algorithm is developed by using backstepping technique to track the pitch and yaw position references independently. Only quantized input signals are used in the system which reduces communication rate and cost. It is shown that not only the ultimate stability is guaranteed by the proposed controller, but also the designers can tune the design parameters in an explicit way to obtain the required closed loop behavior. Experiments are carried out on the Quanser helicopter system to validate the effectiveness, robustness and control capability of the proposed scheme.

A.1 Introduction

The development and interest of distributed and networked control systems (NCSs) have increased recent years, where a control system involves a communication network [1–3]. There are several advantages of networked systems such as reduced wiring and easier maintenance, and with numerous applications e.g. as smart grids and unmanned aerial vehicles. Communication networks also give rise to some disadvantages such as networked-induced delays, packet dropouts and quantization. In a communication network the channel capacity may be limited, restricting number of bits that can be transmitted over the network, and digital rather than continuous signals are used when transmitting data. Quantization is often used for the discontinuous mapping from a continuous space to a finite set. It is nonlinear, since several

different input signals can give the same output and is an irreversible process. This introduces nonlinear errors in the control loop.

Due to its importance, quantized control has received a lot of attention, and it is of interest to see how it will affect the stability of a system. In [4–6] control of linear and nonlinear systems were looked at where either the input, output or the state were quantized. Quantized feedback control was considered in [7] for linear single-input-single-output (SISO) and multiple-input-multiple-output (MIMO) systems, where optimal control and robust control were used for performance purposes. Quantized control for stability of a nonlinear system with uncertainties was considered in [8] using a robust approach, and adaptive approaches have been studied in [9–13]. Here the backstepping technique was used in the control design, and different quantizers were considered including uniform, logarithmic and hysteresis and where either the inputs or the states were quantized. Adaptive control was also considered in [14] for nonlinear MIMO systems with input quantization.

The backstepping technique was proposed in the 1990's, and is a nonlinear controller design method where the control input is designed to compensate for the effects of plant nonlinearity [15]. It has been widely used to design adaptive controllers for uncertain systems, where the controller has a dynamic feedback for estimating the parameters in form of an adaptive update law. This technique has several advantages over the conventional approaches such as providing a promising way to improve the transient performance of adaptive systems by tuning design parameters.

In this paper, a 2-degree-of-freedom (DOF) helicopter system is considered, where the inputs are quantized. It is a nonlinear MIMO system, with challenges in controller design due to its nonlinear behavior, its coupling, and with uncertainties both in the model and the parameters, and with disturbance from the quantized inputs. We consider the adaptive backstepping controller for this system as in [16], where a theoretical proof of stability was given with the use of constructed Lyapunov functions, and where tracking was achieved and also boundedness of all signals in the closed loop system. It was also shown that the tracking error performance can be improved by adjusting the design parameters. This paper extends the results to include quantization of the inputs using a uniform quantization and prove boundedness of the closed loop signals.

The following notations are used. Vectors are denoted by small bold letters and matrices with capitalized bold letters. When the context is sufficient explicit, we may omit to write arguments of a function, vector or matrix.

The paper is organized as follows. In Section A.2 the system model, the quantized feedback system and the uniform quantizer are presented. Section A.3 presents the adaptive control design based on backstepping technique with stability and perform-

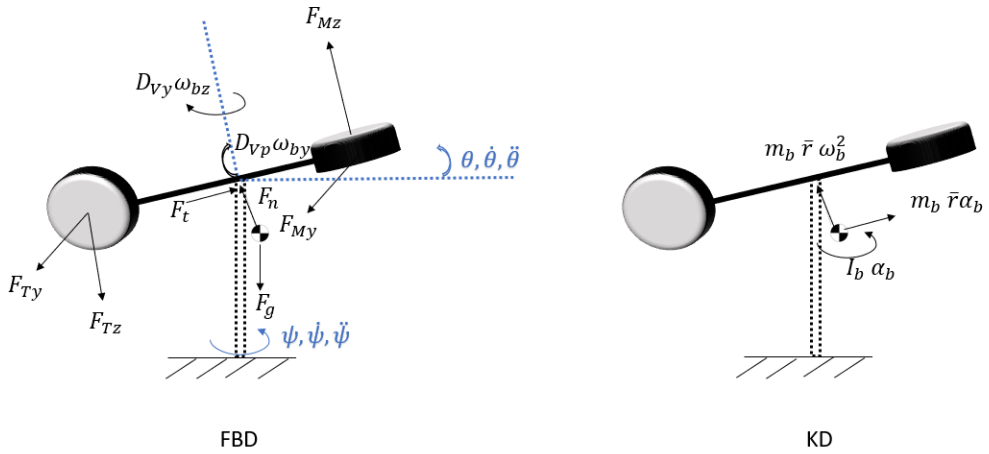

Figure A.1: Free body diagram and kinetic diagram of the Aero body

ance results, Section A.4 presents the experimental results before the conclusion is given in Section A.5.

A.2 Problem Statement

A.2.1 System Model

The helicopter system is visualized in Figure A.1 showing both a free body diagram (FBD) and a kinetic diagram (KD). The main motor is producing two forces, one main force, F_{Mz}, in the z_b-direction that will give a positive pitch angle, and also a force, F_{My}, in the y_b-direction, meaning this will give a yaw angle. This last force is due to the aerodynamic forces. The tail motor is also producing two forces, F_{Tz} and F_{Ty}. This motor is basically here to counteract the yaw from the main motor and thus control the yaw while the main motor is controlling the pitch. These forces are functions of the two system inputs, u_1 and u_2, that are the voltages applied to the main and tail motors. Viscous damping, proportional to the velocity of the Aero body, is also present.

This is a MIMO system with 2 DOF, where each input will change both the pitch and yaw angle. The helicopter model is considered as a rigid body and the equations of motion are derived using Euler-Lagrange equations as given in [16], where the system parameters and control coefficients are uncertain.

The state variables are defined as

$$\boldsymbol{x} = [\vartheta(t), \psi(t), \dot{\vartheta}(t), \dot{\psi}(t)]^\top, \tag{A.1}$$

where ϑ and ψ are pitch and yaw angles, and $\dot{\vartheta}$ and $\dot{\psi}$ are angular velocities of pitch

and yaw angles. The control variables are defined as

$$\boldsymbol{u} = [u_1(t, \boldsymbol{x}), u_2(t, \boldsymbol{x})]^\top, \tag{A.2}$$

and are the inputs that will be quantized. The nonlinear state space model is expressed as

$$\dot{\boldsymbol{x}} = \begin{bmatrix} x_3 \\ x_4 \\ \boldsymbol{\phi}_1^\top \boldsymbol{\theta}_1 \\ \boldsymbol{\phi}_2^\top \boldsymbol{\theta}_2 \end{bmatrix} + \begin{bmatrix} 0 \\ 0 \\ \beta_{1,1} u_1 + \beta_{1,2} u_2 \\ -\beta_{2,1} u_1 + \beta_{2,2} u_2 \end{bmatrix}, \tag{A.3}$$

where $\boldsymbol{\phi}_1$ and $\boldsymbol{\phi}_2$ are known nonlinear functions defined as

$$\boldsymbol{\phi}_1 = \begin{bmatrix} -x_3 \\ -\sin x_1 \\ x_4^2 \cos x_1 \sin x_1 \end{bmatrix}, \quad \boldsymbol{\phi}_2 = \begin{bmatrix} -x_4 \\ -x_2 x_4 \cos x_1 \sin x_1 \end{bmatrix}, \tag{A.4}$$

vectors $\boldsymbol{\theta}_1$ and $\boldsymbol{\theta}_2$ are unknown constant vectors defined as

$$\boldsymbol{\theta}_1 = \frac{1}{I_p + m l_{cm}^2} \begin{bmatrix} D_{Vp} \\ m g l_{cm} \\ m l_{cm}^2 \end{bmatrix}, \quad \boldsymbol{\theta}_2 = \frac{1}{I_y} \begin{bmatrix} D_{Vy} \\ 2 m l_{cm}^2 \end{bmatrix}, \tag{A.5}$$

and $\boldsymbol{\beta}_{i,j},\ i, j \in \{1, 2\}$, are unknown constants defined as

$$\beta_{1,1} = \frac{K_{pp}}{I_p + m l_{cm}^2}, \qquad \beta_{1,2} = \frac{K_{py}}{I_p + m l_{cm}^2}, \tag{A.6}$$

$$\beta_{2,1} = \frac{K_{yp}}{I_y}, \qquad \beta_{2,2} = \frac{K_{yy}}{I_y}. \tag{A.7}$$

The constants K_{pp} and K_{yy} are torque thrust gains from main and tail motors, K_{py} is cross-torque thrust gain acting on pitch from tail motor, K_{yp} is cross-torque thrust gain acting on yaw from main motor, l_{cm} is the distance between the center of mass and the origin of the body-fixed frame, I_p and I_y are the moments of inertia of the pitch and yaw respectively, g is the gravity acceleration, m is the total mass of the Aero body, and D_{V_y} and D_{V_p} are the damping constants for the rotation along the yaw axis and pitch axis separately.

The control objective is to design a control law for u_1 and u_2 to force the outputs x_1 and x_2 to track the reference signals $x_{r1}(t)$ and $x_{r2}(t)$ for pitch and yaw respectively when the inputs are quantized. To achieve the objective, the following

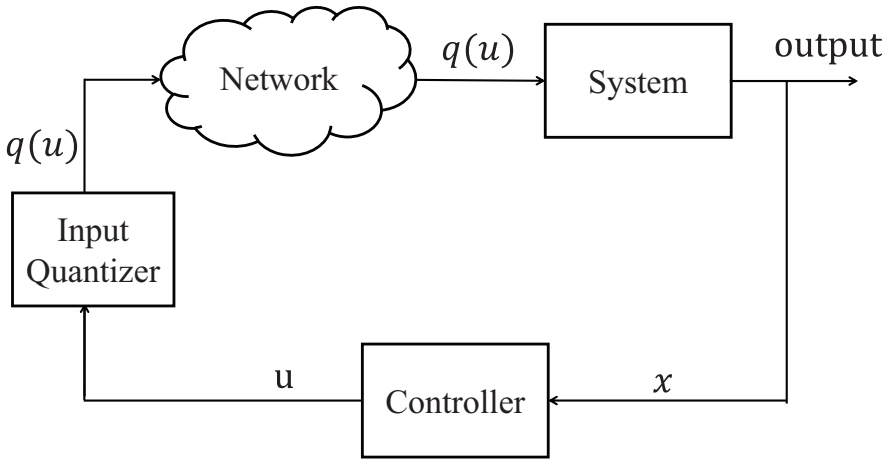

Figure A.2: System with quantized inputs

assumptions are imposed.

Assumption 1. *The reference signals x_{r1} and x_{r2} and first and second order derivatives are known, piecewise continuous and bounded.*

Assumption 2. *All unknown parameters $\boldsymbol{\theta}_1$, $\boldsymbol{\theta}_2$, $\beta_{i,j}$, $i, j \in \{1, 2\}$ are positive constants and within known bounds.*

A.2.2 Quantized System

In this paper, we consider a quantized feedback system as shown in Figure A.2. The inputs u_1 and u_2 in system (A.3) take the quantized values, that are quantized at the encoder side.

A.2.3 Uniform Quantizer

The control inputs u_1 and u_2 are quantized using a uniform quantizer which has intervals of fixed lengths and is defined as follows:

$$q(u_k) = \begin{cases} u_{k,i}\,\mathrm{sgn}(u_k), & u_{k,i} - \frac{l_k}{2} \leq |u_k| < u_{k,i} + \frac{l_k}{2} \\ 0, & |u_k| < u_{k,0} + \frac{l_k}{2} \end{cases} \tag{A.8}$$

where $k = 1, 2$, $u_{k,0} > -l_k/2$ is a constant, $l_k > 0$ is the length of the quantization intervals, $i = 1, 2, ...,$ and $u_{k,i+1} = u_{k,i} + l_k$. The uniform quantization $q(u_k) \in U_k = \{0, \pm u_{k,i}\}$, and a map of the quantization for $u_k > 0$ is shown in Figure A.3.

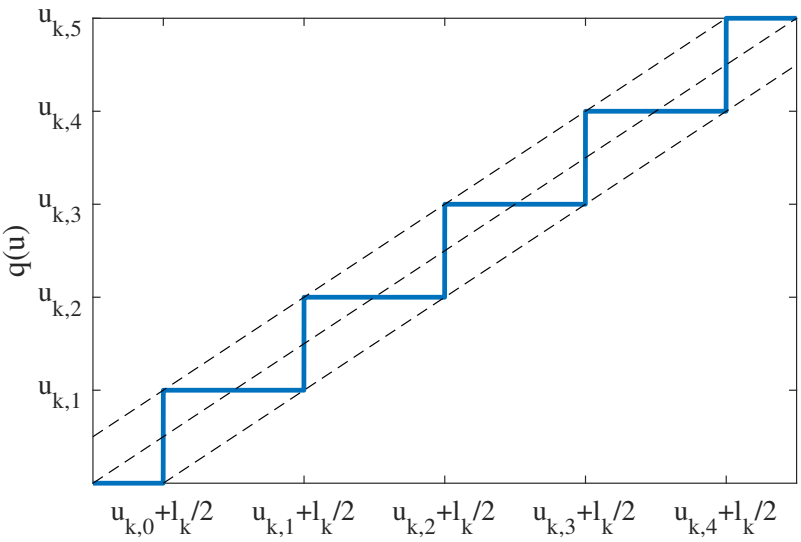

Figure A.3: Map of the uniform quantization, for $u_k > 0$

The smaller the quantization intervals are, the closer the signal is to its continuous counterpart.

A.3 Adaptive Control Design

In this section, we will design adaptive feedback control laws for the helicopter model using backstepping technique. First considering the case when the inputs are continuous and then with quantized inputs.

A.3.1 Continuous Inputs

We begin by introducing the change of coordinates

$$z_1 = x_1 - x_{r1}, \tag{A.9}$$
$$z_2 = x_2 - x_{r2}, \tag{A.10}$$
$$z_3 = x_3 - \alpha_1 - \dot{x}_{r1}, \tag{A.11}$$
$$z_4 = x_4 - \alpha_2 - \dot{x}_{r2}. \tag{A.12}$$

where α_1 and α_2 are the virtual controllers. The design follows the backstepping procedure in [15].

• *Step* 1: The virtual controllers are chosen as

$$\alpha_1 = -c_1 z_1, \tag{A.13}$$
$$\alpha_2 = -c_2 z_2, \tag{A.14}$$

where c_1 and c_2 are positive constants. A control Lyapunov function is chosen as

$$V_1(\boldsymbol{z}, t) = \frac{1}{2} z_1^2 + \frac{1}{2} z_2^2. \tag{A.15}$$

The derivative of V_1 along the solutions of the system is

$$\begin{aligned} \dot{V}_1 &= z_1 \dot{z}_1 + z_2 \dot{z}_2 \\ &= z_1(z_3 + \alpha_1) + z_2(z_4 + \alpha_2) \\ &= -c_1 z_1^2 + z_1 z_3 - c_2 z_2^2 + z_2 z_4. \end{aligned} \tag{A.16}$$

If z_3 and z_4 are zero, then $\dot{V}_1$ is negative and z_1 and z_2 will converge exponentially towards zero.

• *Step* 2: The derivative of z_3 and z_4 are expressed as

$$\dot{z}_3 = \beta_{1,1} u_1 + \beta_{1,2} u_2 + \boldsymbol{\phi}_1^\top \boldsymbol{\theta}_1 + c_1(x_3 - \dot{x}_{r1}) - \ddot{x}_{r1}, \tag{A.17}$$
$$\dot{z}_4 = -\beta_{2,1} u_1 + \beta_{2,2} u_2 + \boldsymbol{\phi}_2^\top \boldsymbol{\theta}_2 + c_2(x_4 - \dot{x}_{r2}) - \ddot{x}_{r2}. \tag{A.18}$$

The control inputs u_1 and u_2 will now be designed so that z_1, z_2, z_3 and z_4 all converge towards zero.
The adaptive control law is designed as follows:

$$\boldsymbol{u} = \begin{bmatrix} u_1 \\ u_2 \end{bmatrix} = \hat{\boldsymbol{B}}^{-1}\bar{\boldsymbol{u}} = \hat{\boldsymbol{R}}\bar{\boldsymbol{u}}, \tag{A.19}$$

where

$$\bar{\boldsymbol{u}} = \begin{bmatrix} \bar{u}_1 \\ \bar{u}_2 \end{bmatrix}, \quad \hat{\boldsymbol{B}} = \begin{bmatrix} \hat{\boldsymbol{\beta}}_1 \\ \hat{\boldsymbol{\beta}}_2 \end{bmatrix}, \tag{A.20}$$

$$\bar{u}_1 = -z_1 - \boldsymbol{\phi}_1^\top \hat{\boldsymbol{\theta}}_1 - c_3 z_3 - c_1(x_3 - \dot{x}_{r1}) + \ddot{x}_{r1}, \tag{A.21}$$

$$\bar{u}_2 = -z_2 - \boldsymbol{\phi}_2^\top \hat{\boldsymbol{\theta}}_2 - c_4 z_4 - c_2\,(x_4 - \dot{x}_{r2}) + \ddot{x}_{r2}, \tag{A.22}$$

$$\hat{\boldsymbol{\beta}}_1 = \begin{bmatrix} \hat{\beta}_{1,1} & \hat{\beta}_{1,2} \end{bmatrix}, \quad \hat{\boldsymbol{\beta}}_2 = \begin{bmatrix} -\hat{\beta}_{2,1} & \hat{\beta}_{2,2} \end{bmatrix}, \tag{A.23}$$

c_3 and c_4 are positive constants, $\hat{\boldsymbol{\theta}}_1$, $\hat{\boldsymbol{\theta}}_2$, $\hat{\beta}_{i,j}$ are the estimates of $\boldsymbol{\theta}_1$, $\boldsymbol{\theta}_2$, $\beta_{i,j}$ and $\hat{\boldsymbol{R}}$ is the inverse of the matrix $\hat{\boldsymbol{B}}$.
The parameter updating laws are chosen as

$$\dot{\hat{\boldsymbol{\theta}}}_1 = \mathrm{Proj}\{\boldsymbol{\Gamma}_1 \boldsymbol{\phi}_1 z_3\}, \tag{A.24}$$

$$\dot{\hat{\boldsymbol{\theta}}}_2 = \mathrm{Proj}\{\boldsymbol{\Gamma}_2 \boldsymbol{\phi}_2 z_4\}, \tag{A.25}$$

$$\dot{\hat{\boldsymbol{\beta}}}_1^\top = \mathrm{Proj}\{\boldsymbol{\Gamma}_3 \boldsymbol{u} z_3\}, \tag{A.26}$$

$$\dot{\hat{\boldsymbol{\beta}}}_2^\top = \mathrm{Proj}\{\boldsymbol{\Gamma}_4 \boldsymbol{u} z_4\}, \tag{A.27}$$

where $\boldsymbol{\Gamma}_k$, $k \in \{1, 2, 3, 4\}$, are positive definite adaptation gain matrices and $\mathrm{Proj}\{\cdot\}$ is the projection operator given in [15] which ensures that the estimates and estimation errors are nonzero and within known bounds. Let $\tilde{\boldsymbol{\theta}}_i = \boldsymbol{\theta}_i - \hat{\boldsymbol{\theta}}_i$ and $\tilde{\boldsymbol{\beta}}_i = \boldsymbol{\beta}_i - \hat{\boldsymbol{\beta}}_i$, $i = 1, 2$, be the parameter estimation errors.
The projection operator $\dot{\hat{\boldsymbol{\theta}}} = \mathrm{Proj}\{\boldsymbol{\tau}\}$ has the following property

$$-\tilde{\boldsymbol{\theta}}^\top \boldsymbol{\Gamma}^{-1} \mathrm{Proj}\{\boldsymbol{\tau}\} \leq -\tilde{\boldsymbol{\theta}}^\top \boldsymbol{\Gamma}^{-1} \boldsymbol{\tau}. \tag{A.28}$$

By using (A.19), we have

$$\boldsymbol{B}\boldsymbol{u} = \boldsymbol{B}\hat{\boldsymbol{R}}\bar{\boldsymbol{u}} = \bar{\boldsymbol{u}} + \tilde{\boldsymbol{B}}\hat{\boldsymbol{R}}\bar{\boldsymbol{u}} = \bar{\boldsymbol{u}} + \tilde{\boldsymbol{B}}\boldsymbol{u}, \tag{A.29}$$

where $\tilde{\boldsymbol{B}} = \boldsymbol{B} - \hat{\boldsymbol{B}}$. The determinant of $\boldsymbol{B}$ matrix will always be positive with the known signs of the parameters and from Assumption 2, where $\det(\boldsymbol{B}) = \beta_{1,1}\beta_{2,2} + \beta_{2,1}\beta_{1,2}$, and from this and also with the projection operator, the matrix $\hat{\boldsymbol{R}}$ does not

have any singularities and is defined for all estimated parameters, given that the initial values are chosen positive. Now the terms $\beta_{1,1}u_1 + \beta_{1,2}u_2$ and $-\beta_{2,1}u_1 + \beta_{2,2}u_2$ in (A.17) and (A.18) can be expressed as

$$\boldsymbol{\beta}_1\boldsymbol{u} = \bar{u}_1 + \tilde{\boldsymbol{\beta}}_1\boldsymbol{u}, \tag{A.30}$$

$$\boldsymbol{\beta}_2\boldsymbol{u} = \bar{u}_2 + \tilde{\boldsymbol{\beta}}_2\boldsymbol{u}. \tag{A.31}$$

We define the final Lyapunov function as

$$\begin{aligned} V_2(\boldsymbol{z}, \tilde{\boldsymbol{\beta}}, \tilde{\boldsymbol{\theta}}, t) =& V_1 + \frac{1}{2}z_3^2 + \frac{1}{2}z_4^2 + \frac{1}{2}\tilde{\boldsymbol{\theta}}_1^\top \boldsymbol{\Gamma}_1^{-1}\tilde{\boldsymbol{\theta}}_1 + \frac{1}{2}\tilde{\boldsymbol{\theta}}_2^\top \boldsymbol{\Gamma}_2^{-1}\tilde{\boldsymbol{\theta}}_2 + \frac{1}{2}\tilde{\boldsymbol{\beta}}_1\boldsymbol{\Gamma}_3^{-1}\tilde{\boldsymbol{\beta}}_1^\top \\ &+ \frac{1}{2}\tilde{\boldsymbol{\beta}}_2\boldsymbol{\Gamma}_4^{-1}\tilde{\boldsymbol{\beta}}_2^\top. \end{aligned} \tag{A.32}$$

The derivative of (A.32) along with (A.17) to (A.31) gives

$$\begin{aligned} \dot{V}_2 =& -c_1z_1^2 - c_2z_2^2 - c_3z_3^2 - c_4z_4^2 + \boldsymbol{\phi}_1^\top\tilde{\boldsymbol{\theta}}_1z_3 + \boldsymbol{\phi}_2^\top\tilde{\boldsymbol{\theta}}_2z_4 - \tilde{\boldsymbol{\theta}}_1^\top\boldsymbol{\Gamma}_1^{-1}\dot{\hat{\boldsymbol{\theta}}}_1 \\ &- \tilde{\boldsymbol{\theta}}_2^\top\boldsymbol{\Gamma}_2^{-1}\dot{\hat{\boldsymbol{\theta}}}_2 + \tilde{\boldsymbol{\beta}}_1\boldsymbol{u}z_3 + \tilde{\boldsymbol{\beta}}_2\boldsymbol{u}z_4 - \tilde{\boldsymbol{\beta}}_1\boldsymbol{\Gamma}_3^{-1}\dot{\hat{\boldsymbol{\beta}}}_1^\top - \tilde{\boldsymbol{\beta}}_2\boldsymbol{\Gamma}_4^{-1}\dot{\hat{\boldsymbol{\beta}}}_2^\top \\ =& -c_1z_1^2 - c_2z_2^2 - c_3z_3^2 - c_4z_4^2 \\ &- \tilde{\boldsymbol{\theta}}_1^\top\boldsymbol{\Gamma}_1^{-1}\left(\dot{\hat{\boldsymbol{\theta}}}_1 - \boldsymbol{\Gamma}_1\boldsymbol{\phi}_1z_3\right) - \tilde{\boldsymbol{\beta}}_1\boldsymbol{\Gamma}_3^{-1}\left(\dot{\hat{\boldsymbol{\beta}}}_1^\top - \boldsymbol{\Gamma}_3\boldsymbol{u}z_3\right) \\ &- \tilde{\boldsymbol{\theta}}_2^\top\boldsymbol{\Gamma}_2^{-1}\left(\dot{\hat{\boldsymbol{\theta}}}_2 - \boldsymbol{\Gamma}_2\boldsymbol{\phi}_2z_4\right) - \tilde{\boldsymbol{\beta}}_2\boldsymbol{\Gamma}_4^{-1}\left(\dot{\hat{\boldsymbol{\beta}}}_2^\top - \boldsymbol{\Gamma}_4\boldsymbol{u}z_4\right). \end{aligned} \tag{A.33}$$

The property of the projection operator in (A.28) and the update laws (A.24)-(A.27) eliminate the last four terms in equation (A.33). Then

$$\dot{V}_2 \leq -c_1z_1^2 - c_2z_2^2 - c_3z_3^2 - c_4z_4^2. \tag{A.34}$$

We then have the following stability and performance results based on the control scheme.

Theorem 1. *Considering the closed-loop adaptive system consisting of the plant* (A.3)*, the adaptive controller* (A.19)*, the virtual control laws* (A.13) *and* (A.14)*, the parameter updating laws* (A.24)-(A.27) *and Assumptions 1 and 2. All signals in the closed loop system are ensured to be uniformly bounded. Furthermore, asymptotic tracking is achieved, i.e.*

$$\lim_{t\to\infty} = [x_i(t) - x_{ri}(t)] = 0, \qquad i = 1, 2. \tag{A.35}$$

Proof: The stability properties of the equilibrium follow from (A.32) and (A.34). By

applying the LaSalle-Yoshizawa theorem, V_2 is uniformly bounded. This implies that z_1, z_2, z_3, z_4 are bounded and are asymptotically stable and z_1, z_2, z_3, $z_4 \to 0$ as $t \to \infty$ and also $\hat{\boldsymbol{\theta}}_1$, $\hat{\boldsymbol{\theta}}_2$, $\hat{\boldsymbol{\beta}}_1$ and $\hat{\boldsymbol{\beta}}_2$ are bounded. Since $z_1 = x_1 - x_{r1}$ and $z_2 = x_2 - x_{r2}$, tracking of the reference signals is also achieved, and x_1 and x_2 are also bounded since z_1 and z_2 are bounded and since x_{r1} and x_{r2} are bounded by definition, cf. Assumption 1. The virtual controls α_1 and α_2 are also bounded from (A.13) and (A.14) and then x_3 and x_4 are also bounded. From (A.19) it follows that the control inputs also are bounded.

Remark 1. *Theorem 1 implies that the error signals will converge to zero. For a real system like the helicopter model, there are disturbances due to e.g. noise from sensors and unmodeled dynamics that are not included in this model, and so the helicopter will have a practical stabilization with the adaptive controller, where the solution is ultimately bounded by a constant μ_0, that is $\|\boldsymbol{z}\| \leq \mu_0, \quad \forall t \geq T$, for some $T > 0$ [17].*

A.3.2 Quantized Inputs

Considering the nonlinear state space model with quantized inputs expressed as

$$\dot{\boldsymbol{x}} = \begin{bmatrix} x_3 \\ x_4 \\ \boldsymbol{\phi}_1^\top \boldsymbol{\theta}_1 \\ \boldsymbol{\phi}_2^\top \boldsymbol{\theta}_2 \end{bmatrix} + \begin{bmatrix} 0 \\ 0 \\ \beta_{1,1} q(u_1) + \beta_{1,2} q(u_2) \\ -\beta_{2,1} q(u_1) + \beta_{2,2} q(u_2) \end{bmatrix}, \tag{A.36}$$

where the control inputs u_1 and u_2 are quantized by the uniform quantizer defined in (A.8). The change of coordinates and step 1 will be the same as when the inputs are continuous and the virtual control laws are designed as in (A.13) and (A.14). In step 2 the control inputs appear, and the derivative of z_3 and z_4 are expressed as

$$\dot{z}_3 = \beta_{1,1} q(u_1) + \beta_{1,2} q(u_2) + \boldsymbol{\phi}_1^\top \boldsymbol{\theta}_1 + c_1(x_3 - \dot{x}_{r1}) - \ddot{x}_{r1}, \tag{A.37}$$

$$\dot{z}_4 = -\beta_{2,1} q(u_1) + \beta_{2,2} q(u_2) + \boldsymbol{\phi}_2^\top \boldsymbol{\theta}_2 + c_2(x_4 - \dot{x}_{r2}) - \ddot{x}_{r2}. \tag{A.38}$$

The quantizer inputs are decomposed into two parts

$$q(u_k) = u_k(t) + d_k(t), \tag{A.39}$$

where d_k is the quantization error and bounded by a constant, $|d_k| \leq \delta_k$, where

$$\delta_k = \max\{u_{k,0} + l_k/2, l_k/2\}. \tag{A.40}$$

Thus the equations (A.37) and (A.38) are expressed as

$$\dot{z}_3 = \beta_{1,1}(u_1 + d_1) + \beta_{1,2}(u_2 + d_2) + \boldsymbol{\phi}_1^\top \boldsymbol{\theta}_1 + c_1(x_3 - \dot{x}_{r1}) - \ddot{x}_{r1}, \tag{A.41}$$

$$\dot{z}_4 = -\beta_{2,1}(u_1 + d_1) + \beta_{2,2}(u_2 + d_2) + \boldsymbol{\phi}_2^\top \boldsymbol{\theta}_2 + c_2(x_4 - \dot{x}_{r2}) - \ddot{x}_{r2}, \tag{A.42}$$

where due to quantization, two extra terms are included in each equation. The inputs are designed in the controller (A.19) together with (A.21)-(A.23) and with the parameter updating laws (A.24)-(A.27). The final Lyapunov function V_2 is defined as in (A.32), the same as without quantization. Then the derivative of V_2 gives

$$\begin{aligned}\dot{V}_2 = &- c_1 z_1^2 - c_2 z_2^2 - c_3 z_3^2 - c_4 z_4^2 + \boldsymbol{\beta_1 d} z_3 + \boldsymbol{\beta_2 d} z_4 - \tilde{\boldsymbol{\theta}}_1^\top \boldsymbol{\Gamma}_1^{-1} \left(\dot{\hat{\boldsymbol{\theta}}}_1 - \boldsymbol{\Gamma}_1 \boldsymbol{\phi}_1 z_3 \right) \\ &- \tilde{\boldsymbol{\beta}}_1 \boldsymbol{\Gamma}_3^{-1} \left(\dot{\hat{\boldsymbol{\beta}}}_1^\top - \boldsymbol{\Gamma}_3 \boldsymbol{u} z_3 \right) - \tilde{\boldsymbol{\theta}}_2^\top \boldsymbol{\Gamma}_2^{-1} \left(\dot{\hat{\boldsymbol{\theta}}}_2 - \boldsymbol{\Gamma}_2 \boldsymbol{\phi}_2 z_4 \right) - \tilde{\boldsymbol{\beta}}_2 \boldsymbol{\Gamma}_4^{-1} \left(\dot{\hat{\boldsymbol{\beta}}}_2^\top - \boldsymbol{\Gamma}_4 \boldsymbol{u} z_4 \right),\end{aligned} \tag{A.43}$$

where $\boldsymbol{d} = [d_1 \;\; d_2]^\top$, and where the property of the projection operator in (A.28) and the update laws (A.24)-(A.27) eliminate the last four terms in equation (A.43). Then

$$\begin{aligned}\dot{V}_2 &\leq - c_1 z_1^2 - c_2 z_2^2 - c_3 z_3^2 - c_4 z_4^2 + \boldsymbol{\beta}_1 \boldsymbol{d} z_3 + \boldsymbol{\beta}_2 \boldsymbol{d} z_4 \\ &\leq - c_0 \|\boldsymbol{z}\|^2 + \sqrt{(|\boldsymbol{\beta}_1|\boldsymbol{\delta})^2 + (|\boldsymbol{\beta}_2|\boldsymbol{\delta})^2} \|\boldsymbol{z}\| \\ &\leq - (1-\lambda) c_0 \|\boldsymbol{z}\|^2 - \lambda c_0 \|\boldsymbol{z}\|^2 + \sqrt{(|\boldsymbol{\beta}_1|\boldsymbol{\delta})^2 + (|\boldsymbol{\beta}_2|\boldsymbol{\delta})^2} \|\boldsymbol{z}\| \\ &\leq - (1-\lambda) c_0 \|\boldsymbol{z}\|^2, \quad \forall \|\boldsymbol{z}\| \geq \frac{\sqrt{(|\boldsymbol{\beta}_1|\boldsymbol{\delta})^2 + (|\boldsymbol{\beta}_2|\boldsymbol{\delta})^2}}{\lambda c_0},\end{aligned} \tag{A.44}$$

where $c_0 = \min\{c_1, c_2, c_3, c_4\}$, the constant $\boldsymbol{\delta} = [\delta_1 \;\; \delta_2]^\top$ is the maximum quantization errors as defined in (A.40) and $0 < \lambda < 1$. We then have the following stability and performance results based on the control scheme.

Theorem 2. *Considering the closed-loop adaptive system consisting of the plant* (A.36)*, the adaptive controller* (A.19)*, the virtual control laws* (A.13) *and* (A.14)*, the parameter updating laws* (A.24)-(A.27)*, the uniform quantizer* (A.8) *and Assumptions 1 and 2. All signals in the closed loop system are ensured to be uniformly bounded. The tracking error signals will converge to a compact set, i.e.*

$$\|\boldsymbol{z}\| \leq \mu = \frac{\sqrt{(|\boldsymbol{\beta}_1|\boldsymbol{\delta})^2 + (|\boldsymbol{\beta}_2|\boldsymbol{\delta})^2}}{\lambda c_0}, \tag{A.45}$$

where μ is a positive constant. The tracking errors $z_i(t) = x_i(t) - x_{ri}(t), i \in \{1, 2\}$, are ultimately bounded by $\|z_i\| \leq \mu$, and tracking is achieved.

Proof: The stability properties of the equilibrium follows from (A.32) and (A.44). The quantization error is bounded by definition (A.40). By applying the LaSalle-Yoshizawa theorem, V_2 is bounded. This implies that z_1, z_2, z_3, z_4, $\hat{\boldsymbol{\theta}}_1$, $\hat{\boldsymbol{\theta}}_2$, $\hat{\boldsymbol{\beta}}_1$ and $\hat{\boldsymbol{\beta}}_2$ are bounded. Furthermore, z_1, z_2, z_3 and z_4, will converge to a compact set containing the equilibrium as $t \to \infty$. Since $z_1 = x_1 - x_{r1}$ and $z_2 = x_2 - x_{r2}$, the states x_1 and x_2 are also bounded since z_1 and z_2 are bounded and since x_{r1} and x_{r2} are bounded by definition, cf. Assumption 1. Tracking of the reference signals is achieved, with a bounded tracking error. The virtual controls α_1 and α_2 are also bounded from (A.13) and (A.14) and then x_3 and x_4 are also bounded. From (A.19) it follows that the control inputs also are bounded.

Remark 2. *The tracking errors are adjustable by tuning the design parameters* $c_i,\ i \in \{1, 2, 3, 4\}$.

Remark 3. *The smaller quantization intervals* l_k*, the smaller the compact set for the error variables* $\|\boldsymbol{z}\|$ *will be, and if* l_k *decreases to zero and there is no quantization, the error will also be zero and the result will be similar to Theorem 1, without quantization.*

Remark 4. *The bound for the error system will also include the bound from Remark 1 for the helicopter model, only shifting the bound to* $\|\boldsymbol{z}\| \leq \mu_0 + \mu, \quad \forall t \geq T$*, for some* $T > 0$.

A.4 Experimental Results

The Quanser Aero helicopter system shown in Figure A.4 is a two-rotor laboratory equipment for flight control-based experiments. The setup is a horizontal position of the main thruster and a vertical position of the tail thruster, which resembles a helicopter with two propellers driven by two DC motors. The proposed controller was simulated using MATLAB/Simulink and tested on the Quanser Aero helicopter system. The initial states were set as $\boldsymbol{x}(0) = 0$ and the design parameters were set as $c_1 = c_2 = 6$, $c_3 = c_4 = 3$, $\boldsymbol{\Gamma}_1 = \boldsymbol{I}_3$, $\boldsymbol{\Gamma}_2 = \boldsymbol{I}_2$ and $\boldsymbol{\Gamma}_3 = \boldsymbol{\Gamma}_4 = 0.01\boldsymbol{I}_2$. The same quantization intervals were used for the two inputs, since the two motors on the helicopter model are equal and where the range of the inputs are similar and in the range of $[-24, 24]$. The interval was chosen $l_1 = l_2 = 1$, and is a quantization level chosen high to show the effect of the quantization, since there are other disturbances that will affect the results as e.g. noise from sensors. The constant $u_{k,0}$ was chosen equal zero for both inputs, and so the upper bound for the quantization errors were $\delta_1 = \delta_2 = l_k/2 = 1/2$. The initial values for the parameters were chosen as

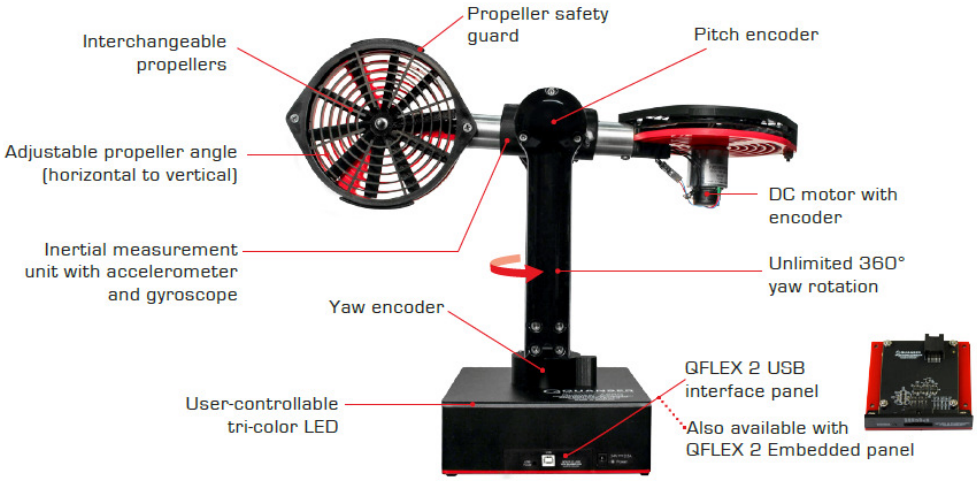

Figure A.4: Quanser Aero, helicopter model

$\hat{\boldsymbol{\beta}}_1(0) = [0.0506 \;\; 0.0506]$, $\hat{\boldsymbol{\beta}}_2(0) = [-0.0645 \;\; 0.0810]$, $\hat{\boldsymbol{\theta}}_1(0) = [0.322 \;\; 1.8436 \;\; 0.0007]^\top$ and $\hat{\boldsymbol{\theta}}_2(0) = [0.4374 \;\; 0.0014]^\top$ based on estimates for the values in [18].

The objective in this test was to track a sinusoidal signal, where a sine wave with amplitude of 40 degrees and frequency of 0.05 Hz was applied to pitch, while there should be no rotation about yaw, and see how the system was affected by quantization of inputs.

A.4.1 Results without Quantization

The results from simulation and testing on the helicopter with continuous inputs are shown in Figures A.5-A.6, where red plots are from simulation and blue plots are from the real system. While the simulations in Figure A.5 show that the tracking errors converge to zero, we see that for the helicopter, the tracking errors converge to bounded errors close to zero. This is due to the unknown disturbances affecting the system as in Remark 1. Tracking of the reference signal is achieved, for both pitch and yaw angle. The inputs are also plotted in Figure A.5.

In Figure A.6, the norm of $\boldsymbol{z}$ is plotted. The simulation shows that $\|\boldsymbol{z}\| \to 0$ as $t \to \infty$, while this is not the case for the real system. From the plot for the helicopter system, we define $\mu_0 = \max\|\boldsymbol{z}\|$.

A.4.2 Results with Quantization

Now the inputs were quantized, with results plotted in Figures A.7-A.9. From Figure A.7, we can see that the desired trajectory for a sine wave in pitch can be followed using the proposed adaptive controller both in simulation and testing on the helicopter system. From the simulation, there is an error for both angles due

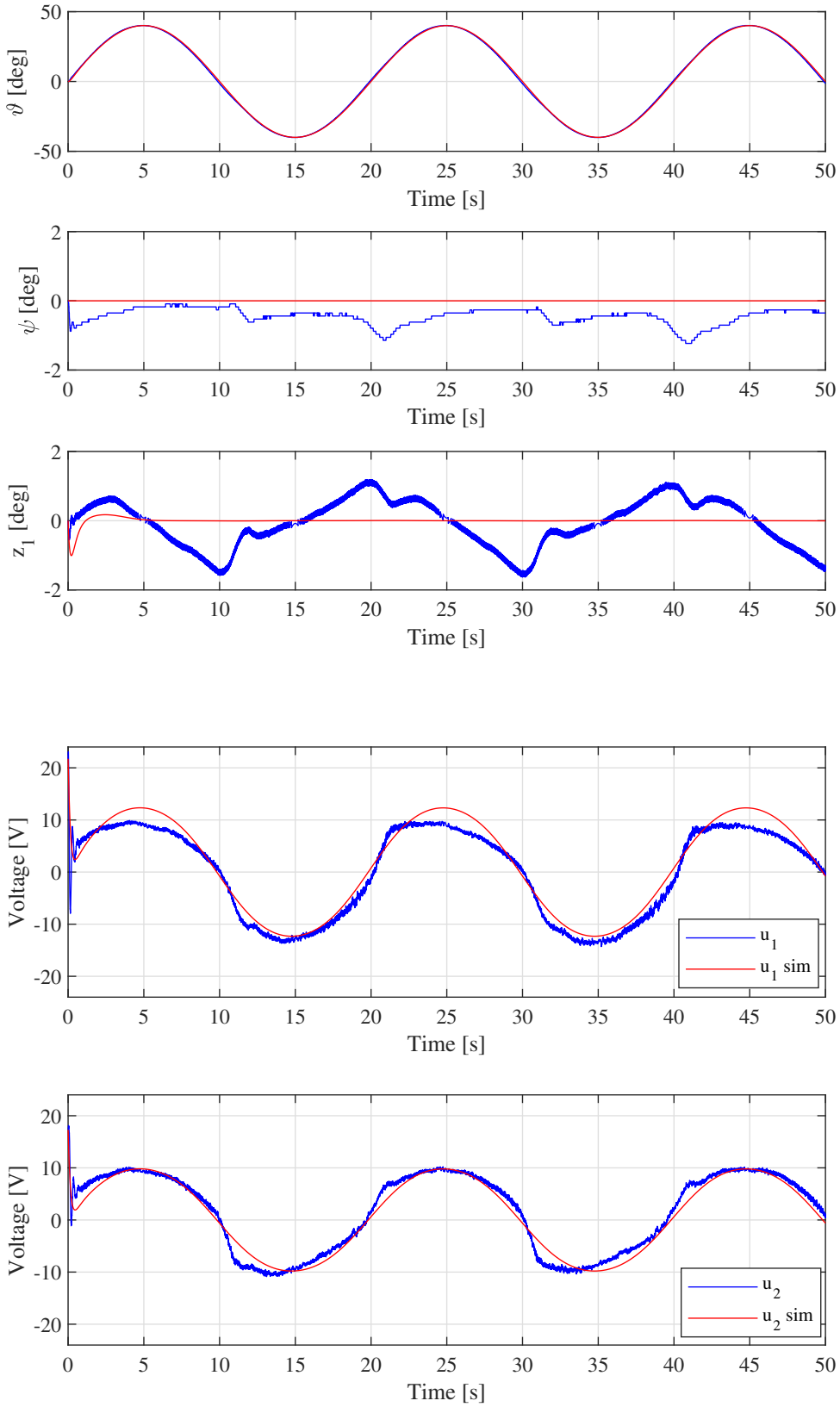

Figure A.5: Results without quantization. 1) Pitch angle. 2) Yaw angle. 3) Pitch angle error. 4-5) Inputs.

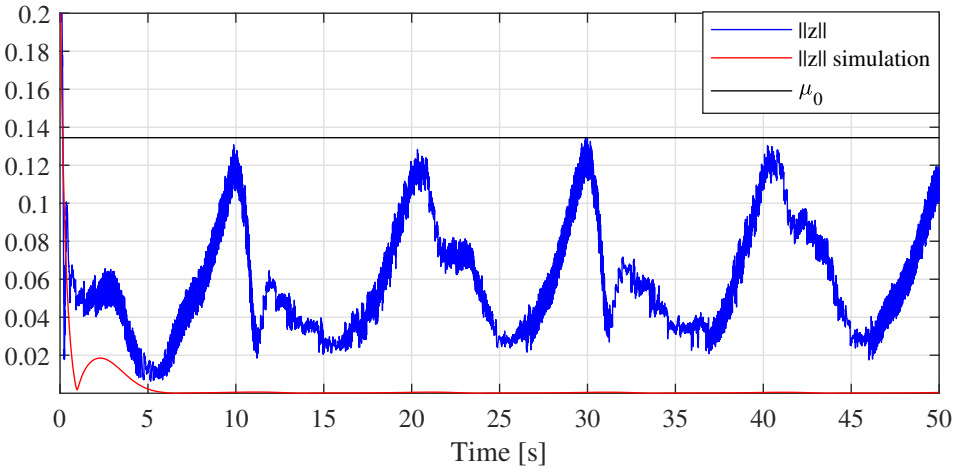

Figure A.6: Norm of z without quantization.

to quantization compared to simulation without quantization in Figure A.5. In Figure A.8, the norm of the error state $\boldsymbol{z}$ from the simulation is plotted and also the bound μ from Theorem 2, computed with $\lambda = 0.999$, and assuming $\boldsymbol{\beta}_1 = \hat{\boldsymbol{\beta}}_1(0)$ and $\boldsymbol{\beta}_2 = \hat{\boldsymbol{\beta}}_2(0)$. In the transient period, the norm enters the bound, but leaves it for a short period, and this is possible due to the LaSalle-Yoshizawa theorem. After this it remains within the bound μ. Looking at the plotted norm for the helicopter in Figure A.9, where μ_0 is the bound found without quantization due to unknown disturbances and $\mu_0 + \mu$ also includes the bound for quantization, we see that $\|\boldsymbol{z}\|$ is within the bound for the whole time period.

A.4.3 Comparing Results

To compare the results with and without quantization, the total tracking error, z_{track}, and the total voltage used, u_{total}, was measured, where

$$z_{track} = \sum_{i=1}^{2} \int_0^t z_i(\tau)^2 d\tau, \tag{A.46}$$

$$u_{total} = \sum_{i=1}^{2} \int_0^t u_i(\tau)^2 d\tau, \tag{A.47}$$

with $t = 50\ s$. There is a trade-off between the error and voltage consumption since the more accurate the controller is, the more voltage is needed to hold the trajectory closer to the reference.

In Table A.1, the results are compared for different quantization intervals. The tracking error is higher when the inputs are quantized, while the total voltage use is lower for most of the tests with quantization. The higher error is due to the quantization error, as expected from Theorems 1 and 2.

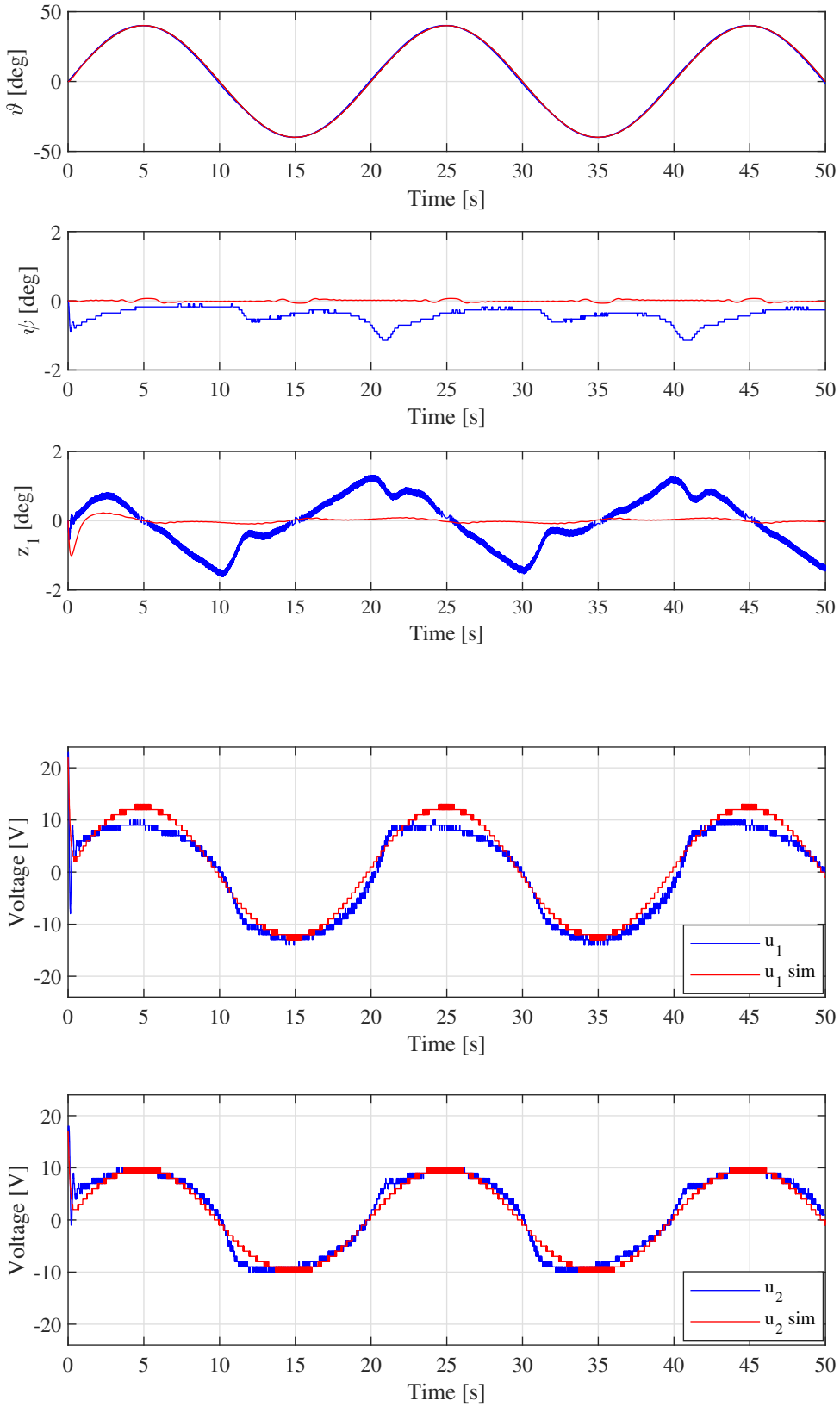

Figure A.7: Results with quantization. 1) Pitch angle. 2) Yaw angle. 3) Pitch angle error. 4-5) Inputs.

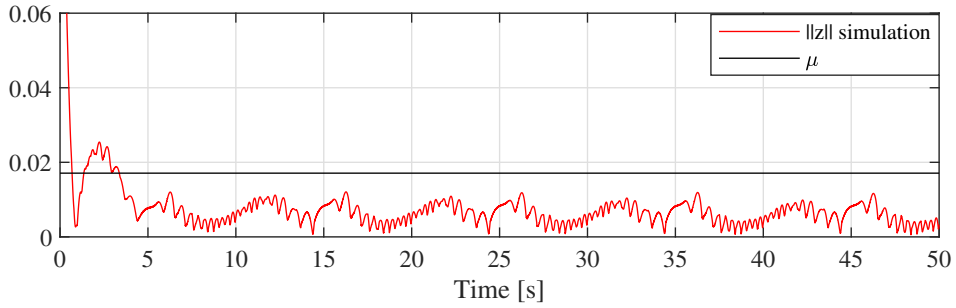

Figure A.8: Simulation of norm of z with quantization and the bound μ.

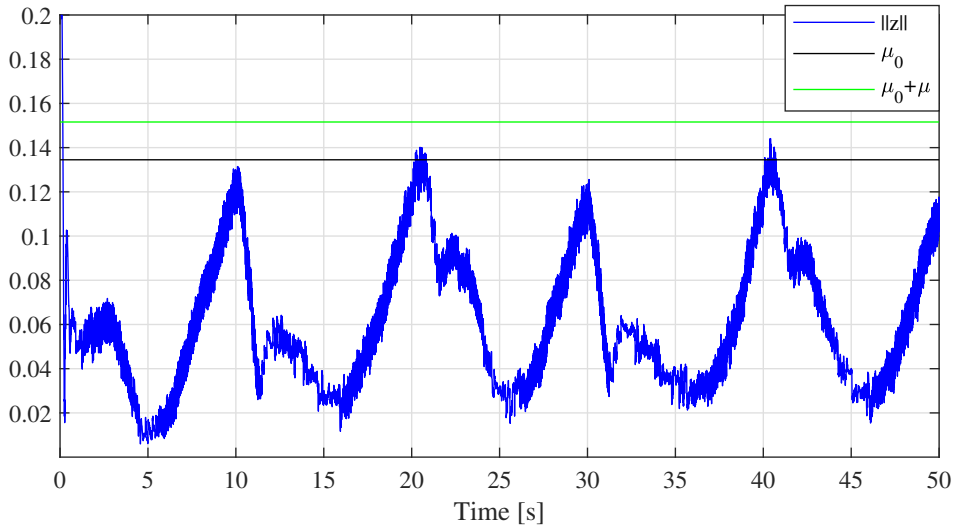

Figure A.9: Norm of z with quantization from the helicopter, with bounds.

Table A.1: Comparison of error and voltage use with and without quantization

Measurement	**Quantization**				
	$l_k = 0$	$l_k = 0.1$	$l_k = 0.5$	$l_k = 1$	$l_k = 1.5$
z_{track}	0.0110	0.0116	0.0114	0.0116	0.0121
u_{total}	6429	6444	6365	6367	6328

A.5 Conclusion

In this paper, an adaptive backstepping control scheme is considered for a MIMO nonlinear helicopter model with input quantization. The system parameters are not required to be fully known for the controller design. A theoretical proof of stability is given with the use of constructed Lyapunov functions, where boundedness of all signals in the closed loop system are achieved and also tracking of a given reference signal. The tracking error signals will converge to a compact set. Experiments and simulations validates the proof, where tracking is achieved and the total tracking error signals are some higher when the inputs are quantized compared to when inputs are not quantized.

References – Paper A

[1] X. Ge, F. Yang, and Q.-L. Han, "Distributed networked control systems: A brief overview," *Information Sciences*, vol. 380, pp. 117–131, 2017.

[2] X.-M. Zhang, Q.-L. Han, X. Ge, D. Ding, L. Ding, D. Yue, and C. Peng, "Networked control systems: A survey of trends and techniques," *IEEE/CAA Journal of Automatica Sinica*, vol. 7, no. 1, pp. 1–17, 2020.

[3] D. Zhang, P. Shi, Q.-G. Wang, and L. Yu, "Analysis and synthesis of networked control systems: A survey of recent advances and challenges," *ISA Transactions 66*, pp. 376–392, 2017.

[4] Z. P. Jiang and T. F. Liu, "Quantized nonlinear control - a survey," *Acta Automatica Sinica*, vol. 39, no. 11, pp. 1820–1830, Nov. 2013.

[5] N. Elia and S. K. Mitter, "Stabilization of linear systems with limited information," *IEEE Transactions on Automatic Control*, vol. 46, no. 9, pp. 1384–1400, 2001.

[6] S. Tatikonda and S. Mitter, "Control under communication constraints," *IEEE Transactions on Automatic Control*, vol. 49, no. 7, pp. 1056–1068, 2004.

[7] M. Fu and L. Xie, "The sector bound approach to quantized feedback control," *IEEE Transactions on Automatic Control*, vol. 50, no. 11, pp. 1698–1711, 2005.

[8] C. D. Persis, "Robust stabilization of nonlinear systems by quantized and ternary control," *Systems & Control Letters*, vol. 58, no. 8, pp. 602–608, 2009.

[9] J. Zhou, C. Wen, and W. Wang, "Adaptive control of uncertain nonlinear systems with quantized input signal," *Automatica*, vol. 95, pp. 152–162, 2018.

[10] J. Zhou and W. Wang, "Adaptive control of quantized uncertain nonlinear systems," *IFAC PapersOnLine*, vol. 50, no. 1, pp. 10 425–10 430, 2017.

[11] J. Zhou, C. Wen, W. Wang, and F. Yang, "Adaptive backstepping control of nonlinear uncertain systems with quantized states," *IEEE Transactions on Automatic Control*, vol. 64, no. 11, pp. 4756–4763, 2019.

[12] J. Zhou and C. Wen, "Adaptive backstepping control of uncertain nonlinear systems with input quantization," in *IEEE Conference on Decision and Control*, Dec. 2013, pp. 5571–5576.

[13] J. Zhou, "Decentralized adaptive control for interconnected nonlinear systems with input quantization," *IFAC PapersOnLine*, vol. 50, no. 1, pp. 10 419–10 424, 2017.

[14] H. Sun, N. Hovakimyan, and T. Basar, "$\mathcal{L}_1$ adaptive controller for uncertain nonlinear multi-input multi-output systems with input quantization," *IEEE Transactions on Automatic Control*, vol. 57, no. 3, pp. 565–578, 2012.

[15] M. Krstić, I. Kanellakopoulos, and P. Kokotović, *Nonlinear and Adaptive Control Design*. John Wiley & Sons, Inc., 1995.

[16] S. M. Schlanbusch and J. Zhou, "Adaptive backstepping control of a 2-dof helicopter," in *Proceedings of the IEEE 7th International Conference on Control, Mechatronics and Automation*, 2019, pp. 210–215.

[17] H. K. Khalil, *Nonlinear Control*. Pearson, 2015.

[18] S. M. Schlanbusch, "Adaptive backstepping control of quanser 2dof helicopter - theory and experiments," Master's thesis, University of Agder, 2019.

Paper B

Adaptive Backstepping Attitude Control of a Rigid Body with State Quantization

Siri Marte Schlanbusch, Jing Zhou and Rune Schlanbusch

This paper has been published as:

S. M. Schlanbusch, J. Zhou and R. Schlanbusch, "Adaptive backstepping attitude control of a rigid body with state quantization," in *Proceedings of 60th IEEE Conference on Decision and Control*, 2021, pp. 372–377, doi: 10.1109/CDC45484.2021.9683579.

Adaptive Backstepping Attitude Control of a Rigid Body with State Quantization

Siri Marte Schlanbusch[1], Jing Zhou[1] and Rune Schlanbusch[2]

[1]Department of Engineering Sciences
University of Agder
4879 Grimstad, Norway

[2]Norwegian Research Centre AS
4879 Grimstad, Norway

Abstract

In this paper, the attitude tracking control problem of a rigid body is investigated where the states are quantized. An adaptive backstepping based control scheme is developed and a new approach to stability analysis is developed by constructing a new compensation scheme for the effects of the vector state quantization. It is shown that all closed-loop signals are ensured uniformly bounded and the tracking errors converge to a compact set containing the origin. Experiments on a 2 degrees-of-freedom helicopter system illustrate the proposed control scheme.

B.1 Introduction

The interest for quantized control has attracted considerable attention in recent years due to its theoretical and practical importance in practical engineering, where signals are required to be quantized and transmitted via a common communication network. An important aspect is to use quantization schemes that yield sufficient precision, but reduce the communication burden over the network.

A great number of representative results have been reported on analysis and control of feedback systems with input quantization, as can be observed in [1–7]. The feedback control problem of systems with state quantization has been studied in [8–11], where the system dynamics in these works are precisely known. As we know, system uncertainties and non-linearity inevitably exist in physical systems. Only a few work using an adaptive approach have been reported to solve the state quantization problem for uncertain linear systems in [12] and uncertain nonlinear systems in [13].

Quantized control of rigid bodies is a potential problem. For example, the remote

control of a group of UAVs or robots, where the signals are transmitted over a shared network with limited communication information. Attitude stabilization with input quantization was investigated in [14] using a fixed-time sliding mode control. Trajectory tracking control for autonomous underwater vehicles with the effect of quantization was investigated in [15] using a sliding mode controller, where the considered systems are completely known. In [16], adaptive tracking control was proposed for underactuated autonomous underwater vehicles with input quantization. Uncertainties and non-linearities always exist in many practical systems. Thus it is more reasonable to consider controller design for uncertain nonlinear systems.

Adaptive backstepping technique was proposed in the 1990's in [17] to deal with plant non-linearity and parameter uncertainties. Several results have been reported on adaptive backstepping control with input quantization, e.g in [6, 7, 18, 19] for uncertain nonlinear systems, in [20] for a 2-DOF helicopter system, in [16] for tracking control for under-actuated autonomous underwater vehicles and in [21] for formation tracking control for a group of UAVs. However, adaptive backstepping control results to address uncertain systems with state quantization are very limited. One major difficulty to deal with the state quantization is that the backstepping technique requires differentiating virtual controls and in turn the states by applying chain rule. If the states are quantized, they become discontinuous and therefore it is difficult to analyze the resulting control system with the current backstepping based approaches. This problem was solved in [13] where the states were quantized by a static bounded quantizer.

This paper is concerned with the attitude tracking control of uncertain nonlinear rigid body systems with state quantization. A new backstepping based adaptive controller and a new approach to stability analysis are proposed. Compared to [13] for single-input-single-output (SISO) systems, this paper considers multiple-input-multiple-output (MIMO) uncertain systems with state quantization. A uniform quantization is included when tested on a 2 degrees-of-freedom (DOF) helicopter system from Quanser, with challenges in controller design due to the nonlinear behavior, the cross coupling effect between inputs and outputs, and with uncertainties both in the model and the parameters. It is analytically shown how the choice of quantization level affects the tracking performance, where a higher quantization level increases the tracking error. The experiments on the helicopter system illustrate the proposed scheme.

B.2 Dynamical Model and Problem Formulation

B.2.1 Notations

The symbol $\boldsymbol{\omega}_{b,a}^{c}$ denotes angular velocity of frame a relative to frame b, expressed in frame c; $\boldsymbol{R}_{a}^{b}$ is the rotation matrix from frame a to frame b; the cross product operator $\times$ between two vectors $\boldsymbol{a}$ and $\boldsymbol{b}$ is written as $\boldsymbol{S}(\boldsymbol{a})\boldsymbol{b}$ where $\boldsymbol{S}$ is skew-symmetric; $\lambda_{\max}(\cdot)$ and $\lambda_{\min}(\cdot)$ denotes the maximum and minimum eigenvalue of the matrix $(\cdot)$, and $\|\cdot\|$ denotes the $\mathcal{L}_2$-norm and induced $\mathcal{L}_2$-norm for vectors and matrices, respectively.

B.2.2 Attitude Dynamics

The orientation of a rigid body in frame b, relative to an inertial frame i, can be described by a unit quaternion, $\boldsymbol{q} = [\eta, \varepsilon_1, \varepsilon_2, \varepsilon_3]^\top = [\eta, \boldsymbol{\varepsilon}^\top]^\top \in \mathbb{S}^3 = \{x \in \mathbb{R}^4 : \boldsymbol{x}^\top \boldsymbol{x} = 1\}$ that is a complex number, where $\eta = \cos(\upsilon/2) \in \mathbb{R}$ is the real part and $\boldsymbol{\varepsilon} = \boldsymbol{k}\sin(\upsilon/2) \in \mathbb{R}^3$ is the imaginary part, where υ is the Euler angle and $\boldsymbol{k}$ is the Euler axis, and $\mathbb{S}^3$ is the non-Euclidean three-sphere. We consider a fully actuated rigid body with equations of motion for the attitude dynamics defined as

$$\dot{\boldsymbol{q}} = \boldsymbol{T}(\boldsymbol{q})\boldsymbol{\omega}, \tag{B.1}$$

$$\boldsymbol{J}\dot{\boldsymbol{\omega}} = \boldsymbol{\Psi}(\boldsymbol{q}, \boldsymbol{\omega}) + \boldsymbol{\Phi}(\boldsymbol{\omega})\boldsymbol{\theta} + \boldsymbol{B}\boldsymbol{u}, \tag{B.2}$$

with $\boldsymbol{\omega}_{i,b}^{b} = \boldsymbol{\omega} \in \mathbb{R}^3$, and where

$$\boldsymbol{T}(\boldsymbol{q}) = \frac{1}{2}\begin{bmatrix} -\boldsymbol{\varepsilon}^\top \\ \eta\boldsymbol{I} + \boldsymbol{S}(\boldsymbol{\varepsilon}) \end{bmatrix} \in \mathbb{R}^{4\times 3}, \tag{B.3}$$

$\boldsymbol{J} = \mathrm{diag}(J_x, J_y, J_z) \in \mathbb{R}^{3\times 3}$ is the inertia matrix about the origin o, and is positive definite,

$$\boldsymbol{\Psi} = -\boldsymbol{S}(\boldsymbol{\omega})(\boldsymbol{J}\boldsymbol{\omega}) - \boldsymbol{g}(\boldsymbol{q}) \ \in \mathbb{R}^3, \tag{B.4}$$

$$\boldsymbol{\Phi} = \mathrm{diag}(-\boldsymbol{\omega}) \ \in \mathbb{R}^{3\times 3}, \tag{B.5}$$

are known nonlinear functions of $\boldsymbol{q}$ and $\boldsymbol{\omega}$, the vector $\boldsymbol{\theta} \in \mathbb{R}^3$ is unknown and constant, the control allocation matrix $\boldsymbol{B} \in \mathbb{R}^{3\times 3}$ and the control input $\boldsymbol{u} \in \mathbb{R}^3$. The matrix $\boldsymbol{I}$ denotes the identity matrix and $\boldsymbol{S}(\cdot)$ is the skew-symmetric matrix given by

$$\boldsymbol{S}(\boldsymbol{\varepsilon}) = \begin{bmatrix} 0 & -\varepsilon_3 & \varepsilon_2 \\ \varepsilon_3 & 0 & -\varepsilon_1 \\ -\varepsilon_2 & \varepsilon_1 & 0 \end{bmatrix}. \tag{B.6}$$

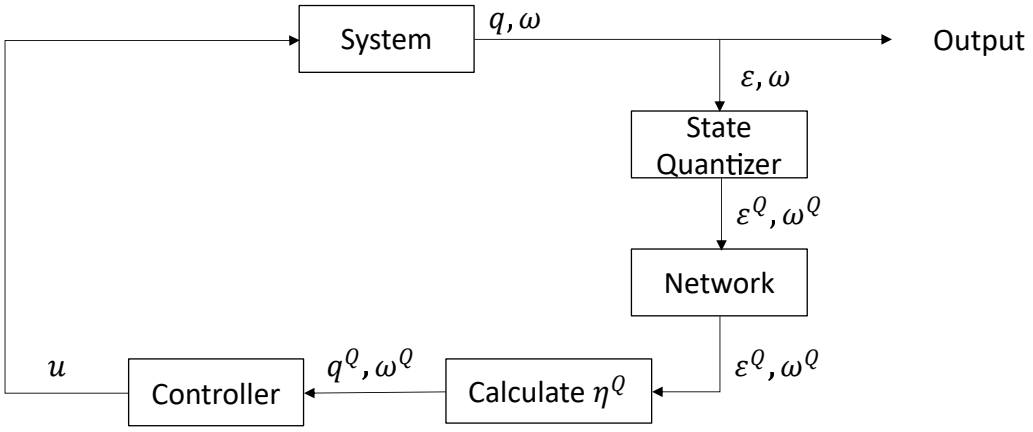

Figure B.1: Control system with state quantization over a network.

The moment caused by the gravitational force is

$$\boldsymbol{g}(\boldsymbol{q}) = -\boldsymbol{S}(\boldsymbol{r}_g^b)\boldsymbol{R}_i^b \boldsymbol{f}_g^i \in \mathbb{R}^3, \tag{B.7}$$

where $\boldsymbol{r}_g^b = [x_g \ y_g \ z_g]^\top$ is the distance from the origin to the center of mass, $\boldsymbol{f}_g^i = [0 \ \ 0 \ \ -mg]^\top$, m is the mass of the rigid body, and g is the gravity acceleration. If $\boldsymbol{r}_g^b = \boldsymbol{0} \implies \boldsymbol{g(q)} = 0$ and the rotation is about center of mass.

The orientation between two frames can be described by a rotation matrix given as

$$\boldsymbol{R}(\boldsymbol{q}) = \boldsymbol{I} + 2\eta \boldsymbol{S}(\boldsymbol{\varepsilon}) + 2\boldsymbol{S}^2(\boldsymbol{\varepsilon}), \tag{B.8}$$

where $\boldsymbol{R} \in SO(3)$ that is a special orthogonal group of order 3, and has the property

$$SO(3) = \{\boldsymbol{R} \in \mathbb{R}^{3\times 3} : \boldsymbol{R}^\top \boldsymbol{R} = \boldsymbol{I}, \det(\boldsymbol{R}) = 1\}. \tag{B.9}$$

The time derivative of a rotation matrix can be expressed as

$$\dot{\boldsymbol{R}}_b^a = \boldsymbol{R}_b^a \boldsymbol{S}(\boldsymbol{\omega}_{a,b}^b) = \boldsymbol{S}(\boldsymbol{\omega}_{a,b}^a)\boldsymbol{R}_b^a. \tag{B.10}$$

Attitude and angular velocities are assumed to be measurable after quantization, and for the control allocation matrix it is assumed that $\det(\boldsymbol{B}) \neq 0$, i.e. the matrix is invertible.

B.2.3 Problem Statement

We consider a control system as shown in Fig. B.1, where the states $\boldsymbol{\varepsilon}, \boldsymbol{\omega}$ are quantized at the encoder side to be sent over a network. The network is assumed noiseless, so that the quantized state signal is recovered and sent to the controller. Only the

quantized states $\boldsymbol{\varepsilon}^Q, \boldsymbol{\omega}^Q$ are measured, and the quantized value of η is calculated as

$$\eta^Q = \pm\sqrt{1 - \boldsymbol{\varepsilon}^{Q\top}\boldsymbol{\varepsilon}^Q}, \tag{B.11}$$

to ensure that the property of unit quaternion, $\boldsymbol{q}^{Q\top}\boldsymbol{q}^Q = 1$, is fulfilled, where the quantized attitude is given by $\boldsymbol{q}^Q = [\eta^Q, \boldsymbol{\varepsilon}^{Q\top}]^\top$.

Remark 1. *The quantized value, η^Q, can be calculated based on the value of $\boldsymbol{\varepsilon}^Q$ and knowledge of the sign of $\eta(t_0)$ and the assumption of sign continuity of $\eta(t)$ based on derivative. We can do the calculation after the network communication, saving bandwidth by sending less data over the network.*

Remark 2. *If we are close to, or at $\eta = 0$, we might end up with $\boldsymbol{\varepsilon}^{Q\top}\boldsymbol{\varepsilon}^Q > 1$, and a scaling is needed to ensure we have a unit quaternion.*

Let $\boldsymbol{q}_{i,d} = \boldsymbol{q}_d$, $\boldsymbol{\omega}^i_{i,d} = \boldsymbol{\omega}_d$ be the desired attitude and angular velocity. The control objective is to design a control law for $\boldsymbol{u}(t)$ by utilizing only quantized states $\boldsymbol{q}^Q(t), \boldsymbol{\omega}^Q(t)$ to ensure that $\boldsymbol{q}^Q(t) \to \boldsymbol{q}_d(t)$ and $\boldsymbol{\omega}^Q(t) \to \boldsymbol{\omega}^Q_{i,d}(t)$ as $t \to \infty$, where the kinematic equation

$$\dot{\boldsymbol{q}}_d = \boldsymbol{T}(\boldsymbol{q}_d)\boldsymbol{\omega}^d_{i,d} = \frac{1}{2}\begin{bmatrix} -\boldsymbol{\varepsilon}_d^\top \\ \eta_d\boldsymbol{I} - \boldsymbol{S}(\boldsymbol{\varepsilon}_d) \end{bmatrix}\boldsymbol{\omega}_d, \tag{B.12}$$

is satisfied, and where all the signals in the closed-loop system are uniformly bounded. To achieve the objective, the following assumptions are imposed.

Assumption 1. *The functions $\boldsymbol{q}_d(t)$, $\boldsymbol{\omega}_d(t)$ and $\dot{\boldsymbol{\omega}}_d(t)$ are known, piecewise continuous and bounded, where $\|\boldsymbol{\omega}_d(t)\| < k_{\omega_d}$ and $\|\dot{\boldsymbol{\omega}}_d(t)\| < k_{\dot{\omega}_d}$ $\forall t \geq t_0$ where $k_{\omega_d}, k_{\dot{\omega}_d} > 0$.*

Assumption 2. *The unknown parameter vector $\boldsymbol{\theta}$ is bounded by $\|\boldsymbol{\theta}\| \leq k_\theta$, where k_θ is a positive constant. Also $\boldsymbol{\theta} \in C_\theta$, where C_θ is a known compact convex set.*

B.2.4 Quantizer

The quantizer considered in this paper has the following property

$$|x^Q - x| \leq \delta_x, \tag{B.13}$$

where x is a scalar signal and $\delta_x > 0$ denotes the quantization bound. A uniform quantizer is considered, which has intervals of fixed length and is defined as

$$x^Q = x_i \operatorname{sgn}(x), \quad x_i - \frac{l}{2} \leq |x| < x_i + \frac{l}{2}, \tag{B.14}$$

where $i = 0, 1, 2, ...$, $x_0 = 0$, $x_{i+1} = x_i + l$, $l > 0$ is the length of the quantization intervals and where $\text{sgn}(\cdot)$ is the signum function. Here $x^Q = x + d$, where d is the quantization error and is bounded by (B.13), where $\delta_x = l/2$. The uniform quantization $x^Q \in U = \{\pm x_i\}$.

B.3 Controller Design and Stability Analysis

In this section we will design adaptive feedback control laws for the rigid body using backstepping technique. We begin with a change of coordinates to the error variables, and first find the error variables when the states are not quantized. The tracking error $\boldsymbol{e}$, is given by the quaternion product

$$\boldsymbol{e} = \bar{\boldsymbol{q}}_{i,d} \otimes \boldsymbol{q}_{i,b} = \begin{bmatrix} \tilde{\eta} \\ \tilde{\boldsymbol{\varepsilon}} \end{bmatrix} = \begin{bmatrix} \eta_d \eta + \boldsymbol{\varepsilon}_d^\top \boldsymbol{\varepsilon} \\ \eta_d \boldsymbol{\varepsilon} - \eta \boldsymbol{\varepsilon}_d - S(\boldsymbol{\varepsilon}_d)\boldsymbol{\varepsilon} \end{bmatrix} \in \mathbb{S}^3, \tag{B.15}$$

where $\bar{\boldsymbol{q}} = [\eta \ \ -\boldsymbol{\varepsilon}^\top]^\top$ is the inverse rotation given by the complex conjugate. If $\boldsymbol{q}_{i,b} = \boldsymbol{q}_{i,d}$ then $\boldsymbol{e} = [\pm 1 \ \mathbf{0}^\top]^\top$. Because there exists two different equilibria using quaternion coordinates, global stability can not be achieved, even though $\boldsymbol{e}$ and $-\boldsymbol{e}$ represents the same physical attitude [22]. We include one further assumption as follows:

Assumption 3. $\text{sgn}(\tilde{\eta}(t_0)) = \text{sgn}(\tilde{\eta}(t)) \ \ \forall t \geq t_0$.

Remark 3. *Assumption 3 is imposed to avoid the problem when the attitude error is close to* $E \triangleq \{\boldsymbol{e} \in \mathbb{S}^3 \ : \ \tilde{\eta} = 0\}$*, where the solution is not robust when a disturbance/quantization is introduced.*

The relative error kinematics is

$$\dot{\boldsymbol{e}} = \boldsymbol{T}(\boldsymbol{e})\boldsymbol{\omega}_e, \tag{B.16}$$

where $\boldsymbol{T}(\cdot)$ is defined in (B.3), and the angular velocity error

$$\boldsymbol{\omega}_e = \boldsymbol{\omega} - \boldsymbol{R}_i^b \boldsymbol{\omega}_d. \tag{B.17}$$

Since we have two equilibrium points, we introduce the change of coordinates

$$\boldsymbol{z}_{1\pm} = \begin{bmatrix} 1 \mp \tilde{\eta} \\ \tilde{\boldsymbol{\varepsilon}} \end{bmatrix}, \quad \boldsymbol{z}_2 = \boldsymbol{\omega}_e - \boldsymbol{\alpha}, \tag{B.18}$$

$$\dot{\boldsymbol{z}}_{1\pm} = \frac{1}{2} \begin{bmatrix} \pm \tilde{\boldsymbol{\varepsilon}}^\top \\ (\tilde{\eta}\boldsymbol{I} + \boldsymbol{S}(\tilde{\boldsymbol{\varepsilon}})) \end{bmatrix} \boldsymbol{\omega}_e \triangleq \frac{1}{2} \boldsymbol{G}(\boldsymbol{e})^\top \boldsymbol{\omega}_e, \tag{B.19}$$

where $\boldsymbol{z}_{1+}$ is the equilibrium point when $\tilde{\eta}(t_0) \geq 0$ and $\boldsymbol{z}_{1-}$ is the equilibrium point when $\tilde{\eta}(t_0) < 0$, the matrix $\boldsymbol{G}^\top \in \mathbb{R}^{4\times 3}$, and where $\boldsymbol{\alpha}$ is a virtual controller chosen as

$$\boldsymbol{\alpha} = -\boldsymbol{C}_1 \boldsymbol{G} \boldsymbol{z}_1 \in \mathbb{R}^3, \tag{B.20}$$

where $\boldsymbol{C}_1 \in \mathbb{R}^{3\times 3}$ is a positive definite matrix.

Remark 4. *Without the change of coordinates to $\boldsymbol{z}_{1\pm}$ one might end up with an unwanted or less optimal rotation of the rigid body.*

By multiplication, it can be shown that $\boldsymbol{G}\boldsymbol{z}_1 = \pm\tilde{\boldsymbol{\varepsilon}}$, and then from (B.20) we have

$$\dot{\boldsymbol{\alpha}} = \mp\frac{1}{2}\boldsymbol{C}_1\left[\tilde{\eta}\boldsymbol{I} + \boldsymbol{S}(\tilde{\boldsymbol{\varepsilon}})\right]\boldsymbol{\omega}_e. \tag{B.21}$$

The angular velocity error and angular velocity are bounded

$$\begin{aligned}\|\boldsymbol{\omega}_e\| &\leq \|\boldsymbol{z}_2 + \boldsymbol{\alpha}\| \leq \|\boldsymbol{z}_2\| + \lambda_{\max}(\boldsymbol{C}_1)\|\boldsymbol{G}\|\|\boldsymbol{z}_1\| \leq [1 + \lambda_{\max}(\boldsymbol{C}_1)]\|\boldsymbol{z}\| \\ &\triangleq d_a\|\boldsymbol{z}\|, \end{aligned} \tag{B.22}$$

$$\begin{aligned}\|\boldsymbol{\omega}\| &\leq \|\boldsymbol{\omega}_e + \boldsymbol{R}_i^b\boldsymbol{\omega}_d\| \leq d_a\|\boldsymbol{z}\| + \|\boldsymbol{R}_i^b\|\|\boldsymbol{\omega}_d\| \\ &\leq d_a\|\boldsymbol{z}\| + k_{\omega_d}, \end{aligned} \tag{B.23}$$

where $\boldsymbol{z} = [\boldsymbol{z}_1^\top, \boldsymbol{z}_2^\top]^\top$. When the states are quantized, the quantization error of the quaternion can be expressed as

$$\boldsymbol{d}_q = \bar{\boldsymbol{q}}_{i,b} \otimes \boldsymbol{q}_{i,Q} = \begin{bmatrix} d_\eta \\ \boldsymbol{d}_\varepsilon \end{bmatrix} = \begin{bmatrix} \eta\eta^Q + \boldsymbol{\varepsilon}^\top\boldsymbol{\varepsilon}^Q \\ \eta\boldsymbol{\varepsilon}^Q - \eta^Q\boldsymbol{\varepsilon} - S(\boldsymbol{\varepsilon})\boldsymbol{\varepsilon}^Q \end{bmatrix}, \tag{B.24}$$

where $\boldsymbol{d}_\varepsilon$ is the quantization error and bounded by $\|\boldsymbol{d}_\varepsilon\| \leq k_\varepsilon\|\boldsymbol{\delta}_\varepsilon\|$ from (B.13) and where $k_\varepsilon > 1$ is a positive constant, and d_η is bounded from the unity property of unit quaternion. If $\boldsymbol{q}^Q = \boldsymbol{q}$ and there is no quantization error, $\boldsymbol{d}_q = [1\ 0\ 0\ 0]^\top$. The tracking error with the quantized value of the unit quaternion $\boldsymbol{e}^Q$, is given by

$$\boldsymbol{e}^Q = \bar{\boldsymbol{q}}_{i,d} \otimes \boldsymbol{q}_{i,Q} = \begin{bmatrix} \tilde{\eta}^Q \\ \tilde{\boldsymbol{\varepsilon}}^Q \end{bmatrix} = \begin{bmatrix} \eta_d\eta^Q + \boldsymbol{\varepsilon}_d^\top\boldsymbol{\varepsilon}^Q \\ \eta_d\boldsymbol{\varepsilon}^Q - \eta^Q\boldsymbol{\varepsilon}_d - S(\boldsymbol{\varepsilon}_d)\boldsymbol{\varepsilon}^Q \end{bmatrix}, \tag{B.25}$$

and can also be described by

$$\begin{aligned}\boldsymbol{e}^Q = \boldsymbol{q}_{d,b} \otimes \boldsymbol{q}_{b,Q} = \boldsymbol{e} \otimes \boldsymbol{d}_q &= \begin{bmatrix} \tilde{\eta}d_\eta - \tilde{\boldsymbol{\varepsilon}}^\top\boldsymbol{d}_\varepsilon \\ d_\eta\tilde{\boldsymbol{\varepsilon}} + \tilde{\eta}\boldsymbol{d}_\varepsilon + S(\tilde{\boldsymbol{\varepsilon}})\boldsymbol{d}_\varepsilon \end{bmatrix} \\ &= \begin{bmatrix} \tilde{\eta}^Q \\ \tilde{\boldsymbol{\varepsilon}} + (d_\eta - 1)\tilde{\boldsymbol{\varepsilon}} + \tilde{\eta}\boldsymbol{d}_\varepsilon + S(\tilde{\boldsymbol{\varepsilon}})\boldsymbol{d}_\varepsilon \end{bmatrix} \triangleq \begin{bmatrix} \tilde{\eta}^Q \\ \tilde{\boldsymbol{\varepsilon}} + \boldsymbol{d}_{\tilde{\varepsilon}} \end{bmatrix}, \end{aligned} \tag{B.26}$$

where the value of $\boldsymbol{d}_{\tilde{\varepsilon}}$ depends on the quantization error given in (B.24). If there is no quantization error, $\boldsymbol{d}_{\tilde{\varepsilon}} = \boldsymbol{0}$. The quantization of the angular velocities $\boldsymbol{\omega}$ can be expressed as

$$\boldsymbol{\omega}^Q = \boldsymbol{\omega} + \boldsymbol{d}_\omega, \tag{B.27}$$

where $\boldsymbol{d}_\omega$ is the quantization error and bounded by $\|\boldsymbol{d}_\omega\| \leq \|\boldsymbol{\delta}_\omega\|$ from (B.13). We choose the adaptive controller

$$\boldsymbol{u}(t) = \boldsymbol{B}^{-1}\Big[-\boldsymbol{G}^Q \boldsymbol{z}_1^Q - \boldsymbol{C}_2 \boldsymbol{z}_2^Q - \boldsymbol{\Phi}^Q \hat{\boldsymbol{\theta}} - \boldsymbol{\Psi}^Q - \boldsymbol{J}\Big(\boldsymbol{S}(\boldsymbol{\omega}^Q)\boldsymbol{R}_i^Q \boldsymbol{\omega}_d - \boldsymbol{R}_i^Q \dot{\boldsymbol{\omega}}_d - \bar{\boldsymbol{\alpha}}^Q\Big)\Big], \tag{B.28}$$

$$\dot{\hat{\boldsymbol{\theta}}} = \mathrm{Proj}\{\boldsymbol{\Gamma}\boldsymbol{\Phi}^Q \boldsymbol{z}_2^Q\}, \tag{B.29}$$

where $\hat{\boldsymbol{\theta}}$ is the estimated value of $\boldsymbol{\theta}$, the vector $\tilde{\boldsymbol{\theta}} = \boldsymbol{\theta} - \hat{\boldsymbol{\theta}}$, the matrices $\boldsymbol{C}_2,\ \boldsymbol{\Gamma} \in \mathbb{R}^{3\times 3}$ are positive definite, and where $\mathrm{Proj}\{\cdot\}$ is the projection operator given in [17], and

$$\boldsymbol{z}_{1\pm}^Q = \begin{bmatrix} 1 \mp \tilde{\eta}^Q \\ \tilde{\boldsymbol{\varepsilon}}^Q \end{bmatrix}, \tag{B.30}$$

$$\boldsymbol{z}_2^Q = \boldsymbol{\omega}_e^Q - \boldsymbol{\alpha}^Q, \tag{B.31}$$

$$\boldsymbol{G}(\boldsymbol{e}^Q)^\top = \begin{bmatrix} \pm\tilde{\boldsymbol{\varepsilon}}^{Q\top} \\ \tilde{\eta}^Q \boldsymbol{I} + \boldsymbol{S}(\tilde{\boldsymbol{\varepsilon}}^Q) \end{bmatrix}, \tag{B.32}$$

$$\boldsymbol{\alpha}^Q = -\boldsymbol{C}_1 \boldsymbol{G}^Q \boldsymbol{z}_1^Q = \mp \boldsymbol{C}_1 \tilde{\boldsymbol{\varepsilon}}^Q, \tag{B.33}$$

$$\boldsymbol{\Psi}^Q = -\boldsymbol{S}(\boldsymbol{\omega}^Q)(\boldsymbol{J}\boldsymbol{\omega}^Q) - \boldsymbol{g}(\boldsymbol{q}^Q), \tag{B.34}$$

$$\boldsymbol{\Phi}^Q = \mathrm{diag}(-\boldsymbol{\omega}^Q), \tag{B.35}$$

$$\boldsymbol{g}(\boldsymbol{q}^Q) = -\boldsymbol{S}(\boldsymbol{r}_g^b)\boldsymbol{R}_i^Q \boldsymbol{f}_g^i, \tag{B.36}$$

$$\bar{\boldsymbol{\alpha}}^Q \triangleq \mp\frac{1}{2}\boldsymbol{C}_1\Big[\tilde{\eta}^Q \boldsymbol{I} + \boldsymbol{S}(\tilde{\boldsymbol{\varepsilon}}^Q)\Big]\boldsymbol{\omega}_e^Q, \tag{B.37}$$

$$\boldsymbol{\omega}_e^Q = \boldsymbol{\omega}^Q - \boldsymbol{R}_i^Q \boldsymbol{\omega}_d, \tag{B.38}$$

$$\boldsymbol{R}_i^Q = \boldsymbol{R}_b^Q \boldsymbol{R}_i^b. \tag{B.39}$$

Remark 5. *The projection operator* $\mathrm{Proj}\{\cdot\}$ *in* (B.29) *ensures that the estimates and estimation errors are nonzero and within known bounds, that is* $\|\hat{\boldsymbol{\theta}}\| \leq k_\theta$ *and* $\|\tilde{\boldsymbol{\theta}}\| \leq k_\theta$*, and has the property* $-\tilde{\boldsymbol{\theta}}^\top \boldsymbol{\Gamma}^{-1}\mathrm{Proj}(\boldsymbol{\tau}) \leq -\tilde{\boldsymbol{\theta}}^\top \boldsymbol{\Gamma}^{-1}\boldsymbol{\tau}$*, which are helpful to guarantee the closed-loop stability.*

Remark 6. *Only the quantized states can be used in the designed controller. Since the quantized states are used in the design of the virtual controller* $\boldsymbol{\alpha}^Q$ *in* (B.33)*, the derivative of the virtual controller is discontinuous and can not be used in the design of the controller, as it is for the case when the states are not quantized. Instead we*

choose a function (B.37)*, that is designed as if the states are not quantized in* (B.21)*, where* $\partial\boldsymbol{\alpha}/\partial\tilde{\boldsymbol{\varepsilon}}$ *is used [13].*

We show the stability of the positive equilibrium point, i.e. $\boldsymbol{z}_1^Q = \boldsymbol{z}_{1+}^Q$. To ensure that all signals are bounded, we first establish some prelimenary results as stated in the following lemma.

Lemma 1. *The effects of state quantization are bounded by the following inequalities:*

$$\text{(i)}\ \boldsymbol{\omega}_e^Q = \boldsymbol{\omega} + \boldsymbol{d}_\omega - \boldsymbol{R}_b^Q \boldsymbol{R}_i^b \boldsymbol{\omega}_d \le \boldsymbol{\omega}_e + \Big(2k_\varepsilon\Big[\boldsymbol{S}(\boldsymbol{\delta}_\varepsilon)+\boldsymbol{S}^2(\boldsymbol{\delta}_\varepsilon)\Big]\boldsymbol{R}_i^b\boldsymbol{\omega}_d + \boldsymbol{\delta}_\omega\Big) \triangleq \boldsymbol{\omega}_e + \boldsymbol{\delta}_{\omega_e}, \tag{B.40}$$

$$\text{(ii)}\ \boldsymbol{z}_2^Q \le \boldsymbol{\omega}_e + \boldsymbol{\delta}_{\omega_e} + \boldsymbol{C}_1\tilde{\boldsymbol{\varepsilon}}^Q \le \boldsymbol{\omega}_e + \boldsymbol{\delta}_{\omega_e} - \boldsymbol{\alpha} + \boldsymbol{C}_1\boldsymbol{d}_{\tilde{\varepsilon}} \le \boldsymbol{z}_2 + (\boldsymbol{\delta}_{\omega_e} + \boldsymbol{C}_1 k_\varepsilon \boldsymbol{\delta}_\varepsilon) \triangleq \boldsymbol{z}_2 + \boldsymbol{\delta}_{z_2}, \tag{B.41}$$

$$\text{(iii)}\ \|\boldsymbol{G}\boldsymbol{z}_1 - \boldsymbol{G}^Q\boldsymbol{z}_1^Q\| = \|\tilde{\boldsymbol{\varepsilon}} - \tilde{\boldsymbol{\varepsilon}}^Q\| \le \|k_\varepsilon\boldsymbol{\delta}_\varepsilon\|, \tag{B.42}$$

$$\text{(iv)}\ \|\boldsymbol{R}_i^Q - \boldsymbol{R}_i^b\| \le \|-2d_\eta\boldsymbol{S}(\boldsymbol{d}_\varepsilon)+2\boldsymbol{S}^2(\boldsymbol{d}_\varepsilon)^\top\|\|\boldsymbol{R}_i^b\| \le 2\Big[k_\varepsilon\|\boldsymbol{\delta}_\varepsilon\| + k_\varepsilon^2\|\boldsymbol{\delta}_\varepsilon\|^2\Big] \triangleq d_R, \tag{B.43}$$

$$\text{(v)}\ \|\boldsymbol{\Psi} - \boldsymbol{\Psi}^Q\| \le \|-\boldsymbol{S}(\boldsymbol{\omega})(\boldsymbol{J}\boldsymbol{\omega})+\boldsymbol{S}(\boldsymbol{\omega}+\boldsymbol{d}_\omega)(\boldsymbol{J}(\boldsymbol{\omega}+\boldsymbol{d}_\omega))+\boldsymbol{S}(\boldsymbol{r}_g^b)\boldsymbol{R}_i^b\boldsymbol{f}_g^i - \boldsymbol{S}(\boldsymbol{r}_g^b)\boldsymbol{R}_i^Q\boldsymbol{f}_g^i\| \le \Big[\lambda_{\max}(\boldsymbol{J})\Big(\|\boldsymbol{\delta}_\omega\|^2 + 2k_{\omega_d}\|\boldsymbol{\delta}_\omega\|\Big) + \|\boldsymbol{r}_g^b\|d_R mg\Big] + \Big[2\lambda_{\max}(\boldsymbol{J})\|\boldsymbol{\delta}_\omega\|d_a\Big]\|\boldsymbol{z}\| \triangleq d_{\Psi_1} + d_{\Psi_2}\|\boldsymbol{z}\|, \tag{B.44}$$

$$\text{(vi)}\ \|\boldsymbol{S}(\boldsymbol{\omega})\boldsymbol{R}_i^b - \boldsymbol{S}(\boldsymbol{\omega}^Q)\boldsymbol{R}_i^Q\| \le \|-\boldsymbol{S}(\boldsymbol{\omega})[-2d_\eta\boldsymbol{S}(\boldsymbol{d}_\varepsilon) + 2\boldsymbol{S}^2(\boldsymbol{d}_\varepsilon)^\top]\boldsymbol{R}_i^b - \boldsymbol{S}(\boldsymbol{d}_\omega)\boldsymbol{R}_i^Q\| \le \|\boldsymbol{\omega}\|d_R + \|\boldsymbol{\delta}_\omega\| \le (k_{\omega_d}d_R + \|\boldsymbol{\delta}_\omega\|) + (d_a d_R)\|\boldsymbol{z}\| \triangleq d_{S_1} + d_{S_2}\|\boldsymbol{z}\|, \tag{B.45}$$

$$\text{(vii)}\ \|\bar{\boldsymbol{\alpha}}^Q - \dot{\boldsymbol{\alpha}}\| = \|\frac{1}{2}\boldsymbol{C}_1\Big[[\tilde{\eta}\boldsymbol{I} + \boldsymbol{S}(\tilde{\varepsilon})]\boldsymbol{\omega}_e - [\tilde{\eta}^Q\boldsymbol{I} + \boldsymbol{S}(\tilde{\varepsilon}^Q)]\boldsymbol{\omega}_e^Q\Big]\| \le \frac{1}{2}\lambda_{\max}(\boldsymbol{C}_1)\Big(2\|\boldsymbol{\omega}_e\| + \|\boldsymbol{\delta}_{\omega_e}\|\Big) \le \lambda_{\max}(\boldsymbol{C}_1)(\frac{1}{2}\|\boldsymbol{\delta}_{\omega_e}\| + d_a\|\boldsymbol{z}\|) \triangleq d_{\bar{\alpha}_1} + d_{\bar{\alpha}_2}\|\boldsymbol{z}\|. \tag{B.46}$$

Proof: The property of (B.40) follows from (B.38), with the use of (B.8), (B.24), (B.27) and (B.39). The property of (B.41) follows from (B.31), with the use of (B.40), (B.33), (B.26), (B.18) and (B.20). The definition in (B.26) is used for inequality (B.42). The property of (B.43) follows by using (B.39) and (B.24), together with the property of (B.8). Using (B.4), (B.7), (B.13), (B.23), (B.27), (B.34), (B.36) and (B.43) the bound in (B.44) is ensured. The property of (B.45) follows by using (B.23), (B.24), (B.27), (B.43), (B.39) together with the properties of (B.8) and (B.13). The property of (B.46) follows by using (B.21), (B.22), (B.37), (B.40) and the property of unit quaternion.

We state our main results based on the control scheme in the following theorem.

Theorem 1. *Considering the closed-loop adaptive system consisting of the plant* (B.1)-(B.2) *with state quantization satisfying the bounded property* (B.13)*, the adaptive controller* (B.28)*, the update law* (B.29) *and Assumptions 1-3. If the gain matrices* $\boldsymbol{C}_1$ *and* $\boldsymbol{C}_2$ *and quantization parameters* $\boldsymbol{\delta}_\varepsilon$ *and* $\boldsymbol{\delta}_\omega$ *are chosen to satisfy*

$$\frac{c_0}{2} - d_{V_1} \geq k > 0, \tag{B.47}$$

where c_0 *is the minimum eigenvalue of* $\boldsymbol{C}_0 = \min\{\boldsymbol{G}^\top \boldsymbol{C}_1 \boldsymbol{G}, \boldsymbol{C}_2\}$*,* k *is a positive constant, and* d_{V_1} *is defined as*

$$d_{V_1} = d_{\Psi_2} + d_{S_2}\lambda_{\max}(\boldsymbol{J})k_{\omega_d} + d_{\bar{\alpha}_2}\lambda_{\max}(\boldsymbol{J}), \tag{B.48}$$

all signals in the closed loop system are ensured to be uniformly bounded. The error signals will converge to a compact set, i.e.

$$\|\boldsymbol{z}(t)\| \leq \sqrt{\frac{a}{k}}, \tag{B.49}$$

where

$$\begin{aligned}
a &= d_{\theta_1} + \frac{1}{2c_0} d_{V_2}^2, && \text{(B.50)}\\
d_{\theta_1} &= k_\theta \|\boldsymbol{\delta}_\omega\| \|\boldsymbol{\delta}_{z_2}\| + k_\theta \|\boldsymbol{\delta}_{z_2}\| k_{\omega_d}, && \text{(B.51)}\\
d_{V_2} &= \lambda_{\max}(\boldsymbol{C}_2)\|\boldsymbol{\delta}_{z_2}\| + \|k_\varepsilon \boldsymbol{\delta}_\varepsilon\| + d_{\Psi_1} + d_{S_1}\lambda_{\max}(\boldsymbol{J})k_{\omega_d} + d_R\lambda_{\max}(\boldsymbol{J})k_{\dot{\omega}_d}\\
&\quad + d_{\bar{\alpha}_1}\lambda_{\max}(\boldsymbol{J}) + d_{\theta_2}, && \text{(B.52)}\\
d_{\theta_2} &= k_\theta \|\boldsymbol{\delta}_\omega\| + k_\theta d_a \|\boldsymbol{\delta}_{z_2}\|, && \text{(B.53)}
\end{aligned}$$

and is ultimately bounded. Tracking of a given reference signal is achieved, with a bounded error.

Proof: Considering the Lyapunov function

$$V(\boldsymbol{z}, \tilde{\boldsymbol{\theta}}, t) = \boldsymbol{z}_1^\top \boldsymbol{z}_1 + \frac{1}{2}\boldsymbol{z}_2^\top \boldsymbol{J}\boldsymbol{z}_2 + \frac{1}{2}\tilde{\boldsymbol{\theta}}^\top \boldsymbol{\Gamma}^{-1}\tilde{\boldsymbol{\theta}}, \tag{B.54}$$

then by following the controller design in (B.28)-(B.29), the derivative of (B.54) is given as

$$\begin{aligned}
\dot{V} &= \boldsymbol{z}_1^\top \boldsymbol{G}^\top \boldsymbol{z}_2 - \boldsymbol{z}_1^\top \boldsymbol{G}^\top \boldsymbol{C}_1 \boldsymbol{G}\boldsymbol{z}_1 + \boldsymbol{z}_2^\top \Big[\boldsymbol{\Phi}\boldsymbol{\theta} + \boldsymbol{\Psi} + \boldsymbol{B}\boldsymbol{u} + \boldsymbol{J}\Big(\boldsymbol{S}(\boldsymbol{\omega})\boldsymbol{R}_i^b \boldsymbol{\omega}_d - \boldsymbol{R}_i^b \dot{\boldsymbol{\omega}}_d - \dot{\boldsymbol{\alpha}}\Big)\Big]\\
&\quad - \tilde{\boldsymbol{\theta}}^\top \boldsymbol{\Gamma}^{-1}\dot{\hat{\boldsymbol{\theta}}}\\
&= -\boldsymbol{z}_1^\top \boldsymbol{G}^\top \boldsymbol{C}_1 \boldsymbol{G}\boldsymbol{z}_1 - \boldsymbol{z}_2^\top \boldsymbol{C}_2 \boldsymbol{z}_2^Q + \boldsymbol{z}_2^\top (\boldsymbol{G}\boldsymbol{z}_1 - \boldsymbol{G}^Q \boldsymbol{z}_1^Q) + \boldsymbol{z}_2^\top (\boldsymbol{\Psi} - \boldsymbol{\Psi}^Q)
\end{aligned}$$

$$+ \boldsymbol{z}_2^\top \boldsymbol{J}(\boldsymbol{S}(\boldsymbol{\omega})\boldsymbol{R}_i^b - \boldsymbol{S}(\boldsymbol{\omega}^Q)\boldsymbol{R}_i^Q)\boldsymbol{\omega}_d + \boldsymbol{z}_2^\top \boldsymbol{J}\Big(\boldsymbol{R}_i^Q - \boldsymbol{R}_i^b\Big)\dot{\boldsymbol{\omega}}_d + \boldsymbol{z}_2^\top \boldsymbol{J}(\bar{\boldsymbol{\alpha}}^Q - \dot{\boldsymbol{\alpha}})$$
$$+ \Big[\boldsymbol{z}_2^\top(\boldsymbol{\Phi}\boldsymbol{\theta} - \boldsymbol{\Phi}^Q\hat{\boldsymbol{\theta}}) - \tilde{\boldsymbol{\theta}}^\top\boldsymbol{\Phi}^Q\boldsymbol{z}_2^Q\Big]. \tag{B.55}$$

By using (B.5), (B.35), (B.29), (B.27), (B.41), (B.23) and Assumption 2 the last terms in (B.55) satisfy the inequality

$$\begin{aligned}\boldsymbol{z}_2^\top(\boldsymbol{\Phi}\boldsymbol{\theta}-\boldsymbol{\Phi}^Q\hat{\boldsymbol{\theta}})-\tilde{\boldsymbol{\theta}}^\top\boldsymbol{\Phi}^Q\boldsymbol{z}_2^Q &= \boldsymbol{\theta}^\top\boldsymbol{\Phi}\boldsymbol{z}_2 - \boldsymbol{\theta}^\top\boldsymbol{\Phi}^Q\boldsymbol{z}_2 + \tilde{\boldsymbol{\theta}}^\top\boldsymbol{\Phi}^Q\boldsymbol{z}_2 - \tilde{\boldsymbol{\theta}}^\top\boldsymbol{\Phi}^Q\boldsymbol{z}_2^Q \\ &\leq \|\boldsymbol{\theta}\|\|\boldsymbol{\Phi}-\boldsymbol{\Phi}^Q\|\|\boldsymbol{z}_2\| + \|\tilde{\boldsymbol{\theta}}\|\|\boldsymbol{\Phi}^Q\|\|\boldsymbol{z}_2-\boldsymbol{z}_2^Q\| \\ &\leq k_\theta\|\mathrm{diag}(-\boldsymbol{\omega})-\mathrm{diag}(-\boldsymbol{\omega}-\boldsymbol{d}_\omega)\|\|\boldsymbol{z}\|+k_\theta(\|\boldsymbol{\omega}\|+\|\boldsymbol{\delta}_\omega\|)\|\boldsymbol{\delta}_{z_2}\| \\ &\leq d_{\theta_1} + d_{\theta_2}\|\boldsymbol{z}\|. \end{aligned} \tag{B.56}$$

By using Young's inequality, the properties in Lemma 1, (B.56) and Assumption 1, the derivative of V in (B.55) can be obtained as

$$\begin{aligned}\dot{V} \leq & -\boldsymbol{z}_1^\top\boldsymbol{G}^\top\boldsymbol{C}_1\boldsymbol{G}\boldsymbol{z}_1 - \boldsymbol{z}_2^\top\boldsymbol{C}_2\boldsymbol{z}_2 + \lambda_{\max}(\boldsymbol{C}_2)\|\boldsymbol{\delta}_{z_2}\|\|\boldsymbol{z}\| + \|k_\varepsilon\boldsymbol{\delta}_\varepsilon\|\|\boldsymbol{z}\| + d_{\Psi_1}\|\boldsymbol{z}\| \\ & + d_{\Psi_2}\|\boldsymbol{z}\|^2 + d_{S_1}\lambda_{\max}(\boldsymbol{J})k_{\omega_d}\|\boldsymbol{z}\| + d_{S_2}\lambda_{\max}(\boldsymbol{J})k_{\omega_d}\|\boldsymbol{z}\|^2 + d_R\lambda_{\max}(\boldsymbol{J})k_{\dot{\omega}_d}\|\boldsymbol{z}\| \\ & + d_{\bar{\alpha}_1}\lambda_{\max}(\boldsymbol{J})\|\boldsymbol{z}\| + d_{\bar{\alpha}_2}\lambda_{\max}(\boldsymbol{J})\|\boldsymbol{z}\|^2 + d_{\theta_1} + d_{\theta_2}\|\boldsymbol{z}\| \\ \leq & -c_0\|\boldsymbol{z}\|^2 + d_{\theta_1} + d_{V_2}\|\boldsymbol{z}\| + d_{V_1}\|\boldsymbol{z}\|^2 \\ \leq & -(\frac{c_0}{2} - d_{V_1})\|\boldsymbol{z}\|^2 + d_{\theta_1} + \frac{1}{2c_0}d_{V_2}^2 \\ \leq & -k\|\boldsymbol{z}\|^2 + a < 0, \quad \forall\|\boldsymbol{z}\| > \sqrt{a/k}. \end{aligned} \tag{B.57}$$

From (B.54) and (B.57) and by applying the LaSalle-Yoshizawa theorem, it follows that $\boldsymbol{z}_1$, $\boldsymbol{z}_2$ and $\tilde{\boldsymbol{\theta}}$ are bounded and satisfy (B.49) under condition (B.47). From (B.28) and Lemma 1 it follows that the control input $\boldsymbol{u}$, where only quantized states are measured, also is bounded. Thus, all signals in the closed loop system are bounded. Tracking of the desired reference signal is achieved, with a bounded tracking error given in (B.49). The value of a depends on the quantization parameters, and higher values of the quantization intervals will increase a, and if there is no quantization then $a = 0$.

B.4 Experimental Results

The proposed controller was simulated using MATLAB/Simulink and tested on the Quanser Aero helicopter system, shown in Fig. B.2. This is a two-rotor laboratory equipment for flight control-based experiments. The setup has a horizontal position of the main thruster and a vertical position of the tail thruster, which resembles a helicopter with two propellers driven by two DC motors. This is a MIMO system

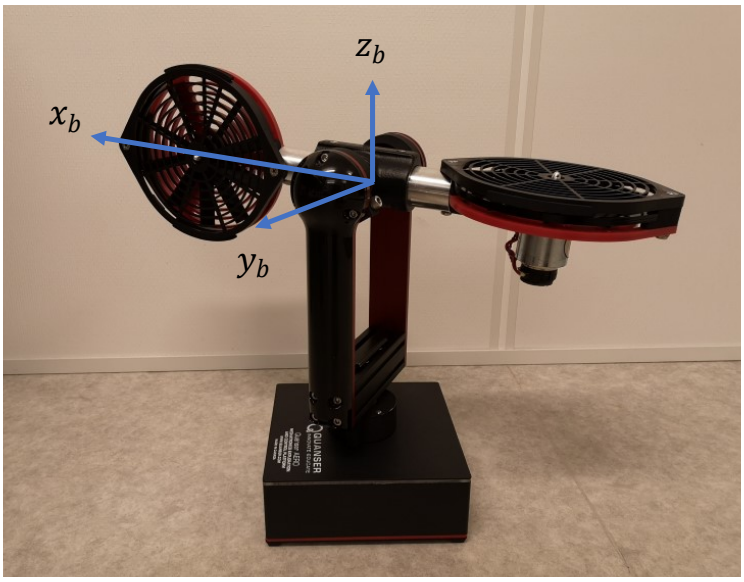

Figure B.2: Quanser Aero helicopter system with body coordinate frame.

Table B.1: Helicopter Parameters.

Symbol	Value	Units
$\boldsymbol{J}$	$\text{diag}(0.0218, 0.0217, 0.0218)$	kgm^2
m	1.075	kg
g	9.81	m/s^2
$\boldsymbol{r}_b^g$	$[0 \;\; 0 \;\; -0.0038]^\top$	m
$\boldsymbol{B}$	$\begin{bmatrix} 1 & 0 & 0 \\ 0 & 0.0011 & 0.0011 \\ 0 & -0.0014 & 0.00176 \end{bmatrix}$	Nm/V

with 2 DOF, and the helicopter can rotate around two axes where each input affects both rotational directions. The body fixed coordinate frame is visualized in Fig. B.2, and the inertial frame is coinciding with the body frame when $\boldsymbol{q} = [\pm 1 \; 0 \; 0 \; 0]^\top$. The mathematical model is described by (B.1) and (B.2), and the parameters used for simulation and experiments are shown in Table B.1. The initial states and estimated parameters were chosen as $\boldsymbol{q}(t_0) = [1 \; 0 \; 0 \; 0]^\top$, $\boldsymbol{\omega}(t_0) = [0 \; 0 \; 0]^\top$ and $\hat{\boldsymbol{\theta}}(t_0) = [0 \; 0.0070 \; 0.0095]^\top$ and the design parameters were set to $C_1 = 0.3\boldsymbol{I}$, $C_2 = 0.15\boldsymbol{I}$ and $\boldsymbol{\Gamma} = 0.02\boldsymbol{I}$. The objective was to track a sinusoidal signal where $r_d = 0$, $p_d = 40\pi/180 \sin(0.1\pi t)$, $y_d = 100\pi/180 \sin(0.05\pi t)$, given in Euler angles, and converted to a quaternion, and see how the system was affected by quantization of the states and validate the findings in Theorem 1. The quantization level for all measured states were chosen as $l = 2/2^R$, where R is number of bits transmitted in the communication. The system was first tested with continuous states, then with different values for R.

The results from the test with quantized states, where $R = 7$ are shown in Figs. B.3-B.5, showing the states $\boldsymbol{q}^Q$, $\boldsymbol{\omega}^Q$, the error in attitude and in angular velocity

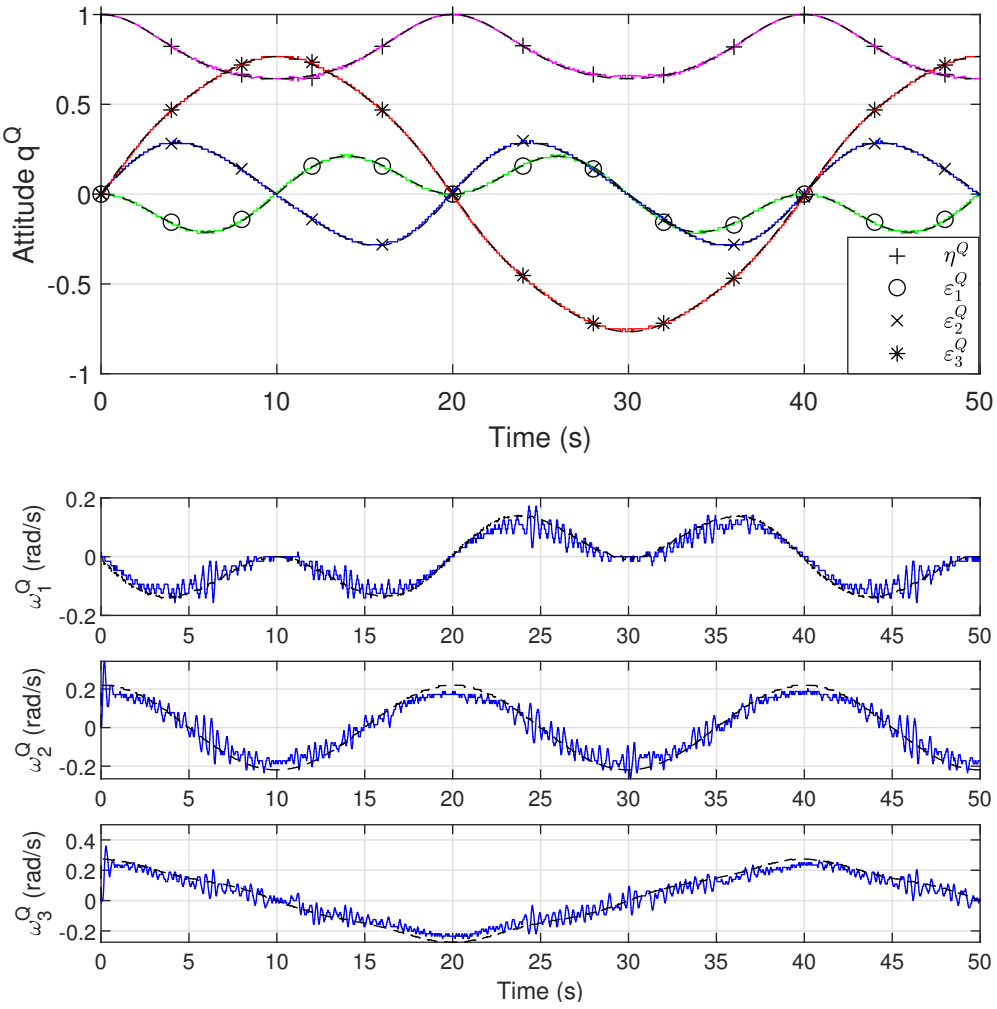

Figure B.3: The attitude $\boldsymbol{q}^Q$ and the angular velocity $\boldsymbol{\omega}^Q$ from experiment.

$\tilde{\boldsymbol{\varepsilon}}^Q$, $\boldsymbol{\omega}_e^Q$, and the input $\boldsymbol{u}(\boldsymbol{q}^Q, \boldsymbol{\omega}^Q)$, respectively. The desired states are shown with a dotted line and measured values from tests on the helicopter model are shown with a solid line. Since we only have 2 motors on the helicopter model, the control allocation matrix $\boldsymbol{B}$, was chosen so that the input $u_1 = 0$, and is not included in the plot of the input in Fig. B.5.

The total tracking error z_{track} was measured, where

$$z_{\text{track}} = \int_{t_0}^{t_f} \tilde{\boldsymbol{\varepsilon}}(\tau)^{Q,\top} \tilde{\boldsymbol{\varepsilon}}(\tau)^Q d\tau, \tag{B.58}$$

with $t_0 = 0$ and $t_f = 50$ s. The tracking errors for different values of R are shown in Table B.2. For values $R \geq 9$, the system does not show a big difference in performance compared to when using continuous signals. A lower value for R is also possible, and will require less data transmission, but with the cost of higher tracking error and also with more chattering for the input.

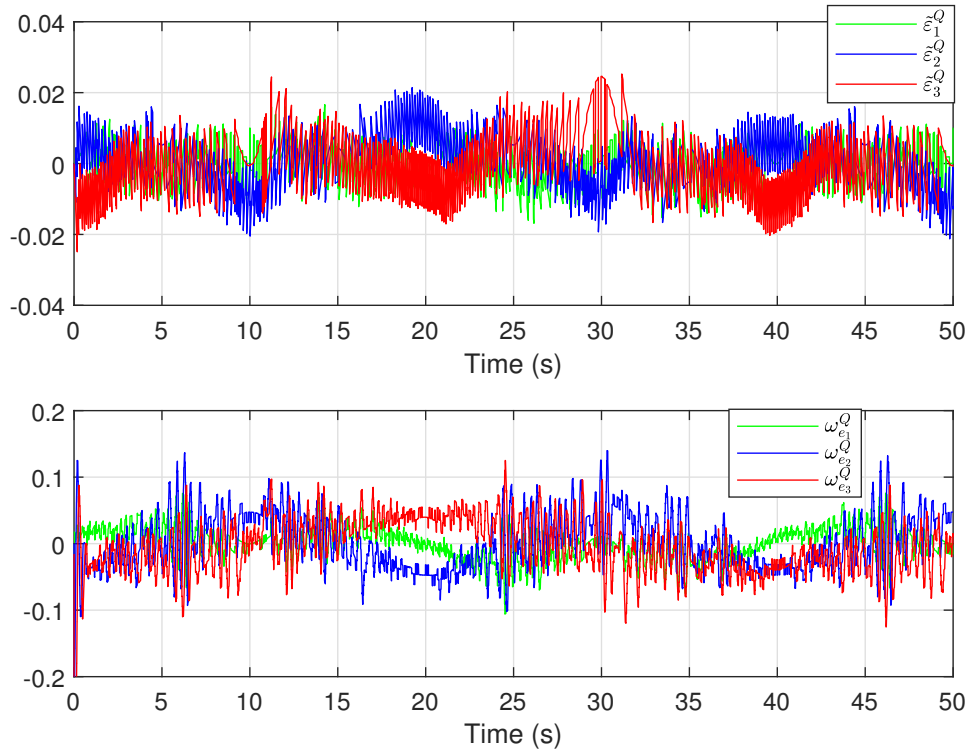

Figure B.4: The error in attitude $\tilde{\boldsymbol{\varepsilon}}^Q$ and the angular velocity error $\boldsymbol{\omega}_{\boldsymbol{e}}^Q$ from experiment.

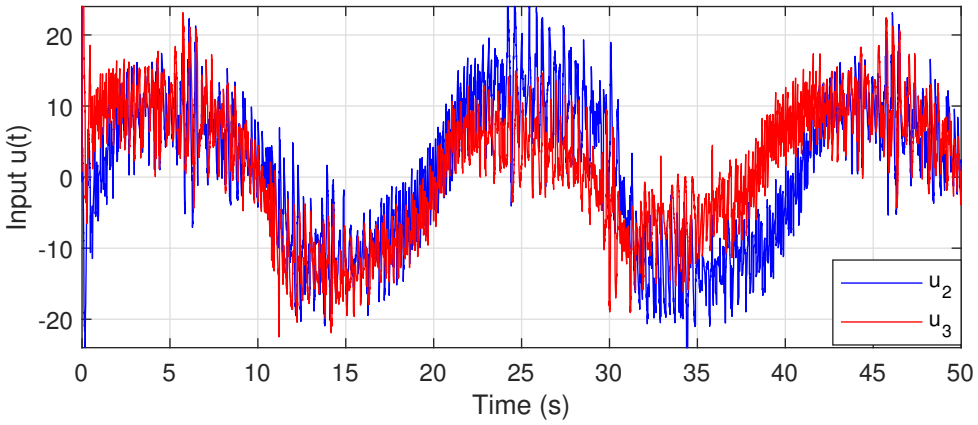

Figure B.5: The input $\boldsymbol{u}(\boldsymbol{q}^Q, \boldsymbol{\omega}^Q)$ from experiment.

Table B.2: Tracking error for different quantization levels, $l = 2/2^R$, from test on helicopter model.

$z_{\mathbf{track}}$	$\boldsymbol{\omega}^Q$				
$\boldsymbol{\varepsilon}^Q$	R	7	8	9	cont.
	7	0.0072	0.0075	0.0074	-
	8	0.0043	0.0043	0.0044	-
	9	0.0042	0.0039	0.0035	-
	cont	-	-	-	0.0035

B.5 Conclusion

In this paper, an adaptive backstepping control scheme is developed for attitude tracking using quaternions where the states are quantized. The quantizer considered satisfies a bounded condition and so the quantization error is bounded. With the use of constructed Lyapunov functions, all signals in the closed loop system are shown to be uniformly bounded and also tracking of a given reference signal is achieved. Experiments support the proof. As illustrated in the experiment, it is possible to reduce the communication burden over the network by including quantization and still have a good performance, where a suitable quantization level must be chosen. Actuators may reach their saturation level at some point, and this is a problem that can be further looked into.

References – Paper B

[1] S. Tatikonda and S. Mitter, "Control under communication constraints," *IEEE Transactions on Automatic Control*, vol. 49, no. 7, pp. 1056–1068, 2004.

[2] M. Fu and L. Xie, "The sector bound approach to quantized feedback control," *IEEE Transactions on Automatic Control*, vol. 50, no. 11, pp. 1698–1711, 2005.

[3] C. D. Persis, "Robust stabilization of nonlinear systems by quantized and ternary control," *Systems & Control Letters*, vol. 58, no. 8, pp. 602–608, 2009.

[4] T. Hayakawa, H. Ishii, and K. Tsumaru, "Adaptive quantized control for nonlinear uncertain systems," *Systems & Control Letters*, vol. 58, no. 9, pp. 625–632, 2009.

[5] H. Sun, N. Hovakimyan, and T. Basar, "$\mathcal{L}_1$ adaptive controller for uncertain nonlinear multi-input multi-output systems with input quantization," *IEEE Transactions on Automatic Control*, vol. 57, no. 3, pp. 565–578, 2012.

[6] J. Zhou, C. Wen, and G. Yang, "Adaptive backstepping stabilization of nonlinear uncertain systems with quantized input signal," in *IEEE Transactions on Automatic Control*, vol. 59, no. 2, 2014, pp. 460–464.

[7] J. Zhou, C. Wen, and W. Wang, "Adaptive control of uncertain nonlinear systems with quantized input signal," *Automatica*, vol. 95, pp. 152–162, 2018.

[8] D. Liberzon, "Hybrid feedback stabilization of systems with quantized signals," *Automatica*, vol. 39, no. 9, pp. 1543–1554, 2003.

[9] T. Liu and Z. Jiang, "Event-triggered control of nonlinear systems with state quantization," *IEEE Transactions on Automatic Control*, vol. 64, no. 2, pp. 797–803, 2019.

[10] T. Liu, Z.-P. Jiang, and D. J. Hill, "A sector bound approach to feedback control of nonlinear systems with state quantization," *Automatica*, vol. 48, no. 1, pp. 145–152, 2012.

[11] K. Liu, E. Fridman, and K. H. Johansson, "Dynamic quantization of uncertain linear networked control systems," *Automatica*, vol. 59, pp. 248–255, 2015.

[12] A. Selivanov, A. Fradkov, and D. Liberzon, "Adaptive control of passifiable linear systems with quantized measurements and bounded disturbances," *Systems and Control Letters*, vol. 88, pp. 62–67, 2016.

[13] J. Zhou, C. Wen, W. Wang, and F. Yang, "Adaptive backstepping control of nonlinear uncertain systems with quantized states," *IEEE Transactions on Automatic Control*, vol. 64, no. 11, pp. 4756–4763, 2019.

[14] R. Sun, A. Shan, C. Zhang, J. Wu, and Q. Jia, "Quantized fault-tolerant control for attitude stabilization with fixed-time disturbance observer," *Journal of Guidance, Control, and Dynamics*, vol. 44, no. 2, pp. 449–455, 2021.

[15] Y. Yan and S. Yu, "Sliding mode tracking control of autonomous underwater vehicles with the effect of quantization," *Ocean Engineering*, vol. 151, pp. 322–328, 2018.

[16] B. Huang, B. Zhou, S. Zhang, and C. Zhu, "Adaptive prescribed performance tracking control for underactuated autonomous underwater vehicles with input quantization," *Ocean Engineering*, vol. 221, 2021.

[17] M. Krstić, I. Kanellakopoulos, and P. Kokotović, *Nonlinear and Adaptive Control Design*. John Wiley & Sons, Inc., 1995.

[18] L. Xing, C. Wen, Y. Zhu, H. Su, and Z. Liu, "Output feedback control for uncertain nonlinear systems with input quantization," *Automatica*, vol. 65, pp. 191–202, 2015.

[19] Y. Li and G. Yang, "Adaptive asymptotic tracking control of uncertain nonlinear systems with input quantization and actuator faults," *Automatica*, vol. 72, pp. 177–185, 2016.

[20] S. M. Schlanbusch and J. Zhou, "Adaptive backstepping control of a 2-DOF helicopter system with uniform quantized inputs," in *IECON 2020 The 46th Annual Conference of the IEEE Industrial Electronics Society*, 2020, pp. 88–94.

[21] Y. Wang, L. He, and C. Huang, "Adaptive time-varying formation tracking control of unmanned aerial vehicles with quantized input," *ISA Transactions*, vol. 85, pp. 76–83, 2019.

[22] R. Schlanbusch, A. Loria, R. Kristiansen, and P. J. Nicklasson, "PD+ attitude control of rigid bodies with improved performance," in *49th IEEE Conference on Decision and Control*, 2010.

Paper C

Adaptive Attitude Control of a Rigid Body with Input and Output Quantization

Siri Marte Schlanbusch, Jing Zhou and Rune Schlanbusch

This paper has been published as:

S. M. Schlanbusch, J. Zhou and R. Schlanbusch, "Adaptive attitude control of a rigid body with input and output quantization," *IEEE Transactions on Industrial Electronics*, vol. 69, no. 8, pp. 8296–8305, 2022, doi: 10.1109/TIE.2021.3105999.

Adaptive Attitude Control of a Rigid Body with Input and Output Quantization

Siri Marte Schlanbusch[1], Jing Zhou[1] and Rune Schlanbusch[2]

[1]Department of Engineering Sciences
University of Agder
4879 Grimstad, Norway

[2]Norwegian Research Centre AS
4879 Grimstad, Norway

Abstract

In this article, the adaptive attitude-tracking problem of a rigid body is investigated, where the input and output are transmitted via a network. To reduce the communication burden in a network, a quantizer is introduced in both uplink and downlink communication channels. An adaptive backstepping-based control scheme is developed for a class of multiple-input and multiple-output (MIMO) rigid body systems. The proposed control algorithm can overcome the difficulty to proceed with the recursive design of virtual controls with quantized output vector and a new approach to stability analysis is developed by constructing a new compensation scheme for the effects of the vector output quantization and input quantization. It is shown that all closed-loop signals are ensured uniformly bounded and the tracking errors converge to a compact set containing the origin. Experiments on a 2 degrees-of-freedom helicopter system illustrate the effectiveness of the proposed control scheme.

Nomenclature

$d_{(\cdot)}$	Quantization error related to $(\cdot)$.
$\boldsymbol{e}$	Tracking error, quaternion.
$\boldsymbol{f}_g^i$	Gravitational force, expressed in i frame.
g	Gravitational acceleration.
$\boldsymbol{g}(\boldsymbol{q})$	Moment caused by the gravitational force.
$\boldsymbol{G}$	Error kinematics matrix.

$\boldsymbol{I}$ Identity matrix.

$\boldsymbol{J}$ Inertia matrix about the origin o, decomposed in the b frame.

$k_{(\cdot)}$ Positive constant related to $(\cdot)$.

$\boldsymbol{k}$ Euler axis.

l Length of quantization interval.

m Mass of the rigid body.

$\boldsymbol{q}$ Attitude.

$\boldsymbol{q}_{a,b}$ Unit quaternion $\boldsymbol{q}$ in b frame relative to a frame.

$\boldsymbol{r}_g^b$ Distance from the origin to the center of mass, decomposed in the b frame.

$\boldsymbol{R}_a^b$ Rotation matrix from frame a to frame b.

R Number of bits.

$\boldsymbol{S}(\boldsymbol{a})\boldsymbol{b}$ Cross product operator $\times$ between two vectors $\boldsymbol{a}$ and $\boldsymbol{b}$, where $\boldsymbol{S}$ is skew-symmetric.

$\boldsymbol{T}, \boldsymbol{\Psi}, \boldsymbol{\Phi}$ Known nonlinear functions of $\boldsymbol{q}$ and $\boldsymbol{\omega}$.

$\boldsymbol{u}$ Control input.

V Lyapunov function candidate.

$\boldsymbol{\tau}_d$ External disturbance.

$\delta_{(\cdot)}$ Maximum bounded value for $d_{(\cdot)}$.

$\boldsymbol{\varepsilon}$ Imaginary parts of a unit quaternion.

η Real part of a unit quaternion.

$\boldsymbol{\theta}$ Unknown constant vector.

$\lambda_{\max}(\cdot)$ Maximum eigenvalue of the matrix $(\cdot)$.

$\lambda_{\min}(\cdot)$ Minimum eigenvalue of the matrix $(\cdot)$.

υ Euler angle.

$\boldsymbol{\omega}$ Angular velocity.

$\boldsymbol{\omega}_{b,a}^c$ Angular velocity of frame a relative to frame b, expressed in frame c.

$\mathbb{R}^n$ Set of real numbers, dimension n.

$\mathbb{S}^3$ The non-Euclidean three-sphere.

$(\cdot)^{\mathcal{Q}}$ Quantized signal of $(\cdot)$.

$\|\cdot\|$ The $\mathcal{L}_2$-norm and induced $\mathcal{L}_2$-norm for vectors and matrices, respectively.

Vectors are denoted by small bold letters and matrices with capitalized bold letters.

C.1 Introduction

Attitude control of rigid bodies has been widely addressed in the literature, see e.g. [1–9], and with applications in marine systems in [10], unmanned aerial vehicles (UAVs) in [11], helicopters in [12], underwater vehicles in [13], and other robotic systems. Rigid body systems are utilized in numerous important applications such as transportation [14], inspection [15], search and rescue [16] and remote sensing [17]. In [6], a robust adaptive controller is proposed for the attitude tracking problem of rigid bodies in the presence of uncertain parameters and where the attitude is represented by rotation matrices. In [7], an adaptive attitude tracking controller is developed for rigid body systems in the presence of unknown inertia and gyro-bias. In [8], an adaptive controller is proposed for a leader-following attitude consensus problem for multiple rigid body systems subject to jointly connected switching networks in the presence of uncertain parameters. In [9], an adaptive backstepping controller is proposed for the trajectory tracking of a rigid body with unknown mass and inertia based on dual-quaternions. Chen *et al.* [11] proposed a robust nonlinear controller for quadrotor UAVs, which combines the sliding-mode control technique and the backstepping control technique. In [12], adaptive backstepping control is proposed for pitch and yaw control of a 2 degrees-of-freedom (DOF) helicopter system. Yan and Yu [13] investigated the sliding mode tracking control of underwater vehicles.

Quantized control has attracted considerable attention in recent years, due to its theoretical and practical importance in practical engineering, where digital processors are widespread used and signals are required to be quantized and transmitted via a common network to reduce the communication burden. However, most of the works on quantized feedback control are concerned with either input quantization [18–25] or state quantization [26, 27].

In practice, it is common that both the inputs and the states of rigid bodies are quantized due to actuator and sensor limitations. Control of rigid bodies with quantized signals is a potential problem and has received attention with a demand on stability and reliability. For example, the remote control of a group of vehicles or robots, where the signals are transmitted over a shared network using quantization

techniques. Attitude stabilization with input quantization is investigated in [28] using a fixed-time sliding mode control. Trajectory tracking control for autonomous underwater vehicles with the effect of quantization is investigated in [13] using a sliding mode controller, where the considered systems are completely known. In [29], adaptive tracking control is proposed for underactuated autonomous underwater vehicles with input quantization.

Uncertainties and non-linearities always exist in many practical systems. Research on adaptive control of rigid bodies with either input quantization or state quantization using backstepping technique has received attention, see for examples, [29–31]. In [30], an adaptive backstepping control scheme with quantized inputs is presented for a 2 DOF helicopter system, considering a uniform quantizer. In [29], adaptive backstepping is investigated for tracking control for under-actuated autonomous underwater vehicles with input quantization. An adaptive backstepping controller is proposed for formation tracking control for a group of UAVs with quantized inputs in [31]. Actually, the above cited attitude control approaches do not consider the problem which takes both the input quantization and state quantization into account.

In this article, we aim to solve the attitude tracking of uncertain nonlinear rigid body systems with both input and output quantization. The system is modeled as a nonlinear multiple-input-multiple-output (MIMO) system, with challenges in controller design due to its nonlinear behavior, its cross coupling effect between inputs and outputs, and with uncertainties both in the model and the parameters. A uniform quantization is used for signals in order to reduce the communication burden. A new backstepping based adaptive controller and a new approach to stability analysis are proposed. The full state vector is considered in the stability, that is often forgotten for quaternion based attitude control, where the scalar part of the quaternion is left out. The proposed method is tested on a 2 DOF helicopter system from Quanser. It is analytically shown how the choice of quantization level affects the tracking performance, where a higher quantization level increases the tracking error. The experiments on the helicopter system illustrate the proposed scheme.

With aforementioned features, the main contributions of this paper are summarized as follows.

- As far as we are concerned, this is the first work which solves the adaptive control problem for rigid body systems with unknown parameters and with both input and output quantization, where a bounded type of quantizer is considered, meanwhile guaranteeing that the attitude error and velocity error will converge to a compact set. Compared with [24] where only input quantization is considered, and [27] where only state quantization is considered, this research studies both input and output quantization problem. The main challenge is that

the designed controller and virtual controls can only utilize quantized states and both the effects of input and output quantization introduce numerous residual terms that need to be dominated. Additionally, the quantization causes discrete phenomenons which complicates the controller design and stability analysis. To overcome this difficulty, differentiable virtual controls are firstly designed by assuming that the system has no quantization. Their partial derivatives multiplied by the quantized signals are then utilized to complete the design of virtual controls for the case with quantized input and output.

- Compared to backstepping control of single-input-single-output (SISO) systems with either input or state quantization in [23–25, 27, 32], this paper considers MIMO uncertain systems with both input and output quantization. The challenge is that the control problem becomes more complicated for MIMO systems due to the coupling among various inputs and outputs. It becomes even more difficult to deal with when there exist uncertain parameters in the coupling matrix and both inputs and outputs are quantized. To overcome the difficulty, a new backstepping based adaptive controller and a new approach to stability analysis are proposed, where the effects of both output and input quantization are compensated for.

C.2 Rigid Body Dynamical Model and Problem Formulation

C.2.1 Attitude Dynamics

The attitude of a rigid body can be represented by e.g. Euler angles in [13, 30], (modified) Rodrigues parameters, rotation matrices in [3, 6] or quaternions in [4, 7, 9], where each representation has different properties. Any three-parameter representations have some kind of singularity, where e.g. Euler angles (roll-pitch-yaw) have kinematic singularities since it is not possible to describe the angular velocity for all angles, and with the potential problem of gimbal lock. Practical applications are often represented by unit quaternions, since this has a nonsingular parameterization. With a desire of a singularity-free representation of the attitude, which is important for agile systems, unit quaternions are used in this paper.

We describe the orientation of a rigid body in the body frame b, relative to an inertial frame i, by a unit quaternion, $\boldsymbol{q} = [\eta, \varepsilon_1, \varepsilon_2, \varepsilon_3]^\top = [\eta, \boldsymbol{\varepsilon}^\top]^\top \in \mathbb{S}^3 = \{x \in \mathbb{R}^4 : \boldsymbol{x}^\top \boldsymbol{x} = 1\}$, that is a complex number, where $\eta = \cos(\upsilon/2) \in \mathbb{R}$ and $\boldsymbol{\varepsilon} = \boldsymbol{k} \sin(\upsilon/2) \in \mathbb{R}^3$. Considering a fully actuated rigid body, the equations of

motion for the attitude dynamics are defined as

$$\dot{\boldsymbol{q}} = \boldsymbol{T}(\boldsymbol{q})\boldsymbol{\omega}, \tag{C.1}$$

$$\boldsymbol{J}\dot{\boldsymbol{\omega}} = \boldsymbol{\Psi}(\boldsymbol{q},\boldsymbol{\omega}) + \boldsymbol{\Phi}(\boldsymbol{\omega})\boldsymbol{\theta} + \boldsymbol{B}\boldsymbol{u}, \tag{C.2}$$

where the angular velocity $\boldsymbol{\omega}_{i,b}^{b} = \boldsymbol{\omega} \in \mathbb{R}^3$, the inertia matrix $\boldsymbol{J} = \mathrm{diag}(J_x, J_y, J_z) \in \mathbb{R}^{3\times3}$ and is positive definite, the unknown constant vector $\boldsymbol{\theta} \in \mathbb{R}^3$, the control allocation matrix $\boldsymbol{B} \in \mathbb{R}^{3\times3}$, the control input $\boldsymbol{u} \in \mathbb{R}^3$, and where

$$\boldsymbol{T}(\boldsymbol{q}) = \frac{1}{2}\begin{bmatrix} -\boldsymbol{\varepsilon}^\top \\ \eta\boldsymbol{I} + \boldsymbol{S}(\boldsymbol{\varepsilon}) \end{bmatrix} \in \mathbb{R}^{4\times3}, \tag{C.3}$$

$$\boldsymbol{\Psi}(\boldsymbol{q},\boldsymbol{\omega}) = -\boldsymbol{S}(\boldsymbol{\omega})(\boldsymbol{J}\boldsymbol{\omega}) - \boldsymbol{g}(\boldsymbol{q}) \ \in \mathbb{R}^3, \tag{C.4}$$

$$\boldsymbol{\Phi}(\boldsymbol{\omega}) = \mathrm{diag}(-\boldsymbol{\omega}) \ \in \mathbb{R}^{3\times3}, \tag{C.5}$$

$$\boldsymbol{g}(\boldsymbol{q}) = -\boldsymbol{S}(\boldsymbol{r}_g^b)\boldsymbol{R}_i^b\boldsymbol{f}_g^i, \tag{C.6}$$

where $\boldsymbol{f}_g^i = [0\ 0\ -mg]^\top$, and the matrix $\boldsymbol{S}(\cdot)$ is the skew-symmetric matrix given by

$$\boldsymbol{S}(\boldsymbol{\varepsilon}) = \begin{bmatrix} 0 & -\varepsilon_3 & \varepsilon_2 \\ \varepsilon_3 & 0 & -\varepsilon_1 \\ -\varepsilon_2 & \varepsilon_1 & 0 \end{bmatrix}. \tag{C.7}$$

If $\boldsymbol{r}_g^b = \boldsymbol{0} \implies \boldsymbol{g}(\boldsymbol{q}) = 0$ and the rotation is about the center of mass. In applications, such as underwater vehicle dynamics, the equations of motion is described by a rotation about a point o, that is not the center of mass [33].
The orientation between two frames can be described by a rotation matrix given as

$$\boldsymbol{R}(\boldsymbol{q}) = \boldsymbol{I} + 2\eta\boldsymbol{S}(\boldsymbol{\varepsilon}) + 2\boldsymbol{S}^2(\boldsymbol{\varepsilon}), \tag{C.8}$$

and the rotation matrix $\boldsymbol{R} \in SO(3)$ that is a special orthogonal group of order 3, and has the property

$$SO(3) = \{\boldsymbol{R} \in \mathbb{R}^{3\times3} : \boldsymbol{R}^\top\boldsymbol{R} = \boldsymbol{I}, \det(\boldsymbol{R}) = 1\}. \tag{C.9}$$

The derivative of a rotation matrix can be expressed as [33]

$$\dot{\boldsymbol{R}}_b^a = \boldsymbol{R}_b^a\boldsymbol{S}(\boldsymbol{\omega}_{a,b}^b) = \boldsymbol{S}(\boldsymbol{\omega}_{a,b}^a)\boldsymbol{R}_b^a. \tag{C.10}$$

Attitude and angular velocities are assumed to be measurable after quantization, and for the control allocation matrix it is assumed that $\det(\boldsymbol{B}) \neq 0$, i.e. the matrix is invertible.

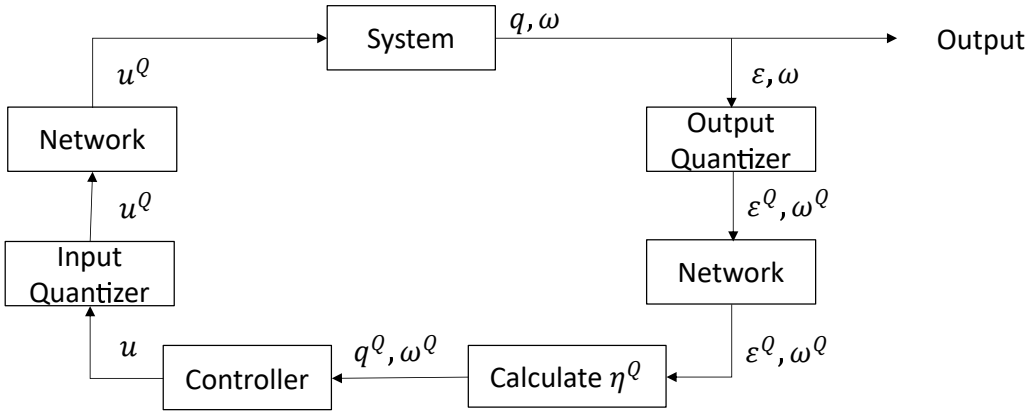

Figure C.1: Control system with quantization over a network.

C.2.2 Problem Statement

We consider a control system as shown in Fig. C.1, where the outputs $\boldsymbol{\varepsilon}, \boldsymbol{\omega}$ and input $\boldsymbol{u}$ are quantized at the encoder side to be sent over the network. It is noted that $\boldsymbol{q} = [\eta, \boldsymbol{\varepsilon}^\top]^\top$. To reduce the communication burden, we have limited the feedback part of the quaternion to only contain $\boldsymbol{\varepsilon}$, as η can be reconstructed due to the unity of the quaternion. The network is assumed noiseless, so that the quantized output signals $\boldsymbol{\varepsilon}^Q, \boldsymbol{\omega}^Q$ are recovered and sent to the controller, and the quantized input signal $\boldsymbol{u}^Q(t)$ is recovered and sent to the plant.

Only the quantized output $\boldsymbol{\varepsilon}^Q, \boldsymbol{\omega}^Q$ are measured, and the quantized value of η is calculated as

$$\eta^Q = \pm\sqrt{1 - (\boldsymbol{\varepsilon}^Q)^\top \boldsymbol{\varepsilon}^Q}, \tag{C.11}$$

to ensure that the property of unit quaternion, $(\boldsymbol{q}^Q)^\top \boldsymbol{q}^Q = 1$, is fulfilled, where the quantized attitude is given by $\boldsymbol{q}^Q = [\eta^Q, (\boldsymbol{\varepsilon}^Q)^\top]^\top$.

Remark 1. *If the state variable η is quantized and sent over the network, we can not ensure that $\boldsymbol{q}^Q$ is a unit quaternion, and a correction/scaling will be needed to ensure this. Since η^Q can be calculated based on the value of $\boldsymbol{\varepsilon}^Q$ and knowledge of the sign of $\eta(t_0)$ and the assumption of sign continuity of $\eta(t)$ based on derivative, we can do the calculation after the network communication. This will also save bandwidth by sending less data over the network.*

Remark 2. *If we are close to, or at $\eta = 0$, we might end up with $(\boldsymbol{\varepsilon}^Q)^\top \boldsymbol{\varepsilon}^Q > 1$, and a scaling is needed to ensure we have a unit quaternion.*

Let $\boldsymbol{q}_{i,d} = \boldsymbol{q}_d$, $\boldsymbol{\omega}^i_{i,d} = \boldsymbol{\omega}_d$, be the desired attitude and angular velocity. The control objective is to design a control law for $\boldsymbol{u}(t) = \boldsymbol{u}(\boldsymbol{q}^Q, \boldsymbol{\omega}^Q)$ by utilizing only quantized outputs $\boldsymbol{q}^Q(t)$ and $\boldsymbol{\omega}^Q(t)$ to ensure that $\boldsymbol{q}^Q(t) \to \boldsymbol{q}_d(t)$ and $\boldsymbol{\omega}^Q(t) \to \boldsymbol{\omega}^Q_{i,d}(t)$

as $t \to \infty$, where the kinematic equation

$$\dot{\boldsymbol{q}}_d = \boldsymbol{T}(\boldsymbol{q}_d)\boldsymbol{\omega}_{i,d}^d = \frac{1}{2}\begin{bmatrix} -\boldsymbol{\varepsilon}_d^\top \\ \eta_d \boldsymbol{I} - \boldsymbol{S}(\boldsymbol{\varepsilon}_d) \end{bmatrix} \boldsymbol{\omega}_d, \tag{C.12}$$

is satisfied, and where all the signals in the closed-loop system are uniformly bounded. To achieve the objective, the following assumptions are imposed.

Assumption 1. *The desired attitude $\boldsymbol{q}_d(t)$, the desired angular velocity $\boldsymbol{\omega}_d(t)$ and the desired angular acceleration $\dot{\boldsymbol{\omega}}_d(t)$ are known, piecewise continuous and bounded functions, that is, there exist $k_{\omega_d}, k_{\dot{\omega}_d} > 0$ such that $\|\boldsymbol{\omega}_d(t)\| < k_{\omega_d}$ and $\|\dot{\boldsymbol{\omega}}_d(t)\| < k_{\dot{\omega}_d}$ $\forall t \geq t_0$.*

Assumption 2. *The unknown parameter vector $\boldsymbol{\theta}$ is bounded by $\|\boldsymbol{\theta}\| \leq k_\theta$, where k_θ is a positive constant. Also $\boldsymbol{\theta} \in C_\theta$, where C_θ is a known compact convex set.*

C.2.3 Quantizer

The quantizer considered in this paper has the following property

$$|y^Q - y| \leq \delta_y, \tag{C.13}$$

where y is a scalar signal and $\delta_y > 0$ denotes the quantization bound. A uniform quantizer is chosen, which has intervals of fixed length and is defined as follows:

$$y^Q = \begin{cases} y_i \operatorname{sgn}(y), & y_i - \frac{l}{2} < |y| \leq y_i + \frac{l}{2} \\ 0, & |y| \leq y_0 \end{cases}, \tag{C.14}$$

where $y_0 > 0, y_1 = y_0 + \frac{l}{2}$, $y_{i+1} = y_i + l$, $l > 0$ is the length of the quantization interval, $\operatorname{sgn}(y)$ is the sign function. The uniform quantization $y^Q \in U = \{0, \pm y_i\}$, and a map of the quantization for $y_i > 0$ is shown in Fig. C.2. Clearly, the property in (C.13) is satisfied with $\delta_y = \max\{y_0, \frac{l}{2}\}$.

When a vector is quantized, we have

$$\boldsymbol{y}^Q = \begin{bmatrix} y_1^Q & y_2^Q & \cdots & y_n^Q \end{bmatrix}^\top, \tag{C.15}$$

and so each vector element is bounded by (C.13), and we have $\|\boldsymbol{y}^Q - \boldsymbol{y}\| = \|\boldsymbol{d}_y\| \leq \|\boldsymbol{\delta}_y\| \triangleq \delta_y$.

Other bounded quantizers such as hysteresis-uniform quantizer and logarithmic-uniform quantizer as presented in [27] can also be considered.

Remark 3. *Communication in a network only has to occur when the quantization levels change. Thus, a higher value for length of the quantization intervals requires less data transmission.*

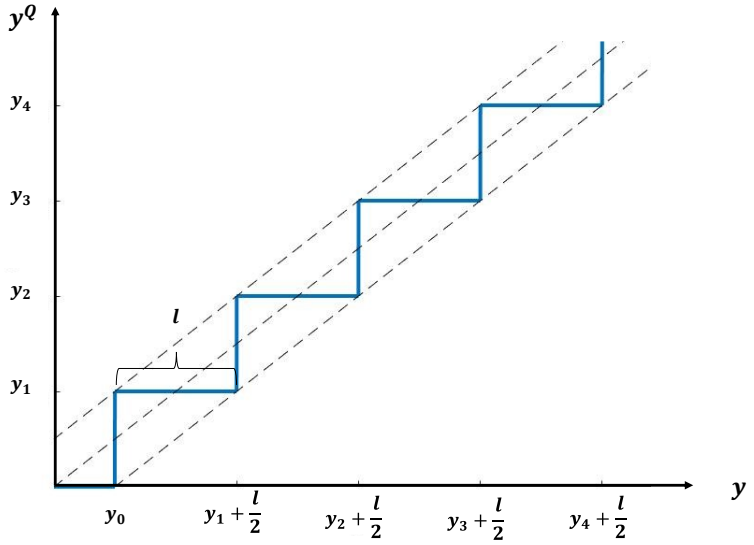

Figure C.2: Map of the uniform quantizer for $y > 0$.

C.3 Controller Design

In this section we will design adaptive feedback control laws for the rigid body using backstepping technique.

C.3.1 Without Quantization

We first consider the case that the output and input are not quantized. For our model, two steps are included, where the control signal is designed in the last step. We begin with a change of coordinates to the error variables. The tracking error $\boldsymbol{e}$ is defined by the quaternion product

$$\boldsymbol{e} = \bar{\boldsymbol{q}}_{i,d} \otimes \boldsymbol{q}_{i,b} = \begin{bmatrix} \tilde{\eta} \\ \tilde{\boldsymbol{\varepsilon}} \end{bmatrix} = \begin{bmatrix} \eta_d \eta + \boldsymbol{\varepsilon}_d^\top \boldsymbol{\varepsilon} \\ \eta_d \boldsymbol{\varepsilon} - \eta \boldsymbol{\varepsilon}_d - S(\boldsymbol{\varepsilon}_d)\boldsymbol{\varepsilon} \end{bmatrix} \in \mathbb{S}^3, \tag{C.16}$$

where $\bar{\boldsymbol{q}} = [\eta \ \ -\boldsymbol{\varepsilon}^\top]^\top$ is the inverse rotation given by the complex conjugate. If $\boldsymbol{q}_{i,b} = \boldsymbol{q}_{i,d}$ then $\boldsymbol{e} = [\pm 1 \ \mathbf{0}_3^\top]^\top$, where $\mathbf{0}_3^\top$ is the zero vector of dimension three. Because there exist two different equilibria using quaternion coordinates, global stability can not be achieved, even though $\boldsymbol{e}$ and $-\boldsymbol{e}$ represent the same physical attitude [2]. We include one further assumption as follows.

Assumption 3. *We assume that* $\operatorname{sgn}(\tilde{\eta}(t_0)) = \operatorname{sgn}(\tilde{\eta}(t)) \ \ \forall t \geq t_0$.

Remark 4. *Assumption 3 is imposed to avoid the problem when the attitude error is close to* $E = \{\boldsymbol{e} \in \mathbb{S}^3 \ : \ \tilde{\eta} = 0\}$.

The relative error kinematics is

$$\dot{\boldsymbol{e}} = \boldsymbol{T}(\boldsymbol{e})\boldsymbol{\omega}_e, \tag{C.17}$$

where $\boldsymbol{T}(\cdot)$ is defined in (C.3) and the angular velocity error is

$$\boldsymbol{\omega}_e = \boldsymbol{\omega} - \boldsymbol{R}_i^b \boldsymbol{\omega}_d. \tag{C.18}$$

Following the backstepping design procedure, the change of coordinates are introduced as

$$\boldsymbol{z}_{1\pm} = \begin{bmatrix} 1 \mp \tilde{\eta} \\ \tilde{\boldsymbol{\varepsilon}} \end{bmatrix}, \quad \boldsymbol{z}_2 = \boldsymbol{\omega}_e - \boldsymbol{\alpha}, \tag{C.19}$$

where $\boldsymbol{z}_{1+}$ is the equilibrium point when $\tilde{\eta}(t_0) \geq 0$ and $\boldsymbol{z}_{1-}$ is the equilibrium point when $\tilde{\eta}(t_0) < 0$ and where $\boldsymbol{\alpha}$ is a virtual controller designed in step 1 as

$$\boldsymbol{\alpha} = -\boldsymbol{C}_1 \boldsymbol{G} \boldsymbol{z}_{1\pm}, \tag{C.20}$$

where $\boldsymbol{C}_1 \in \mathbb{R}^{3\times 3}$ is a positive definite matrix and

$$\begin{aligned} \boldsymbol{G}(\boldsymbol{e})^\top &\triangleq \begin{bmatrix} \pm\tilde{\boldsymbol{\varepsilon}}^\top \\ \tilde{\eta}\boldsymbol{I} + \boldsymbol{S}(\tilde{\boldsymbol{\varepsilon}}) \end{bmatrix} \in \mathbb{R}^{4\times 3}, \\ \dot{\boldsymbol{z}}_{1\pm} &= \frac{1}{2}\boldsymbol{G}^\top \boldsymbol{\omega}_e = -\frac{1}{2}\boldsymbol{G}^\top \boldsymbol{C}_1 \boldsymbol{G} \boldsymbol{z}_{1\pm} + \frac{1}{2}\boldsymbol{G}^\top \boldsymbol{z}_2. \end{aligned} \tag{C.21}$$

For ease of notation we denote $\boldsymbol{z}_1 = \boldsymbol{z}_{1\pm}$ further in the paper. In step 2, the final controller $\boldsymbol{u}(t)$ and parameter update law $\dot{\hat{\boldsymbol{\theta}}}$ are designed as

$$\boldsymbol{u} = \boldsymbol{B}^{-1}\Big[-\boldsymbol{G}\boldsymbol{z}_1 - \boldsymbol{C}_2\boldsymbol{z}_2 - \boldsymbol{\Phi}\hat{\boldsymbol{\theta}} - \boldsymbol{\Psi} - \boldsymbol{J}\Big(\boldsymbol{S}(\boldsymbol{\omega})\boldsymbol{R}_i^b\boldsymbol{\omega}_d - \boldsymbol{R}_i^b\dot{\boldsymbol{\omega}}_d - \dot{\boldsymbol{\alpha}}\Big)\Big], \tag{C.22}$$

$$\dot{\hat{\boldsymbol{\theta}}} = \boldsymbol{\Gamma}\boldsymbol{\Phi}\boldsymbol{z}_2, \tag{C.23}$$

where $\boldsymbol{C}_2 \in \mathbb{R}^{3\times 3}$ and $\boldsymbol{\Gamma} \in \mathbb{R}^{3\times 3}$ are positive definite matrices. We choose a Lyapunov function candidate as

$$V(\boldsymbol{z}_1, \boldsymbol{z}_2, \tilde{\boldsymbol{\theta}}, t) = \boldsymbol{z}_1^\top \boldsymbol{z}_1 + \frac{1}{2}\boldsymbol{z}_2^\top \boldsymbol{J}\boldsymbol{z}_2 + \frac{1}{2}\tilde{\boldsymbol{\theta}}^\top \boldsymbol{\Gamma}^{-1}\tilde{\boldsymbol{\theta}}, \tag{C.24}$$

where $\hat{\boldsymbol{\theta}}$ is the estimated value of $\boldsymbol{\theta}$, and the unknown parameter error is $\tilde{\boldsymbol{\theta}} = \boldsymbol{\theta} - \hat{\boldsymbol{\theta}}$. The derivative of V can be computed as

$$\begin{aligned} \dot{V} = {} & \boldsymbol{z}_1^\top \boldsymbol{G}^\top \boldsymbol{z}_2 - \boldsymbol{z}_1^\top \boldsymbol{G}^\top \boldsymbol{C}_1 \boldsymbol{G}\boldsymbol{z}_1 + \boldsymbol{z}_2^\top \Big[\boldsymbol{\Phi}\boldsymbol{\theta} + \boldsymbol{\Psi} + \boldsymbol{B}\boldsymbol{u} + \boldsymbol{J}\Big(\boldsymbol{S}(\boldsymbol{\omega})\boldsymbol{R}_i^b\boldsymbol{\omega}_d - \boldsymbol{R}_i^b\dot{\boldsymbol{\omega}}_d - \dot{\boldsymbol{\alpha}}\Big)\Big] \\ & - \tilde{\boldsymbol{\theta}}^\top \boldsymbol{\Gamma}^{-1}\dot{\hat{\boldsymbol{\theta}}} \end{aligned}$$

$$= -\boldsymbol{z}_1^\top \boldsymbol{G}^\top \boldsymbol{C}_1 \boldsymbol{G} \boldsymbol{z}_1 - \boldsymbol{z}_2^\top \boldsymbol{C}_2 \boldsymbol{z}_2. \tag{C.25}$$

By applying the LaSalle-Yoshizawa theorem [34], it follows that all signals are uniformly bounded and asymptotic tracking is achieved as $(\boldsymbol{z}_1(t), \boldsymbol{z}_2(t)) \to (\boldsymbol{0}, \boldsymbol{0})$ as $t \to \infty$. The angular velocity error and the angular velocity are bounded by

$$\begin{aligned} \|\boldsymbol{\omega}_e\| &\le \|\boldsymbol{z}_2\| + \lambda_{\max}(\boldsymbol{C}_1)\|\boldsymbol{G}\|\|\boldsymbol{z}_1\| \le \Big[1 + \lambda_{\max}(\boldsymbol{C}_1)\Big]\|\boldsymbol{z}\| \\ &\triangleq k_{\omega_e}\|\boldsymbol{z}\|, \end{aligned} \tag{C.26}$$

$$\begin{aligned} \|\boldsymbol{\omega}\| &\le \|\boldsymbol{\omega}_e + \boldsymbol{R}_i^b \boldsymbol{\omega}_d\| \le k_{\omega_e}\|\boldsymbol{z}\| + \|\boldsymbol{R}_i^b\|\|\boldsymbol{\omega}_d\| \\ &\le k_{\omega_e}\|\boldsymbol{z}\| + k_{\omega_d}, \end{aligned} \tag{C.27}$$

where $\boldsymbol{z} = [\boldsymbol{z}_1^\top, \boldsymbol{z}_2^\top]^\top$.

C.3.2 Quantized Input and Output

When the outputs $\boldsymbol{\varepsilon}$ and $\boldsymbol{\omega}$ and input $\boldsymbol{u}$ are quantized with the property (C.13), we have

$$|{\varepsilon_k}^Q - \varepsilon_k| \le \delta_{\varepsilon_k},\ k = 1, 2, 3, \tag{C.28}$$

$$|{\omega_k}^Q - \omega_k| \le \delta_{\omega_k},\ k = 1, 2, 3, \tag{C.29}$$

$$|u_k^Q - u_k| \le \delta_{u_k},\ k = 1, 2, 3. \tag{C.30}$$

The quantization error of the quaternion can be expressed as

$$\boldsymbol{d}_q = \bar{\boldsymbol{q}}_{i,b} \otimes \boldsymbol{q}_{i,Q} = \begin{bmatrix} d_\eta \\ \boldsymbol{d}_\varepsilon \end{bmatrix} = \begin{bmatrix} \eta\eta^Q + \boldsymbol{\varepsilon}^\top \boldsymbol{\varepsilon}^Q \\ \eta\boldsymbol{\varepsilon}^Q - \eta^Q\boldsymbol{\varepsilon} - S(\boldsymbol{\varepsilon})\boldsymbol{\varepsilon}^Q \end{bmatrix}, \tag{C.31}$$

where $\boldsymbol{d}_\varepsilon$ is the quantization error and bounded by $\|\boldsymbol{d}_\varepsilon\| \le k_\varepsilon \|\boldsymbol{\delta}_\varepsilon\|$ from (C.28) and where $k_\varepsilon > 1$ is a positive constant, and d_η is bounded from the unity property of unit quaternion. If $\boldsymbol{q}^Q = \boldsymbol{q}$ and there is no quantization error, then $\boldsymbol{d}_q = [1\ 0\ 0\ 0]^\top$. The tracking error with the quantized value of the unit quaternion, $\boldsymbol{e}^Q$, is given by

$$\boldsymbol{e}^Q = \begin{bmatrix} \tilde{\eta}^Q \\ \tilde{\boldsymbol{\varepsilon}}^Q \end{bmatrix} = \begin{bmatrix} \eta_d\eta^Q + \boldsymbol{\varepsilon}_d^\top \boldsymbol{\varepsilon}^Q \\ \eta_d\boldsymbol{\varepsilon}^Q - \eta^Q\boldsymbol{\varepsilon}_d - S(\boldsymbol{\varepsilon}_d)\boldsymbol{\varepsilon}^Q \end{bmatrix}, \tag{C.32}$$

and can also be described by

$$\begin{aligned} \boldsymbol{e}^Q = \boldsymbol{q}_{d,b} \otimes \boldsymbol{q}_{b,Q} = \boldsymbol{e} \otimes \boldsymbol{d}_q &= \begin{bmatrix} \tilde{\eta} d_\eta - \tilde{\boldsymbol{\varepsilon}}^\top \boldsymbol{d}_\varepsilon \\ d_\eta \tilde{\boldsymbol{\varepsilon}} + \tilde{\eta}\boldsymbol{d}_\varepsilon + S(\tilde{\boldsymbol{\varepsilon}})\boldsymbol{d}_\varepsilon \end{bmatrix} \\ &= \begin{bmatrix} \tilde{\eta}^Q \\ \tilde{\boldsymbol{\varepsilon}} + (d_\eta - 1)\tilde{\boldsymbol{\varepsilon}} + \tilde{\eta}\boldsymbol{d}_\varepsilon + S(\tilde{\boldsymbol{\varepsilon}})\boldsymbol{d}_\varepsilon \end{bmatrix} \triangleq \begin{bmatrix} \tilde{\eta}^Q \\ \tilde{\boldsymbol{\varepsilon}} + \boldsymbol{d}_{\tilde{\varepsilon}} \end{bmatrix}, \end{aligned} \tag{C.33}$$

where the value of $\boldsymbol{d}_{\tilde{\varepsilon}}$ depends on the quantization error that is bounded by (C.28). If there is no quantization error, $\boldsymbol{d}_{\tilde{\varepsilon}} = \boldsymbol{0}$.
The quantized angular velocity $\boldsymbol{\omega}^Q$ is expressed as

$$\boldsymbol{\omega}^Q = \boldsymbol{\omega} + \boldsymbol{d}_\omega, \tag{C.34}$$

where $\boldsymbol{d}_\omega$ is the quantization error and is bounded by $\|\boldsymbol{d}_\omega\| \leq \|[\delta_{\omega_1}\ \delta_{\omega_2}\ \delta_{\omega_3}]^\top\| = \|\boldsymbol{\delta}_\omega\| \triangleq \delta_\omega$ from (C.29).
To propose a suitable control scheme, the quantized input $\boldsymbol{u}^Q(t)$ is decomposed into two parts

$$\boldsymbol{u}^Q(t) = \boldsymbol{u}(t) + \boldsymbol{d}_u(t), \tag{C.35}$$

where $\boldsymbol{d}_u$ is the quantization error of the input, which is bounded by $\|\boldsymbol{d}_u\| \leq \|[\delta_{u1}\ \delta_{u2}\ \delta_{u3}]^\top\| = \|\boldsymbol{\delta}_u\| \triangleq \delta_u$, from (C.30).
The adaptive controller is designed as

$$\boldsymbol{u}^Q(t) = Q(\boldsymbol{u}), \tag{C.36}$$

$$\boldsymbol{u}(t) = \boldsymbol{B}^{-1}\Big[-\boldsymbol{G}^Q\boldsymbol{z}_1^Q - \boldsymbol{C}_2\boldsymbol{z}_2^Q - \boldsymbol{\Phi}^Q\hat{\boldsymbol{\theta}} - \boldsymbol{\Psi}^Q - \boldsymbol{J}\Big(\boldsymbol{S}(\boldsymbol{\omega}^Q)\boldsymbol{R}_i^Q\boldsymbol{\omega}_d - \boldsymbol{R}_i^Q\dot{\boldsymbol{\omega}}_d - \bar{\boldsymbol{\alpha}}^Q\Big)\Big], \tag{C.37}$$

$$\dot{\hat{\boldsymbol{\theta}}} = \mathrm{Proj}\{\boldsymbol{\Gamma}\boldsymbol{\Phi}^Q\boldsymbol{z}_2^Q\}, \tag{C.38}$$

where $\mathrm{Proj}\{\cdot\}$ is the projection operator given in [34], and

$$\boldsymbol{z}_1^Q = \begin{bmatrix} 1 \mp \tilde{\eta}^Q \\ \tilde{\boldsymbol{\varepsilon}}^Q \end{bmatrix}, \tag{C.39}$$

$$\boldsymbol{z}_2^Q = \boldsymbol{\omega}_e^Q - \boldsymbol{\alpha}^Q, \tag{C.40}$$

$$\boldsymbol{G}(\boldsymbol{e}^Q)^\top = \begin{bmatrix} \pm(\tilde{\boldsymbol{\varepsilon}}^Q)^\top \\ \tilde{\eta}^Q\boldsymbol{I} + \boldsymbol{S}(\tilde{\boldsymbol{\varepsilon}}^Q) \end{bmatrix}, \tag{C.41}$$

$$\boldsymbol{\alpha}^Q = -\boldsymbol{C}_1\boldsymbol{G}^Q\boldsymbol{z}_1^Q = \mp\boldsymbol{C}_1\tilde{\boldsymbol{\varepsilon}}^Q, \tag{C.42}$$

$$\boldsymbol{\Psi}^Q = -\boldsymbol{S}(\boldsymbol{\omega}^Q)(\boldsymbol{J}\boldsymbol{\omega}^Q) - \boldsymbol{g}(\boldsymbol{q}^Q), \tag{C.43}$$

$$\boldsymbol{\Phi}^Q = \mathrm{diag}(-\boldsymbol{\omega}^Q), \tag{C.44}$$

$$\boldsymbol{g}(\boldsymbol{q}^Q) = -\boldsymbol{S}(\boldsymbol{r}_g^b)\boldsymbol{R}_i^Q\boldsymbol{f}_g^i, \tag{C.45}$$

$$\bar{\boldsymbol{\alpha}}^Q \triangleq \mp\frac{1}{2}\boldsymbol{C}_1\Big[\tilde{\eta}^Q\boldsymbol{I} + \boldsymbol{S}(\tilde{\boldsymbol{\varepsilon}}^Q)\Big]\boldsymbol{\omega}_e^Q, \tag{C.46}$$

$$\boldsymbol{\omega}_e^Q = \boldsymbol{\omega}^Q - \boldsymbol{R}_i^Q\boldsymbol{\omega}_d, \tag{C.47}$$

$$\boldsymbol{R}_i^Q = \boldsymbol{R}_b^Q\boldsymbol{R}_i^b, \tag{C.48}$$

where $\boldsymbol{R}_b^Q$ is the rotation due to the quantization error. It is noted that the following manipulation is used in (C.42).

$$\boldsymbol{G}^Q \boldsymbol{z}_1^Q = \pm\tilde{\boldsymbol{\varepsilon}}^Q - \tilde{\eta}^Q\tilde{\boldsymbol{\varepsilon}}^Q + \tilde{\boldsymbol{\varepsilon}}^Q\tilde{\eta}^Q + (\boldsymbol{S}(\tilde{\boldsymbol{\varepsilon}})^Q)^\top\tilde{\boldsymbol{\varepsilon}}^Q = \pm\tilde{\boldsymbol{\varepsilon}}^Q. \tag{C.49}$$

Remark 5. *The projection operator Proj$\{\cdot\}$ in* (C.38) *ensures that the estimates and estimation errors are nonzero and within known bounds, that is $\|\hat{\boldsymbol{\theta}}\| \leq k_\theta$ and $\|\tilde{\boldsymbol{\theta}}\| \leq k_\theta$, and has the property $-\tilde{\boldsymbol{\theta}}^\top\boldsymbol{\Gamma}^{-1}Proj(\boldsymbol{\tau}) \leq -\tilde{\boldsymbol{\theta}}^\top\boldsymbol{\Gamma}^{-1}\boldsymbol{\tau}$, which are helpful to guarantee the closed-loop stability.*

Remark 6. *Only the quantized output can be used in the designed controller. Since the quantized output is used in the design of the virtual controller $\boldsymbol{\alpha}^Q$ in* (C.42)*, the derivative of the virtual controller is discontinuous and can not be used in the design of the controller. Instead, a function $\bar{\boldsymbol{\alpha}}^Q$ is used in* (C.46)*, which is designed as if the output is not quantized.*

C.4 Stability Analysis

To analyze the closed-loop system stability, we first establish some preliminary results as stated in the following lemma.

Lemma 1. *The effects of output quantization are bounded by the following inequalities:*

$$\text{(i)}\ \boldsymbol{\omega}_e^Q \leq \boldsymbol{\omega}_e + \boldsymbol{\delta}_{\omega_e}, \tag{C.50}$$
$$\text{(ii)}\ \boldsymbol{z}_2^Q \leq \boldsymbol{z}_2 + \boldsymbol{\delta}_{z_2}, \tag{C.51}$$
$$\text{(iii)}\ \|\boldsymbol{G}\boldsymbol{z}_1 - \boldsymbol{G}^Q\boldsymbol{z}_1^Q\| \leq \delta_{z_1}, \tag{C.52}$$
$$\text{(iv)}\ \|\boldsymbol{R}_i^Q - \boldsymbol{R}_i^b\| \leq \delta_R, \tag{C.53}$$
$$\text{(v)}\ \|\boldsymbol{\Psi} - \boldsymbol{\Psi}^Q\| \leq \delta_{\Psi_1} + \delta_{\Psi_2}\|\boldsymbol{z}\|, \tag{C.54}$$
$$\text{(vi)}\ \|\boldsymbol{S}(\boldsymbol{\omega})\boldsymbol{R}_i^b - \boldsymbol{S}(\boldsymbol{\omega}^Q)\boldsymbol{R}_i^Q\| \leq \delta_{S_1} + \delta_{S_2}\|\boldsymbol{z}\|, \tag{C.55}$$
$$\text{(vii)}\ \|\bar{\boldsymbol{\alpha}}^Q - \dot{\boldsymbol{\alpha}}\| \leq \delta_{\bar{\alpha}_1} + \delta_{\bar{\alpha}_2}\|\boldsymbol{z}\|, \tag{C.56}$$
$$\text{(viii)}\ \|\boldsymbol{\Phi} - \boldsymbol{\Phi}^Q\| \leq \delta_\omega. \tag{C.57}$$

Proof: With the use of (C.8), (C.31), (C.34), (C.47), and (C.48), we have

$$\begin{aligned}
\boldsymbol{\omega}_e^Q &= \boldsymbol{\omega} + \boldsymbol{d}_\omega - \boldsymbol{R}_b^Q\boldsymbol{R}_i^b\boldsymbol{\omega}_d \\
&\leq \boldsymbol{\omega}_e + \Big(\Big[2d_\eta\boldsymbol{S}(\boldsymbol{d}_\varepsilon) - 2\boldsymbol{S}^2(\boldsymbol{d}_\varepsilon)^\top\Big]\boldsymbol{R}_i^b\boldsymbol{\omega}_d + \boldsymbol{\delta}_\omega\Big) \\
&\leq \boldsymbol{\omega}_e + \Big(2k_\varepsilon\Big[\boldsymbol{S}(\boldsymbol{\delta}_\varepsilon) + \boldsymbol{S}^2(\boldsymbol{\delta}_\varepsilon)\Big]\boldsymbol{R}_i^b\boldsymbol{\omega}_d + \boldsymbol{\delta}_\omega\Big) \triangleq \boldsymbol{\omega}_e + \boldsymbol{\delta}_{\omega_e}.
\end{aligned} \tag{C.58}$$

Using (C.28), (C.40), (C.42), and (C.50), we have

$$\begin{aligned}\boldsymbol{z}_2^Q &\le \boldsymbol{\omega}_e + \boldsymbol{\delta}_{\omega_e} \pm \boldsymbol{C}_1 \tilde{\boldsymbol{\varepsilon}}^Q \\ &\le \boldsymbol{\omega}_e + \boldsymbol{\delta}_{\omega_e} - \boldsymbol{\alpha} \pm \boldsymbol{C}_1 \boldsymbol{d}_{\tilde{\varepsilon}} \\ &\le \boldsymbol{z}_2 + (\boldsymbol{\delta}_{\omega_e} + \boldsymbol{C}_1 k_\varepsilon \boldsymbol{\delta}_\varepsilon) \triangleq \boldsymbol{z}_2 + \boldsymbol{\delta}_{z_2}. \end{aligned} \tag{C.59}$$

From the definition in (C.33) and the fact that $\boldsymbol{G}\boldsymbol{z}_1 = \pm\tilde{\boldsymbol{\varepsilon}}$ and $\boldsymbol{G}^Q \boldsymbol{z}_1^Q = \pm\tilde{\boldsymbol{\varepsilon}}^Q$, it is shown that

$$\|\boldsymbol{G}\boldsymbol{z}_1 - \boldsymbol{G}^Q \boldsymbol{z}_1^Q\| = \|\pm\tilde{\boldsymbol{\varepsilon}} - (\pm\tilde{\boldsymbol{\varepsilon}}^Q)\| \le \|\boldsymbol{d}_{\tilde{\varepsilon}}\| \le \|k_\varepsilon \boldsymbol{\delta}_\varepsilon\| \triangleq \delta_{z_1}. \tag{C.60}$$

By using (C.31) and (C.48) and the property of (C.8) and (C.9), we have

$$\begin{aligned}\|\boldsymbol{R}_i^Q - \boldsymbol{R}_i^b\| &= \|\boldsymbol{R}_b^Q \boldsymbol{R}_i^b - \boldsymbol{R}_i^b\| = \|(\boldsymbol{R}_b^Q - \boldsymbol{I})\boldsymbol{R}_i^b\| \\ &\le \|-2d_\eta \boldsymbol{S}(\boldsymbol{d}_\varepsilon) + 2\boldsymbol{S}^2(\boldsymbol{d}_\varepsilon)^\top\| \|\boldsymbol{R}_i^b\| \\ &\le 2\Big[k_\varepsilon \|\boldsymbol{\delta}_\varepsilon\| + k_\varepsilon^2 \|\boldsymbol{\delta}_\varepsilon\|^2\Big] \triangleq \delta_R. \end{aligned} \tag{C.61}$$

Using (C.4), (C.13), (C.31), (C.34), (C.43), (C.45), and (C.48), together with the property of (C.8) and Assumption 1, we have

$$\begin{aligned}\|\boldsymbol{\Psi} - \boldsymbol{\Psi}^Q\| &\le \|-\boldsymbol{S}(\boldsymbol{\omega})(\boldsymbol{J}\boldsymbol{\omega}) + \boldsymbol{S}(\boldsymbol{\omega}+\boldsymbol{d}_\omega)(\boldsymbol{J}(\boldsymbol{\omega}+\boldsymbol{d}_\omega)) + \boldsymbol{S}(\boldsymbol{r}_g^b)\boldsymbol{R}_i^b \boldsymbol{f}_g^i - \boldsymbol{S}(\boldsymbol{r}_g^b)\boldsymbol{R}_i^Q \boldsymbol{f}_g^i\| \\ &\le \Big[\lambda_{\max}(\boldsymbol{J})\Big(2k_{\omega_d}\|\boldsymbol{\delta}_\omega\| + \|\boldsymbol{\delta}_\omega\|^2\Big) + \|\boldsymbol{r}_g^b\|\delta_R mg\Big] + \Big[2\lambda_{\max}(\boldsymbol{J})\|\boldsymbol{\delta}_\omega\| k_{\omega_e}\Big]\|\boldsymbol{z}\| \\ &\triangleq \delta_{\Psi_1} + \delta_{\Psi_2}\|\boldsymbol{z}\|. \end{aligned} \tag{C.62}$$

By using (C.8), (C.27), (C.31), (C.34), (C.48) and (C.61), we have

$$\begin{aligned}\|\boldsymbol{S}(\boldsymbol{\omega})\boldsymbol{R}_i^b - \boldsymbol{S}(\boldsymbol{\omega}^Q)\boldsymbol{R}_i^Q\| &\le \|-\boldsymbol{S}(\boldsymbol{\omega})[-2d_\eta \boldsymbol{S}(\boldsymbol{d}_\varepsilon) + 2\boldsymbol{S}^2(\boldsymbol{d}_\varepsilon)^\top]\boldsymbol{R}_i^b - \boldsymbol{S}(\boldsymbol{d}_\omega)\boldsymbol{R}_i^Q\| \\ &\le \|\boldsymbol{\omega}\|\delta_R + \|\boldsymbol{\delta}_\omega\| \\ &\le (k_{\omega_d}\delta_R + \delta_\omega) + (k_{\omega_e}\delta_R)\|\boldsymbol{z}\| \triangleq \delta_{S_1} + \delta_{S_2}\|\boldsymbol{z}\|. \end{aligned} \tag{C.63}$$

By using (C.20), (C.26) (C.42), (C.46), and (C.50), we have

$$\begin{aligned}\|\bar{\boldsymbol{\alpha}}^Q - \dot{\boldsymbol{\alpha}}\| &= \|\frac{1}{2}\boldsymbol{C}_1\Big[\mp[\tilde{\eta}^Q \boldsymbol{I} + \boldsymbol{S}(\tilde{\boldsymbol{\varepsilon}}^Q)]\boldsymbol{\omega}_e^Q - [\mp[\tilde{\eta}\boldsymbol{I} + \boldsymbol{S}(\tilde{\boldsymbol{\varepsilon}})]]\boldsymbol{\omega}_e\Big]\| \\ &\le \frac{1}{2}\lambda_{\max}(\boldsymbol{C}_1)\Big(2\|\boldsymbol{\omega}_e\| + \|\boldsymbol{\delta}_{\omega_e}\|\Big) \\ &\le \lambda_{\max}(\boldsymbol{C}_1)(\frac{1}{2}\|\boldsymbol{\delta}_{\omega_e}\| + k_{\omega_e}\|\boldsymbol{z}\|) \triangleq \delta_{\bar{\alpha}_1} + \delta_{\bar{\alpha}_2}\|\boldsymbol{z}\|. \end{aligned} \tag{C.64}$$

From (C.5), (C.34) and (C.44), we have

$$\|\boldsymbol{\Phi} - \boldsymbol{\Phi}^Q\| \le \|\mathrm{diag}(-\boldsymbol{\omega}) - \mathrm{diag}(-\boldsymbol{\omega} - \boldsymbol{d}_\omega)\| \le \|\boldsymbol{\delta}_\omega\| = \delta_\omega. \tag{C.65}$$

We state our main results in the following theorem.

Theorem 1. *Considering the closed-loop adaptive system consisting of the plant* (C.1)-(C.2) *with output and input quantization satisfying the bounded properties* (C.28)-(C.30)*, the adaptive controller* (C.36)-(C.37)*, the update law* (C.38) *and Assumptions 1-3. If the gain matrices* $\boldsymbol{C}_1$ *and* $\boldsymbol{C}_2$ *and quantization parameters* $\boldsymbol{\delta}_\varepsilon$*,* $\boldsymbol{\delta}_\omega$ *and* $\boldsymbol{\delta}_u$ *are chosen to satisfy*

$$\frac{c_0}{2} - \delta_{V_1} \geq k > 0, \tag{C.66}$$

where c_0 *is the minimum eigenvalue of* $\boldsymbol{C}_0 = \min\{\boldsymbol{G}^\top \boldsymbol{C}_1 \boldsymbol{G}, \boldsymbol{C}_2\}$*,* k *is a positive constant, and* δ_{V_1} *is defined as*

$$\delta_{V_1} = \delta_{\Psi_2} + \delta_{S_2}\lambda_{\max}(\boldsymbol{J})k_{\omega_d} + \delta_{\bar{\alpha}_2}\lambda_{\max}(\boldsymbol{J}), \tag{C.67}$$

then, all signals in the closed loop system are ensured to be uniformly bounded. The error signals will converge to a compact set, i.e.,

$$\|\boldsymbol{z}(t)\| \leq \sqrt{\frac{\delta_Q}{k}}, \tag{C.68}$$

where

$$\delta_Q = \delta_{\theta_1} + \frac{1}{2c_0}\delta_{V_2}^2, \tag{C.69}$$

$$\delta_{\theta_1} = k_\theta \delta_\omega \|\boldsymbol{\delta}_{z_2}\| + k_\theta \|\boldsymbol{\delta}_{z_2}\| k_{\omega_d}, \tag{C.70}$$

$$\begin{aligned}\delta_{V_2} = {} & \lambda_{\max}(\boldsymbol{C}_2)\|\boldsymbol{\delta}_{z_2}\| + \delta_{z_1} + \delta_{\Psi_1} + \delta_{S_1}\lambda_{\max}(\boldsymbol{J})k_{\omega_d} + \delta_R\lambda_{\max}(\boldsymbol{J})k_{\dot{\omega}_d} + \delta_{\bar{\alpha}_1}\lambda_{\max}(\boldsymbol{J}) \\ & + \delta_{\theta_2} + \delta_{Bu},\end{aligned} \tag{C.71}$$

$$\delta_{\theta_2} = k_\theta \delta_\omega + k_\theta k_{\omega_e}\|\boldsymbol{\delta}_{z_2}\|. \tag{C.72}$$

Proof: Consider the Lyapunov function candidate

$$V(\boldsymbol{z}, \tilde{\boldsymbol{\theta}}, t) = \boldsymbol{z}_1^\top \boldsymbol{z}_1 + \frac{1}{2}\boldsymbol{z}_2^\top \boldsymbol{J}\boldsymbol{z}_2 + \frac{1}{2}\tilde{\boldsymbol{\theta}}^\top \boldsymbol{\Gamma}^{-1}\tilde{\boldsymbol{\theta}}. \tag{C.73}$$

Following (C.36)-(C.38), the derivative of (C.73) is given as

$$\begin{aligned}\dot{V} = {} & \boldsymbol{z}_1^\top \boldsymbol{G}^\top \boldsymbol{z}_2 - \boldsymbol{z}_1^\top \boldsymbol{G}^\top \boldsymbol{C}_1 \boldsymbol{G}\boldsymbol{z}_1 + \boldsymbol{z}_2^\top \Big[\boldsymbol{\Phi}\boldsymbol{\theta} + \boldsymbol{\Psi} + \boldsymbol{B}\boldsymbol{u}^Q + \boldsymbol{J}\Big(\boldsymbol{S}(\boldsymbol{\omega})\boldsymbol{R}_i^b\boldsymbol{\omega}_d - \boldsymbol{R}_i^b\dot{\boldsymbol{\omega}}_d - \dot{\boldsymbol{\alpha}}\Big)\Big] \\ & - \tilde{\boldsymbol{\theta}}^\top \boldsymbol{\Gamma}^{-1}\dot{\hat{\boldsymbol{\theta}}} \\ \leq {} & - \boldsymbol{z}_1^\top \boldsymbol{G}^\top \boldsymbol{C}_1 \boldsymbol{G}\boldsymbol{z}_1 - \boldsymbol{z}_2^\top \boldsymbol{C}_2 \boldsymbol{z}_2^Q + \boldsymbol{z}_2^\top (\boldsymbol{G}\boldsymbol{z}_1 - \boldsymbol{G}^Q \boldsymbol{z}_1^Q) + \boldsymbol{z}_2^\top (\boldsymbol{\Psi} - \boldsymbol{\Psi}^Q) \\ & + \boldsymbol{z}_2^\top \boldsymbol{J}(\boldsymbol{S}(\boldsymbol{\omega})\boldsymbol{R}_i^b - \boldsymbol{S}(\boldsymbol{\omega}^Q)\boldsymbol{R}_i^Q)\boldsymbol{\omega}_d + \boldsymbol{z}_2^\top \boldsymbol{J}\Big(\boldsymbol{R}_i^Q - \boldsymbol{R}_i^b\Big)\dot{\boldsymbol{\omega}}_d + \boldsymbol{z}_2^\top \boldsymbol{J}(\bar{\boldsymbol{\alpha}}^Q - \dot{\boldsymbol{\alpha}}) \\ & + \boldsymbol{z}_2^\top \boldsymbol{B}\boldsymbol{d}_u + \Big[\boldsymbol{z}_2^\top (\boldsymbol{\Phi}\boldsymbol{\theta} - \boldsymbol{\Phi}^Q\hat{\boldsymbol{\theta}}) - \tilde{\boldsymbol{\theta}}^\top \boldsymbol{\Phi}^Q \boldsymbol{z}_2^Q\Big].\end{aligned} \tag{C.74}$$

Using (C.30), the term containing the quantization error from the input in (C.74) satisfies

$$\boldsymbol{z}_2^\top \boldsymbol{B}\boldsymbol{d}_u \leq \|\boldsymbol{z}_2\|\|\boldsymbol{B}\|\delta_u \leq \delta_u\|\boldsymbol{B}\|\|\boldsymbol{z}\| \triangleq \delta_{Bu}\|\boldsymbol{z}\|. \tag{C.75}$$

By using (C.5), (C.34), (C.38), (C.44), (C.51), (C.27) and Assumption 2, the last terms in (C.74) satisfy the inequality

$$\begin{aligned}
\boldsymbol{z}_2^\top(\boldsymbol{\Phi}\boldsymbol{\theta} - \boldsymbol{\Phi}^Q\hat{\boldsymbol{\theta}}) - \tilde{\boldsymbol{\theta}}^\top\boldsymbol{\Phi}^Q\boldsymbol{z}_2^Q &= \boldsymbol{\theta}^\top\boldsymbol{\Phi}\boldsymbol{z}_2 - \boldsymbol{\theta}^\top\boldsymbol{\Phi}^Q\boldsymbol{z}_2 + \tilde{\boldsymbol{\theta}}^\top\boldsymbol{\Phi}^Q\boldsymbol{z}_2 - \tilde{\boldsymbol{\theta}}^\top\boldsymbol{\Phi}^Q\boldsymbol{z}_2^Q \\
&\leq \|\boldsymbol{\theta}\|\|\boldsymbol{\Phi} - \boldsymbol{\Phi}^Q\|\|\boldsymbol{z}_2\| + \|\tilde{\boldsymbol{\theta}}\|\|\boldsymbol{\Phi}^Q\|\|\boldsymbol{z}_2 - \boldsymbol{z}_2^Q\| \\
&\leq k_\theta\delta_\omega\|\boldsymbol{z}\| + k_\theta(\|\boldsymbol{\omega}\| + \|\boldsymbol{\delta}_\omega\|)\|\boldsymbol{\delta}_{z_2}\| \\
&\leq (k_\theta\delta_\omega\|\boldsymbol{\delta}_{z_2}\| + k_\theta\|\boldsymbol{\delta}_{z_2}\|k_{\omega_d}) + (k_\theta\delta_\omega + k_\theta k_{\omega_e}\|\boldsymbol{\delta}_{z_2}\|)\|\boldsymbol{z}\| \\
&\triangleq \delta_{\theta_1} + \delta_{\theta_2}\|\boldsymbol{z}\|.
\end{aligned} \tag{C.76}$$

By using Young's inequality, the properties in Lemma 1, (C.75), (C.76) and Assumption 1, (C.74) becomes

$$\begin{aligned}
\dot{V} \leq & -\boldsymbol{z}_1^\top\boldsymbol{G}^\top\boldsymbol{C}_1\boldsymbol{G}\boldsymbol{z}_1 - \boldsymbol{z}_2^\top\boldsymbol{C}_2\boldsymbol{z}_2 + \lambda_{\max}(\boldsymbol{C}_2)\|\boldsymbol{\delta}_{z_2}\|\|\boldsymbol{z}\| + \delta_{z_1}\|\boldsymbol{z}\| + \delta_{\Psi_1}\|\boldsymbol{z}\| + \delta_{\Psi_2}\|\boldsymbol{z}\|^2 \\
& + \delta_{S_1}\lambda_{\max}(\boldsymbol{J})k_{\omega_d}\|\boldsymbol{z}\| + \delta_{S_2}\lambda_{\max}(\boldsymbol{J})k_{\omega_d}\|\boldsymbol{z}\|^2 + \delta_R\lambda_{\max}(\boldsymbol{J})k_{\dot{\omega}_d}\|\boldsymbol{z}\| + \delta_{Bu}\|\boldsymbol{z}\| \\
& + \delta_{\bar{\alpha}_1}\lambda_{\max}(\boldsymbol{J})\|\boldsymbol{z}\| + \delta_{\bar{\alpha}_2}\lambda_{\max}(\boldsymbol{J})\|\boldsymbol{z}\|^2 + \delta_{\theta_1} + \delta_{\theta_2}\|\boldsymbol{z}\| \\
\leq & -c_0\|\boldsymbol{z}\|^2 + \delta_{\theta_1} + \delta_{V_2}\|\boldsymbol{z}\| + \delta_{V_1}\|\boldsymbol{z}\|^2 \\
\leq & -(\frac{c_0}{2} - \delta_{V_1})\|\boldsymbol{z}\|^2 + \delta_{\theta_1} + \frac{1}{2c_0}\delta_{V_2}^2 \\
\leq & -k\|\boldsymbol{z}\|^2 + \delta_Q < 0, \quad \forall\|\boldsymbol{z}\| > \sqrt{\delta_Q/k}.
\end{aligned} \tag{C.77}$$

From (C.73) and (C.77) and by applying the LaSalle-Yoshizawa theorem, it follows that $\boldsymbol{z}_1$, $\boldsymbol{z}_2$ and $\tilde{\boldsymbol{\theta}}$ are bounded and satisfy (C.68) under condition (C.66). From (C.37) and Lemma 1, it follows that the control input $\boldsymbol{u}$, where only the quantized output is measured, also is bounded. Thus, all signals in the closed loop system are bounded. Tracking of the desired reference signal is achieved, with a bounded tracking error given in (C.68).

Remark 7. *The value of δ_Q depends on the quantization parameters, and higher values of the quantization intervals will increase δ_Q. If there is no quantization, $\delta_Q = 0$. In principle, the quantization level can be chosen arbitrarily as long as the inequality* (C.66) *is satisfied, where δ_{V_1} depends on the quantization parameters $\boldsymbol{\delta}_\omega$ and $\boldsymbol{\delta}_\varepsilon$, and c_0 depends on the control design parameters. Therefore,* (C.66) *provides some insights on how to choose these quantization parameters.*

Next, we consider the case where external disturbances $\boldsymbol{\tau}_d$, assumed unknown

but bounded by $\|\boldsymbol{\tau}_d\| \leq k_{\tau_d}$, are present to the system, and the attitude dynamics are described by

$$\boldsymbol{J}\dot{\boldsymbol{\omega}} = \boldsymbol{\Psi}(\boldsymbol{q}, \boldsymbol{\omega}) + \boldsymbol{\Phi}(\boldsymbol{\omega})\boldsymbol{\theta} + \boldsymbol{B}\boldsymbol{u} + \boldsymbol{\tau}_d. \tag{C.78}$$

Corollary 1. *Let Assumptions 1-3 hold. Consider the closed-loop adaptive system consisting of the plant* (C.1), (C.78) *with output and input quantization satisfying the bounded properties* (C.28)-(C.30), *the adaptive controller* (C.36)-(C.37) *and the update law* (C.38). *Choosing the gain matrices* $\boldsymbol{C}_1$ *and* $\boldsymbol{C}_2$ *and quantization parameters* $\boldsymbol{\delta}_\varepsilon$, $\boldsymbol{\delta}_\omega$ *and* $\boldsymbol{\delta}_u$ *to satisfy* (C.66), *all signals in the closed loop system are ensured to be uniformly bounded. The error signals will converge to a compact set, i.e.,*

$$\|\boldsymbol{z}(t)\| \leq \sqrt{\frac{\delta_{Qdist}}{k}}, \tag{C.79}$$

where

$$\delta_{Qdist} = \delta_{\theta_1} + \frac{1}{2c_0}(\delta_{V_2} + k_{\tau_d})^2. \tag{C.80}$$

The proof follows along the same lines as the proof of Theorem 1.

Remark 8. *The proposed control method considered in this paper needs information of all system states, which is reasonable for rigid body systems where the attitude and the angular velocity are measured by sensors. If some states are not available, an observer will be needed. Another limitation is that only a bounded type of quantizer is considered in this paper, where the quantization error is bounded. The proposed method can be extended to compensate for unbounded quantization error caused by the logarithmic or hysteresis quantizers.*

C.5 Experimental Results

The proposed controller was tested on the Quanser Aero helicopter system, shown in Fig. C.3. This is a two-rotor laboratory equipment for flight control-based experiments. The setup has a horizontal position of the main thruster and a vertical position of the tail thruster, which resembles a helicopter with two propellers driven by two DC motors. This is a MIMO system with 2 DOF, and the helicopter can rotate around two axes where each input affects both rotational directions. The body fixed coordinate frame is visualized in Fig. C.3, and the inertial frame is coinciding with the body frame when $\boldsymbol{q} = [\pm 1\ 0\ 0\ 0]^\top$. The mathematical model is described by (C.1) and (C.2), and the parameters used for simulation and experiments are

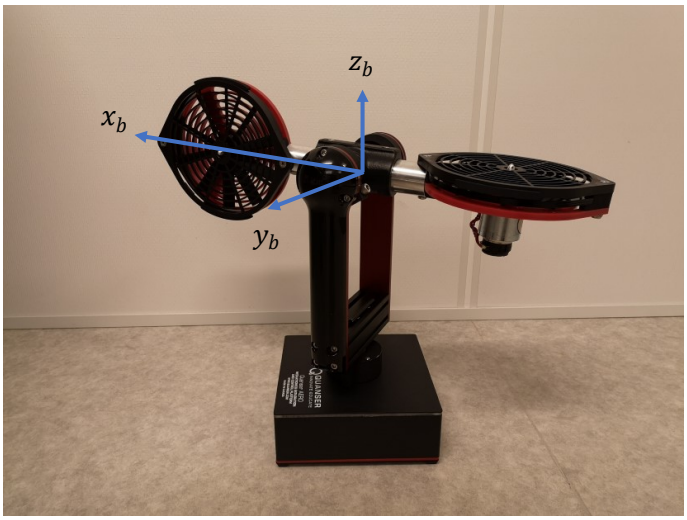

Figure C.3: Quanser Aero helicopter system with body coordinate frame.

Table C.1: Helicopter Parameters.

Symbol	Value	Units
$\boldsymbol{J}$	$\text{diag}(0.0218, 0.0217, 0.0218)$	kgm^2
m	1.075	kg
g	9.81	m/s^2
$\boldsymbol{r}_b^g$	$[0 \;\; 0 \;\; -0.0038]^\top$	m
$\boldsymbol{B}$	$\begin{bmatrix} 1 & 0 & 0 \\ 0 & 0.0011 & 0.0011 \\ 0 & -0.0014 & 0.00176 \end{bmatrix}$	Nm/V

shown in Table C.1. The initial states and estimated parameters were chosen as $\boldsymbol{q}(t_0) = [1\ 0\ 0\ 0]^\top$, $\boldsymbol{\omega}(t_0) = [0\ 0\ 0]^\top$ and $\hat{\boldsymbol{\theta}}(t_0) = [0\ 0.0070\ 0.0095]^\top$, where t_0 defines the start of experiment, and the design parameters were set to $\boldsymbol{C}_1 = 0.3\boldsymbol{I}$, $\boldsymbol{C}_2 = 0.15\boldsymbol{I}$ and $\boldsymbol{\Gamma} = 0.02\boldsymbol{I}$.

The objective was to track a sinusoidal signal where $r_d = 0$, $p_d = 40\pi/180 \sin(0.1\pi t)$, $y_d = 100\pi/180 \sin(0.05\pi t)$, given in Euler angles, that was converted to a quaternion, and also to track the angular velocities as given in (C.12), and see how the system was affected by quantization of the output and the input. The inputs have limits of $\pm$ 24 V. The length of the quantization interval for the outputs were chosen as $l_{\varepsilon_k} = l_{\omega_k} = 2/(2^R - 1),\ k = 1, 2, 3$, and for the inputs $l_{u_k} = 48/(2^R - 1),\ k = 1, 2, 3$, where R is number of bits transmitted in the communication. The system was tested with different values for R. The performance of the proposed control system was also tested subject to an external disturbance, where we set a fan to blow wind at the helicopter system.

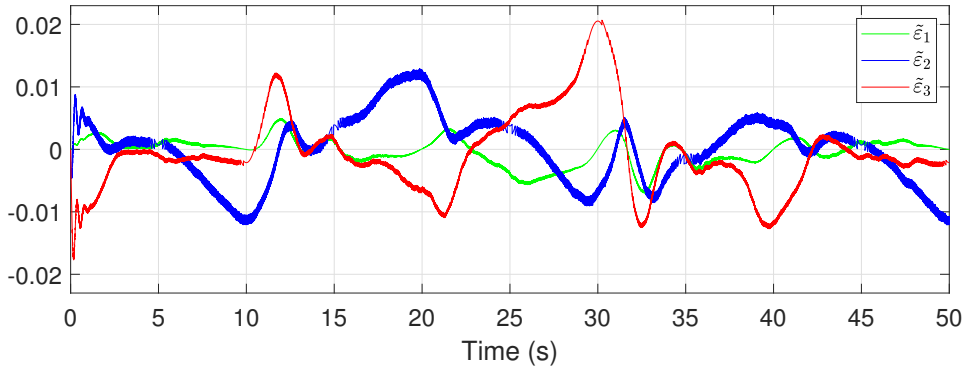

Figure C.4: Error in attitude $\tilde{\boldsymbol{\varepsilon}}$, from experiment, without quantization.

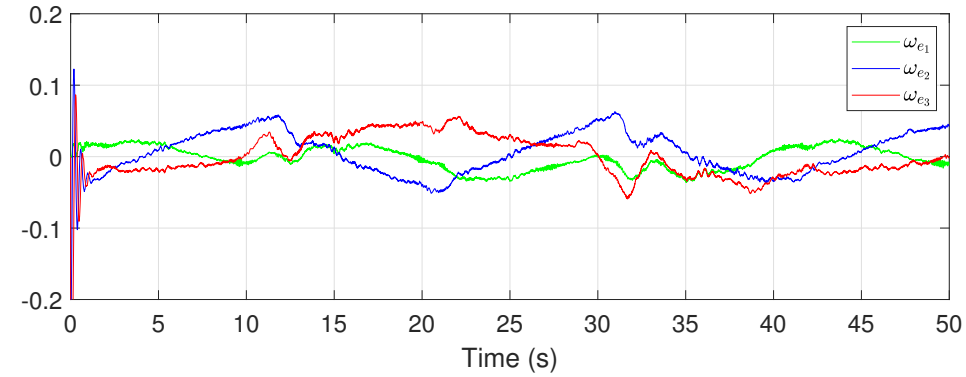

Figure C.5: Angular velocity error $\boldsymbol{\omega}_e$, from experiment, without quantization.

C.5.1 Results

The results from test without quantization are shown in Figs. C.4–C.6, showing the error in attitude $\tilde{\boldsymbol{\varepsilon}}$, the error in angular velocity $\boldsymbol{\omega}_e$, and the input $\boldsymbol{u}$, respectively. From Figs. C.4 and C.5, tracking of the desired reference signals are achieved and the tracking errors are bounded. The value of $\tilde{\varepsilon}_{(\cdot)}$ is within $[-0.02 \quad +0.02]$, that corresponds to an error of about ± 0.04 rad or ± 2.3 deg in Euler angles. The input signal in Fig. C.6 is also bounded.

The system was then tested with quantized output and input. We tested with different values for R, and plots for quantization levels chosen as $R = 8$ for the output, and $R = 6$ for the input, are shown in Figs. C.7–C.11, showing the outputs $\boldsymbol{q}^Q$ and $\boldsymbol{\omega}^Q$, the error in attitude $\tilde{\boldsymbol{\varepsilon}}^Q$, the error in angular velocity $\boldsymbol{\omega}_e^Q$ and the input $\boldsymbol{u}^Q$, respectively. The desired states are shown with a dotted line, and measured values from tests on the helicopter model are shown with a solid line. The results show that tracking is achieved and that all signals are uniformly bounded, in accordance with the findings of Theorem 1.

Next, an external disturbance was added to the system in form of wind, where the input and outputs were quantized. Figs. C.12–C.14 show the attitude error $\tilde{\boldsymbol{\varepsilon}}^Q$, the angular velocity error $\boldsymbol{\omega}_e^Q$ and the input $\boldsymbol{u}^Q$, respectively. As can be seen from

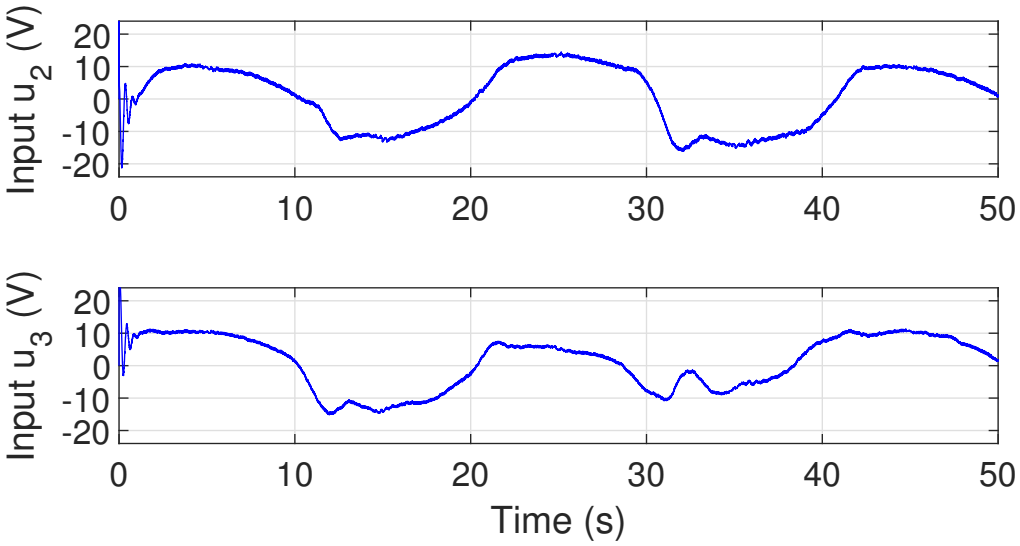

Figure C.6: Inputs u_2 and u_3 from experiment, without quantization.

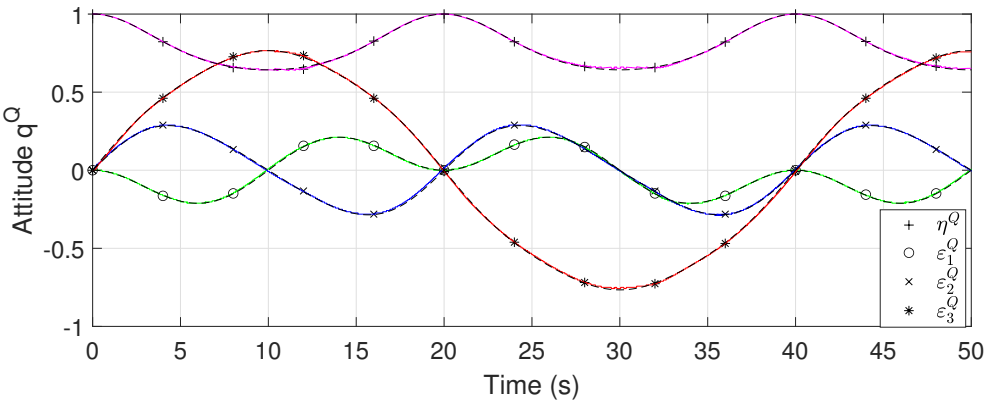

Figure C.7: Attitude $\boldsymbol{q}^Q$ from experiment with quantization.

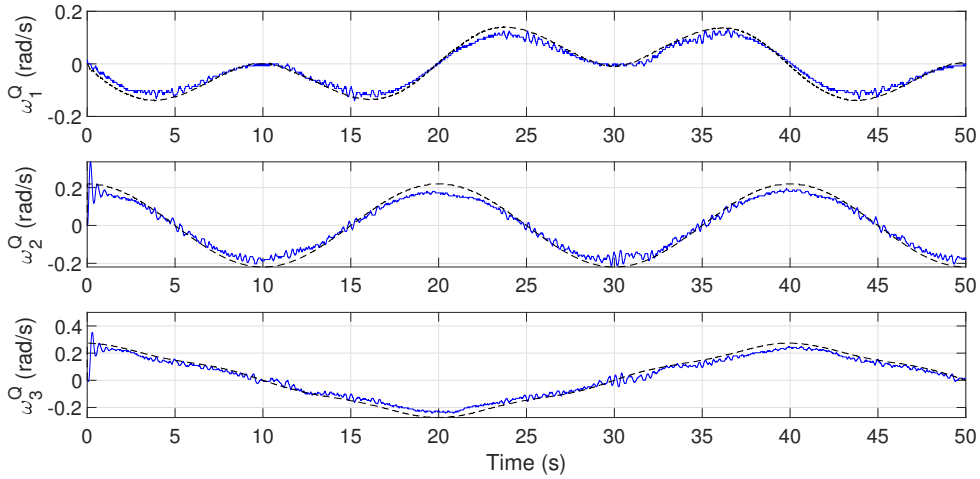

Figure C.8: Angular velocity $\boldsymbol{\omega}^Q$ from experiment with quantization.

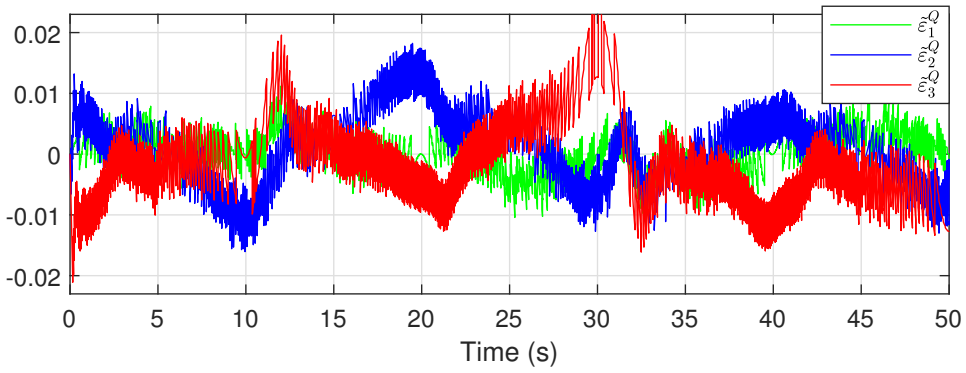

Figure C.9: Error in attitude $\tilde{\boldsymbol{\varepsilon}}^Q$ from experiment with quantization.

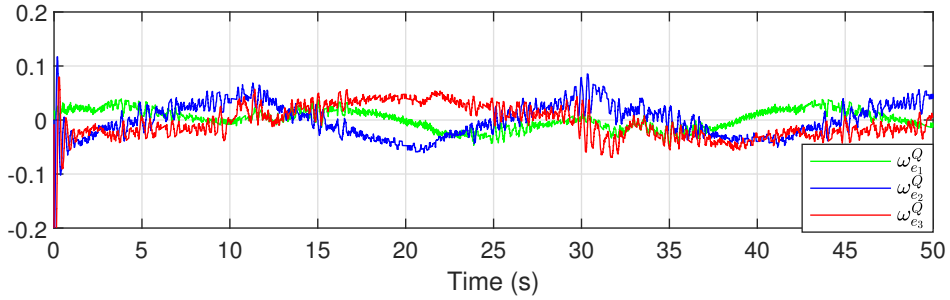

Figure C.10: Angular velocity error $\boldsymbol{\omega}_e^Q$ from experiment with quantization.

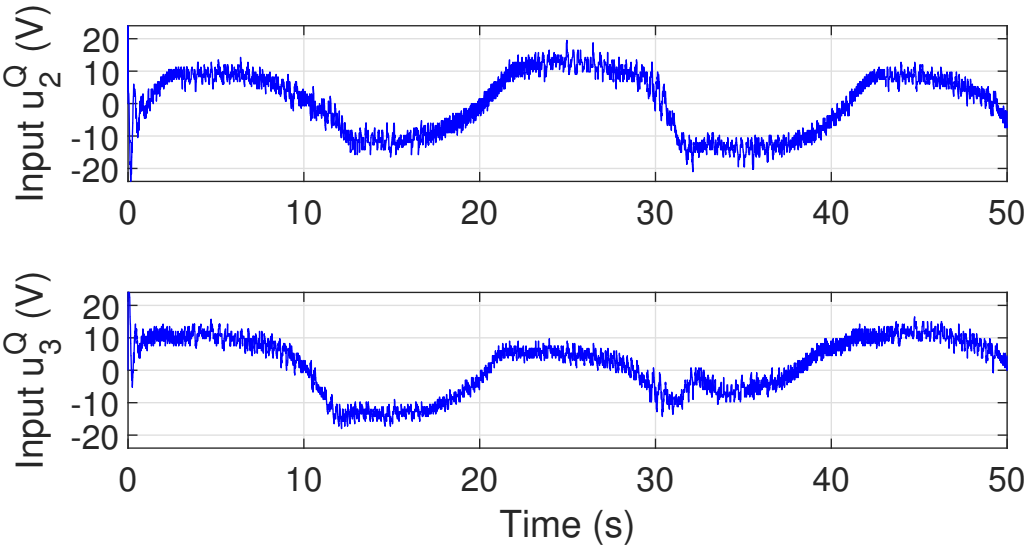

Figure C.11: Inputs u_2^Q and u_3^Q from experiment with quantization.

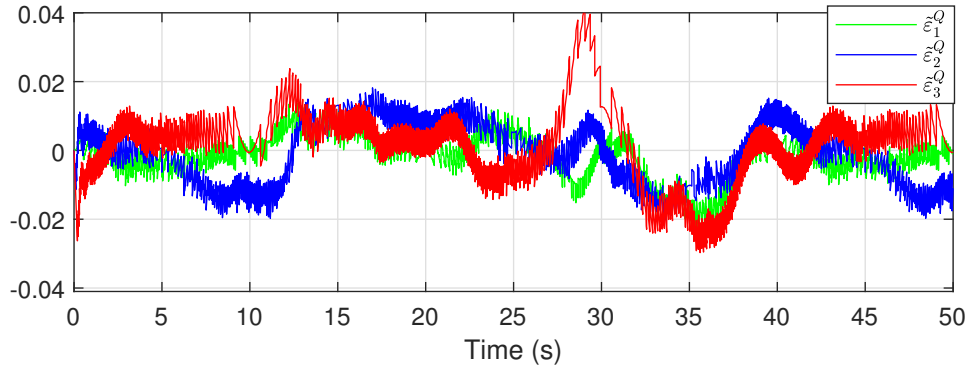

Figure C.12: Error in attitude $\tilde{\boldsymbol{\varepsilon}}^Q$ from experiment with external disturbance.

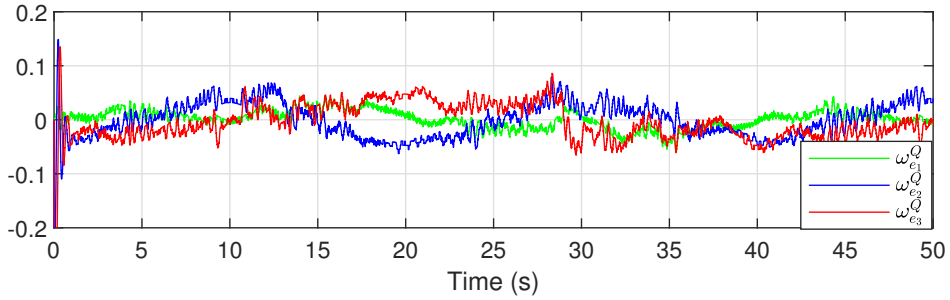

Figure C.13: Angular velocity error $\boldsymbol{\omega}_e^Q$ from experiment with external disturbance.

the plots, the errors in attitude and angular velocity are kept close to zero during tracking of the reference signals in presence of an external disturbance.

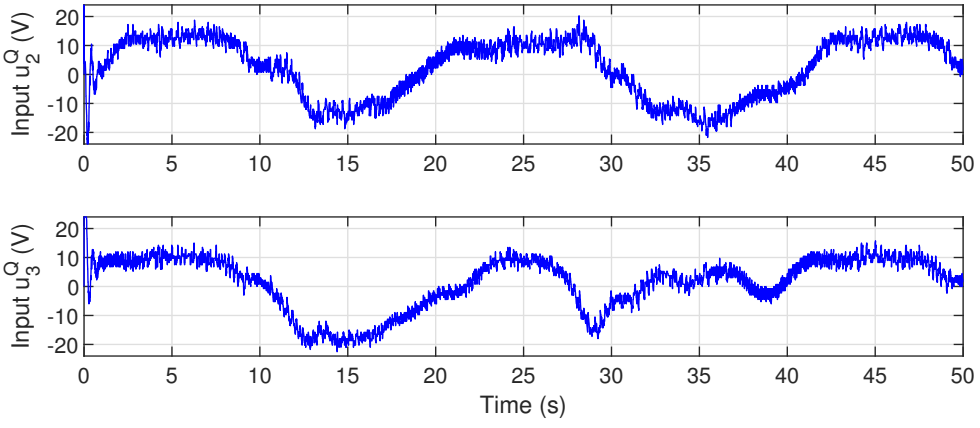

Figure C.14: Inputs u_2^Q and u_3^Q from experiment with external disturbance.

Table C.2: Tracking error for different quantization levels

z_{track} $\times 10^{-4}$	**Output $\boldsymbol{\varepsilon}^Q$, $\boldsymbol{\omega}^Q$ with $l_s = 2/(2^R-1)$**				
Input $\boldsymbol{u}^Q$ with $l_u = 48/(2^R-1)$	R	8	9	10	cont.
	6	49	51	38	38
	7	43	40	37	40
	8	45	40	39	45
	9	45	40	40	43
	10	47	40	39	38
	cont	43	35	34	35

Table C.3: Total energy use for different quantization levels

u_{total}	**Output $\boldsymbol{\varepsilon}^Q$, $\boldsymbol{\omega}^Q$ with $l_s = 2/(2^R-1)$**				
Input $\boldsymbol{u}^Q$ with $l_u = 48/(2^R-1)$	R	8	9	10	cont.
	6	8042	8168	7884	7945
	7	7881	7935	7897	8023
	8	8095	7895	7898	8017
	9	8055	7857	7959	8034
	10	8121	7970	7892	7899
	cont	8147	7854	7767	7980

C.5.2 Comparing Results

To compare the results with and without quantization, the total tracking error, z_{track}, and the total use of energy, u_{total}, were measured, where

$$z_{\text{track}} = \int_{t_0}^{t_f} (\tilde{\boldsymbol{\varepsilon}}^Q)^\top \tilde{\boldsymbol{\varepsilon}}^Q d\tau, \;\; u_{\text{total}} = \int_{t_0}^{t_f} (\boldsymbol{u}^Q)^\top \boldsymbol{u}^Q d\tau, \tag{C.81}$$

where t_0 and t_f define start and end of experiment, respectively. The experiments were run for 50 s. The tracking error and total use of energy for different values of R are shown in Tables C.2 and C.3.

From Table C.2, it is observed that for higher quantization levels, the tracking error increases. This is according to the findings of Theorem 1. For high values of R, i.e. for small quantization intervals, the system does not show a big difference in performance compared to when using continuous signals. A lower value for R is also possible, and will require less data transmission, but with the cost of higher tracking error, and also with more chattering for the input. The system is more affected by quantization of the output than of the input in terms of tracking error. Table C.4 compares the tracking error and total use of energy when an external disturbance was added. The quantization levels were chosen as $R = 8$ for the output, and $R = 6$ for the input. From this experiment, the tracking error increased when a disturbance was introduced, in accordance with the findings of Corollary 1, and also the total use of energy increased. By choosing a small quantization interval, the communication

Table C.4: Tracking error and total use of energy with and without external disturbance

	No disturbance		**External disturbance**	
	z_{track} $\times 10^{-4}$	u_{total}	z_{track} $\times 10^{-4}$	u_{total}
Continuous signals	35	7980	97	9241
Quantized signals	49	8042	119	9699

burden over a network can be reduced, and still achieve a good performance.

C.6 Conclusion

In this article, an adaptive backstepping control scheme is developed for attitude tracking using quaternions where the output and the input are quantized. The quantizer considered satisfies a bounded condition and so the quantization error is bounded. The full state is considered in the stability analysis, and with the use of constructed Lyapunov functions, all signals in the closed loop system are shown to be uniformly bounded and also tracking of a given reference signal is achieved. Experiments on a 2-DOF helicopter system supports the proof, where a uniform quantizer is tested for the system. As illustrated in the experiment, it is possible to reduce the communication burden over the network by including quantization, where a suitable quantization level must be chosen, depending on the performance requirement for the application.

References – Paper C

[1] J. T.-Y. Wen and K. Kreutz-Delgado, "The attitude control problem," *IEEE Transactions on Automatic Control*, vol. 36, no. 10, pp. 1148–1162, 1991.

[2] R. Schlanbusch, A. Loria, R. Kristiansen, and P. J. Nicklasson, "PD+ attitude control of rigid bodies with improved performance," in *49th IEEE Conference on Decision and Control*, 2010.

[3] N. A. Chaturvedi, A. K. Sanyal, and N. H. McClamroch, "Rigid-body attitude control," *IEEE Control Systems Magazine*, vol. 31, no. 3, pp. 30–51, 2011.

[4] C. G. Mayhew, R. G. Sanfelice, and A. R. Teel, "Quaternion-based hybrid control for robust global attitude tracking," *IEEE Transactions on Automatic Control*, vol. 56, no. 11, pp. 2555–2566, 2011.

[5] R. Schlanbusch, "Control of rigid bodies," Ph.D. dissertation, NTNU - Norwegian University of Science and Technology, 2012.

[6] T. Lee, "Robust adaptive attitude tracking on SO(3) with an application to a quadrotor UAV," *IEEE Transactions on Control Systems Technology*, vol. 21, no. 5, pp. 1924–1930, 2013.

[7] A. Benallegue, Y. Chitour, and A. Tayebi, "Adaptive attitude tracking control of rigid body systems with unknown inertia and gyro-bias," *IEEE Transactions on Automatic Control*, vol. 63, no. 11, pp. 3986–3993, 2018.

[8] T. Wang and J. Huang, "Leader-following adaptive consensus of multiple uncertain rigid body systems over jointly connected networks," *Unmanned Systems*, vol. 08, no. 02, pp. 85–93, 2020.

[9] T. S. Andersen and R. Kristiansen, "Adaptive backstepping control for a fully-actuated rigid-body in a dual-quaternion framework," in *2019 IEEE 58th Conference on Decision and Control (CDC)*, 2019.

[10] T. I. Fossen, *Marine Control Systems: Guidance, Navigation, and Control of Ships, Rigs and Underwater Vehicles*. Trondheim, Norway: Marine Cybernetics AS, 2002.

[11] F. Chen, R. Jiang, K. Zhang, B. Jiang, and G. Tao, "Robust backstepping sliding-mode control and observer-based fault estimation for a quadrotor uav," *IEEE Transactions on Industrial Electronics*, vol. 63, no. 6, pp. 5044–5056, 2016.

[12] S. M. Schlanbusch and J. Zhou, "Adaptive backstepping control of a 2-dof helicopter," in *Proceedings of the IEEE 7th International Conference on Control, Mechatronics and Automation*, 2019, pp. 210–215.

[13] Y. Yan and S. Yu, "Sliding mode tracking control of autonomous underwater vehicles with the effect of quantization," *Ocean Engineering*, vol. 151, pp. 322–328, 2018.

[14] X. Liang, Y. Fang, N. Sun, and H. Lin, "Nonlinear hierarchical control for unmanned quadrotor transportation systems," *IEEE Transactions on Industrial Electronics*, vol. 65, no. 4, pp. 3395–3405, 2018.

[15] A. E. Jimenez-Cano, P. J. Sanchez-Cuevas, P. Grau, A. Ollero, and G. Heredia, "Contact-based bridge inspection multirotors: Design, modeling, and control considering the ceiling effect," *IEEE Robotics and Automation Letters*, vol. 4, no. 4, pp. 3561–3568, 2019.

[16] C. Sampedro, A. Rodriguez-Ramos, H. Bavle, A. Carrio, P. de la Puente, and P. Campoy, "A fully-autonomous aerial robot for search and rescue applications in indoor environments using learning-based techniques," *Journal of Intelligent & Robotic Systems*, vol. 95, no. 2, pp. 601–627, 2018.

[17] J. Yan, J. Gao, X. Yang, X. Luo, and X. Guan, "Position tracking control of remotely operated underwater vehicles with communication delay," *IEEE Transactions on Control Systems Technology*, vol. 28, no. 6, pp. 2506–2514, 2020.

[18] S. Tatikonda and S. Mitter, "Control under communication constraints," *IEEE Transactions on Automatic Control*, vol. 49, no. 7, pp. 1056–1068, 2004.

[19] M. Fu and L. Xie, "The sector bound approach to quantized feedback control," *IEEE Transactions on Automatic Control*, vol. 50, no. 11, pp. 1698–1711, 2005.

[20] C. D. Persis, "Robust stabilization of nonlinear systems by quantized and ternary control," *Systems & Control Letters*, vol. 58, no. 8, pp. 602–608, 2009.

[21] T. Hayakawa, H. Ishii, and K. Tsumaru, "Adaptive quantized control for nonlinear uncertain systems," *Systems & Control Letters*, vol. 58, no. 9, pp. 625–632, 2009.

[22] H. Sun, N. Hovakimyan, and T. Basar, "$\mathcal{L}_1$ adaptive controller for uncertain nonlinear multi-input multi-output systems with input quantization," *IEEE Transactions on Automatic Control*, vol. 57, no. 3, pp. 565–578, 2012.

[23] J. Zhou, C. Wen, and G. Yang, "Adaptive backstepping stabilization of nonlinear uncertain systems with quantized input signal," in *IEEE Transactions on Automatic Control*, vol. 59, no. 2, 2014, pp. 460–464.

[24] J. Zhou, C. Wen, and W. Wang, "Adaptive control of uncertain nonlinear systems with quantized input signal," *Automatica*, vol. 95, pp. 152–162, 2018.

[25] Y. Li and G. Yang, "Adaptive asymptotic tracking control of uncertain nonlinear systems with input quantization and actuator faults," *Automatica*, vol. 72, pp. 177–185, 2016.

[26] A. Selivanov, A. Fradkov, and D. Liberzon, "Adaptive control of passifiable linear systems with quantized measurements and bounded disturbances," *Systems and Control Letters*, vol. 88, pp. 62–67, 2016.

[27] J. Zhou, C. Wen, W. Wang, and F. Yang, "Adaptive backstepping control of nonlinear uncertain systems with quantized states," *IEEE Transactions on Automatic Control*, vol. 64, no. 11, pp. 4756–4763, 2019.

[28] R. Sun, A. Shan, C. Zhang, J. Wu, and Q. Jia, "Quantized fault-tolerant control for attitude stabilization with fixed-time disturbance observer," *Journal of Guidance, Control, and Dynamics*, vol. 44, no. 2, pp. 449–455, 2021.

[29] B. Huang, B. Zhou, S. Zhang, and C. Zhu, "Adaptive prescribed performance tracking control for underactuated autonomous underwater vehicles with input quantization," *Ocean Engineering*, vol. 221, 2021.

[30] S. M. Schlanbusch and J. Zhou, "Adaptive backstepping control of a 2-DOF helicopter system with uniform quantized inputs," in *IECON 2020 The 46th Annual Conference of the IEEE Industrial Electronics Society*, 2020, pp. 88–94.

[31] Y. Wang, L. He, and C. Huang, "Adaptive time-varying formation tracking control of unmanned aerial vehicles with quantized input," *ISA Transactions*, vol. 85, pp. 76–83, 2019.

[32] L. Xing, C. Wen, Y. Zhu, H. Su, and Z. Liu, "Output feedback control for uncertain nonlinear systems with input quantization," *Automatica*, vol. 65, pp. 191–202, 2015.

[33] O. Egeland and J. T. Gravdahl, *Modeling and Simulation for Automatic Control*. Marine Cybernetics AS, 2003.

[34] M. Krstić, I. Kanellakopoulos, and P. Kokotović, *Nonlinear and Adaptive Control Design*. John Wiley & Sons, Inc., 1995.

Paper D

Adaptive Backstepping Control of a 2-DOF Helicopter System in the Presence of Quantization

Siri Marte Schlanbusch and Jing Zhou

This paper has been published as:

S. M. Schlanbusch and J. Zhou, "Adaptive backstepping control of a 2-DOF helicopter system in the presence of quantization," in *9th International Conference on Control, Mechatronics and Automation*, 2021, pp. 110–115, doi: 10.1109/ICCMA54375.2021.9646184.

Adaptive Backstepping Control of a 2-DOF Helicopter System in the Presence of Quantization

Siri Marte Schlanbusch and Jing Zhou

Department of Engineering Sciences
University of Agder
4879 Grimstad, Norway

Abstract

This paper studies the attitude tracking control for an uncertain 2-degrees of freedom helicopter system where the inputs and the states are quantized. An adaptive backstepping based control scheme is proposed to handle the effect of quantization for tracking of reference angles for pitch and yaw. All closed-loop signals are ensured uniformly bounded and the tracking errors will converge to a compact set containing the origin. Experiments on the helicopter system illustrate the proposed control scheme.

D.1 Introduction

The interest for wireless communication, remote controlled systems and other network control systems (NCSs) where the control loops are closed through a communication network has increased recent years. The network bandwidth might be limited and signals are required to be quantized before transmitted over the network. Then it is important to choose a quantization scheme that can reduce the communication burden over the network, and at the same time ensure sufficient precision for the system. Quantization introduces nonlinear errors in the control loop that may lead to degradation of system performance or even unstable control systems.

Various results have been reported for quantized feedback control systems with input quantization, see e.g [1–4], where only the information from controller to the plant is quantized, while the controller is designed by continuous measures of the state feedback. The feedback control problem of systems with state quantization has been studied in [5–8], where the system dynamics in these works are precisely known.

Uncertainties often appears in systems, and adaptive control is a control method

that can be used to handle such uncertainties. Adaptive control schemes were developed in [2, 9, 10] for uncertain systems with input quantization. Adaptive backstepping technique was proposed in the 1990's in [11] to deal with plant nonlinearity and parameter uncertainties. The backstepping technique has several advantages over the conventional approaches such as providing a promising way to improve the transient performance of adaptive systems by tuning design parameters. Several results have been reported for adaptive backstepping control for systems with input quantization, e.g. in [12, 13] for uncertain nonlinear systems, in [14] for a 2-degrees of freedom (DOF) helicopter system, in [4] for tracking control for under-actuated autonomous underwater vehicles and in [15] for formation tracking control for a group of UAVs. Adaptive backstepping-based stabilization of uncertain systems with state quantization are very limited, since the backstepping technique requires differentiating the quantized states that are discontinuous. This problem was solved in [16] where the states were quantized by a static bounded quantizer for uncertain nonlinear systems. The solution in [16] to handle the discontinuous states was considered in [17] for attitude control of a rigid body.

Both inputs and states are in practice quantized due to actuator and sensor limitations, but there are only a few results handling both input and state quantization. In [18], trajectory tracking control for autonomous underwater vehicles with the effect of quantization was investigated using a sliding mode controller. In [19], adaptive attitude control for a rigid body with input and output quantization was studied. In [20], adaptive tracking control for nonholonomic mobile robots with input and state quantization was considered. In [21], an adaptive neural network controller was developed for a 2-DOF helicopter system with saturated input and quantized input and state.

In this paper we extend the results from [22] and [14], where the adaptive backstepping control of a 2-DOF helicopter was considered in [22] and with input quantization in [14], to now deal with both input and state quantization for the same helicopter system. The helicopter is a nonlinear multiple-input and multiple-output (MIMO) system, with challenges in controller design due to its nonlinear behavior, its cross coupling effect between inputs and outputs, and with uncertainties both in the model and the parameters. Based on Lyapunov stability theory, the stability of the helicopter system is analyzed, were the tracking errors are shown to converge to an ultimate bound. Experiments on the helicopter system illustrate the proposed control scheme.

The main contributions in this paper are summarized as follows.

- Compared to [14] where the problem of input quantization was considered, this paper studies the problem where both the inputs and the states are quantized. The main challenge is that the designed controller and virtual control can only

utilize quantized states, and this problem is being addressed.

- The attitude, i.e. orientation, of a MIMO 2-DOF helicopter system is to be controlled, where the system has challenges due to uncertain parameters, there is a coupling between the inputs and the outputs that makes control more complicated, and quantization of both the inputs and the states introduce errors that need to be handled in the control design and in the stability analysis. We propose an adaptive control algorithm using the backstepping technique to deal with these problems.

The paper is organized as follows. In Section D.2, the system model, problem statement and the considered quantizer are presented. Section D.3 presents the adaptive control design based on backstepping technique. In Section D.4 a stability analysis is given, Section D.5 presents the results from experiment before a conclusion is given in Section D.6.

D.2 Dynamical Model and Problem Formulation

D.2.1 Notations

Vectors are denoted by small bold letters and matrices with capitalized bold letters. $\lambda_{\max}(\cdot)$ and $\lambda_{\min}(\cdot)$ denotes the maximum and minimum eigenvalue of the matrix $(\cdot)$, and $\|\cdot\|$ denotes the $\mathcal{L}_2$-norm and induced $\mathcal{L}_2$-norm for vectors and matrices, respectively.

D.2.2 System Model

The considered helicopter system is visualized in Fig. D.1 showing the body fixed coordinate frame. This is a two-rotor laboratory equipment for flight control-based experiments. The setup is a horizontal position of the main thruster and a vertical position of the tail thruster, which resembles a helicopter with two propellers driven by two DC motors. The main motor is producing a force in the z_b-direction that will give a positive pitch angle, and at the same time the rotation of the propeller generates a torque about the motor shaft causing a motion in the y_b-direction, meaning this will give a yaw angle. The tail motor is producing a force in the y_b direction and at the same time a torque changing the pitch angle. Thus, this is a MIMO system with 2 DOF, where each input will change both the pitch and the yaw angle. The helicopter model is considered as a rigid body and the equations of motion are derived using Euler-Lagrange equations as given in [22], where the system parameters are uncertain.

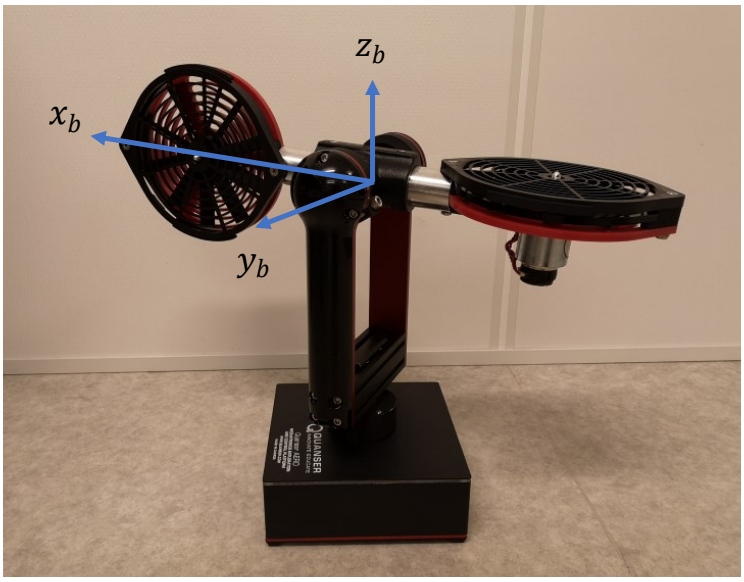

Figure D.1: Quanser Aero helicopter system with body coordinate frame

The state variables are defined as

$$\boldsymbol{x}_1 = [\vartheta(t)\ \psi(t)]^\top \in \mathbb{R}^2, \quad \boldsymbol{x}_2 = [\dot{\vartheta}(t), \dot{\psi}(t)]^\top \in \mathbb{R}^2, \tag{D.1}$$

where ϑ and ψ are pitch and yaw angles, and $\dot{\vartheta}$ and $\dot{\psi}$ are angular velocities of pitch and yaw. The nonlinear state space model is expressed as

$$\dot{\boldsymbol{x}} = \begin{bmatrix} \boldsymbol{x}_2 \\ \boldsymbol{\Phi}_1^\top \boldsymbol{\theta}_1 + \boldsymbol{\Phi}_2^\top \boldsymbol{\theta}_2 + \boldsymbol{K}\boldsymbol{u}^q \end{bmatrix} \in \mathbb{R}^4, \tag{D.2}$$

where

$$\boldsymbol{\Phi}_1 = \begin{bmatrix} -x_{2,1} & 0 \\ -\sin x_{1,1} & 0 \\ x_{2,2}^2 \cos x_{1,1} \sin x_{1,1} & 0 \end{bmatrix} \in \mathbb{R}^{3\times 2}, \tag{D.3}$$

$$\boldsymbol{\Phi}_2 = \begin{bmatrix} 0 & -x_{2,2} \\ 0 & -x_{1,2}x_{2,2} \cos x_{1,1} \sin x_{1,1} \end{bmatrix} \in \mathbb{R}^{2\times 2}, \tag{D.4}$$

are known nonlinear functions,

$$\boldsymbol{\theta}_1 = \frac{1}{I_p} \begin{bmatrix} d_p \\ mgr \\ mr^2 \end{bmatrix} \in \mathbb{R}^3, \quad \boldsymbol{\theta}_2 = \frac{1}{I_y} \begin{bmatrix} d_y \\ 2mr^2 \end{bmatrix} \in \mathbb{R}^2, \tag{D.5}$$

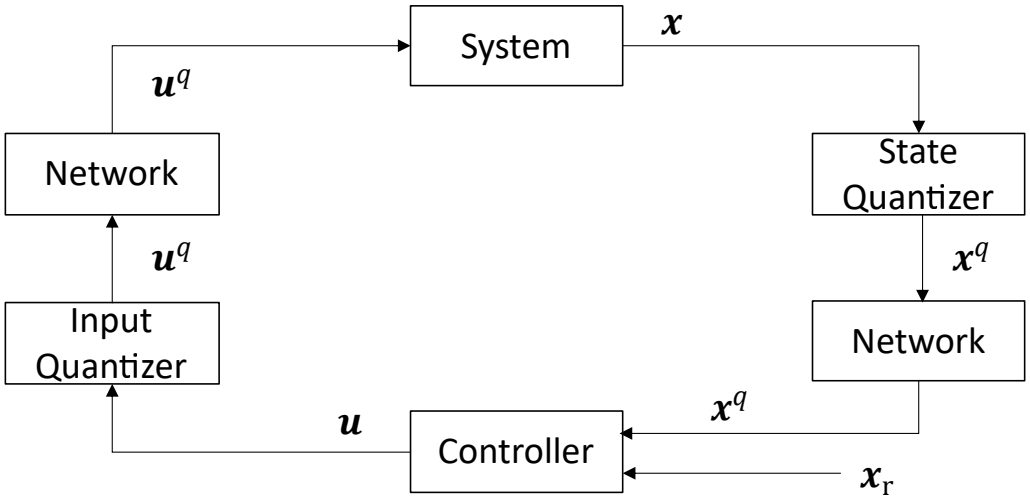

Figure D.2: Control system with input and state quantization over a network.

are unknown constant vectors,

$$\boldsymbol{K} = \begin{bmatrix} \frac{k_1}{I_p} & \frac{k_2}{I_p} \\ \frac{-k_3}{I_y} & \frac{k_4}{I_y} \end{bmatrix} \in \mathbb{R}^{2\times 2}, \tag{D.6}$$

is the control allocation matrix. The constants k_1 and k_4 are torque thrust gains from the main and the tail motors, k_2 is a cross-torque thrust gain acting on pitch from the tail motor, k_3 is a cross-torque thrust gain acting on yaw from the main motor, r is the distance between the center of mass and the origin of the body-fixed frame, I_p and I_y are the moments of inertia of pitch and yaw respectively, g is the gravity acceleration, m is the total mass of the Aero body, and d_y and d_p are damping constants.

D.2.3 Problem Statement

We consider a control system as shown in Fig. D.2, where the state vector $\boldsymbol{x}$ and the input vector $\boldsymbol{u}$ are quantized at the encoder side to be sent over a network. The network is assumed noiseless, so that the quantized state signal $\boldsymbol{x}^q$ is recovered and sent to the controller and the quantized input signal $\boldsymbol{u}^q$ is recovered and sent to the plant.

The quantizers for the state and control input are modeled as follows.

$$\boldsymbol{x}^q = Q_1(\boldsymbol{x}), \tag{D.7}$$

$$\boldsymbol{u}^q = Q_2(\boldsymbol{u}), \tag{D.8}$$

where the control input $\boldsymbol{u}$ can only use the quantized state as follows:

$$\boldsymbol{u} = [u_1(t, \boldsymbol{x}^q), u_2(t, \boldsymbol{x}^q)]^\top \in \mathbb{R}^2. \tag{D.9}$$

Given reference signal $\boldsymbol{x}_r(t)$, the control objective is to design a control law for $\boldsymbol{u} = \boldsymbol{u}(t, \boldsymbol{x}^q)$ by utilizing only quantized state $\boldsymbol{x}^q(t)$, to force the state $\boldsymbol{x}_1(t)$ to track the reference signal $\boldsymbol{x}_r(t)$ when the inputs are quantized, and to ensure that all the signals in the closed-loop system are uniformly bounded. To achieve the objective, the following assumptions are imposed.

Assumption 1. *The reference signal $\boldsymbol{x}_r$ and first and second order derivatives are known, piecewise continuous and bounded. Then there exists $k_{x_r}, k_{\dot{x}_r}, k_{\ddot{x}_r} > 0$ such that $\|\boldsymbol{x}_r\| < k_{x_r}$, $\|\dot{\boldsymbol{x}}_r\| < k_{\dot{x}_r}$ and $\|\ddot{\boldsymbol{x}}_r\| < k_{\ddot{x}_r}, \forall t \geq t_0$.*

Assumption 2. *The unknown parameter vectors $\boldsymbol{\theta}_1$ and $\boldsymbol{\theta}_2$ are bounded by $\|\boldsymbol{\theta}_1\| \leq k_{\theta_1}$, $\|\boldsymbol{\theta}_2\| \leq k_{\theta_2}$ where $k_{\theta_1}, k_{\theta_2}$ are positive constants. Also $\boldsymbol{\theta}_1 \in C_{\theta_1}$, $\boldsymbol{\theta}_2 \in C_{\theta_2}$ where C_{θ_1} and C_{θ_2} are known compact convex sets.*

Assumption 3. *The functions $\boldsymbol{\Phi}_1$ and $\boldsymbol{\Phi}_2$ satisfy locally Lipschitz conditions such that*

$$\|\boldsymbol{\Phi}_1(t, \boldsymbol{y}_1) - \boldsymbol{\Phi}_1(t, \boldsymbol{y}_2)\| \leq L_{\Phi_1}\|\boldsymbol{y}_1 - \boldsymbol{y}_2\|, \tag{D.10}$$

$$\|\boldsymbol{\Phi}_2(t, \boldsymbol{y}_1) - \boldsymbol{\Phi}_2(t, \boldsymbol{y}_2)\| \leq L_{\Phi_2}\|\boldsymbol{y}_1 - \boldsymbol{y}_2\|, \tag{D.11}$$

where L_{Φ_1} and L_{Φ_2} are constants and $\boldsymbol{y}_1, \boldsymbol{y}_2$ are real vectors.

D.2.4 Quantizer

In this paper, a uniform quantizer is considered for both state quantization $Q_1(\boldsymbol{x})$ and input quantization $Q_2(\boldsymbol{u})$, which has intervals of fixed length and is defined as follows:

$$y^q = Q(y) = \begin{cases} y_i \operatorname{sgn}(y), & y_i - \frac{l}{2} < |y| \leq y_i + \frac{l}{2} \\ 0, & |y| \leq y_0 \end{cases}, \tag{D.12}$$

where $y_0 > 0, y_1 = y_0 + \frac{l}{2}$, $y_{i+1} = y_i + l$, $l > 0$ is the length of the quantization interval, $\operatorname{sgn}(y)$ is the sign function. The uniform quantization $y^q \in U = \{0, \pm y_i\}$, and a map of the quantization for $y_i > 0$ is shown in Fig. D.3. The quantizer considered in this paper has the following property

$$|y^q - y| = |d_y| \leq \delta_y, \tag{D.13}$$

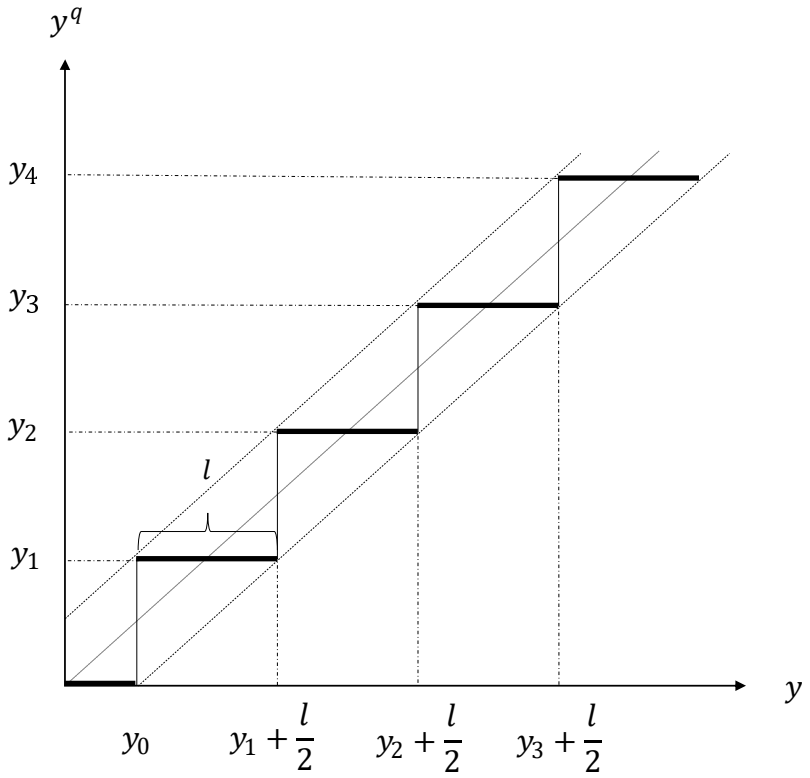

Figure D.3: Map of the uniform quantizer for $y > 0$.

where y is a scalar signal, d is the quantization error and $\delta_y > 0$ denotes the quantization bound. Clearly, the property in (D.13) is satisfied with $\delta_y = \max\{y_0, \frac{l}{2}\}$. When a vector is quantized, we have

$$\boldsymbol{y}^q = \begin{bmatrix} y_1^q & y_2^q & \cdots & y_n^q \end{bmatrix}^\top, \tag{D.14}$$

and so each vector element is bounded by (D.13), and we have $\|\boldsymbol{y}^q - \boldsymbol{y}\| = \|\boldsymbol{d}_y\| \leq \|\boldsymbol{\delta}_y\| \triangleq \delta_y$.

D.3 Adaptive Control Design

In this section we will design adaptive feedback control laws for the helicopter system using backstepping technique. For this model, two steps are included, where the control signal is designed in the last step. We first introduce the change of coordinates

$$\boldsymbol{z}_1 = \boldsymbol{x}_1 - \boldsymbol{x}_r, \tag{D.15}$$

$$\boldsymbol{z}_2 = \boldsymbol{x}_2 - \boldsymbol{\alpha} - \dot{\boldsymbol{x}}_r, \tag{D.16}$$

where $\boldsymbol{\alpha}$ is a virtual controller designed in the first step and chosen as

$$\boldsymbol{\alpha} = -\boldsymbol{C}_1 \boldsymbol{z}_1, \tag{D.17}$$

where $\boldsymbol{C}_1 \in \mathbb{R}^{2\times 2}$ is a positive definite matrix. The derivative of (D.15) and (D.16) are given as

$$\dot{\boldsymbol{z}}_1 = \boldsymbol{x}_2 - \dot{\boldsymbol{x}}_r = \boldsymbol{z}_2 + \boldsymbol{\alpha}, \tag{D.18}$$

$$\dot{\boldsymbol{z}}_2 = \boldsymbol{\Phi}_1^\top \boldsymbol{\theta}_1 + \boldsymbol{\Phi}_2^\top \boldsymbol{\theta}_2 + \boldsymbol{K}\boldsymbol{u}^q - \dot{\boldsymbol{\alpha}} - \ddot{\boldsymbol{x}}_r. \tag{D.19}$$

To propose a suitable control scheme, the quantized input $\boldsymbol{u}^q(t)$ is decomposed into two parts

$$\boldsymbol{u}^q(t) = \boldsymbol{u}(t) + \boldsymbol{d}_u(t), \tag{D.20}$$

where $\boldsymbol{d}_u$ is the quantization error of the input, which is bounded by $\|\boldsymbol{d}_u\| \leq \|[\delta_{u_1}\ \delta_{u_2}]^\top\| = \|\boldsymbol{\delta}_u\| \triangleq \delta_u$, from (D.13).
The adaptive controller is designed as

$$\boldsymbol{u}(t) = \boldsymbol{K}^{-1}\Big[-\boldsymbol{z}_1^q - \boldsymbol{C}_2\boldsymbol{z}_2^q - \boldsymbol{\Phi}_1(\boldsymbol{x}^q)^\top\hat{\boldsymbol{\theta}}_1 - \boldsymbol{\Phi}_2(\boldsymbol{x}^q)^\top\hat{\boldsymbol{\theta}}_2 + \bar{\boldsymbol{\alpha}}^q + \ddot{\boldsymbol{x}}_r\Big], \tag{D.21}$$

$$\dot{\hat{\boldsymbol{\theta}}}_1 = \mathrm{Proj}\{\boldsymbol{\Gamma}_1\boldsymbol{\Phi}_1(\boldsymbol{x}^q)\boldsymbol{z}_2^q\}, \tag{D.22}$$

$$\dot{\hat{\boldsymbol{\theta}}}_2 = \mathrm{Proj}\{\boldsymbol{\Gamma}_2\boldsymbol{\Phi}_2(\boldsymbol{x}^q)\boldsymbol{z}_2^q\}, \tag{D.23}$$

where $\boldsymbol{C}_2, \boldsymbol{\Gamma}_2 \in \mathbb{R}^{2\times 2}$ and $\boldsymbol{\Gamma}_1 \in \mathbb{R}^{3\times 3}$ are positive definite gain matrices, $\hat{\boldsymbol{\theta}}$ is the estimated value of $\boldsymbol{\theta}$, the vector $\tilde{\boldsymbol{\theta}} = \boldsymbol{\theta} - \hat{\boldsymbol{\theta}}$, and where $\mathrm{Proj}\{\cdot\}$ is the projection operator given in [11] and where

$$\boldsymbol{z}_1^q = \boldsymbol{x}_1^q - \boldsymbol{x}_r, \tag{D.24}$$

$$\boldsymbol{z}_2^q = \boldsymbol{x}_2^q - \boldsymbol{\alpha}^q - \dot{\boldsymbol{x}}_r, \tag{D.25}$$

$$\boldsymbol{\alpha}^q = -\boldsymbol{C}_1\boldsymbol{z}_1^q, \tag{D.26}$$

$$\boldsymbol{\Phi}_1(\boldsymbol{x}^q) = \begin{bmatrix} -x_{2,1}^q & 0 \\ -\sin x_{1,1}^q & 0 \\ (x_{2,2}^q)^2 \cos x_{1,1}^q \sin x_{1,1}^q & 0 \end{bmatrix} \tag{D.27}$$

$$\boldsymbol{\Phi}_2(\boldsymbol{x}^q) = \begin{bmatrix} 0 & -x_{2,2}^q \\ 0 & -x_{1,2}^q x_{2,2}^q \cos x_{1,1}^q \sin x_{1,1}^q \end{bmatrix} \tag{D.28}$$

$$\bar{\boldsymbol{\alpha}}^q \triangleq -\boldsymbol{C}_1(\boldsymbol{x}_2^q - \dot{\boldsymbol{x}}_r). \tag{D.29}$$

Remark 1. *The projection operator* $\mathrm{Proj}\{\cdot\}$ *in* (D.22) *and* (D.23) *ensures that the estimates and estimation errors are nonzero and within known bounds, that is* $\|\hat{\boldsymbol{\theta}}\| \leq k_\theta$ *and* $\|\tilde{\boldsymbol{\theta}}\| \leq k_\theta$*, and has the property* $-\tilde{\boldsymbol{\theta}}^\top\boldsymbol{\Gamma}^{-1}\mathrm{Proj}(\boldsymbol{\tau}) \leq -\tilde{\boldsymbol{\theta}}^\top\boldsymbol{\Gamma}^{-1}\boldsymbol{\tau}$*, which are helpful to guarantee the closed-loop stability.*

Remark 2. *Only the quantized state can be used in the designed controller. Since*

the quantized state is used in the design of the virtual controller $\boldsymbol{\alpha}^q$ in (D.26)*, the derivative of the virtual controller is discontinuous and can not be used in the design of the controller. Instead, a function $\bar{\boldsymbol{\alpha}}^q$ is used in* (D.29)*, which is designed as if the state is not quantized.*

D.4 Stability Analysis

To analyze the closed-loop system stability, we first establish some preliminary results as stated in the following lemmas.

Lemma 1. *The effects of state quantization are bounded by the following inequalities:*

$$\|\boldsymbol{z}_1^q - \boldsymbol{z}_1\| = \|(\boldsymbol{x}_1^q - \boldsymbol{x}_r) - (\boldsymbol{x}_1 - \boldsymbol{x}_r)\| \leq \delta_{x_1}, \tag{D.30}$$

$$\|\boldsymbol{\alpha}^q - \boldsymbol{\alpha}\| = \|-\boldsymbol{C}_1\boldsymbol{z}_1^q + \boldsymbol{C}_1\boldsymbol{z}_1\| \leq \lambda_{\max}(\boldsymbol{C}_1)\delta_{x_1} \triangleq \delta_\alpha \tag{D.31}$$

$$\|\boldsymbol{z}_2^q - \boldsymbol{z}_2\| = \|(\boldsymbol{x}_2^q - \boldsymbol{x}_2) + (\boldsymbol{\alpha} - \boldsymbol{\alpha}^q)\| \leq \delta_{x_2} + \delta_\alpha \triangleq \delta_{z_2} \tag{D.32}$$

$$\|\boldsymbol{\Phi}_1(\boldsymbol{x}^q) - \boldsymbol{\Phi}_1(\boldsymbol{x})\| \leq L_{\Phi_1}\|\boldsymbol{x}^q - \boldsymbol{x}\| = L_{\Phi_1}\delta_x \triangleq \delta_{\Phi_1} \tag{D.33}$$

$$\|\boldsymbol{\Phi}_2(\boldsymbol{x}^q) - \boldsymbol{\Phi}_2(\boldsymbol{x})\| \leq L_{\Phi_2}\|\boldsymbol{x}^q - \boldsymbol{x}\| = L_{\Phi_2}\delta_x \triangleq \delta_{\Phi_2} \tag{D.34}$$

$$\|\bar{\boldsymbol{\alpha}}^q - \dot{\boldsymbol{\alpha}}\| = \|-\boldsymbol{C}_1(\boldsymbol{x}_2^q - \dot{\boldsymbol{x}}_r) + \boldsymbol{C}_1(\boldsymbol{x}_2 - \dot{\boldsymbol{x}}_r)\| \leq \lambda_{\max}(\boldsymbol{C}_1)\delta_{x_2} \triangleq \delta_{\bar{\alpha}}, \tag{D.35}$$

where $\delta_{(\cdot)}$ are positive constants.

Proof: Using the property (D.13) of the quantizer, we have

$$\|\boldsymbol{x}_1^q - \boldsymbol{x}_1\| = \|\boldsymbol{d}_{x_1}\| \leq \|[\delta_{x_{1,1}}\ \delta_{x_{1,2}}]^\top\| = \|\boldsymbol{\delta}_{x_1}\| \triangleq \delta_{x_1}, \tag{D.36}$$

$$\|\boldsymbol{x}_2^q - \boldsymbol{x}_2\| = \|\boldsymbol{d}_{x_2}\| \leq \|[\delta_{x_{2,1}}\ \delta_{x_{2,2}}]^\top\| = \|\boldsymbol{\delta}_{x_2}\| \triangleq \delta_{x_2}, \tag{D.37}$$

$$\|\boldsymbol{x}^q - \boldsymbol{x}\| = \|[\delta_{x_1}\ \delta_{x_2}]^\top\| = \|\boldsymbol{\delta}_x\| \triangleq \delta_x. \tag{D.38}$$

Then from (D.15)-(D.18), (D.24)-(D.26), Assumption 3 and (D.36)-(D.38) the inequalities (D.30)-(D.35) holds.

Lemma 2. *The state $\boldsymbol{x}$ satisfies the following inequality:*

$$\|\boldsymbol{x}\| \leq k_{x_1} + k_{x_2}\|\boldsymbol{z}\|, \tag{D.39}$$

where $\boldsymbol{z} = [\boldsymbol{z}_1^\top\ \boldsymbol{z}_2^\top]^\top$.

Proof: From the definitions in (D.15)-(D.17) and Assumption 1 we have

$$\|\boldsymbol{x}_1\| \leq \|\boldsymbol{z}_1 + \boldsymbol{x}_r\| \leq k_{x_r} + \|\boldsymbol{z}_1\| \leq k_{x_r} + \|\boldsymbol{z}\|, \tag{D.40}$$

$$\|\boldsymbol{\alpha}\| \leq \lambda_{\max}(\boldsymbol{C}_1)\|\boldsymbol{z}_1\|, \tag{D.41}$$

$$\|\boldsymbol{x}_2\| \leq \|\boldsymbol{z}_2 + \boldsymbol{\alpha} + \dot{\boldsymbol{x}}_r\| \leq \|\boldsymbol{z}_2\| + \lambda_{\max}(\boldsymbol{C}_1)\|\boldsymbol{z}_1\| + k_{\dot{x}_r}$$

$$\leq k_{\dot{x}_r} + [1 + \lambda_{\max}(\boldsymbol{C}_1)]\|\boldsymbol{z}\|. \tag{D.42}$$

Then

$$\begin{aligned}\|\boldsymbol{x}\| = \|[\boldsymbol{x}_1^\top \ \boldsymbol{x}_2^\top]^\top\| &= \sqrt{(\|\boldsymbol{x}_1\|)^2 + (\|\boldsymbol{x}_2\|)^2} \\ &\leq (k_{x_r} + k_{\dot{x}_r}) + (2 + \lambda_{\max}(\boldsymbol{C}_1))\|\boldsymbol{z}\| \\ &\triangleq k_{x_1} + k_{x_2}\|\boldsymbol{z}\|. \end{aligned} \tag{D.43}$$

The main results are now stated in the following theorem.

Theorem 1. *Consider the closed-loop adaptive system consisting of the plant* (D.2) *with input and state quantization satisfying the bounded property* (D.13)*, the adaptive controller* (D.21)*, the parameter updating laws* (D.22)-(D.23) *and Assumptions 1-3. All signals in the closed-loop system are ensured to be uniformly bounded and the error signals will converge to a compact set, i.e.*

$$\|\boldsymbol{z}(t)\| \leq \sqrt{\frac{2a}{c_0}}, \tag{D.44}$$

where c_0 is the minimum eigenvalue of $\boldsymbol{C}_0 = \min\{\boldsymbol{C}_1, \boldsymbol{C}_2\}$, and where

$$a = \delta_{V_1} + \frac{1}{2c_0} d_{V_2}^2, \tag{D.45}$$

$$\delta_{V_1} = \delta_{\theta_{11}} + \delta_{\theta_{21}}, \tag{D.46}$$

$$\delta_{V_2} = \delta_{z_2} + \delta_{x_1} + \delta_{\bar{\alpha}} + \|\boldsymbol{K}\|\delta_u + \delta_{\theta_{12}} + \delta_{\theta_{22}}, \tag{D.47}$$

and is ultimately bounded. Tracking of a given reference signal is achieved, with a bounded error.

Proof: We choose a Lyapunov function candidate as

$$V = \frac{1}{2}\boldsymbol{z}_1^\top \boldsymbol{z}_1 + \frac{1}{2}\boldsymbol{z}_2^\top \boldsymbol{z}_2 + \frac{1}{2}\tilde{\boldsymbol{\theta}}_1^\top \boldsymbol{\Gamma}_1^{-1}\tilde{\boldsymbol{\theta}}_1 + \frac{1}{2}\tilde{\boldsymbol{\theta}}_2^\top \boldsymbol{\Gamma}_2^{-1}\tilde{\boldsymbol{\theta}}_2. \tag{D.48}$$

Following the controller design in (D.21)-(D.23), the derivative of (D.48) is

$$\begin{aligned}\dot{V} =& -\boldsymbol{z}_1^\top \boldsymbol{C}_1 \boldsymbol{z}_1 + \boldsymbol{z}_1^\top \boldsymbol{z}_2 - \tilde{\boldsymbol{\theta}}_1^\top \boldsymbol{\Gamma}_1^{-1}\dot{\hat{\boldsymbol{\theta}}}_1 - \tilde{\boldsymbol{\theta}}_2^\top \boldsymbol{\Gamma}_2^{-1}\dot{\hat{\boldsymbol{\theta}}}_2 + \boldsymbol{z}_2^\top[\boldsymbol{\Phi}_1^\top \boldsymbol{\theta}_1 + \boldsymbol{\Phi}_2^\top \boldsymbol{\theta}_2 + \boldsymbol{K}\boldsymbol{u}^q - \dot{\boldsymbol{\alpha}} - \ddot{\boldsymbol{x}}_r] \\ =& -\boldsymbol{z}_1^\top \boldsymbol{C}_1 \boldsymbol{z}_1 - \boldsymbol{z}_2^\top \boldsymbol{C}_2 \boldsymbol{z}_2^q + \boldsymbol{z}_2^\top(\boldsymbol{z}_1 - \boldsymbol{z}_1^q) + \boldsymbol{z}_2^\top(\bar{\boldsymbol{\alpha}}^q - \dot{\boldsymbol{\alpha}}) + \boldsymbol{z}_2^\top \boldsymbol{K}\boldsymbol{d}_u \\ &+ \left[\boldsymbol{z}_2^\top\left(\boldsymbol{\Phi}_1(\boldsymbol{x})^\top \boldsymbol{\theta}_1 - \boldsymbol{\Phi}_1(\boldsymbol{x}^q)^\top \hat{\boldsymbol{\theta}}_1\right) - \tilde{\boldsymbol{\theta}}_1^\top \boldsymbol{\Phi}_1(\boldsymbol{x}^q)\boldsymbol{z}_2^q\right] \\ &+ \left[\boldsymbol{z}_2^\top\left(\boldsymbol{\Phi}_2(\boldsymbol{x})^\top \boldsymbol{\theta}_2 - \boldsymbol{\Phi}_2(\boldsymbol{x}^q)^\top \hat{\boldsymbol{\theta}}_2\right) - \tilde{\boldsymbol{\theta}}_2^\top \boldsymbol{\Phi}_2(\boldsymbol{x}^q)\boldsymbol{z}_2^q\right]. \end{aligned} \tag{D.49}$$

By using (D.10), (D.33), (D.38) and (D.43) and Assumption 2, The following in-

equality is satisfied for the terms in (D.49) containing $\boldsymbol{\theta}_1$ and $\hat{\boldsymbol{\theta}}_1$:

$$\begin{aligned}
&\boldsymbol{z}_2^\top(\boldsymbol{\Phi}_1(\boldsymbol{x})^\top\boldsymbol{\theta}_1 - \boldsymbol{\Phi}_1(\boldsymbol{x}^q)^\top\hat{\boldsymbol{\theta}}_1) - \tilde{\boldsymbol{\theta}}_1^\top\boldsymbol{\Phi}_1(\boldsymbol{x}^q)\boldsymbol{z}_2^q \\
&= \boldsymbol{\theta}_1^\top\boldsymbol{\Phi}_1(\boldsymbol{x})\boldsymbol{z}_2 - \boldsymbol{\theta}_1^\top\boldsymbol{\Phi}_1(\boldsymbol{x}^q)\boldsymbol{z}_2 + \tilde{\boldsymbol{\theta}}_1^\top\boldsymbol{\Phi}_1(\boldsymbol{x}^q)\boldsymbol{z}_2 - \tilde{\boldsymbol{\theta}}_1^\top\boldsymbol{\Phi}_1(\boldsymbol{x}^q)\boldsymbol{z}_2^q \\
&\leq \|\boldsymbol{\theta}_1\|\|\boldsymbol{\Phi}_1(\boldsymbol{x}) - \boldsymbol{\Phi}_1(\boldsymbol{x}^q)\|\|\boldsymbol{z}_2\| + \|\tilde{\boldsymbol{\theta}}_1\|\|\boldsymbol{\Phi}_1(\boldsymbol{x}^q)\|\|\boldsymbol{z}_2 - \boldsymbol{z}_2^Q\| \\
&\leq k_{\theta_1}\delta_{\Phi_1}\|\boldsymbol{z}\| + k_{\theta_1}L_{\Phi_1}\|\boldsymbol{x}^{\boldsymbol{q}}\|\delta_{z_2} \\
&\leq k_{\theta_1}\delta_{\Phi_1}\|\boldsymbol{z}\| + k_{\theta_1}\delta_{z_2}L_{\Phi_1}(k_{x_1} + k_{x_2}\|\boldsymbol{z}\| + \delta_x) \\
&= [k_{\theta_1}\delta_{z_2}L_{\Phi_1}(k_{x_1} + \delta_x)] + [k_{\theta_1}\delta_{\Phi_1} + k_{\theta_1}\delta_{z_2}L_{\Phi_1}k_{x_2}]\|\boldsymbol{z}\| \\
&\triangleq \delta_{\theta_{11}} + \delta_{\theta_{12}}\|\boldsymbol{z}\|.
\end{aligned} \tag{D.50}$$

In a similar way, by using (D.11), (D.34), (D.38) and (D.43) and Assumptions 2, the following inequality is satisfied for the terms in (D.49) containing $\boldsymbol{\theta}_2$ and $\hat{\boldsymbol{\theta}}_2$:

$$\begin{aligned}
&\boldsymbol{z}_2^\top(\boldsymbol{\Phi}_2(\boldsymbol{x})^\top\boldsymbol{\theta}_2 - \boldsymbol{\Phi}_2(\boldsymbol{x}^q)^\top\hat{\boldsymbol{\theta}}_2) - \tilde{\boldsymbol{\theta}}_2^\top\boldsymbol{\Phi}_2(\boldsymbol{x}^q)\boldsymbol{z}_2^q \\
&= [k_{\theta_2}\delta_{z_2}L_{\Phi_2}(k_{x_1} + \delta_x)] + [k_{\theta_2}\delta_{\Phi_2} + k_{\theta_2}\delta_{z_2}L_{\Phi_2}k_{x_2}]\|\boldsymbol{z}\| \\
&\triangleq \delta_{\theta_{21}} + \delta_{\theta_{22}}\|\boldsymbol{z}\|.
\end{aligned} \tag{D.51}$$

Using the properties (D.30), (D.32) and (D.35) in Lemma 1 together with (D.50) and (D.51) and Young's inequality, we have

$$\begin{aligned}
\dot{V} \leq& -\boldsymbol{z}_1^\top\boldsymbol{C}_1\boldsymbol{z}_1 - \boldsymbol{z}_2^\top\boldsymbol{C}_2\boldsymbol{z}_2 + \|\boldsymbol{z}_2\|\delta_{z_2} + \|\boldsymbol{z}_2\|\delta_{x_1} + \|\boldsymbol{z}_2\|\delta_{\bar{\alpha}} + \|\boldsymbol{z}_2\|\|\boldsymbol{K}\|\delta_u + \delta_{\theta_{11}} \\
&+ \delta_{\theta_{12}}\|\boldsymbol{z}\| + \delta_{\theta_{21}} + \delta_{\theta_{22}}\|\boldsymbol{z}\| \\
\leq& -c_0\|\boldsymbol{z}\|^2 + \delta_{V_1} + \delta_{V_2}\|\boldsymbol{z}\| \\
\leq& -\frac{c_0}{2}\|\boldsymbol{z}\|^2 + \delta_{V_1} + \frac{1}{2c_0}\delta_{V_2}^2 \\
=& -\frac{c_0}{2}\|\boldsymbol{z}\|^2 + a.
\end{aligned} \tag{D.52}$$

From (D.48) and (D.52) it is shown that $\dot{V} < 0\ \forall\|\boldsymbol{z}\| > \sqrt{\frac{2a}{c_0}}$, thus $\boldsymbol{z}(t)$ is ultimately bounded and satisfies (D.44). The boundedness of $\boldsymbol{z}$ and (D.30) and (D.32) ensure the boundedness of the quantized error states $\boldsymbol{z}_1^q$ and $\boldsymbol{z}_2^q$. Then $\boldsymbol{\alpha}^q$ in (D.31) is also bounded. Since $\boldsymbol{x}$ is bounded in (D.43), then from (D.38) also $\boldsymbol{x}^q$ is bounded. From the projection operator, $\hat{\boldsymbol{\theta}}_1$ and $\hat{\boldsymbol{\theta}}_2$ are ensured bounded. Then, together with Assumptions 1-3, $\boldsymbol{u}$ in (D.21) is also bounded, and so all the closed-loop signals are uniformly bounded. Tracking is achieved, where the tracking error is ultimately bounded by (D.44).

Table D.1: Helicopter Parameters and initial values.

Symbol	Value
$\boldsymbol{x}(t_0)$	$[0\ 0\ 0\ 0]^\top$
$\hat{\boldsymbol{\theta}}_1(t_0)$	$[0.3218\ 1.8423\ 0.0007]^\top$
$\hat{\boldsymbol{\theta}}_2(t_0)$	$[0.4374\ 0.0014]^\top$
$\boldsymbol{K}$	$\begin{bmatrix} 0.0506 & 0.0506 \\ -0.0645 & 0.0810 \end{bmatrix}$

D.5 Experimental Results

The proposed controller was simulated using MATLAB/Simulink and tested on the Quanser Aero helicopter system. The mathematical model is described by (D.2), and the initial states and parameters used for simulation and experiments are shown in Table D.1.

The objective was to track a reference signal chosen as $\boldsymbol{x}_r(t) = [40\pi/180 \sin(0.1\pi t)\ 100\pi/180 \sin(0.05\pi t)]^\top$ when both the inputs and the states were quantized, and to ensure that all the signals in the closed-loop system were uniformly bounded. The inputs have limits of ± 24 V. The quantization levels were chosen as $l_u = 0.3$ for both inputs, and $l_s = 0.02$ for all the states. The gain matrices were set to $\boldsymbol{C}_1 = 6\boldsymbol{I}_3$, $\boldsymbol{C}_2 = 3\boldsymbol{I}_2$, $\boldsymbol{\Gamma}_1 = \boldsymbol{I}_3$ and $\boldsymbol{\Gamma}_2 = \boldsymbol{I}_2$.

The trajectories of the quantized states $\boldsymbol{x}^q = [\vartheta^q(t), \psi^q(t), \dot{\vartheta}^q(t), \dot{\psi}^q(t)]^\top$ are shown in Fig. D.4, where the desired states are shown with a dotted line and measured values from test on the helicopter system are shown with a solid line. The error in states $\boldsymbol{x}_1^q - \boldsymbol{x}_r$ and $\boldsymbol{x}_2^q - \dot{\boldsymbol{x}}_r$ are shown in Fig. D.5, and Fig. D.6 shows the quantized input $\boldsymbol{u}^q$. The results here illustrate the theoretical findings in Theorem 1, where tracking is achieved and all signals are shown to be uniformly bounded.

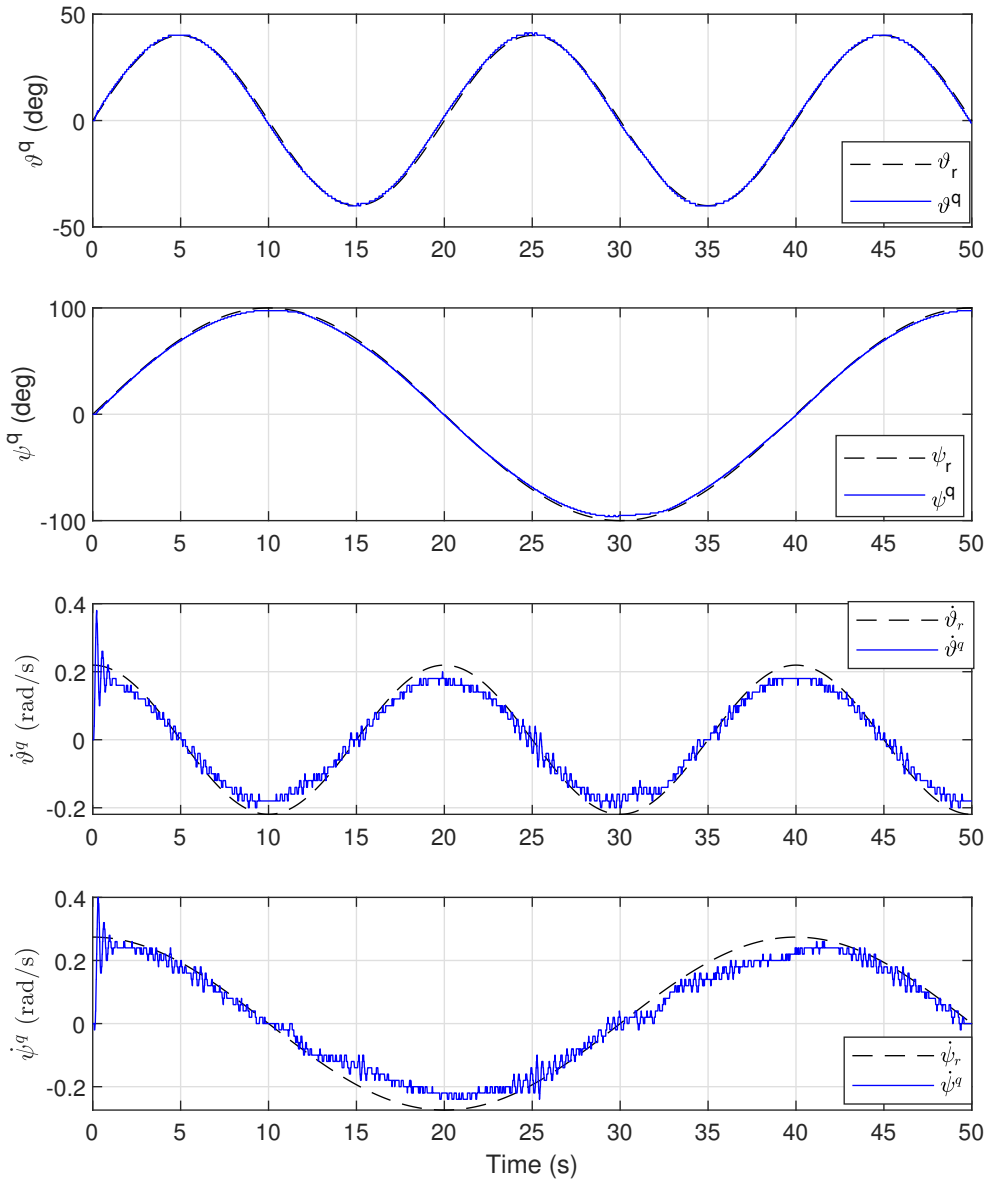

Figure D.4: Trajectories of the quantized states $\boldsymbol{x}^q$ from experiment.

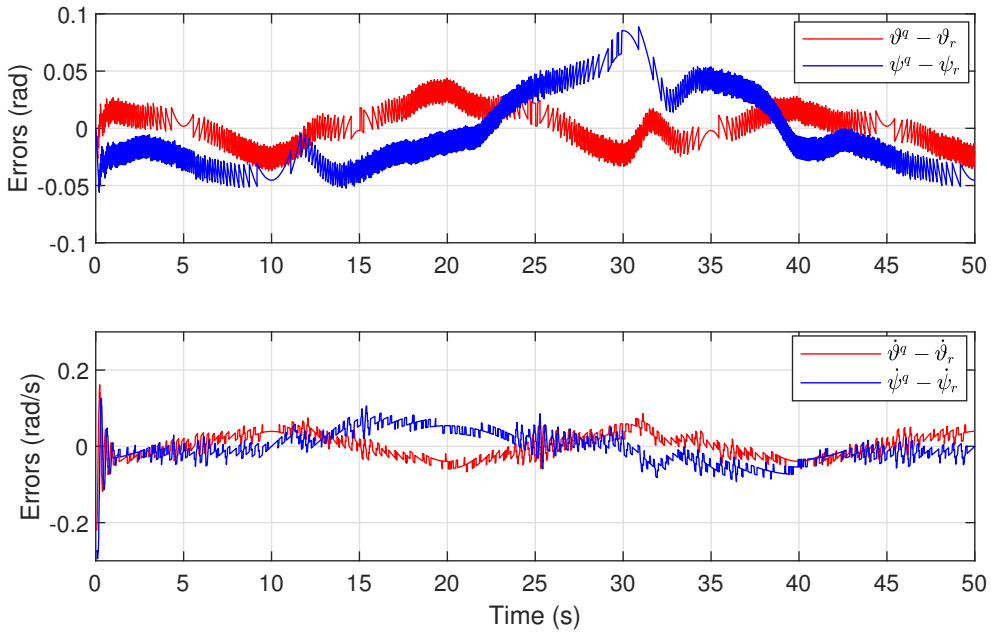

Figure D.5: Errors $\boldsymbol{x}_1^q - \boldsymbol{x}_r$ and $\boldsymbol{x}_2^q - \dot{\boldsymbol{x}}_r$.

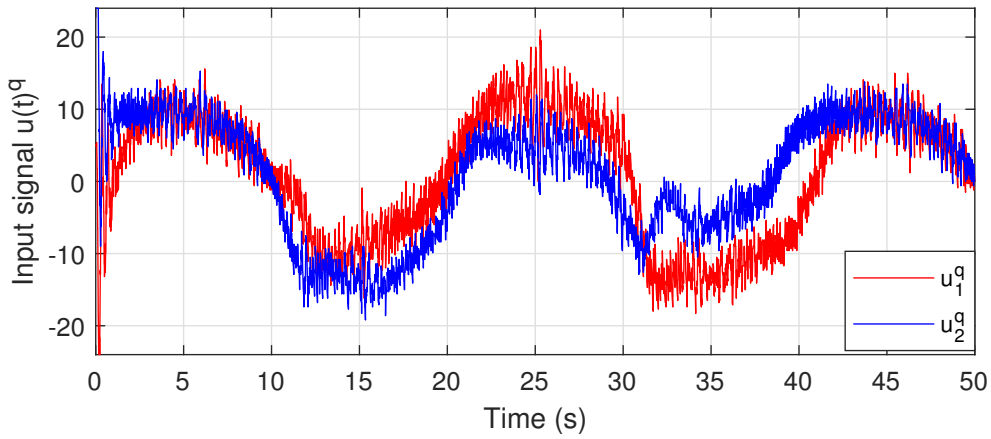

Figure D.6: Quantized input $\boldsymbol{u}(t)^q$.

D.6 Conclusion

In this paper, an adaptive backstepping control scheme for an uncertain nonlinear MIMO helicopter system with both input and state quantization was developed. The quantizer considered satisfies a bounded condition and so the quantization error is bounded. For the closed loop system, all signals are shown to be uniformly bounded where the error signals will converge to a compact set containing the origin. Tracking of a given reference signal is achieved, with a bounded error. Experiments on the helicopter system support the proof.

References – Paper D

[1] S. Tatikonda and S. Mitter, "Control under communication constraints," *IEEE Transactions on Automatic Control*, vol. 49, no. 7, pp. 1056–1068, 2004.

[2] L. Xing, C. Wen, Y. Zhu, H. Su, and Z. Liu, "Output feedback control for uncertain nonlinear systems with input quantization," *Automatica*, vol. 65, pp. 191–202, 2015.

[3] X. Shao, L. Xu, and W. Zhang, "Quantized control capable of appointed-time performances for quadrotor attitude tracking: Experimental validation," *IEEE Transactions on Industrial Electronics*, 2021.

[4] B. Huang, B. Zhou, S. Zhang, and C. Zhu, "Adaptive prescribed performance tracking control for underactuated autonomous underwater vehicles with input quantization," *Ocean Engineering*, vol. 221, 2021.

[5] D. Liberzon, "Hybrid feedback stabilization of systems with quantized signals," *Automatica*, vol. 39, no. 9, pp. 1543–1554, 2003.

[6] T. Liu and Z. Jiang, "Event-triggered control of nonlinear systems with state quantization," *IEEE Transactions on Automatic Control*, vol. 64, no. 2, pp. 797–803, 2019.

[7] T. Liu, Z.-P. Jiang, and D. J. Hill, "A sector bound approach to feedback control of nonlinear systems with state quantization," *Automatica*, vol. 48, no. 1, pp. 145–152, 2012.

[8] K. Liu, E. Fridman, and K. H. Johansson, "Dynamic quantization of uncertain linear networked control systems," *Automatica*, vol. 59, pp. 248–255, 2015.

[9] T. Hayakawa, H. Ishii, and K. Tsumaru, "Adaptive quantized control for nonlinear uncertain systems," *Systems & Control Letters*, vol. 58, no. 9, pp. 625–632, 2009.

[10] H. Sun, N. Hovakimyan, and T. Basar, "$\mathcal{L}_1$ adaptive controller for uncertain nonlinear multi-input multi-output systems with input quantization," *IEEE Transactions on Automatic Control*, vol. 57, no. 3, pp. 565–578, 2012.

[11] M. Krstić, I. Kanellakopoulos, and P. Kokotović, *Nonlinear and Adaptive Control Design*. John Wiley & Sons, Inc., 1995.

[12] J. Zhou and C. Wen, "Adaptive backstepping control of uncertain nonlinear systems with input quantization," in *IEEE Conference on Decision and Control*, 2013, pp. 5571–5576.

[13] J. Zhou, C. Wen, and W. Wang, "Adaptive control of uncertain nonlinear systems with quantized input signal," *Automatica*, vol. 95, pp. 152–162, 2018.

[14] S. M. Schlanbusch and J. Zhou, "Adaptive backstepping control of a 2-DOF helicopter system with uniform quantized inputs," in *IECON 2020 The 46th Annual Conference of the IEEE Industrial Electronics Society*, 2020, pp. 88–94.

[15] Y. Wang, L. He, and C. Huang, "Adaptive time-varying formation tracking control of unmanned aerial vehicles with quantized input," *ISA Transactions*, vol. 85, pp. 76–83, 2019.

[16] J. Zhou, C. Wen, W. Wang, and F. Yang, "Adaptive backstepping control of nonlinear uncertain systems with quantized states," *IEEE Transactions on Automatic Control*, vol. 64, no. 11, pp. 4756–4763, 2019.

[17] S. M. Schlanbusch, J. Zhou, and R. Schlanbusch, "Adaptive backstepping attitude control of a rigid body with state quantization," in *Proceedings of 60th IEEE Conference on Decision and Control*, 2021.

[18] Y. Yan and S. Yu, "Sliding mode tracking control of autonomous underwater vehicles with the effect of quantization," *Ocean Engineering*, vol. 151, pp. 322–328, 2018.

[19] S. M. Schlanbusch, J. Zhou, and R. Schlanbusch, "Adaptive attitude control of a rigid body with input and output quantization," *IEEE Transactions on Industrial Electronics*, 2021.

[20] S. J. Yoo and B. S. Park, "Quantized-states-based adaptive control against unknown slippage effects of uncertain mobile robots with input and state quantization," *Nonlinear Analysis: Hybrid Systems*, vol. 42, pp. 1–17, 2021, article 101077.

[21] B. M. Kim and S. J. Yoo, "Approximation-based quantized state feedback tracking of uncertain input-saturated MIMO nonlinear systems with application to 2-DOF helicopter," *Mathematics*, vol. 9, no. 9, 2021.

[22] S. M. Schlanbusch and J. Zhou, "Adaptive backstepping control of a 2-dof helicopter," in *Proceedings of the IEEE 7th International Conference on Control, Mechatronics and Automation*, 2019, pp. 210–215.

Paper E

Attitude Control of a 2-DOF Helicopter System with Input Quantization and Delay

Siri Marte Schlanbusch, Ole Morten Aamo and Jing Zhou

This paper has been published as:

S. M. Schlanbusch, O. M. Aamo and J. Zhou, "Attitude control of a 2-DOF helicopter system with input quantization and delay," in *IECON 2022 The 48th Annual Conference of the IEEE Industrial Electronics Society*, 2022, doi: 10.1109/IECON49645.2022.9968994.

Attitude Control of a 2-DOF Helicopter System with Input Quantization and Delay

Siri Marte Schlanbusch[1], Ole Morten Aamo[2] and Jing Zhou[1]

[1]Department of Engineering Sciences
University of Agder
Grimstad N-4879, Norway

[2]Department of Engineering Cybernetics
Norwegian University of Science and Technology
Trondheim N-7491, Norway

Abstract

In this paper the attitude tracking control problem of a 2 degrees-of-freedom helicopter system with network induced constraints is studied. A predictor feedback control law is developed to compensate a known delay in the communication, where the inputs are quantized before transmitted over the network. Stability of the closed-loop system is established, where tracking is achieved with bounded tracking errors due to the network issues. The developed predictor-based controller is experimentally tested on the helicopter system, where we demonstrate that tracking is achieved in presence of both input delay and quantization.

E.1 Introduction

Air vehicles such as unmanned aerial vehicles (UAVs) and helicopters provide great accessibility and have a wide range of applications such as transport, search and rescue, inspection, monitoring and photography. Unmanned aircraft are controlled by a human operator from ground or fully autonomously by electronic systems, where remote controlled systems are sensitive to time delays and also the sampling and quantization of signals before transmitted in the communication network affect the performance of such systems.

For an attitude tracking control problem where signals are sent through a network, both quantization and delay have impact on the tracking performance. Quantization naturally exists in networked control systems (NCSs), where a quantizer can be

considered as a devise that converts a continuous signal into a piecewise constant signal, which leads to quantization errors that are nonlinear. These errors can not be ignored when the resolution in the network is low, since it will affect the performance and stability of the system. Quantization can also be considered as useful, from the advantage of reducing occupation rate of transmission bandwidth in the communication channel [1]. Tracking control of systems with input quantization has been investigated in e.g. [2–5] for uncertain nonlinear systems, in [6] for a group of unmanned aerial vehicles with unknown parameters, in [7] for under-actuated autonomous underwater vehicles (AUVs) and in [8] for a 2 degrees-of-freedom (DOF) helicoper system.

One of the first tools for handling delays was the Smith predictor used for compensating a pure time-delay for open-loop stable plants. A modified Smith predictor compensates for both the predicted effect of the control input and of the future evolution of the system state, and also works for unstable plants [9]. Several predictor based approaches have been proposed to compensate input delays for linear systems in [10–12] and nonlinear systems in [13–19] where a backstepping transformation was introduced in the control design in [13], which makes it possible to show stability of the closed-loop system using a Lyapunov functional. In [20] the attitude stabilization of a quadrotor with a known input delay was considered where a predictor feedback controller was developed to compensate the delay. Compared to stabilization to a desired attitude, the problem of tracking a changing reference signal with time is more difficult. Unless knowing the reference signal in advance, and by sending the reference signal the delayed-time units ahead to the controller, it is not possible to track the desired signal perfectly in presence of a delay. In [21], the tracking control problem of nonlinear networked and quantized control systems was studied. In [22] a predictor feedback controller was developed for trajectory tracking where both input delay and parameters were unknown.

In this paper we are focusing on the problem of tracking a given reference attitude for a nonlinear multiple-input multiple-output (MIMO) helicopter system with 2 DOF, when there is a known constant time-delay of D-time units for the inputs and at the same time, the inputs are quantized before transmitted over the network. The main contributions in this paper are dealing with the simultaneous issues caused by quantization and delay, where the effect of the delay is compensated for by the design of a predictor feedback controller, and where the effect of quantization is analytically shown to be related to the tracking error. A higher quantization level increases the tracking error. Simulations and experiments are carried out to illustrate the proposed control scheme.

The paper is organized as follows. In Section E.2, the dynamical model of the helicopter system, the control problem and the considered quantizer are presented.

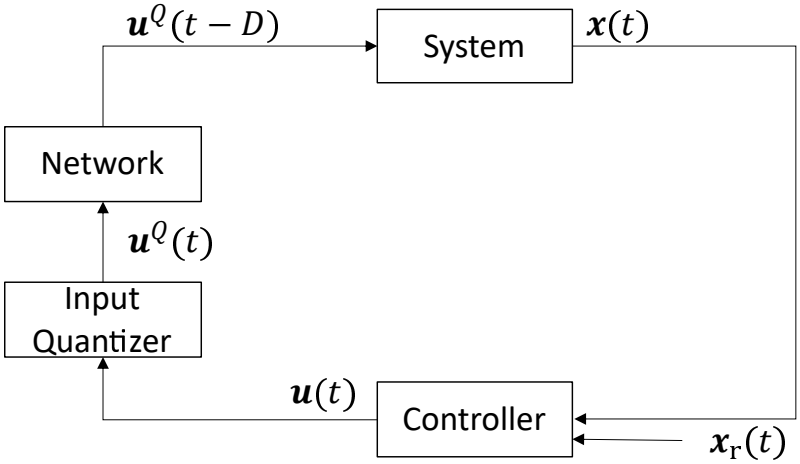

Figure E.1: Control system with input quantization and delay over a network.

Section E.3 provides the predictor-feedback control design, in Section E.4 a proof of stability on the basis of a Lyapunov functional is given and in Section E.5 experimental results of the proposed method implemented on the helicopter system are presented and Section E.6 sums up the paper in a conclusion.

E.2 Dynamical Model and Problem Statement

E.2.1 Notations

Vectors are denoted by small bold letters and matrices with capitalized bold letters. $\lambda_{\max}(\cdot)$ and $\lambda_{\min}(\cdot)$ denote the maximum and minimum eigenvalue of the matrix $(\cdot)$, and $\|\cdot\|$ denotes the $\mathcal{L}_2$-norm and induced $\mathcal{L}_2$-norm for vectors and matrices, respectively. For vector functions, the norm $\|\boldsymbol{u}(t)\|_2 = \sqrt{\int_0^D \boldsymbol{u}(x,t)^\top \boldsymbol{u}(x,t)dx}$ denotes the spatial $\mathcal{L}_2$ norm.

E.2.2 Problem Statement

We are considering a control problem as shown in Fig. E.1, where the input vector $\boldsymbol{u}$ is quantized before transmitted in the communication network and there is a time-delay D in the network. The system is assumed noiseless, so that the quantized signals are recovered after transmission, and so the system receives the quantized delayed input $\boldsymbol{u}^Q(t-D)$.

The control objective is to develop a predictor based control law to compensate for a constant known input delay for a multi input nonlinear helicopter system to track a given reference attitude signal. From the derived error dynamics, we will design a controller so that stability of the origin of the error system is maintained in the presence of both quantization and delay of the input.

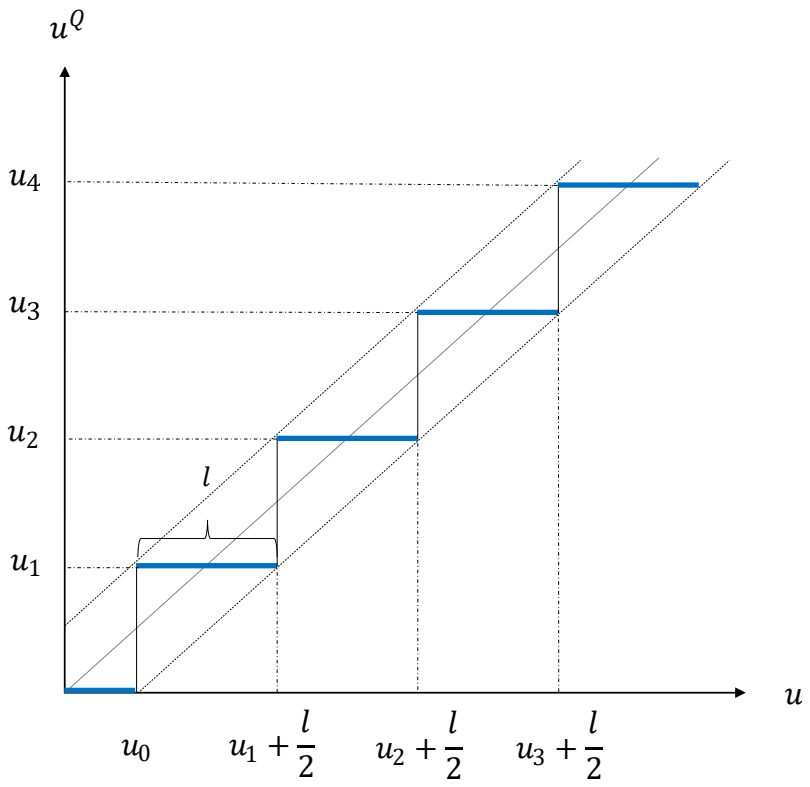

Figure E.2: Map of the uniform quantizer for $u > 0$.

E.2.3 Quantizer

In this paper we consider a uniform quantizer for the inputs, where the quantizer for each input signal is modeled as

$$Q(u) = u^Q = \begin{cases} u_i \operatorname{sgn}(u), & u_i - \frac{l}{2} < |u| \leq u_i + \frac{l}{2} \\ 0, & |u| \leq u_0 \end{cases}, \tag{E.1}$$

where $Q(\cdot)$ is a quantizer, $u_0 > 0, u_1 = u_0 + \frac{l}{2}$, $u_{i+1} = u_i + l$, $l > 0$ is the length of the quantization interval, $\operatorname{sgn}(u)$ is the sign function. The uniform quantization $u^Q \in U = \{0, \pm u_i\}$, and a map of the quantization for $u_i > 0$ is shown in Fig. E.2.

The following property holds for the uniform quantizer

$$|u^Q - u| \leq \delta, \tag{E.2}$$

where $\delta > 0$ denotes the quantization bound. Clearly, the property in (E.2) is satisfied with $\delta = \max\{u_0, \frac{l}{2}\}$. When a vector is quantized, we have

$$\boldsymbol{u}^Q = \begin{bmatrix} u_1^Q & u_2^Q & \cdots & u_n^Q \end{bmatrix}^\top, \tag{E.3}$$

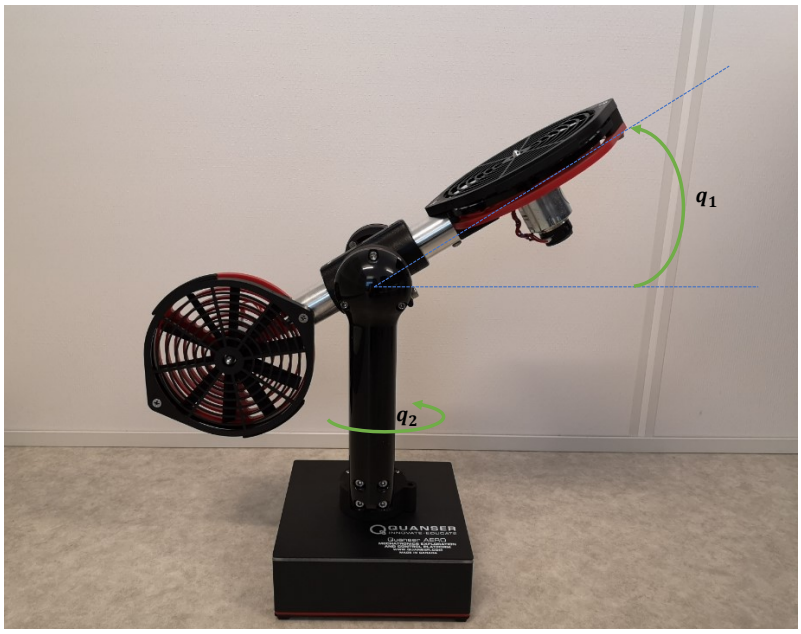

Figure E.3: Quanser Aero helicopter system.

and so each vector element is bounded by (E.2), and we have

$$\|\boldsymbol{u}^Q - \boldsymbol{u}\| = \|\boldsymbol{d}\| \leq \|\boldsymbol{\delta}\| \triangleq \delta_u, \tag{E.4}$$

where $\boldsymbol{d}$ is the quantization error.

E.2.4 Mathematical Model

The helicopter system shown in Fig. E.3 is a two-rotor laboratory equipment for flight control-based experiments. With a horizontal position of the main thruster and a vertical position of the tail thruster, this resembles a helicopter with two propellers driven by two DC motors. The helicopter is a MIMO system with 2 DOF, and can rotate around two axes. This is considered as a rigid body and a mathematical model is derived using Euler-Lagrange equations and expressed as:

$$\boldsymbol{M}(\boldsymbol{q})\ddot{\boldsymbol{q}} + \boldsymbol{C}(\boldsymbol{q}, \dot{\boldsymbol{q}})\dot{\boldsymbol{q}} + \boldsymbol{D}\dot{\boldsymbol{q}} + \boldsymbol{g}(\boldsymbol{q}) = \boldsymbol{u}^Q(t - D), \tag{E.5}$$

where

$$\boldsymbol{M}(\boldsymbol{q}) = \begin{bmatrix} I_p + mr^2 & 0 \\ 0 & I_y + mr^2 \sin^2 q_1 \end{bmatrix}, \tag{E.6}$$

$$\boldsymbol{C}(\boldsymbol{q}, \dot{\boldsymbol{q}}) = \begin{bmatrix} 0 & -mr^2 \sin q_1 \cos q_1 \dot{q}_2 \\ mr^2 \sin q_1 \cos q_1 \dot{q}_2 & mr^2 \sin q_1 \cos q_1 \dot{q}_1 \end{bmatrix}, \tag{E.7}$$

$$\boldsymbol{g}(\boldsymbol{q}) = \begin{bmatrix} mgr \sin q_1 & 0 \end{bmatrix}^\top, \quad \boldsymbol{q} = \begin{bmatrix} q_1 & q_2 \end{bmatrix}^\top, \tag{E.8}$$

and where $\boldsymbol{q}, \dot{\boldsymbol{q}}, \ddot{\boldsymbol{q}} \in \mathbb{R}^2$ are angles, angular velocities and accelerations, $\boldsymbol{M}(\boldsymbol{q})$, $\boldsymbol{C}(\boldsymbol{q}, \dot{\boldsymbol{q}}), \boldsymbol{D} \in \mathbb{R}^{2\times 2}$ are the inertia, Coriolis and damping matrices, respectively, where $\boldsymbol{D}$ is a constant matrix, $\boldsymbol{g}(\boldsymbol{q}) \in \mathbb{R}^2$ is a vector of gravitational loading, r is the distance between the center of mass and the origin of the body-fixed frame, I_p and I_y are the moments of inertia of q_1 and q_2 respectively, g is the gravitational acceleration, and m is the total mass of the Aero body.

Defining $\boldsymbol{x} = [\boldsymbol{q}^\top, \dot{\boldsymbol{q}}^\top]^\top = [\boldsymbol{x}_1^\top, \boldsymbol{x}_2^\top] \in \mathbb{R}^4$, and $\boldsymbol{u} \in \mathbb{R}^2$, the system can be written in state space form as

$$\dot{\boldsymbol{x}}(t) = f(\boldsymbol{x}(t), \boldsymbol{u}^Q(t - D)). \tag{E.9}$$

For tracking of a reference signal $\boldsymbol{x}_r(t)$, the error states are defined as

$$\boldsymbol{z}_1 = \boldsymbol{x}_r - \boldsymbol{x}_1, \tag{E.10}$$

$$\boldsymbol{z}_2 = \dot{\boldsymbol{z}}_1 + \boldsymbol{A}\boldsymbol{z}_1, \tag{E.11}$$

where $\boldsymbol{A}$ is a constant positive definite matrix, and the error dynamics is given as

$$\dot{\boldsymbol{z}}(t) = f(\boldsymbol{z}(t), \boldsymbol{u}^Q(t - D)) = \begin{bmatrix} \boldsymbol{z}_2 - \boldsymbol{A}\boldsymbol{z}_1 \\ \boldsymbol{A}\boldsymbol{z}_2 + \boldsymbol{h} - \boldsymbol{M}^{-1}\boldsymbol{u}^Q(t - D) \end{bmatrix}, \tag{E.12}$$

$$\boldsymbol{h} = \ddot{\boldsymbol{x}}_r - \boldsymbol{A}^\top \boldsymbol{A}\boldsymbol{z}_1 + \boldsymbol{M}^{-1}\left[(\boldsymbol{C} + \boldsymbol{D})(\dot{\boldsymbol{x}}_r + \boldsymbol{A}\boldsymbol{z}_1 - \boldsymbol{z}_2) + \boldsymbol{g}\right]. \tag{E.13}$$

The change of coordinates (E.10)–(E.11) are chosen by following the backstepping design procedure [23], where a similar design is given in e.g. [24]. To achieve the control objective, the following assumption regarding the reference signal is imposed:

Assumption 1. *The desired angles, angular velocities and accelerations,* $\boldsymbol{x}_r(t), \dot{\boldsymbol{x}}_r(t), \ddot{\boldsymbol{x}}_r(t) \in \mathbb{R}^2$*, are known, continuous and bounded for all* $t \geq t_0 \geq 0$*.*

E.3 Predictor-Feedback Control Design

To compensate for the input delay, we derive a predictor-feedback controller for the system. A nominal controller for the error system (E.12) without quantization and delay $D = 0$, can be formulated as

$$\boldsymbol{u}(t) = \kappa\left(\boldsymbol{z}(t), \boldsymbol{x}_r(t)\right) = \boldsymbol{M}(\boldsymbol{h} + (\boldsymbol{A} + \boldsymbol{B})\boldsymbol{z}_2 + \boldsymbol{z}_1), \tag{E.14}$$

where $\boldsymbol{B}$ is a positive definite matrix, and makes the origin exponentially stable in the absence of delay and quantization. System (E.12) can be equivalently modeled

by a cascade of ODE-PDE [17]

$$\dot{\boldsymbol{z}}(t) = f(\boldsymbol{z}(t), \boldsymbol{u}(0,t)), \tag{E.15}$$

$$\boldsymbol{u}_t(x,t) = \boldsymbol{u}_x(x,t), \tag{E.16}$$

$$\boldsymbol{u}(D,t) = \boldsymbol{u}^Q(t), \tag{E.17}$$

where the actuator state is modeled by a transport PDE and where the solution to (E.16)–(E.17) is given by $\boldsymbol{u}(x,t) = \boldsymbol{u}^Q(t+x-D)$ for all $x \in [0, D]$.

The predictor feedback controller is defined as [14]

$$\boldsymbol{u}^Q(t) = Q\left(\kappa[\boldsymbol{p}(D,t), \boldsymbol{x}_r(t+D)]\right), \tag{E.18}$$

where the predictor state is given as

$$\boldsymbol{p}(x,t) = \boldsymbol{z}(t) + \int_0^x f(\boldsymbol{p}(y,t), \boldsymbol{u}(y,t))dy, \forall x \in [0, D], \tag{E.19}$$

where, assuming perfect model f, $\boldsymbol{p}(x,t) = \boldsymbol{z}(t+x)\ \forall x \in [0, D]$, and so $\boldsymbol{p}(D,t) = \boldsymbol{z}(t+D)$ is the D-time units ahead predictor of $\boldsymbol{z}(t)$. Then the delayed input

$$\boldsymbol{u}(0,t) = \boldsymbol{u}^Q(t-D) = Q\left(\kappa[t, \boldsymbol{p}(0,t)]\right) = \kappa(t, \boldsymbol{z}(t)) + \boldsymbol{d}(t), \tag{E.20}$$

where $\boldsymbol{d}(t)$ is the quantization error which satisfies (E.4).

E.4 Stability Analysis

To analyze the closed-loop stability, we first establish some preliminary results as stated in the following Lemma.

Lemma 1. *The open loop system $\dot{\boldsymbol{z}} = f(\boldsymbol{z}, \boldsymbol{\omega})$ is forward complete.*

Proof. Consider the nonnegative-valued, radially unbounded, smooth Lyapunov function and its derivative [18]

$$V_1(\boldsymbol{z}) = \frac{1}{2}\boldsymbol{z}^\top \boldsymbol{z}, \tag{E.21}$$

$$\begin{aligned}\dot{V}_1 &= \boldsymbol{z}_1^\top(\boldsymbol{z}_2 - \boldsymbol{A}\boldsymbol{z}_1) + \boldsymbol{z}_2^\top(\boldsymbol{A}\boldsymbol{z}_2 + \boldsymbol{h} - \boldsymbol{M}^{-1}\boldsymbol{\omega}) \\ &\leq c_1 V_1 + \frac{1}{2}\boldsymbol{\omega}^\top\boldsymbol{\omega} + c_2(\boldsymbol{x}_r^\top\boldsymbol{x}_r + \dot{\boldsymbol{x}}_r^\top\dot{\boldsymbol{x}}_r + \ddot{\boldsymbol{x}}_r^\top\ddot{\boldsymbol{x}}_r) \\ &\leq c_1 V_1 + c_3, \quad \forall \boldsymbol{z} \in \mathbb{R}^4, \boldsymbol{\omega} \in \mathbb{R}^2,\end{aligned} \tag{E.22}$$

where $c_{(\cdot)}$ are positive constants, Assumption 1 is used, and where $\boldsymbol{\omega}$ is a bounded input. Then, the system $\dot{\boldsymbol{z}}$ is forward complete and solutions exist globally. □

A definition of forward completeness is given in e.g.[14]. Since the system is forward complete, the problem of a finite escape phenomenon is avoided, and ensures that for every initial condition and every bounded input signal, the corresponding solution is defined for all $t \geq 0$.

Following [17], we define the direct and inverse backstepping transformation

$$\boldsymbol{w}(x,t) = \boldsymbol{u}(x,t) - Q\left(\kappa[x+t, \boldsymbol{p}(x,t)]\right), \tag{E.23}$$

$$\boldsymbol{u}(x,t) = \boldsymbol{w}(x,t) + Q\left(\kappa[x+t, \boldsymbol{\pi}(x,t)]\right), \tag{E.24}$$

where for all $x \in [0, D]$,

$$\boldsymbol{\pi}(x,t) = \boldsymbol{z}(t) + \int_0^x f(\boldsymbol{\pi}(y,t), Q\left(\kappa[t+y, \boldsymbol{\pi}(y,t)]\right) + \boldsymbol{w}(y,t))dy, \tag{E.25}$$

where $\boldsymbol{\pi}(x,t)$ are used to generate the target predictor state $\boldsymbol{\pi}(D,t)$.

By [17, Lemma 1], the transformation (E.23) maps the closed loop system consisting of the error system (E.15)–(E.17) and the control law (E.18)–(E.19) into the target system

$$\begin{aligned}\dot{\boldsymbol{z}}(t) &= f(\boldsymbol{z}(t), \boldsymbol{w}(0,t) + \kappa(t, \boldsymbol{z}(t)) + \boldsymbol{d}(t)) \\ &= \begin{bmatrix} \boldsymbol{z}_2(t) - \boldsymbol{A}\boldsymbol{z}_1(t) \\ -\boldsymbol{z}_1(t) - \boldsymbol{B}\boldsymbol{z}_2(t) - \boldsymbol{M}^{-1}\boldsymbol{w}(0,t) - \boldsymbol{M}^{-1}\boldsymbol{d}(t) \end{bmatrix}, \end{aligned} \tag{E.26}$$

$$\boldsymbol{w}_x(x,t) = \boldsymbol{w}_t(x,t), \ \forall x \in [0, D], \tag{E.27}$$

$$\boldsymbol{w}(D,t) = 0. \tag{E.28}$$

By [17, Lemma 2], (E.24) is the inverse of (E.23). We now state our main result in the following theorem.

Theorem 1. *Consider the closed-loop system consisting of the error dynamics of the helicopter system* (E.15)–(E.17)*, the control law* (E.18)–(E.19) *with input quantization satisfying the bounded property* (E.4)*, and the reference signal* $\boldsymbol{x}_r(t)$ *satisfying Assumption 1. If the gain matrices* $\boldsymbol{A}$ *and* $\boldsymbol{B}$ *are chosen to satisfy the inequality*

$$\min\{2\lambda_{\min}(\boldsymbol{A}), 2\lambda_{\min}(\boldsymbol{B}) - 2, 1\} > c_4 > 0, \tag{E.29}$$

where c_4 *is a positive constant, then for all initial conditions* $\boldsymbol{z}(t_0) \in \mathbb{R}^4$*,* $\boldsymbol{u}(x,t_0) \in \mathbb{R}^2 \ \forall x \in [0, D]$ *and for all* $t \geq t_0 \geq 0$*, the following holds:*

$$\|\boldsymbol{z}(t)\| + \|\boldsymbol{w}(t)\|_2 \leq c_6 \left(\|\boldsymbol{z}(t_0)\| + \|\boldsymbol{w}(t_0)\|_2\right) e^{-\frac{c_4}{2}(t-t_0)} + c_5\delta_u, \tag{E.30}$$

where

$$c_5 = \sqrt{\frac{2k}{c_4}} > 0, \qquad c_6 = \sqrt{2ke^D} > 0, \tag{E.31}$$

where $k = \max\{1, \lambda_{\max}(\boldsymbol{M}^{-1})^2\}$.

Proof. Due to forward completeness of (E.15) (Lemma 1), the predictor state (E.19) is well defined and therefore $\boldsymbol{w}(x,t)$ in (E.23) is well defined. It follows that the target system (E.26)–(E.28) is well defined and that we can select the Lyapunov function candidate

$$V_2(t) = \frac{1}{2}\boldsymbol{z}(t)^\top \boldsymbol{z}(t) + \frac{k}{2}\int_0^D e^x \boldsymbol{w}(x,t)^\top \boldsymbol{w}(x,t)dx, \tag{E.32}$$

that satisfies

$$\frac{1}{2}E(t) \leq V_2(t) \leq \frac{1}{2}ke^D E(t), \tag{E.33}$$

where

$$E(t) = \boldsymbol{z}(t)^\top \boldsymbol{z}(t) + \int_0^D \boldsymbol{w}(x,t)^\top \boldsymbol{w}(x,t)dx. \tag{E.34}$$

The derivative of (E.32) is

$$\begin{aligned}\dot{V}_2 =& -\boldsymbol{z}_1^\top \boldsymbol{A}\boldsymbol{z}_1 - \boldsymbol{z}_2^\top \boldsymbol{B}\boldsymbol{z}_2 - \boldsymbol{z}_2^\top \boldsymbol{M}^{-1}\boldsymbol{w}(0,t) - \boldsymbol{z}_2^\top \boldsymbol{M}^{-1}\boldsymbol{d}(t) + k\int_0^D e^x \boldsymbol{w}(x,t)^\top \boldsymbol{w}_t(x,t)dx \\ \leq& -\boldsymbol{z}_1^\top \boldsymbol{A}\boldsymbol{z}_1 - \boldsymbol{z}_2^\top \boldsymbol{B}\boldsymbol{z}_2 + \boldsymbol{z}_2^\top \boldsymbol{z}_2 - \frac{k}{2}\boldsymbol{w}(0,t)^\top \boldsymbol{w}(0,t) - \frac{k}{2}\int_0^D e^x \boldsymbol{w}(x,t)^\top \boldsymbol{w}(x,t)dx \\ &+ \frac{k}{2}\left(\boldsymbol{w}(0,t)^\top \boldsymbol{w}(0,t) + \delta_u^2\right),\end{aligned} \tag{E.35}$$

where Young's inequality and integration by parts are used. By choosing matrices $\boldsymbol{A}$ and $\boldsymbol{B}$ such that (E.29) holds, we have

$$\dot{V}_2 \leq -c_4 V_2 + \frac{k}{2}\delta_u^2. \tag{E.36}$$

From (E.36) and by using the comparison lemma [25, Lemma 3.4], then for all $t \geq t_0 \geq 0$,

$$\begin{aligned}V_2(t) &\leq V_2(t_0)e^{-c_4(t-t_0)} + \frac{k}{2c_4}\delta_u^2(1 - e^{-c_4(t-t_0)}) \\ &\leq V_2(t_0)e^{-c_4(t-t_0)} + \frac{k}{2c_4}\delta_u^2.\end{aligned} \tag{E.37}$$

Table E.1: Helicopter Parameters.

Symbol	Value	Units
I_p, I_y	0.0217	kgm^2
m	1.075	kg
g	9.81	m/s^2
r	0.0038	m
$\boldsymbol{D}$	[0.007 0;0 0.0095]	kgm^2/s

From (E.37) and (E.33) we have

$$E(t) \leq \frac{k}{c_4}\delta_u^2 + ke^D E(t_0)e^{-c_4(t-t_0)}, \tag{E.38}$$

and by using the inequality $\left(\|\boldsymbol{z}(t)\| + \|\boldsymbol{w}(t)\|_2\right)^2 \leq 2E(t)$ we get estimate (E.30). This shows that the target system is uniformly ultimately bounded with an ultimate bound that is directly related to the value of the quantization parameter.

□

Remark 1. *From* (E.30)*, tracking is achieved with a bounded error proportional to the quantization.*

E.5 Simulation and Experimental Results

In this section, the attitude tracking control problem is considered for the Quanser Aero helicopter system, where both simulation using MATLAB/Simulink and experiments on the helicopter system have been carried out. The initial values were set to $\boldsymbol{x}(t_0) = \boldsymbol{0}$, where t_0 defines the start of experiment. The parameters used for simulation and experiment are shown in Table E.1, and the design parameters were chosen as $\boldsymbol{A} = 3\boldsymbol{I}$ and $\boldsymbol{B} = 1.6\boldsymbol{I}$ and satisfies the inequality (E.29). The objective in the experiment was to track a given sinusoidal signal for the attitude $\boldsymbol{x}_r(t)$ in presence of both quantization and delay of the inputs.

To illustrate the performance of the proposed predictor-based controller, we first tested without the predictor and without quantization when there was a delay for the input, and so the system received the delayed inputs $\boldsymbol{u}(t-D)$, where the input vector is defined in (E.14). By increasing the delay, the system had more oscillation, and when $D = 0.1s$, the oscillations increased during the experiment and was stopped after about $4s$. Figs. E.4–E.5 show the tracking of angle $q_1(t)$ and the inputs $\boldsymbol{u}(t-D)$, respectively, from this experiment. This shows that the closed-loop system becomes unstable without the predictor for delays greater or equal to $0.1s$.

The proposed control law was then tested for different delays and quantization parameters. The initial condition of the actuator state was set to $\boldsymbol{u}(x, t_0) = \boldsymbol{0}\ \forall\ x \in$

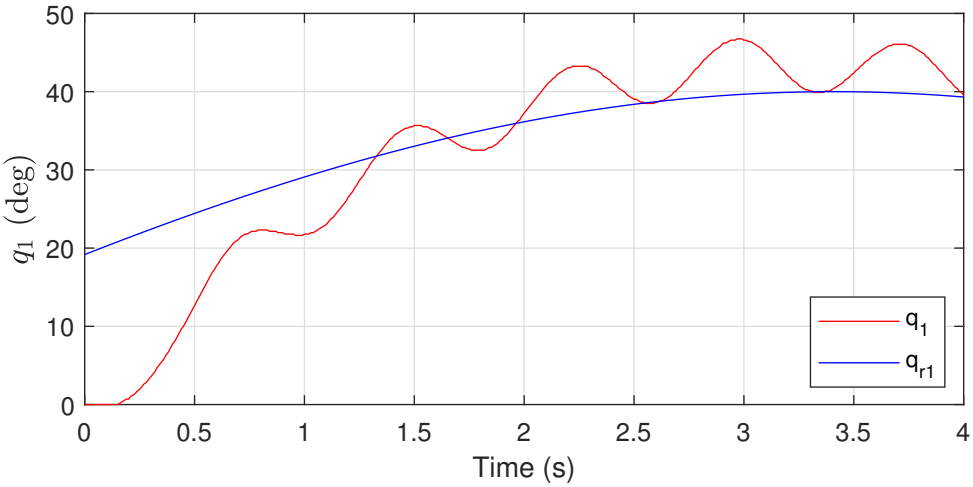

Figure E.4: Tracking of angle $q_1(t)$, with delay, without predictor.

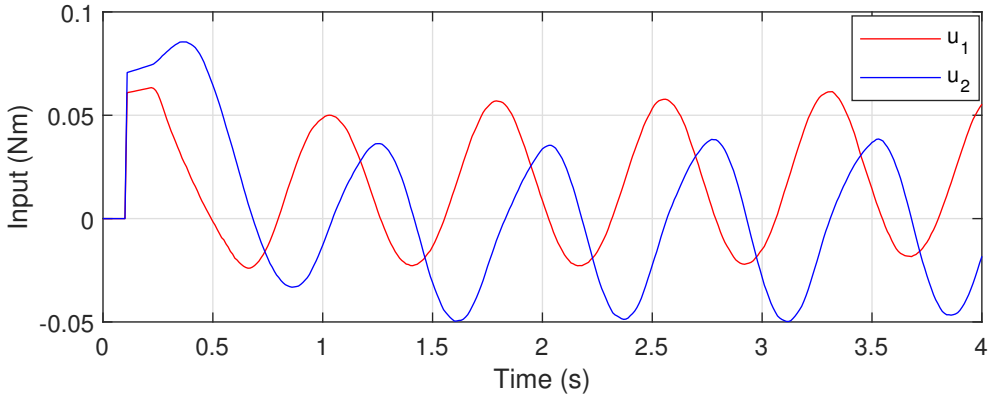

Figure E.5: Input $\boldsymbol{u}(t-D)$ without predictor.

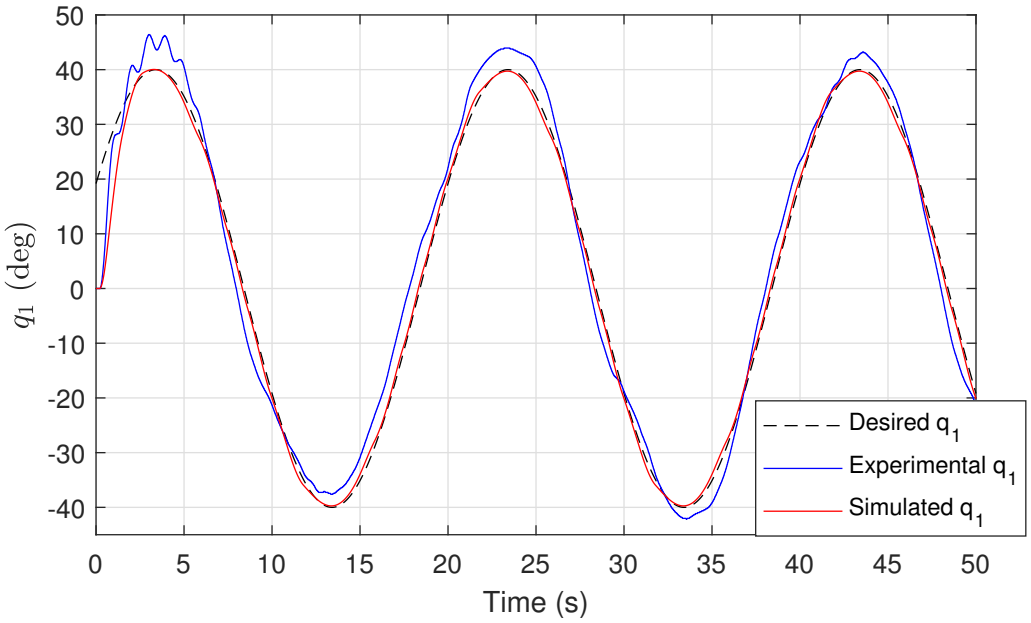

Figure E.6: Tracking of angle $q_1(t)$ from simulation and experiment with delay $D = 0.2$s and quantization.

$[0, D]$, and so the system received zero input until $t = t_0 + D$. The results from simulation and experiment, where the quantization parameters were set to $l = 0.01$, $u_0 = l/2$ and with a time delay $D = 0.2s$, are shown in Figs. E.6–E.11, showing tracking of the angles $\boldsymbol{q}(t)$, the tracking errors $\boldsymbol{z}(t)$ and the inputs $\boldsymbol{u}^Q(t - D)$, respectively, where the red plots are from simulation and the blue plots are from experiment.

From Figs. E.6–E.9 we can see that the desired trajectory can be followed both in simulation and when tested on the helicopter, illustrating our main results in Theorem 1. From the simulation, there are only small tracking errors that are due to the quantization. From the experiment, the tracking errors are higher relative to the simulations due to several other disturbances to the system such as unmodeled dynamics and sensor noise that affects the performance, and the helicopter have a practical stabilization with this controller.

To compare results for different delays and quantization parameters, the total tracking error was defined as

$$z_{\text{track}} = \int_{t_0}^{t_f} \boldsymbol{z}_1^\top \boldsymbol{z}_1 d\tau, \tag{E.39}$$

where t_0 and t_f define start and end of experiment, respectively, and the experiments were run for 50 s where results are provided in Table E.2. From the results we see that by increasing the delay, the total tracking error also increases for the helicopter system, for mainly two reasons. First, since the system receives no input until D

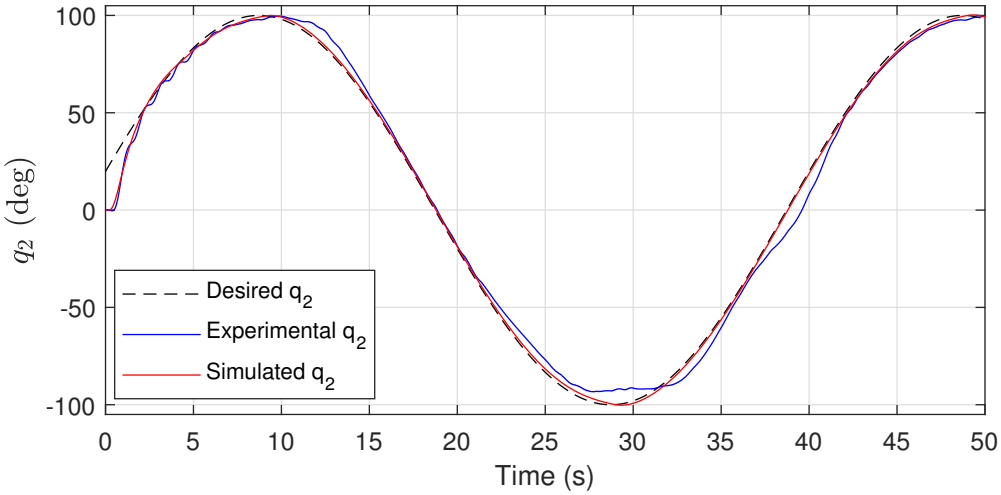

Figure E.7: Tracking of angle $q_2(t)$ from simulation and experiment with delay $D = 0.2$s and quantization.

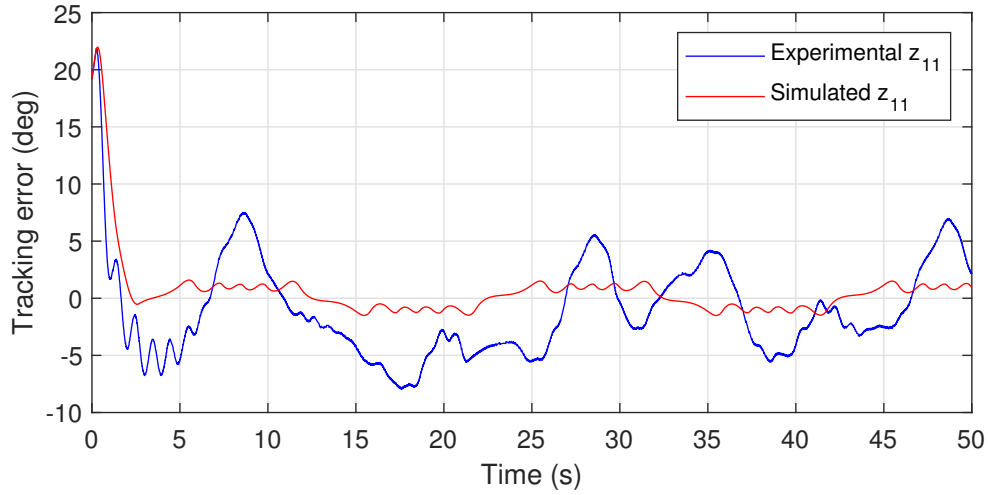

Figure E.8: Tracking error $z_{11}(t)$ from simulation and experiment with delay $D = 0.2$s and quantization.

Table E.2: Total tracking error from experiment with and without delay and quantization. System receives input $\boldsymbol{u}^Q(t - D)$.

Experiment z_{track} $\times 10^{-4}$		**Quantization**			
		No q.	$l = 0.010$	$l = 0.012$	$l = 0.014$
Delay	$D = 0$	3222	3271	3305	3490
	$D = 0.1$	4866	5278	5741	5689
	$D = 0.2$	7274	8692	8518	9114
	$D = 0.3$	13748	11788	13868	14038

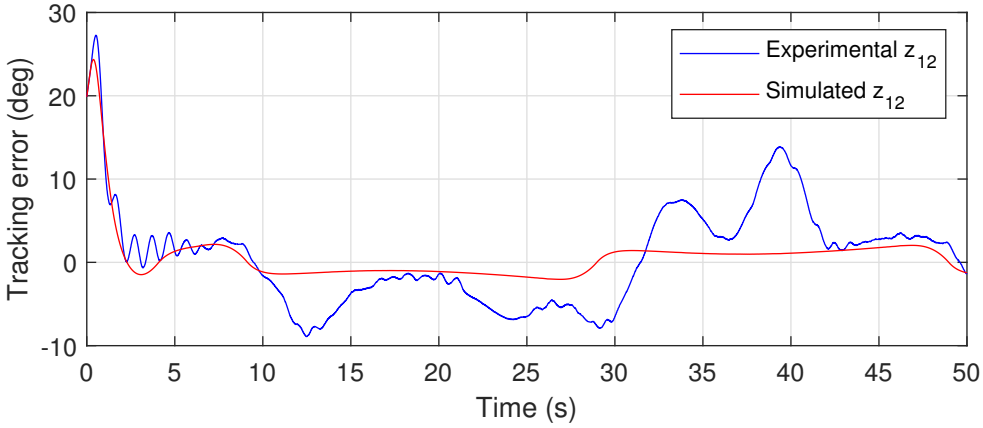

Figure E.9: Tracking error $z_{12}(t)$ from simulation and experiment with delay $D = 0.2$s and quantization.

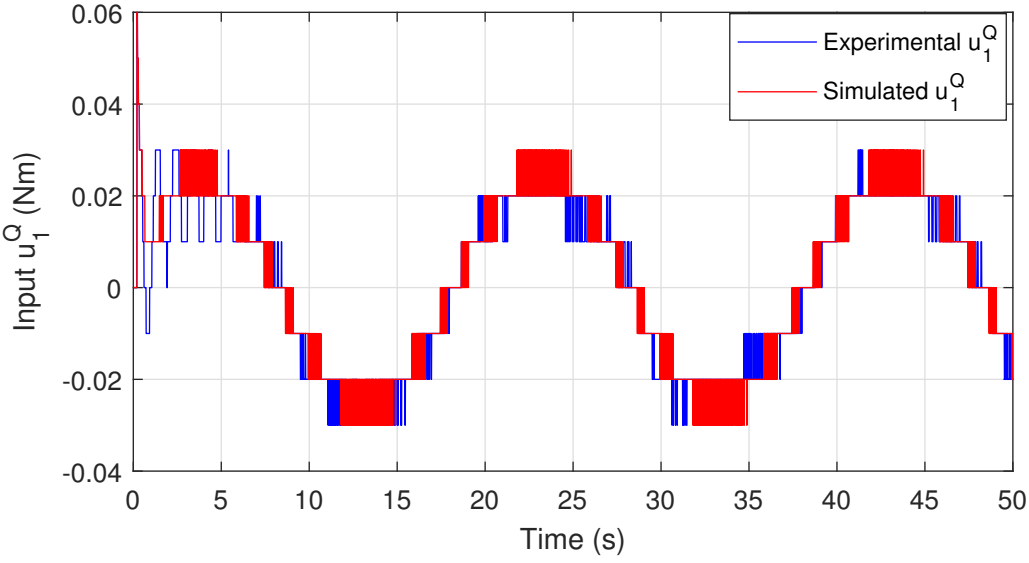

Figure E.10: Input $u_1^Q(t - D)$ from simulation and experiment with delay $D = 0.2$s and quantization.

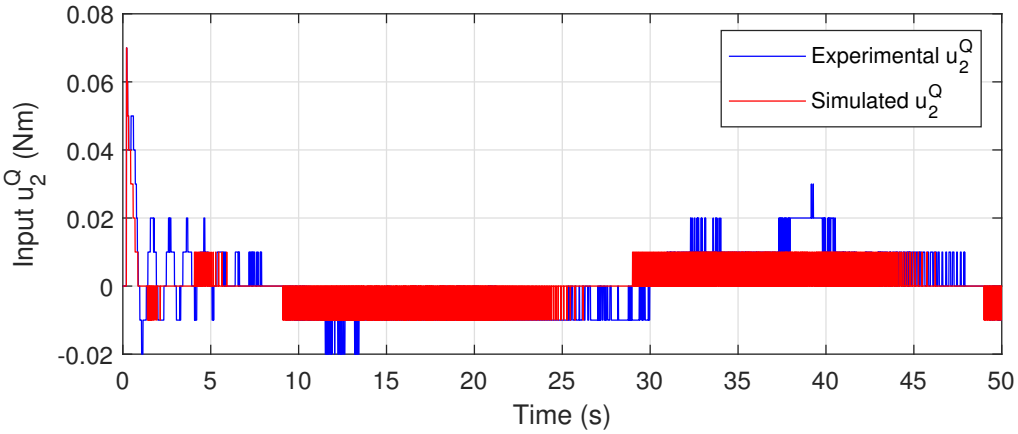

Figure E.11: Input $u_2^Q(t-D)$ from simulation and experiment with delay $D = 0.2$s and quantization.

seconds after the start of experiment, the total tracking error increases during an initial time period, since the reference signal is changing while the helicopter remains stationary. Then, the system receives control input by the predictor based controller and starts tracking the desired signal. So increasing D, increases the time before control kicks in, and z_{track} increases initially. Secondly, because the model is not perfect and from other effects such as measurement errors, the tracking error increases by an increase in the delay. From a perfect model without quantization, the total tracking error will not increase after an initial time period since then $\boldsymbol{z}_1$ becomes zero. The effect of quantization is also shown, where by increasing the quantization, the measurement of the total tracking error increases. This is also affected by other disturbances.

E.6 Conclusion

In this paper, the attitude tracking control problem of a nonlinear system with networked induced delay and quantization for the inputs has been considered. A predictor-feedback controller is proposed to compensate for the input delay. Based on a Lyapunov approach, stability of the closed loop system is ensured and tracking of a desired reference signal is achieved with a bounded tracking error that is directly related to the quantization parameter. Simulations and experiments illustrate the proof.

References – Paper E

[1] N. Elia and S. K. Mitter, "Stabilization of linear systems with limited information," *IEEE Transactions on Automatic Control*, vol. 46, no. 9, pp. 1384–1400, 2001.

[2] L. Xing, C. Wen, Y. Zhu, H. Su, and Z. Liu, "Output feedback control for uncertain nonlinear systems with input quantization," *Automatica*, vol. 65, pp. 191–202, 2015.

[3] J. Zhou and W. Wang, "Adaptive control of quantized uncertain nonlinear systems," *IFAC PapersOnLine*, vol. 50, no. 1, pp. 10 425–10 430, 2017.

[4] Y. Li and G. Yang, "Adaptive asymptotic tracking control of uncertain nonlinear systems with input quantization and actuator faults," *Automatica*, vol. 72, pp. 177–185, 2016.

[5] L. Xing, C. Wen, H. Su, Z. Liu, and J. Cai, "Robust control for a class of uncertain nonlinear systems with input quantization," *International journal of robust and nonlinear control*, vol. 26, no. 8, pp. 1585–1596, 2015.

[6] Y. Wang, L. He, and C. Huang, "Adaptive time-varying formation tracking control of unmanned aerial vehicles with quantized input," *ISA Transactions*, vol. 85, pp. 76–83, 2019.

[7] B. Huang, B. Zhou, S. Zhang, and C. Zhu, "Adaptive prescribed performance tracking control for underactuated autonomous underwater vehicles with input quantization," *Ocean Engineering*, vol. 221, 2021.

[8] S. M. Schlanbusch and J. Zhou, "Adaptive backstepping control of a 2-DOF helicopter system with uniform quantized inputs," in *IECON 2020 The 46th Annual Conference of the IEEE Industrial Electronics Society*, 2020, pp. 88–94.

[9] M. Krstić, "On compensating long actuator delays in nonlinear control," in *American Control Conference*. IEEE, 2008.

[10] Z. Artstein, "Linear systems with delayed controls: A reduction," *IEEE Transactions on Automatic Control*, vol. 27, no. 4, pp. 869–879, 1982.

[11] M. Krstić, "Lyapunov stability of linear predictor feedback for time-varying input delay," *IEEE Transactions on Automatic Control*, vol. 55, no. 2, pp. 554–559, 2010.

[12] Y. Zhu, M. Krstić, and H. Su, "Adaptive global stabilization of uncertain multi-input linear time-delay systems by PDE full-state feedback," *Automatica*, vol. 96, pp. 270–279, 2018.

[13] M. Krstić, "Input delay compensation for forward complete and strict-feedforward nonlinear systems," *IEEE Transactions on Automatic Control*, vol. 55, no. 2, pp. 287–303, 2010.

[14] N. Bekiaris-Liberis and M. Krstić, *Nonlinear control under nonconstant delays*. SIAM, 2013.

[15] D. Bresch-Pietri and M. Krstić, "Backstepping transformation of input delay nonlinear systems," *arXiv:1305.5305*, 2013.

[16] ——, "Delay-adaptive control for nonlinear systems," *IEEE Transactions on Automatic Control*, vol. 59, no. 5, pp. 1203–1218, 2014.

[17] N. Bekiaris-Liberis and M. Krstić, "Predictor-feedback stabilization of multi-input nonlinear systems," *IEEE Transactions on Automatic Control*, vol. 62, no. 2, pp. 516–531, 2017.

[18] M. Bagheri, P. Naseradinmousavi, and M. Krstić, "Feedback linearization based predictor for time delay control of a high-DOF robot manipulator," *Automatica*, vol. 108, 2019.

[19] A. Bertino, P. Naseradinmousavi, and M. Krstić, "Experimental and analytical delay-adaptive control of a 7-DOF robot manipulator," in *American Control Conference*. IEEE, 2021.

[20] M. Sharma and I. Kar, "Attitude stabilization of quadrotor with input time delay," *IFAC-PapersOnLine*, vol. 53, no. 2, pp. 9360–9365, 2020.

[21] W. Ren and J. Xiong, "Tracking control of nonlinear networked and quantized control systems with communication delays," *IEEE Transactions on Automatic Control*, vol. 65, no. 8, pp. 3685–3692, 2020.

[22] D. Bresch-Pietri and M. Krstić, "Adaptive trajectory tracking despite unknown input delay and plant parameters," *Automatica*, vol. 45, no. 9, pp. 2074–2081, 2009.

[23] M. Krstić, I. Kanellakopoulos, and P. Kokotović, *Nonlinear and Adaptive Control Design*. John Wiley & Sons, Inc., 1995.

[24] S. M. Schlanbusch and J. Zhou, "Adaptive backstepping control of a 2-DOF helicopter system in the presence of quantization," in *9th International Conference on Control, Mechatronics and Automation*. IEEE, 2021, pp. 110–115.

[25] H. K. Khalil, *Nonlinear Systems, third edition*. Pearson Education International Inc., 2002.

Paper F

Adaptive Quantized Control of Uncertain Nonlinear Rigid Body Systems

Siri Marte Schlanbusch and Jing Zhou

This paper has been published as:

S. M. Schlanbusch and J. Zhou, "Adaptive quantized control of uncertain nonlinear rigid body systems," *Systems & Control Letters*, vol. 175, 2023, 105513, doi: 10.1016/j.sysconle.2023.105513.

Adaptive Quantized Control of Uncertain Nonlinear Rigid Body Systems

Siri Marte Schlanbusch and Jing Zhou

Department of Engineering Sciences
University of Agder
4879 Grimstad, Norway

Abstract

This paper investigates the attitude tracking control problem for uncertain nonlinear rigid body systems, where both inputs and states are quantized. It is common in networked control systems that sensor and control signals are quantized before they are transmitted via a communication network. An adaptive backstepping control algorithm is developed for a class of uncertain multiple-input multiple-output (MIMO) systems where a class of sector bounded quantizers is considered. It is shown that all the closed-loop signals are ensured uniformly bounded and tracking is achieved. Further, the tracking errors are shown to converge towards a compact set containing the origin and the set can be made small by the choice of the quantization parameters and control parameters. For illustration of the proposed control scheme, experiments were conducted on a 2 degrees-of-freedom (DOF) helicopter system.

F.1 Introduction

Quantized control has gained increasing interest during the past decades due to the use of information technology in the development of modern engineering applications, such as digital control systems and networked control systems. A quantizer maps a continuous signal into a set of discrete values and introduces nonlinear errors that need to be handled. Quantization is not only inevitable owing to the widespread use of digital processors, but also useful due to the advantage of reducing occupation rate of transmission bandwidth in the communication of signals, see e.g. [1].

The quantized feedback stabilization problem for linear systems where the dynamics are precisely known, has been considered in [1–4]. In [1], it was shown that a logarithmic quantizer is the coarsest one to stabilize a single input linear system, where the number of control values is finite. This work was extended in [3] to consider stabilizaton of multiple input linear systems.

Stabilization of nonlinear systems in presence of quantization has been investigated in [5–9]. The main results in [1] was further extended to single input nonlinear systems in [5], and for nonlinear uncertain systems in [6–8], where two different adaptive approaches were used in [6, 7], while a robust approach was considered in [8]. If there are uncertainties to the system, the quantization problem would become more challenging. Since exact system parameters are often unknown for real systems, adaptive control is a useful approach to deal with such uncertainties, where an online estimation of the parameters can be provided. The work in [7], where a backstepping-based adaptive control scheme was presented, was further developed in [9] for the same stabilization problem to consider a hysteresis quantizer, that compared to a logarithmic quantizer has additional quantization levels to avoid chattering. Tracking control in the presence of input quantization has been considered in [10–13] for uncertain nonlinear systems, in [14] for a group of unmanned aerial vehicles with unknown parameters, in [15] for under-actuated autonomous underwater vehicles (AUVs), in [16] for a 2-DOF helicoper system. The developed methods in [5–16] all focused on the input quantization problem, while the controllers were designed by continuous measures of the state feedback.

Control of uncertain systems with state or output quantization has been studied in [17–20] using robust or adaptive approaches. In [17], an adaptive controller was developed for uncertain linear systems with quantized outputs. In [18], a robust controller for a linear MIMO uncertain system was designed with quantized output measurements. In [19], the stabilization problem for uncertain nonlinear systems with quantized states was investigated, and in [20], the attitude tracking control problem of rigid bodies with quantized states was considered, where in [19, 20] adaptive backstepping-based control algorithms were designed.

Although research on quantized control has received much attention recent years, most work focus on either input or output quantization. In practice, the control signal sent to the actuator(s) and the signals sent from sensors to the control module need to be quantized before transmitted due to the use of digital processors and considering the accuracy of sensors. Also, for remotely controlled systems, the control signals and sensor measurements are shared via a common digital network where the bandwidth might be limited and it is natural to suppose that both input and output signals are quantized. Some work that considered both input and state quantization are [21–27]. In [21], the quantization effects on remotely controlled single-input single-output (SISO) linear systems were studied, where the stabilization problem was transformed into a robust control problem. Sliding mode controllers were developed in [22, 23] for trajectory tracking in the presence of both input and state quantization, of AUVs in [22], and of mechanical systems in [23]. Neural-network based adaptive

tracking controllers in presence of quantization were designed in [24] for uncertain nonholonomic mobile robots, and in [25] for uncertain MIMO nonlinear systems. Adaptive backstepping based control schemes were developed in [26, 27], where the attitude tracking control problem for uncertain rigid bodies was investigated in [26], and a class of uncertain nonlinear systems was considered in [27].

This paper investigates the attitude tracking control problem for a class of uncertain rigid body systems with quantization for both inputs and states. The system is modeled as a nonlinear MIMO system, with challenges in controller design due to its nonlinear behavior and uncertain parameters. A quantizer is used for the signals in order to reduce the communication burden, and a new adaptive backstepping based control scheme is developed to achieve tracking of a given reference signal, where the tracking error is shown to converge towards a residual. The proposed control scheme is implemented by experiments on a 2-degrees-of-freedom helicopter system. The main contributions of this paper are as follows.

- The attitude tracking control problem of uncertain nonlinear rigid body systems is investigated where both inputs and states are quantized. As far as we are concerned, this is the first paper that solves this problem with uncertain parameters and where both inputs and states are quantized by a class of quantizers, that satisfies the sector bounded property. A new adaptive backstepping-based controller is developed and a new approach to stability analysis is proposed. By choosing proper design parameters, all signals in the closed-loop system are ensured bounded and tracking is achieved.

- Note that some techniques are presented in [26] to handle the uniform quantization, where the quantization error is bounded by a constant. By contrast, a more general quantizer is considered in this paper. Since the quantization errors depend on the inputs of quantizers, they cannot be ensured bounded automatically. Several difficulties are introduced both in the control design and stability analysis for MIMO uncertain systems due to the fact that the quantization errors are not bounded by constants. Instead the quantization error is linearly dependent on the input to the quantizer, and is the main challenge to be handled. Other challenges:

  - Only the quantized states can be used to construct the control input and the virtual controller.
  - Since the virtual controllers are discontinuous after quantization, the derivative can not be computed as is normally done in the standard backstepping procedure. To overcome the difficulty, differentiable virtual controls are designed by assuming that the system has no quantization.

Their partial derivatives multiplied by the quantized signals are then utilized to complete the design of virtual controls.

– The effects of both input and state quantization introduces several residual terms that need to be dominated.

- By well establishing the relations between the input signals and error states and functions of continuous signals and quantized signals, the stability of the closed-loop system equilibrium can be achieved by choosing proper design parameters.

F.2 Mathematical Model and Problem Statement

F.2.1 Notations

Vectors are denoted by small bold letters and matrices with capitalized bold letters. The symbol $\boldsymbol{\omega}_{b,a}^{c}$ denotes angular velocity of frame a relative to frame b, expressed in frame c; $\boldsymbol{R}_{a}^{b}$ is the rotation matrix from frame a to frame b; the cross product operator $\times$ between two vectors $\boldsymbol{a}$ and $\boldsymbol{b}$ is written as $\boldsymbol{S}(\boldsymbol{a})\boldsymbol{b}$ where $\boldsymbol{S}$ is skew-symmetric; $\lambda_{\max}(\cdot)$ and $\lambda_{\min}(\cdot)$ denotes the maximum and minimum eigenvalue of the matrix $(\cdot)$, and $\|\cdot\|$ denotes the $\mathcal{L}_2$-norm and induced $\mathcal{L}_2$-norm for vectors and matrices, respectively.

F.2.2 Problem Statement

For systems where data transmission are transferred through a common communication network, quantization errors are introduced due to the limited communication rate of the network. For low resolution, these errors can not be ignored, and must be considered in the analysis and controller design since it will affect the performance and stability of the system.

We consider a control system as shown in Fig. F.1, where the inputs $\boldsymbol{u}(t)$ and the states $\boldsymbol{\varepsilon}(t), \boldsymbol{\omega}(t)$ are quantized at the encoder side to be sent over a network. The network is assumed noiseless, so that the quantized signals $\boldsymbol{u}^{Q}(t), \boldsymbol{\varepsilon}^{Q}(t), \boldsymbol{\omega}^{Q}(t)$ are recovered after transmission. The control problem is to design a control law by utilizing only quantized measurement of the states, so that tracking of a desired attitude is achieved.

F.2.3 Rigid Body Model

The orientation of a rigid body in frame b, relative to an inertial frame i, can be described by a unit quaternion [28–30], $\boldsymbol{q} = [\eta, \varepsilon_1, \varepsilon_2, \varepsilon_3]^{\top} = [\eta, \boldsymbol{\varepsilon}^{\top}]^{\top} \in \mathbb{S}^3 = \{\boldsymbol{x} \in$

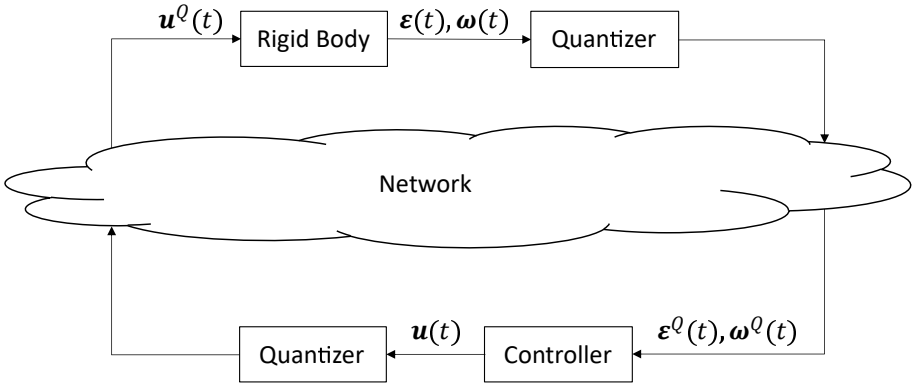

Figure F.1: Control system with input and state quantization over a network.

$\mathbb{R}^4 : \boldsymbol{x}^\top \boldsymbol{x} = 1\}$ that is a complex number, where $\eta = \cos(\upsilon/2) \in \mathbb{R}$ is the real part and $\boldsymbol{\varepsilon} = \boldsymbol{k}\sin(\upsilon/2) \in \mathbb{R}^3$ is the imaginary part, where υ is the Euler angle and $\boldsymbol{k}$ is the Euler axis, and $\mathbb{S}^3$ is the non-Euclidean three-sphere. The kinematic and dynamic equations for the rigid body are defined as

$$\dot{\boldsymbol{q}} = \boldsymbol{T}(\boldsymbol{q})\boldsymbol{\omega}, \tag{F.1}$$

$$\boldsymbol{J}\dot{\boldsymbol{\omega}} = -\boldsymbol{S}(\boldsymbol{\omega})(\boldsymbol{J}\boldsymbol{\omega}) + \boldsymbol{\Phi}(\boldsymbol{\varepsilon}, \boldsymbol{\omega})^\top \boldsymbol{\theta} + \boldsymbol{u}^Q, \tag{F.2}$$

where the angular velocity $\boldsymbol{\omega}_{i,b}^b = \boldsymbol{\omega} \in \mathbb{R}^3$, the inertia matrix $\boldsymbol{J} \in \mathbb{R}^{3\times 3}$ is positive definite and invertible, the vector $\boldsymbol{\theta} \in \mathbb{R}^n$ is unknown and constant, the matrix $\boldsymbol{\Phi} \in \mathbb{R}^{n\times 3}$ are known nonlinear functions, and where we have

$$\boldsymbol{T}(\boldsymbol{q}) = \frac{1}{2}\begin{bmatrix} -\boldsymbol{\varepsilon}^\top \\ \eta\boldsymbol{I} + \boldsymbol{S}(\boldsymbol{\varepsilon}) \end{bmatrix} \in \mathbb{R}^{4\times 3}. \tag{F.3}$$

The matrix $\boldsymbol{I}$ denotes the identity matrix and $\boldsymbol{S}(\cdot)$ is the skew-symmetric matrix given by

$$\boldsymbol{S}(\boldsymbol{\varepsilon}) = \begin{bmatrix} 0 & -\varepsilon_3 & \varepsilon_2 \\ \varepsilon_3 & 0 & -\varepsilon_1 \\ -\varepsilon_2 & \varepsilon_1 & 0 \end{bmatrix}. \tag{F.4}$$

The orientation between two frames can be described by a rotation matrix given as

$$\boldsymbol{R}(\boldsymbol{q}) = \boldsymbol{I} + 2\eta\boldsymbol{S}(\boldsymbol{\varepsilon}) + 2\boldsymbol{S}^2(\boldsymbol{\varepsilon}), \tag{F.5}$$

where $\boldsymbol{R} \in SO(3)$ that is a special orthogonal group of order three, and has the property

$$SO(3) = \{\boldsymbol{R} \in \mathbb{R}^{3\times 3} : \boldsymbol{R}^\top \boldsymbol{R} = \boldsymbol{I}, \det(\boldsymbol{R}) = 1\}. \tag{F.6}$$

The mapping $\boldsymbol{R} : \mathbb{S}^3 \to SO(3)$ is everywhere a local diffeomorphism, but globally two-to-one, where $\boldsymbol{R}(\boldsymbol{q}) = \boldsymbol{R}(-\boldsymbol{q})$ [31]. The time derivative of a rotation matrix can be expressed as [30]

$$\dot{\boldsymbol{R}}_b^a = \boldsymbol{R}_b^a \boldsymbol{S}\left(\boldsymbol{\omega}_{a,b}^b\right) = \boldsymbol{S}\left(\boldsymbol{\omega}_{a,b}^a\right) \boldsymbol{R}_b^a. \tag{F.7}$$

Attitude and angular velocities are assumed to be measurable.

F.2.4 Quantizer

In this paper, we consider a class of quantizers satisfying the following inequality [32]

$$|y^Q - y| = |d| \leq \delta |y| + y_{\min}, \tag{F.8}$$

where d is the quantization error, and $0 \leq \delta < 1$ and $y_{\min} > 0$ are quantization parameters. If $\delta = 0$, the quantization error will only depend on $y_{\min}$, and so the quantization error is bounded by a constant. When $0 < \delta < 1$, the quantization error also depends on the input to the quantizer and is a sector bounded quantizer.

The quantized signals are modeled as

$$Q\left(\boldsymbol{u}(t)\right) = \boldsymbol{u}^Q(t), \tag{F.9}$$

$$Q(\boldsymbol{\varepsilon}(t)) = \boldsymbol{\varepsilon}^Q(t), \quad Q(\boldsymbol{\omega}(t)) = \boldsymbol{\omega}^Q(t), \tag{F.10}$$

where $Q(\cdot)$ is a quantizer, $\boldsymbol{u}(t) \in \mathbb{R}^3$ are the control inputs, $\boldsymbol{u}^Q(t) = [u_1^Q \ u_2^Q \ u_3^Q]^\top$ are the quantized inputs, $\boldsymbol{\varepsilon} \in \mathbb{R}^3$ and $\boldsymbol{\omega} \in \mathbb{R}^3$ are the measured states, and $\boldsymbol{\varepsilon}^Q(t) = [\varepsilon_1^Q \ \varepsilon_2^Q \ \varepsilon_3^Q]^\top$ and $\boldsymbol{\omega}^Q(t) = [\omega_1^Q \ \omega_2^Q \ \omega_3^Q]^\top$ are the quantized states, where each vector element satisfies (F.8) and so

$$\|\boldsymbol{u}^Q - \boldsymbol{u}\| = \|\boldsymbol{d}_u\| \leq \|\boldsymbol{\delta}_u\| \ \|\boldsymbol{u}\| + \|\boldsymbol{u}_{\min}\| \triangleq \delta_u \|\boldsymbol{u}\| + u_{\min}, \tag{F.11}$$

$$\|\boldsymbol{\omega}^Q - \boldsymbol{\omega}\| = \|\boldsymbol{d}_\omega\| \leq \|\boldsymbol{\delta}_\omega\| \ \|\boldsymbol{\omega}\| + \|\boldsymbol{\omega}_{\min}\| \triangleq \delta_\omega \|\boldsymbol{\omega}\| + \omega_{\min}, \tag{F.12}$$

$$\|\boldsymbol{\varepsilon}^Q - \boldsymbol{\varepsilon}\| = \|\boldsymbol{d}_\varepsilon\| \leq \|\boldsymbol{\delta}_\varepsilon\| \ \|\boldsymbol{\varepsilon}\| + \|\boldsymbol{\varepsilon}_{\min}\| \leq \|\boldsymbol{\delta}_\varepsilon\| + \|\boldsymbol{\varepsilon}_{\min}\| \triangleq \delta_\varepsilon, \tag{F.13}$$

where in (F.13), the unity property of the unit quaternion is used.

Most practical quantizers satisfy the property in (F.8), such as a uniform-, a logarithmic- and a logarithmic-uniform quantizer, and will be presented next.

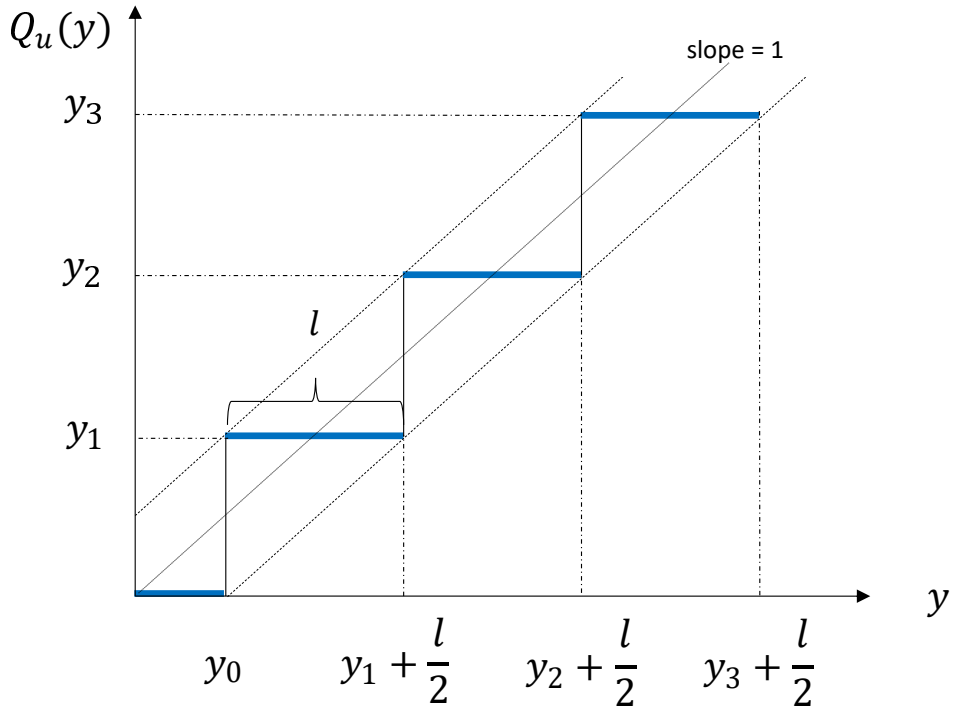

Figure F.2: Map of the uniform quantizer $Q_u(y)$ for $y > 0$.

F.2.4.1 Uniform Quantizer

A uniform quantizer has equal quantization levels and can be described as

$$Q_u(y) = \begin{cases} y_i \operatorname{sgn}(y), & y_i - \frac{l}{2} < |y| \leq y_i + \frac{l}{2} \\ 0, & |y| \leq y_0 \end{cases}, \tag{F.14}$$

where $y_0 > 0$ and $y_1 = y_0 + \frac{l}{2}$, $y_i = y_{i-1} + l$ with $i = 2, 3, \ldots$, l is the length of the quantization interval and $\operatorname{sgn}(\cdot)$ is the sign function. The uniform quantization $Q_u(y)$ is in the set $U = \{0, \pm y_i\}$. The quantization error is bounded by a positive constant $y_{\min} = \max\{y_0, l/2\}$, and satisfies (F.8) with $\delta = 0$. A map of the uniform quantizer (F.14) for $y > 0$ is shown in Fig. F.2. The uniform quantizer has equal quantization levels and is optimal for uniformly distributed signals.

F.2.4.2 Logarithmic Quantizer

A logarithmic quantizer is defined as [33]

$$Q_{\log}(y) = \begin{cases} y_i \operatorname{sgn}(y), & \frac{y_i}{1+\delta} < |y| \leq \frac{y_i}{1-\delta} \\ 0, & |y| \leq y_{\min} \end{cases}, \tag{F.15}$$

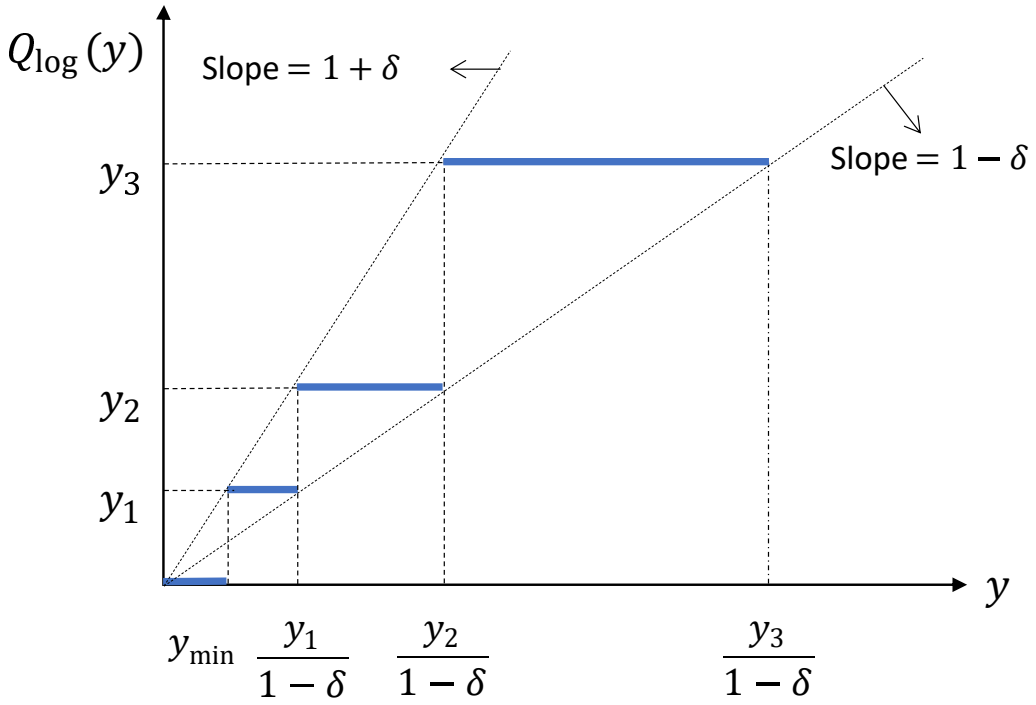

Figure F.3: Map of the logarithmic quantizer $Q_{\log}(y)$ for $y > 0$.

where $y_{\min} = \frac{y_0}{1+\delta}$ determines the size of the dead-zone for $Q_{\log}(y)$, $0 < \delta < 1$, $y_0 > 0$, $y_i = \rho^{(1-i)} y_0$, with $i = 1, 2, \ldots$, and parameter $\rho = \frac{1-\delta}{1+\delta}$. The parameter ρ can be regarded as a measure of the quantization density, where smaller values of ρ implies that the quantizer is coarser. The quantized signal $Q_{\log}(y)$ is in the set $U = \{0, \pm y_i\}$ and satisfies the property in (F.8). A map of the logarithmic quantizer (F.15) for $y > 0$ is shown in Fig. F.3. The logarithmic quantizer has unequal quantization levels, and is useful where the signals are more concentrated near the equilibrium or have higher resolution around the equilibrium, e.g. for speech signal compression, image processing, etc. Several remarks about the logarithmic quantizer can be found in [7, 34, 35].

F.2.4.3 Logarithmic-Uniform Quantizer

A logarithmic-uniform quantizer combines a uniform quantizer and a logarithmic quantizer and is defined as

$$Q_{\text{lu}}(y) = \begin{cases} Q_{\log}(y_{\text{th}}) + Q_u\left(y - y_{\text{th}}\right), & |y| \geq y_{\text{th}} \\ Q_{\log}(y) & |y| < y_{\text{th}} \end{cases}, \tag{F.16}$$

where y_{th} is a positive constant specified by designer denoting the threshold to switch between the logarithmic and uniform quantizer. The uniform quantizer, Q_u, is defined in (F.14) and the logarithmic quantizer, $Q_{\log}$, is defined in (F.15). The

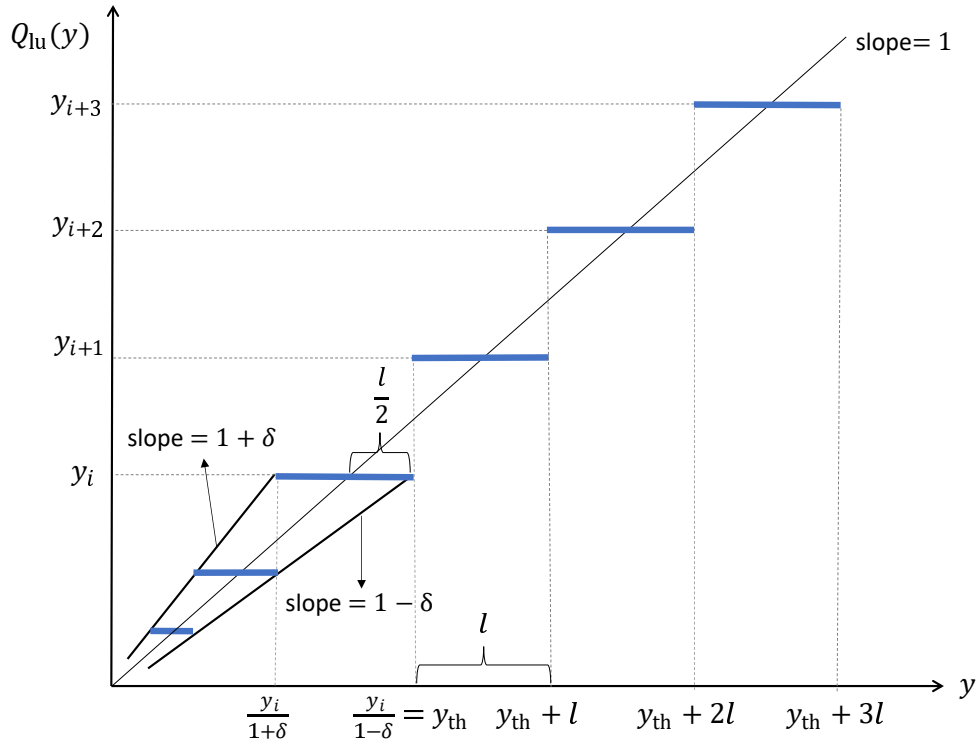

Figure F.4: Map of the logarithmic-uniform quantizer $Q_{\text{lu}}(y)$ for $y > 0$.

quantizer $Q_{\text{lu}}(y)$ takes advantage of a logarithmic quantizer having high resolution close to the origin, and switch to a uniform quantizer for higher values, and satisfies (F.8) with $\delta = 0$ and $y_{\min} \geq \frac{l}{2}$. A map of the logarithmic-uniform quantizer (F.16) for $y > 0$ is shown in Fig. F.4.

F.2.5 Control Objective

We want to track a given desired attitude $\boldsymbol{q}_{i,d} = \boldsymbol{q}_d$ and a desired angular velocity $\boldsymbol{\omega}_{i,d}^i = \boldsymbol{\omega}_d$ where the kinematic equation

$$\dot{\boldsymbol{q}}_d = \boldsymbol{T}(\boldsymbol{q}_d)\boldsymbol{\omega}_{i,d}^d = \frac{1}{2}\begin{bmatrix} -\boldsymbol{\varepsilon}_d^\top \\ \eta_d \boldsymbol{I} - \boldsymbol{S}(\boldsymbol{\varepsilon}_d) \end{bmatrix} \boldsymbol{\omega}_d, \tag{F.17}$$

is satisfied. The tracking error $\boldsymbol{e}$, is given by the quaternion product

$$\boldsymbol{e} = \bar{\boldsymbol{q}}_{i,d} \otimes \boldsymbol{q}_{i,b} = \begin{bmatrix} \tilde{\eta} \\ \tilde{\boldsymbol{\varepsilon}} \end{bmatrix} = \begin{bmatrix} \eta_d \eta + \boldsymbol{\varepsilon}_d^\top \boldsymbol{\varepsilon} \\ \eta_d \boldsymbol{\varepsilon} - \eta \boldsymbol{\varepsilon}_d - S(\boldsymbol{\varepsilon}_d)\boldsymbol{\varepsilon} \end{bmatrix} \in \mathbb{S}^3, \tag{F.18}$$

where $\bar{\boldsymbol{q}} = [\eta \ \ -\boldsymbol{\varepsilon}^\top]^\top$ is the inverse rotation given by the complex conjugate. If $\boldsymbol{q}_{i,b} = \boldsymbol{q}_{i,d}$, then $\boldsymbol{e} = [\pm 1 \ \mathbf{0}_3^\top]^\top$ where $\mathbf{0}_3$ is the zero vector of dimension three. Since there exist two equilibria using the quaternion representation, we conclude that global stability cannot be achieved. Physically $\boldsymbol{e}$ and $-\boldsymbol{e}$ represent the same attitude,

only rotated $\pm 2\pi$ about an axis relative to each other, but mathematically the two equilibria are distinct.

The relative error kinematics is

$$\dot{\boldsymbol{e}} = \boldsymbol{T}(\boldsymbol{e})\boldsymbol{\omega}_e, \tag{F.19}$$

where $\boldsymbol{T}(\cdot)$ is defined in (F.3), and the angular velocity error

$$\boldsymbol{\omega}_e = \boldsymbol{\omega} - \boldsymbol{R}_i^b \boldsymbol{\omega}_d. \tag{F.20}$$

The control objective is to design a control law for $\boldsymbol{u}(t) = \boldsymbol{u}(\boldsymbol{\varepsilon}^Q, \boldsymbol{\omega}^Q)$ by utilizing only the quantized states $\boldsymbol{\varepsilon}^Q$ and $\boldsymbol{\omega}^Q$ to drive $\tilde{\boldsymbol{\varepsilon}}$ and $\boldsymbol{\omega}_e$ towards zero and where all the signals in the closed-loop system are uniformly bounded. To achieve the objective, the following assumptions are imposed.

Assumption 1. *The desired attitude, angular velocity and angular acceleration, $\boldsymbol{q}_d(t)$, $\boldsymbol{\omega}_d(t)$ and $\dot{\boldsymbol{\omega}}_d(t)$ are known, piecewise continuous and bounded, where $\|\boldsymbol{\omega}_d(t)\| < k_{\omega_d}$ and $\|\dot{\boldsymbol{\omega}}_d(t)\| < k_{\dot{\omega}_d}$ $\forall t \geq t_0$ where $k_{\omega_d}, k_{\dot{\omega}_d} > 0$.*

Assumption 2. *The unknown parameter vector $\boldsymbol{\theta}$ is bounded by $\|\boldsymbol{\theta}\| \leq k_\theta$, where k_θ is a positive constant. Also $\boldsymbol{\theta} \in C_\theta$, where C_θ is a known compact convex set.*

Assumption 3. *The function $\boldsymbol{\Phi}$ satisfy a locally Lipschitz condition such that*

$$\|\boldsymbol{\Phi}(\boldsymbol{x}_1, \boldsymbol{y}_1) - \boldsymbol{\Phi}(\boldsymbol{x}_2, \boldsymbol{y}_2)\| \leq L_1\|\boldsymbol{x}_1 - \boldsymbol{x}_2\| + L_2\|\boldsymbol{y}_1 - \boldsymbol{y}_2\|, \tag{F.21}$$

where L_1 and L_2 are positive constants, and $\boldsymbol{x}_{(\cdot)}, \boldsymbol{y}_{(\cdot)} \in \mathbb{R}^3$ are real vectors.

Assumption 4. $\operatorname{sgn}(\tilde{\eta}(t_0)) = \operatorname{sgn}(\tilde{\eta}(t))$ $\forall t \geq t_0$.

Remark 1. *These assumptions are reasonable for most practical systems. Assumption 1 ensures that the reference signal is bounded in t, and is a standard condition for attitude tracking control problems, see e.g [36–38]. Since the vector $\boldsymbol{\theta}$ has constant vector elements, Assumption 2 holds, knowing the bounds for each vector element. Assumption 3 is a fairly mild assumption to ensure the existence and uniqueness of solutions for the system* (F.2) *and applies for a broad class of practical systems, where similar assumptions are made in e.g [19, 27]. By Assumption 4, the equilibrium point that initially are closest is chosen and kept throughout the tracking maneuver.*

F.3 Controller Design

In this section we will design adaptive feedback control laws for the rigid body using backstepping technique in [39]. Since the design of an adaptive controller with

quantized signals is based on the design with continuous measurement of the signals, we start by the case of continuous signals before proceeding to the case of quantized signals.

F.3.1 Continuous Signals

We here consider the case that the signals are not quantized. First, introducing a change of coordinates

$$\boldsymbol{z}_{1\pm} = \begin{bmatrix} 1 \mp \tilde{\eta} \\ \tilde{\boldsymbol{\varepsilon}} \end{bmatrix}, \tag{F.22}$$

$$\boldsymbol{z}_2 = \boldsymbol{\omega}_e - \boldsymbol{\alpha}, \tag{F.23}$$

where $\boldsymbol{z}_{1\pm}$ is an error vector, which shifts the equilibria to the origin [40], where $\boldsymbol{z}_{1+}$ is for the positive equilibrium point when $\tilde{\eta}(t_0) \geq 0$, and $\boldsymbol{z}_{1-}$ is for the negative equilibrium point when $\tilde{\eta}(t_0) < 0$, and where $\boldsymbol{\alpha}$ is a virtual controller chosen as

$$\boldsymbol{\alpha} = -\boldsymbol{C}_1 \boldsymbol{G} \boldsymbol{z}_{1\pm} \in \mathbb{R}^3, \tag{F.24}$$

where $\boldsymbol{C}_1 \in \mathbb{R}^{3\times 3}$ is a positive definite matrix and

$$\boldsymbol{G}(\boldsymbol{e})^\top \triangleq \begin{bmatrix} \pm\tilde{\boldsymbol{\varepsilon}}^\top \\ \tilde{\eta}\boldsymbol{I} + \boldsymbol{S}(\tilde{\boldsymbol{\varepsilon}}) \end{bmatrix} \in \mathbb{R}^{4\times 3}. \tag{F.25}$$

Remark 2. *By introducing the change of coordinates $\boldsymbol{z}_{1\pm}$ we are avoiding that one of the mathematical representations of a given attitude is left unstable. The initial condition of $\tilde{\eta}$ given by Assumption 4 is also helpful in the control strategy, where we choose a target equilibrium point before we start the maneuver. If we were considering that only one of the equilibria was stable, the other would be unstable. Then, if we initially were close to the unstable equilibrium point, we would need a large rotation to reach the stable equilibrium point. We are thus avoiding the problem of unwinding since we now are regulating towards the closest equilibrium point, i.e the equilibrium point which requires the shortest rotation and thus minimizing the path length.*

Remark 3. *By choosing a target equilibrium point prior to the maneuver we will minimize the path length, but not necessarily the input energy. If there is an initial velocity in the opposite direction to the desired rotation it might be more efficient to converge towards the equilibrium that is further away to save energy [40].*

For ease of notation we now denote $\boldsymbol{z}_1 = \boldsymbol{z}_{1\pm}$. The derivative of (F.22)-(F.23),

inserting the dynamics from (F.2) is given as

$$\dot{\boldsymbol{z}}_1 = \frac{1}{2}\boldsymbol{G}^\top \boldsymbol{\omega}_e = -\frac{1}{2}\boldsymbol{G}^\top \boldsymbol{C}_1 \boldsymbol{G}\boldsymbol{z}_1 + \frac{1}{2}\boldsymbol{G}^\top \boldsymbol{z}_2, \tag{F.26}$$

$$\boldsymbol{J}\dot{\boldsymbol{z}}_2 = -\boldsymbol{S}(\boldsymbol{\omega})(\boldsymbol{J}\boldsymbol{\omega}) + \boldsymbol{\Phi}^\top \boldsymbol{\theta} + \boldsymbol{u}^Q + \boldsymbol{J}\left(\boldsymbol{S}(\boldsymbol{\omega})\boldsymbol{R}_i^b \boldsymbol{\omega}_d - \boldsymbol{R}_i^b \dot{\boldsymbol{\omega}}_d - \dot{\boldsymbol{\alpha}}\right), \tag{F.27}$$

where the derivative of (F.24) is

$$\dot{\boldsymbol{\alpha}} = \mp\frac{1}{2}\boldsymbol{C}_1\left[\tilde{\eta}\boldsymbol{I} + \boldsymbol{S}(\tilde{\boldsymbol{\varepsilon}})\right]\boldsymbol{\omega}_e, \tag{F.28}$$

where we have used that $\boldsymbol{G}\boldsymbol{z}_1 = \pm\tilde{\boldsymbol{\varepsilon}}$. Since the inputs are not quantized, we have $\boldsymbol{u}^Q = \boldsymbol{u}$, and an adaptive controller and parameter update law can be designed as

$$\begin{aligned}\boldsymbol{u} = &-\boldsymbol{G}\boldsymbol{z}_1 - \boldsymbol{C}_2\boldsymbol{z}_2 - \boldsymbol{\Phi}^\top\hat{\boldsymbol{\theta}} + \boldsymbol{S}(\boldsymbol{R}_i^b\boldsymbol{\omega}_d)(\boldsymbol{J}\boldsymbol{\omega}) + \boldsymbol{S}(\boldsymbol{\alpha})(\boldsymbol{J}\boldsymbol{\omega}) \\ &- \boldsymbol{J}\left(\boldsymbol{S}(\boldsymbol{\omega})\boldsymbol{R}_i^b\boldsymbol{\omega}_d - \boldsymbol{R}_i^b\dot{\boldsymbol{\omega}}_d - \dot{\boldsymbol{\alpha}}\right),\end{aligned} \tag{F.29}$$

$$\dot{\hat{\boldsymbol{\theta}}} = \boldsymbol{\Gamma}\boldsymbol{\Phi}\boldsymbol{z}_2, \tag{F.30}$$

where $\boldsymbol{C}_2 \in \mathbb{R}^{3\times3}, \boldsymbol{\Gamma} \in \mathbb{R}^{n\times n}$ are positive definite matrices, and the vector $\hat{\boldsymbol{\theta}}$ is the estimated value of $\boldsymbol{\theta}$. A Lyapunov function candidate is chosen as

$$V(\boldsymbol{z}_1, \boldsymbol{z}_2, \tilde{\boldsymbol{\theta}}, t) = \boldsymbol{z}_1^\top\boldsymbol{z}_1 + \frac{1}{2}\boldsymbol{z}_2^\top\boldsymbol{J}\boldsymbol{z}_2 + \frac{1}{2}\tilde{\boldsymbol{\theta}}^\top\boldsymbol{\Gamma}^{-1}\tilde{\boldsymbol{\theta}}, \tag{F.31}$$

where $\tilde{\boldsymbol{\theta}} = \boldsymbol{\theta} - \hat{\boldsymbol{\theta}}$ is the unknown parameter error. By inserting (F.29)–(F.30) in the derivative of (F.31) yields

$$\begin{aligned}\dot{V} = &-\boldsymbol{z}_1^\top\boldsymbol{G}^\top\boldsymbol{C}_1\boldsymbol{G}\boldsymbol{z}_1 + \boldsymbol{z}_1^\top\boldsymbol{G}^\top\boldsymbol{z}_2 + \boldsymbol{z}_2^\top\Big[-\boldsymbol{S}(\boldsymbol{\omega})(\boldsymbol{J}\boldsymbol{\omega}) + \boldsymbol{\Phi}^\top\boldsymbol{\theta} + \boldsymbol{u} \\ &+\boldsymbol{J}\left(\boldsymbol{S}(\boldsymbol{\omega})\boldsymbol{R}_i^b\boldsymbol{\omega}_d - \boldsymbol{R}_i^b\dot{\boldsymbol{\omega}}_d - \dot{\boldsymbol{\alpha}}\right)\Big] - \tilde{\boldsymbol{\theta}}^\top\boldsymbol{\Gamma}^{-1}\dot{\hat{\boldsymbol{\theta}}} \\ = &-\boldsymbol{z}_1^\top\boldsymbol{G}^\top\boldsymbol{C}_1\boldsymbol{G}\boldsymbol{z}_1 - \boldsymbol{z}_2^\top\left[\boldsymbol{S}(\boldsymbol{\omega} - \boldsymbol{\alpha} - \boldsymbol{R}_i^b\boldsymbol{\omega}_d)(\boldsymbol{J}\boldsymbol{\omega})\right] - \boldsymbol{z}_2^\top\boldsymbol{C}_2\boldsymbol{z}_2 \\ = &-\boldsymbol{z}_1^\top\boldsymbol{G}^\top\boldsymbol{C}_1\boldsymbol{G}\boldsymbol{z}_1 - \boldsymbol{z}_2^\top\boldsymbol{C}_2\boldsymbol{z}_2,\end{aligned} \tag{F.32}$$

where we have used the fact that $\boldsymbol{z}_2^\top\boldsymbol{S}(\boldsymbol{z}_2) = 0$. Then it follows that asymptotic tracking is achieved and all signals in the closed-loop system are uniformly bounded.

F.3.2 Quantized Signals

Now we consider the case that both the inputs and the states are quantized, and satisfy the sector bounded property in (F.8). Since only the quantized states $\boldsymbol{\varepsilon}^Q, \boldsymbol{\omega}^Q$ are measured, the quantized value of η is calculated as

$$\eta^Q = \pm\sqrt{1 - (\boldsymbol{\varepsilon}^Q)^\top\boldsymbol{\varepsilon}^Q}, \tag{F.33}$$

where the quantized attitude is given by $\boldsymbol{q}^Q = [\eta^Q, (\boldsymbol{\varepsilon}^Q)^\top]^\top$.

Remark 4. *The value of η^Q can be calculated based on the value of $\boldsymbol{\varepsilon}^Q$ and knowledge of the sign of $\eta(t_0)$ and the assumption of sign continuity of $\eta(t)$ based on derivative. If we are close to, or at $\eta = 0$, we might end up with $(\boldsymbol{\varepsilon}^Q)^\top \boldsymbol{\varepsilon}^Q > 1$, and a scaling is needed to ensure we have a unit quaternion.*

The quantization error of the quaternion can be expressed as

$$\boldsymbol{d}_q = \bar{\boldsymbol{q}}_{i,b} \otimes \boldsymbol{q}_{i,Q} = \begin{bmatrix} d_\eta \\ \boldsymbol{d}_{\tilde{\varepsilon}} \end{bmatrix} = \begin{bmatrix} \eta\eta^Q + \boldsymbol{\varepsilon}^\top \boldsymbol{\varepsilon}^Q \\ \eta\boldsymbol{\varepsilon}^Q - \eta^Q\boldsymbol{\varepsilon} - S(\boldsymbol{\varepsilon})\boldsymbol{\varepsilon}^Q \end{bmatrix}, \tag{F.34}$$

where $\boldsymbol{d}_{\tilde{\varepsilon}}$ is bounded by $\|\boldsymbol{d}_{\tilde{\varepsilon}}\| \leq k_\varepsilon \delta_\varepsilon$ from (F.13) and where $k_\varepsilon > 1$ is a positive constant, and d_η is bounded from the unity property of unit quaternion. If $\boldsymbol{q}^Q = \boldsymbol{q}$ and there is no quantization error, then $\boldsymbol{d}_q = [1\ 0\ 0\ 0]^\top$. The tracking error with the quantized value of the unit quaternion is given by

$$\boldsymbol{e}^Q = \begin{bmatrix} \tilde{\eta}^Q \\ \tilde{\boldsymbol{\varepsilon}}^Q \end{bmatrix} = \begin{bmatrix} \eta_d\eta^Q + \boldsymbol{\varepsilon}_d^\top \boldsymbol{\varepsilon}^Q \\ \eta_d\boldsymbol{\varepsilon}^Q - \eta^Q\boldsymbol{\varepsilon}_d - S(\boldsymbol{\varepsilon}_d)\boldsymbol{\varepsilon}^Q \end{bmatrix}, \tag{F.35}$$

and can also be described by

$$\boldsymbol{e}^Q = \boldsymbol{q}_{d,b} \otimes \boldsymbol{q}_{b,Q} = \boldsymbol{e} \otimes \boldsymbol{d}_q \triangleq \begin{bmatrix} \tilde{\eta}^Q \\ \tilde{\boldsymbol{\varepsilon}} + \boldsymbol{d}_{\tilde{\varepsilon}} \end{bmatrix}, \tag{F.36}$$

where the value of $\boldsymbol{d}_{\tilde{\varepsilon}}$ depends on the quantization error that is bounded by (F.13), and if there is no quantization error, $\boldsymbol{d}_{\tilde{\varepsilon}} = \boldsymbol{0}$.
The adaptive controller and parameter update law are designed as

$$\boldsymbol{u}^Q(t) = \boldsymbol{u}(t) + \boldsymbol{d}_u(t), \tag{F.37}$$

$$\begin{aligned} \boldsymbol{u} = &- \boldsymbol{G}^Q\boldsymbol{z}_1^Q - \boldsymbol{C}_2\boldsymbol{z}_2^Q - (\boldsymbol{\Phi}^Q)^\top\hat{\boldsymbol{\theta}} + \boldsymbol{S}(\boldsymbol{R}_i^Q\boldsymbol{\omega}_d)(\boldsymbol{J}\boldsymbol{\omega}^Q) + \boldsymbol{S}(\boldsymbol{\alpha}^Q)(\boldsymbol{J}\boldsymbol{\omega}^Q) \\ &- \boldsymbol{J}\Big(\boldsymbol{S}(\boldsymbol{\omega}^Q)\boldsymbol{R}_i^Q\boldsymbol{\omega}_d - \boldsymbol{R}_i^Q\dot{\boldsymbol{\omega}}_d - \bar{\boldsymbol{\alpha}}^Q\Big), \end{aligned} \tag{F.38}$$

$$\dot{\hat{\boldsymbol{\theta}}} = \mathrm{Proj}\{\boldsymbol{\Gamma}\boldsymbol{\Phi}^Q\boldsymbol{z}_2^Q\}, \tag{F.39}$$

where $\mathrm{Proj}\{\cdot\}$ is the projection operator given in [39] and where

$$\boldsymbol{z}_1^Q = \begin{bmatrix} 1 \mp \tilde{\eta}^Q \\ \tilde{\boldsymbol{\varepsilon}}^Q \end{bmatrix}, \tag{F.40}$$

$$\boldsymbol{z}_2^Q = \boldsymbol{\omega}_e^Q - \boldsymbol{\alpha}^Q, \tag{F.41}$$

$$\boldsymbol{G}(\boldsymbol{e}^Q)^\top = \begin{bmatrix} \pm(\tilde{\boldsymbol{\varepsilon}}^Q)^\top \\ \tilde{\eta}^Q\boldsymbol{I} + \boldsymbol{S}(\tilde{\boldsymbol{\varepsilon}}^Q) \end{bmatrix}, \tag{F.42}$$

$$\boldsymbol{\alpha}^Q = -\boldsymbol{C}_1\boldsymbol{G}^Q\boldsymbol{z}_1^Q = \mp\boldsymbol{C}_1\tilde{\boldsymbol{\varepsilon}}^Q, \tag{F.43}$$

$$\boldsymbol{\Phi}^Q = \boldsymbol{\Phi}(\boldsymbol{\varepsilon}^Q, \boldsymbol{\omega}^Q), \tag{F.44}$$

$$\bar{\boldsymbol{\alpha}}^Q \triangleq \mp\frac{1}{2}\boldsymbol{C}_1\Big[\tilde{\eta}^Q\boldsymbol{I} + \boldsymbol{S}(\tilde{\boldsymbol{\varepsilon}}^Q)\Big]\boldsymbol{\omega}_e^Q, \tag{F.45}$$

$$\boldsymbol{\omega}_e^Q = \boldsymbol{\omega}^Q - \boldsymbol{R}_i^Q\boldsymbol{\omega}_d, \tag{F.46}$$

$$\boldsymbol{R}_i^Q = \boldsymbol{R}_b^Q\boldsymbol{R}_i^b, \tag{F.47}$$

where $\boldsymbol{R}_b^Q$ is the rotation due to the quantization error. The projection operator is ensuring that the estimates are nonzero and within known bounds, that is $\|\hat{\boldsymbol{\theta}}\| \leq k_\theta$. A function $\bar{\boldsymbol{\alpha}}^Q$ is used in (F.45), which is designed as if the states were not quantized. See e.g. [remark 7] in [19] for a note about this design.

F.4 Stability Analysis

To analyze the closed-loop stability, we first establish some preliminary results as stated in the following Lemmas, and with proofs provided in Appendix A–Appendix D, respectively. The results in this section are applicable for the quantizers satisfying the sector bounded property in (F.8), including the uniform quantizer in Section F.2.4.1, the logarithmic quantizer in Section F.2.4.2, and the logarithmic-uniform quantizer in Section F.2.4.3.

Lemma 1. *The virtual control law $\boldsymbol{\alpha}$, the output $\boldsymbol{\omega}$ and angular velocity error $\boldsymbol{\omega}_e$ are bounded by the following inequalities:*

$$\|\boldsymbol{\alpha}\| \leq \lambda_{\max}(\boldsymbol{C}_1), \tag{F.48}$$

$$\|\boldsymbol{\omega}_e\| \leq \lambda_{\max}(\boldsymbol{C}_1) + \|\boldsymbol{z}\|, \tag{F.49}$$

$$\|\boldsymbol{\omega}\| \leq k_\omega + \|\boldsymbol{z}\|, \tag{F.50}$$

where $\boldsymbol{z} = [\boldsymbol{z}_1^\top, \boldsymbol{z}_2^\top]^\top$, and

$$k_\omega \triangleq \lambda_{\max}(\boldsymbol{C}_1) + k_{\omega_d}. \tag{F.51}$$

Lemma 2. *The effects of state quantization are bounded by the following inequalities:*

$$\text{(i)}\ \|\boldsymbol{R}_i^Q - \boldsymbol{R}_i^b\| \leq \delta_\varepsilon k_R, \tag{F.52}$$

$$\text{(ii)}\ \|\boldsymbol{G}^Q\boldsymbol{z}_1^Q - \boldsymbol{G}\boldsymbol{z}_1\| \leq \delta_\varepsilon k_\varepsilon, \tag{F.53}$$

$$\text{(iii)}\ \|\boldsymbol{\alpha}^Q - \boldsymbol{\alpha}\| \leq \delta_\varepsilon k_\alpha, \tag{F.54}$$

$$\text{(iv)}\ \|\boldsymbol{\omega}^Q - \boldsymbol{\omega}\| \leq \delta_\omega k_\omega + \omega_{\min} + \delta_\omega\|\boldsymbol{z}\|, \tag{F.55}$$

$$\text{(v)}\ \|\boldsymbol{\omega}_e^Q - \boldsymbol{\omega}_e\| \leq \delta_\varepsilon k_R k_{\omega_d} + \delta_\omega k_\omega + \omega_{\min} + \delta_\omega\|\boldsymbol{z}\|, \tag{F.56}$$

$$\text{(vi)}\ \|\boldsymbol{z}_2^Q - \boldsymbol{z}_2\| \leq \delta_\varepsilon k_{z_2} + \delta_\omega k_\omega + \omega_{\min} + \delta_\omega \|\boldsymbol{z}\|, \tag{F.57}$$

$$\text{(vii)}\ \|\bar{\boldsymbol{\alpha}}^Q - \dot{\boldsymbol{\alpha}}\| \leq \delta_\varepsilon k_{\bar{\alpha}_1} + \delta_\omega k_{\bar{\alpha}_2} + \omega_{\min} k_{\bar{\alpha}_3} + \lambda_{\max}(\boldsymbol{C}_1)^2 + (\lambda_{\max}(\boldsymbol{C}_1) + \delta_\omega)\|\boldsymbol{z}\|, \tag{F.58}$$

$$\text{(viii)}\ \|\boldsymbol{\Phi}^Q - \boldsymbol{\Phi}\| \leq \delta_\varepsilon L_1 + \delta_\omega L_2 k_\omega + \omega_{\min} L_2 + \delta_\omega L_2 \|\boldsymbol{z}\|, \tag{F.59}$$

where

$$k_R \triangleq 2k_\varepsilon + 2k_\varepsilon^2 \delta_\varepsilon, \tag{F.60}$$

$$k_\alpha \triangleq \lambda_{\max}(\boldsymbol{C}_1) k_\varepsilon, \tag{F.61}$$

$$k_{z_2} \triangleq k_R k_{\omega_d} + k_\alpha, \tag{F.62}$$

$$k_{\bar{\alpha}_1} \triangleq \frac{1}{2}\lambda_{\max}(\boldsymbol{C}_1) k_R k_{\omega_d}, \tag{F.63}$$

$$k_{\bar{\alpha}_2} \triangleq \frac{1}{2}\lambda_{\max}(\boldsymbol{C}_1) k_\omega, \tag{F.64}$$

$$k_{\bar{\alpha}_3} \triangleq \frac{1}{2}\lambda_{\max}(\boldsymbol{C}_1), \tag{F.65}$$

are positive constants.

Lemma 3. *The effect of input quantization is bounded by the following inequality:*

$$\|\boldsymbol{u}^Q - \boldsymbol{u}\| \leq \delta_u \left(\delta_\varepsilon k_{u_1} + \delta_\omega k_{u_2} + \omega_{\min} k_{u_3} + k_{u_4}\right) + u_{\min} + \delta_u \left(\delta_\varepsilon k_{u_5} + \delta_\omega k_{u_6} + k_{u_7}\right) \|\boldsymbol{z}\|, \tag{F.66}$$

where

$$\begin{aligned} k_{u_1} \triangleq & k_\varepsilon + \lambda_{\max}(\boldsymbol{C}_2) k_{z_2} + k_\theta L_1 + \lambda_{\max}(\boldsymbol{J}) k_\alpha \left(\delta_\omega k_\omega + \omega_{\min} + k_\omega\right) \\ & + \lambda_{\max}(\boldsymbol{J}) k_{\bar{\alpha}_1}, \end{aligned} \tag{F.67}$$

$$k_{u_2} \triangleq \lambda_{\max}(\boldsymbol{C}_2) k_\omega + L_2 k_\omega k_\theta + \lambda_{\max}(\boldsymbol{J}) \left(2k_{\omega_d} k_\omega + \lambda_{\max}(\boldsymbol{C}_1) k_\omega + k_{\bar{\alpha}_2}\right), \tag{F.68}$$

$$k_{u_3} \triangleq \lambda_{\max}(\boldsymbol{C}_2) + L_2 k_\theta + \lambda_{\max}(\boldsymbol{J}) \left(2k_{\omega_d} + \lambda_{\max}(\boldsymbol{C}_1) + k_{\bar{\alpha}_3}\right), \tag{F.69}$$

$$\begin{aligned} k_{u_4} \triangleq & 1 + k_\theta \left(1 + k_\omega\right) + \lambda_{\max}(\boldsymbol{J}) \left(2k_{\omega_d} k_\omega + \lambda_{\max}(\boldsymbol{C}_1) k_\omega + k_{\dot{\omega}_d}\right) \\ & + \frac{3}{2}\lambda_{\max}(\boldsymbol{J}) \lambda_{\max}(\boldsymbol{C}_1)^2, \end{aligned} \tag{F.70}$$

$$k_{u_5} \triangleq \lambda_{\max}(\boldsymbol{J}) k_\alpha, \tag{F.71}$$

$$k_{u_6} \triangleq \lambda_{\max}(\boldsymbol{C}_2) + L_2 k_\theta + \lambda_{\max}(\boldsymbol{J}) \left(2k_{\omega_d} + \delta_\varepsilon k_\alpha + \lambda_{\max}(\boldsymbol{C}_1) + 1\right), \tag{F.72}$$

$$k_{u_7} \triangleq \lambda_{\max}(\boldsymbol{C}_2) + k_\theta + \lambda_{\max}(\boldsymbol{J}) \left(2k_{\omega_d} + \frac{5}{4}\lambda_{\max}(\boldsymbol{C}_1)\right), \tag{F.73}$$

are positive constants.

Lemma 4. *The following inequality holds:*

$$\frac{1}{2}\lambda_{\min}(\boldsymbol{C}_1)\boldsymbol{z}_1^\top\boldsymbol{z}_1 \leq \boldsymbol{z}_1^\top\boldsymbol{G}^\top\boldsymbol{C}_1\boldsymbol{G}\boldsymbol{z}_1. \tag{F.74}$$

By using the properties of Lemmas 1 and 2, we can show the following inequalities,

$$\begin{aligned}
&\boldsymbol{S}(\boldsymbol{\omega})(\boldsymbol{J}\boldsymbol{\omega}) - \boldsymbol{S}(\boldsymbol{R}_i^Q\boldsymbol{\omega}_d)(\boldsymbol{J}\boldsymbol{\omega}^Q) - \boldsymbol{S}(\boldsymbol{\alpha}^Q)(\boldsymbol{J}\boldsymbol{\omega}^Q)\\
\leq\ &\boldsymbol{S}(\boldsymbol{\omega})(\boldsymbol{J}\boldsymbol{\omega}) - \boldsymbol{S}(\boldsymbol{R}_i^b\boldsymbol{\omega}_d)(\boldsymbol{J}\boldsymbol{\omega}) - \boldsymbol{S}(\boldsymbol{\alpha})(\boldsymbol{J}\boldsymbol{\omega})\\
&+\lambda_{\max}(\boldsymbol{J})\left[(\delta_\varepsilon k_R k_{\omega_d}+\delta_\varepsilon k_\alpha)\|\boldsymbol{\omega}^Q\| + (k_{\omega_d}+\|\boldsymbol{\alpha}\|)\|\boldsymbol{d}_\omega\|\right]\\
\leq\ &\boldsymbol{S}(\boldsymbol{z}_2)(\boldsymbol{J}\boldsymbol{\omega})+\lambda_{\max}(\boldsymbol{J})\left[(k_{\omega_d}+\lambda_{\max}(\boldsymbol{C}_1))(\delta_\omega k_\omega+\omega_{\min}+\delta_\omega\|\boldsymbol{z}\|)\right.\\
&\left.+(\delta_\varepsilon k_R k_{\omega_d}+\delta_\varepsilon k_\alpha)(\delta_\omega k_\omega+\omega_{\min}+\delta_\omega\|\boldsymbol{z}\|+k_\omega+\|\boldsymbol{z}\|)\right]\\
\triangleq\ &\boldsymbol{S}(\boldsymbol{z}_2)(\boldsymbol{J}\boldsymbol{\omega})+\delta_\varepsilon k_{T_1}+\delta_\omega k_\omega k_{T_2}+\omega_{\min}k_{T_2}+(\delta_\varepsilon k_{T_3}+\delta_\omega k_{T_2})\,\|\boldsymbol{z}\|,
\end{aligned} \tag{F.75}$$

where

$$k_{T_1} \triangleq \lambda_{\max}(\boldsymbol{J})\,(k_R k_{\omega_d}+k_\alpha)\,(k_\omega+\delta_\omega k_\omega+\omega_{\min})\,, \tag{F.76}$$

$$k_{T_2} \triangleq \lambda_{\max}(\boldsymbol{J})\,(k_{\omega_d}+\lambda_{\max}(\boldsymbol{C}_1))\,, \tag{F.77}$$

$$k_{T_3} \triangleq \lambda_{\max}(\boldsymbol{J})\,(k_R k_{\omega_d}+k_\alpha)\,(1+\delta_\omega)\,, \tag{F.78}$$

and

$$\begin{aligned}
\|\boldsymbol{S}(\boldsymbol{\omega})\boldsymbol{R}_i^b-\boldsymbol{S}(\boldsymbol{\omega}^Q)\boldsymbol{R}_i^Q\| &\leq \|\boldsymbol{\omega}\|\delta_\varepsilon k_R+\|\boldsymbol{d}_\omega\|\\
&\leq \delta_\varepsilon k_\omega k_R+\delta_\omega k_\omega+\omega_{\min}+(\delta_\varepsilon k_R+\delta_\omega)\,\|\boldsymbol{z}\|.
\end{aligned} \tag{F.79}$$

We now state our main result in the following theorem.

Theorem 1. *Consider the closed-loop adaptive system consisting of the plant* (F.26)–(F.27)*, the quantized inputs and states* (F.9)–(F.10) *satisfying* (F.11)–(F.13)*, the adaptive controller* (F.37)–(F.38)*, the parameter update law* (F.39) *and Assumptions 1–4. If the gain matrices* $\boldsymbol{C}_1$ *and* $\boldsymbol{C}_2$ *and quantization parameters are chosen to satisfy*

$$\frac{c_0}{2}-\delta_{V_2} \geq k > 0, \tag{F.80}$$

where $c_0 = \min\{\frac{1}{2}\lambda_{\min}(\boldsymbol{C}_1), \lambda_{\min}(\boldsymbol{C}_2)\}$*,* k *is a positive constant, and*

$$\delta_{V_2} = \delta_\varepsilon k_{V_1}+\delta_\omega k_{V_2}+\delta_u\,(\delta_\varepsilon k_{u_5}+\delta_\omega k_{u_6}+k_{u_7})+\lambda_{\max}(\boldsymbol{J})\lambda_{\max}(\boldsymbol{C}_1), \tag{F.81}$$

where

$$k_{V_1} \triangleq k_{T_3} + \lambda_{\max}(\boldsymbol{J}) k_R k_{\omega_d}, \tag{F.82}$$

$$k_{V_2} \triangleq \lambda_{\max}(\boldsymbol{C}_2) + k_{T_2} + \lambda_{\max}(\boldsymbol{J})\left(k_{\omega_d} + 1\right) + k_{\Phi_4}, \tag{F.83}$$

then, all signals in the closed-loop system are ensured to be uniformly bounded. The $\mathcal{L}_2$-norm of the error states is ultimately bounded by

$$\|\boldsymbol{z}(t)\| \leq \sqrt{\frac{\delta_Q}{k}}, \tag{F.84}$$

where

$$\delta_Q = \frac{1}{2c_0}\delta_{V_1}^2 + \delta_{V_0}, \tag{F.85}$$

$$\delta_{V_0} = \delta_\varepsilon k_{\Phi_1} + \delta_\omega k_\omega k_{\Phi_2} + \omega_{\min} k_{\Phi_2}, \tag{F.86}$$

$$\begin{aligned}\delta_{V_1} =& \delta_\varepsilon k_{V_3} + \delta_\omega k_{V_4} + \omega_{\min} k_{V_5} + \delta_u\left(\delta_\varepsilon k_{u_1} + \delta_\omega k_{u_2} + \omega_{\min} k_{u_3} + k_{u_4}\right) + u_{\min} \\ &+ \lambda_{\max}(\boldsymbol{J})\lambda_{\max}(\boldsymbol{C}_1)^2,\end{aligned} \tag{F.87}$$

$$k_{V_3} \triangleq \lambda_{\max}(\boldsymbol{C}_2) k_{z_2} + k_\varepsilon + k_{T_1} + \lambda_{\max}(\boldsymbol{J})\left(k_\omega k_R k_{\omega_d} + k_R k_{\dot{\omega}_d} + k_{\bar{\alpha}_1}\right) + k_{\Phi_3}, \tag{F.88}$$

$$k_{V_4} \triangleq k_\omega\left(\lambda_{\max}(\boldsymbol{C}_2) + k_{T_2} + \lambda_{\max}(\boldsymbol{J}) k_{\omega_d}\right) + \lambda_{\max}(\boldsymbol{J}) k_{\bar{\alpha}_2} + k_{\Phi_5}, \tag{F.89}$$

$$k_{V_5} \triangleq \lambda_{\max}(\boldsymbol{C}_2) + k_{T_2} + \lambda_{\max}(\boldsymbol{J}) k_{\omega_d} + \lambda_{\max}(\boldsymbol{J}) k_{\bar{\alpha}_2} + k_{\Phi_4}. \tag{F.90}$$

Tracking of a given reference signal is achieved, with a bounded error.

Proof: We choose a Lyapunov function candidate

$$V(\boldsymbol{z}_1, \boldsymbol{z}_2, \tilde{\boldsymbol{\theta}}, t) = \boldsymbol{z}_1^\top \boldsymbol{z}_1 + \frac{1}{2}\boldsymbol{z}_2^\top \boldsymbol{J}\boldsymbol{z}_2 + \frac{1}{2}\tilde{\boldsymbol{\theta}}^\top \boldsymbol{\Gamma}^{-1}\tilde{\boldsymbol{\theta}}. \tag{F.91}$$

By following the control design in (F.37)–(F.39), the derivative of (F.91) is given as

$$\begin{aligned}\dot{V} =& -\boldsymbol{z}_1^\top \boldsymbol{G}^\top \boldsymbol{C}_1 \boldsymbol{G}\boldsymbol{z}_1 + \boldsymbol{z}_1^\top \boldsymbol{G}^\top \boldsymbol{z}_2 + \boldsymbol{z}_2^\top\Big[-\boldsymbol{S}(\boldsymbol{\omega})(\boldsymbol{J}\boldsymbol{\omega}) + \boldsymbol{\Phi}^\top\boldsymbol{\theta} + \boldsymbol{u}^Q \\ &+ \boldsymbol{J}\left(\boldsymbol{S}(\boldsymbol{\omega})\boldsymbol{R}_i^b\boldsymbol{\omega}_d - \boldsymbol{R}_i^b\dot{\boldsymbol{\omega}}_d - \dot{\boldsymbol{\alpha}}\right)\Big] - \tilde{\boldsymbol{\theta}}^\top\boldsymbol{\Gamma}^{-1}\dot{\hat{\boldsymbol{\theta}}} \\ \leq& -\boldsymbol{z}_1^\top \boldsymbol{G}^\top \boldsymbol{C}_1 \boldsymbol{G}\boldsymbol{z}_1 - \boldsymbol{z}_2^\top \boldsymbol{C}_2 \boldsymbol{z}_2^Q + \boldsymbol{z}_2^\top\left(\boldsymbol{G}\boldsymbol{z}_1 - \boldsymbol{G}^Q\boldsymbol{z}_1^Q\right) \\ &+ \boldsymbol{z}_2^\top\left[-\boldsymbol{S}(\boldsymbol{\omega})(\boldsymbol{J}\boldsymbol{\omega}) + \boldsymbol{S}(\boldsymbol{R}_i^Q\boldsymbol{\omega}_d)(\boldsymbol{J}\boldsymbol{\omega}^Q) + \boldsymbol{S}(\alpha^Q)(\boldsymbol{J}\boldsymbol{\omega}^Q)\right] \\ &+ \boldsymbol{z}_2^\top\boldsymbol{J}\left[\boldsymbol{S}(\boldsymbol{\omega})\boldsymbol{R}_i^b - \boldsymbol{S}(\boldsymbol{\omega}^Q)\boldsymbol{R}_i^Q\right]\boldsymbol{\omega}_d + \boldsymbol{z}_2^\top\boldsymbol{J}\Big(\boldsymbol{R}_i^Q - \boldsymbol{R}_i^b\Big)\dot{\boldsymbol{\omega}}_d + \boldsymbol{z}_2^\top\boldsymbol{J}(\bar{\boldsymbol{\alpha}}^Q - \dot{\boldsymbol{\alpha}}) \\ &+ \boldsymbol{z}_2^\top\boldsymbol{d}_u + \Big[\boldsymbol{z}_2^\top(\boldsymbol{\Phi}^\top\boldsymbol{\theta} - (\boldsymbol{\Phi}^Q)^\top\hat{\boldsymbol{\theta}}) - \tilde{\boldsymbol{\theta}}^\top\boldsymbol{\Phi}^Q\boldsymbol{z}_2^Q\Big].\end{aligned} \tag{F.92}$$

The last terms in (F.92) satisfy

$$\boldsymbol{z}_2^\top(\boldsymbol{\Phi}^\top\boldsymbol{\theta} - (\boldsymbol{\Phi}^Q)^\top\hat{\boldsymbol{\theta}}) - \tilde{\boldsymbol{\theta}}^\top\boldsymbol{\Phi}^Q\boldsymbol{z}_2^Q$$

$$
\begin{aligned}
&= \boldsymbol{\theta}^\top \boldsymbol{\Phi} \boldsymbol{z}_2 - \boldsymbol{\theta}^\top \boldsymbol{\Phi}^Q \boldsymbol{z}_2 + \tilde{\boldsymbol{\theta}}^\top \boldsymbol{\Phi}^Q \boldsymbol{z}_2 - \tilde{\boldsymbol{\theta}}^\top \boldsymbol{\Phi}^Q \boldsymbol{z}_2^Q \\
&\leq \|\boldsymbol{\theta}\| \, \|\boldsymbol{\Phi} - \boldsymbol{\Phi}^Q\| \, \|\boldsymbol{z}_2\| + \|\tilde{\boldsymbol{\theta}}\| \, \|\boldsymbol{\Phi}^Q\| \, \|\boldsymbol{z}_2 - \boldsymbol{z}_2^Q\| \\
&\leq k_\theta \|\boldsymbol{\Phi} - \boldsymbol{\Phi}^Q\| \, \|\boldsymbol{z}\| + k_\theta (1 + \|\boldsymbol{\omega}\| + \|\boldsymbol{\Phi} - \boldsymbol{\Phi}^Q\|) \|\boldsymbol{z}_2 - \boldsymbol{z}_2^Q\| \\
&\leq \delta_\varepsilon k_{\Phi_1} + \delta_\omega k_\omega k_{\Phi_2} + \omega_{\min} k_{\Phi_2} + (\delta_\varepsilon k_{\Phi_3} + \delta_\omega k_{\Phi_5} + \omega_{\min} k_{\Phi_4}) \, \|\boldsymbol{z}\| + \delta_\omega k_{\Phi_4} \|\boldsymbol{z}\|^2, \quad \text{(F.93)}
\end{aligned}
$$

where the properties from Lemmas 1–2 are used, and where

$$k_{\Phi_1} \triangleq k_\theta L_1 \left(\delta_\varepsilon k_{z_2} + \delta_\omega k_\omega + \omega_{\min}\right) + \left(k_\theta + k_\theta k_\omega\right) k_{z_2}, \tag{F.94}$$

$$k_{\Phi_2} \triangleq k_\theta L_2 \left(\delta_\varepsilon k_{z_2} + \delta_\omega k_\omega + \omega_{\min}\right) + \left(k_\theta + k_\theta k_\omega\right), \tag{F.95}$$

$$k_{\Phi_3} \triangleq k_\theta L_1 \left(1 + \delta_\omega\right) + k_\theta k_{z_2}, \tag{F.96}$$

$$k_{\Phi_4} \triangleq k_\theta \left(1 + L_2 + L_2 \delta_\omega\right), \tag{F.97}$$

$$k_{\Phi_5} \triangleq k_{\Phi_2} + k_\omega k_{\Phi_4}. \tag{F.98}$$

By using the properties from Lemmas 1–4 together with (F.75), (F.79) and (F.93) and using Young's inequality, we have

$$
\begin{aligned}
\dot{V} \leq & \; - c_0 \|\boldsymbol{z}\|^2 + \delta_{V_0} + \delta_{V_1} \|\boldsymbol{z}\| + \delta_{V_2} \|\boldsymbol{z}\|^2 \\
& \leq - \left(\frac{c_0}{2} - \delta_{V_2}\right) \|\boldsymbol{z}\|^2 + \frac{1}{2c_0} \delta_{V_1}^2 + \delta_{V_0} \\
& \leq - k \|\boldsymbol{z}\|^2 + \delta_Q < 0, \quad \forall \|\boldsymbol{z}\| > \sqrt{\delta_Q / k}.
\end{aligned} \tag{F.99}
$$

This shows that the ultimate bound for $\boldsymbol{z}(t)$ satisfies (F.84) under condition (F.80). Since $\boldsymbol{z}$ is bounded, then by Lemma 2, $\boldsymbol{z}^Q$ is bounded. Then the estimated parameter vector $\hat{\boldsymbol{\theta}}$ is ensured bounded by the projection operator (F.39). Since $\boldsymbol{z}$ is bounded, then by Lemmas 1–3 and the property of unity of the unit quaternion, all signals in the closed loop are ensured bounded. □

Remark 5. *The quantization parameters should be chosen to guarantee the stability and control performances of the attitude tracking control system, and* (F.80) *give some insight to this. Since both the control signals and the states are shown to be bounded, the required number of quantization levels are finite and only a finite number of quantization levels are required to stabilize the system. It can be observed from* (F.85)–(F.87) *that the upper bound of the errors in the sense of* (F.84) *can be decreased if the quantization parameters* $\delta_{(\cdot)}$, $\omega_{\min}$ *and* $u_{\min}$ *are decreased, while all design parameters* $\boldsymbol{C}_{(\cdot)}$ *are kept unchanged. The choice of quantization parameters will depend on the application and the available data-rate for the communication network.*

Remark 6. *A logarithmic quantizer has a better resolution close to zero. Since we are considering a tracking problem where the states are quantized and not the error*

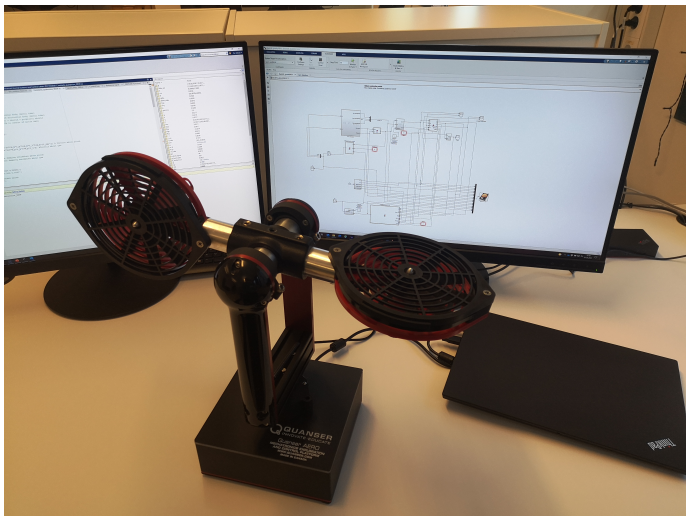

Figure F.5: Quanser Aero helicopter system connected with computer.

states, this would also imply that the error from quantization will be larger if the reference signal is far from the origin. For tracking of a reference signal further away from the equilibrium, one option is to use a logarithmic-uniform quantizer, described in Sec. F.2.4.3, for the state signals. For the stability analysis, this only imply that $\delta_\omega = 0$*, and the value of* δ_ε *is smaller, which again implies that the error signals will converge towards a smaller compact set.*

Remark 7. *Time-delays in the communication channels have significant effects in networked control systems, where the presence of delays may result in a poor performance and can also lead to instability, see e.g. [4, 34]. Extending present results to handle both quantization and time-delay is nontrivial, and is an interesting problem to investigate further.*

F.5 Experimental Results

To illustrate the presented adaptive control scheme, we implemented the controller on the Quanser Aero helicopter system, shown in Fig. F.5. This is a two-rotor laboratory equipment for flight control-based experiments. With a horizontal position of the main thruster and a vertical position of the tail thruster, this resembles a helicopter with two propellers driven by two DC motors. The helicopter is a MIMO system with 2 DOF, and can rotate around two axes where each input affects both rotational directions. The dynamic equation for the helicopter model is defined as

$$\boldsymbol{J}\dot{\boldsymbol{\omega}} = -\boldsymbol{S}(\boldsymbol{\omega})(\boldsymbol{J}\boldsymbol{\omega}) + \boldsymbol{\Phi}(\boldsymbol{\varepsilon}, \boldsymbol{\omega})^\top \boldsymbol{\theta} + \boldsymbol{u}^Q - \boldsymbol{g}(\boldsymbol{q}) + \boldsymbol{\tau}_g, \tag{F.100}$$

Table F.1: Helicopter Parameters.

Symbol	Value	Units
$\boldsymbol{J}$	$\text{diag}(0.0218, 0.0217, 0.0218)$	kgm^2
m	1.075	kg
g	9.81	m/s^2
$\boldsymbol{r}_b^g$	$[0 \;\; 0 \;\; -0.0038]^\top$	m

where $\boldsymbol{g}(\boldsymbol{q}) = -\boldsymbol{S}(\boldsymbol{r}_g^b)\boldsymbol{R}_i^b\boldsymbol{f}_g^i \in \mathbb{R}^3$, $\boldsymbol{r}_g^b = [x_g \; y_g \; z_g]^\top$ is the distance from the origin to the center of mass, $\boldsymbol{f}_g^i = [0 \;\; 0 \;\; -mg]^\top$, m is the mass of the rigid body, and g is the gravitational acceleration. The torque $\boldsymbol{g}(\boldsymbol{q})$ is caused by the gravitational force, because the rotation of the helicopter is not about the center of mass. We assume that this torque can be compensated for directly by measurements of $\boldsymbol{q}$, where $\boldsymbol{\tau}_g = \boldsymbol{g}(\boldsymbol{q})$, and is not sent over the network. The mathematical model is then described by (F.1)–(F.2), and the system receives the driving toques $\boldsymbol{\tau} = \boldsymbol{u}^Q + \boldsymbol{\tau}_g$. The parameters used for simulation and experiments are shown in Table F.1, where $\boldsymbol{\Phi} = \text{diag}(-\boldsymbol{\omega})$, the initial states and estimated parameters were chosen as $\boldsymbol{q}(t_0) = [1 \; 0 \; 0 \; 0]^\top$, $\boldsymbol{\omega}(t_0) = [0 \; 0 \; 0]^\top$ and $\hat{\boldsymbol{\theta}}(t_0) = [0 \;\; 0.0070 \;\; 0.0095]^\top$, where t_0 defines the start of experiment, and the design parameters were set to $\boldsymbol{C}_1 = 0.3\boldsymbol{I}$, $\boldsymbol{C}_2 = 0.15\boldsymbol{I}$ and $\boldsymbol{\Gamma} = 0.02\boldsymbol{I}$. The quantization parameters were chosen as $\delta_{\varepsilon_i} = \delta_{\omega_i} = 0.02$, $\varepsilon_{0_i} = \omega_{0_i} = 0.005$ $i = 1, 2, 3$ for the states, and $\delta_{u_i} = 0.05$, $u_{0_i} = 0.0055$ $i = 1, 2, 3$ for the inputs. For the chosen values, Eq. (F.80) holds. The term $\boldsymbol{\Phi}(\boldsymbol{\omega})^\top\boldsymbol{\theta}$ in the dynamical model of the practical setup relates to viscous damping in the system. The true values of the damping coefficients $\boldsymbol{\theta}$ are not known, and the update law (F.39) for the estimated values does not provide convergence towards the true values. The objective in the experiment was to track a given sinusoidal signal for the attitude, where $r_d = 0$, $p_d = 20\pi/180\sin(0.1\pi t + \pi/2)$, $y_d = 20\pi/180\sin(0.05\pi t + \pi/2)$, given in Euler angles, that was converted to a quaternion, and also to track the angular velocities as given in (F.17), while the inputs sent to the helicopter and the measured states sent to the controller were quantized. The initial value for the desired attitude was $\boldsymbol{q}_d(t_0) = [0.9698, \;\; -0.0302, \;\; 0.1710, \;\; 0.1710]^\top$ and so initially we have a tracking error $\boldsymbol{e}^Q(t_0) = [0.9698, 0.0302, -0.1710, -0, 1710]^\top$, see Eq. (F.35). Since $\text{sgn}(\tilde{\eta}^Q(t_0)) \geq 0$, we choose the positive equilibrium point (F.40) for our maneuver.

Figs. F.6–F.10 show the attitude $\boldsymbol{\varepsilon}^Q$, the angular velocity $\boldsymbol{\omega}^Q$, the error in attitude $\tilde{\boldsymbol{\varepsilon}}^Q$, the error in angular velocity $\boldsymbol{\omega}_e^Q$, and the inputs $\boldsymbol{u}^Q$, respectively. The dotted lines show the desired reference signals, while measured values from experiments on the helicopter system are shown with a solid line. The same experiment was also conducted with continuous measurements of the inputs and the states with results given in Figs. F.11–F.13 showing the error in attitude $\tilde{\boldsymbol{\varepsilon}}$, the error in angular velocity $\boldsymbol{\omega}_e$, and the inputs $\boldsymbol{u}$, respectively.

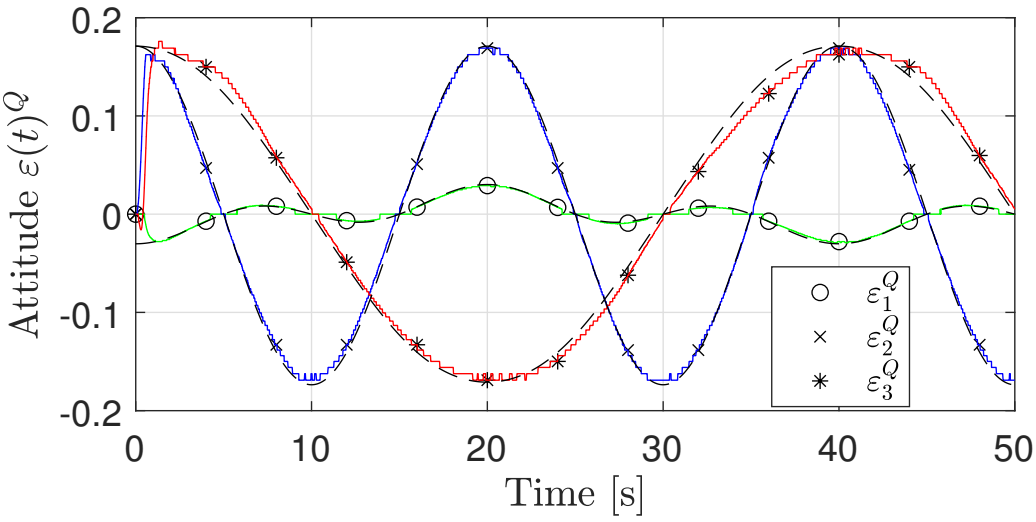

Figure F.6: Attitude $\boldsymbol{\varepsilon}^Q$ from experiment with quantization.

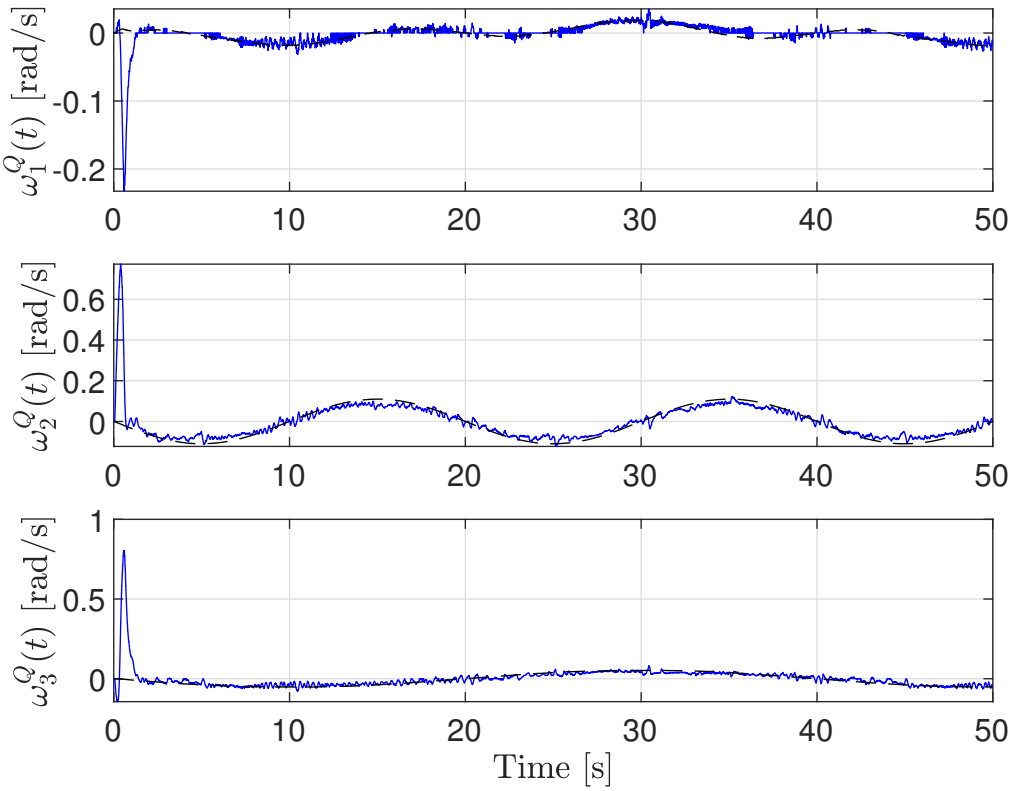

Figure F.7: Angular velocity $\boldsymbol{\omega}^Q$ from experiment with quantization.

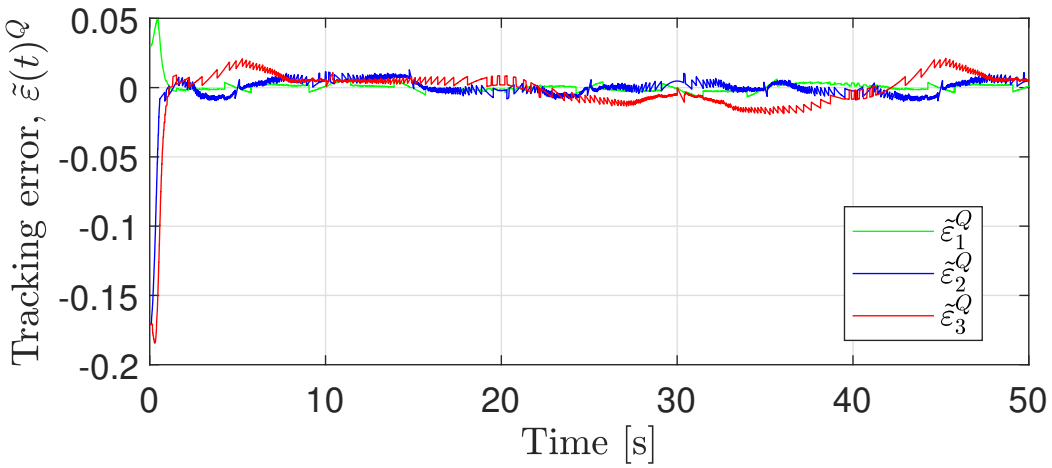

Figure F.8: Tracking error $\tilde{\boldsymbol{\varepsilon}}^Q$ from experiment with quantization.

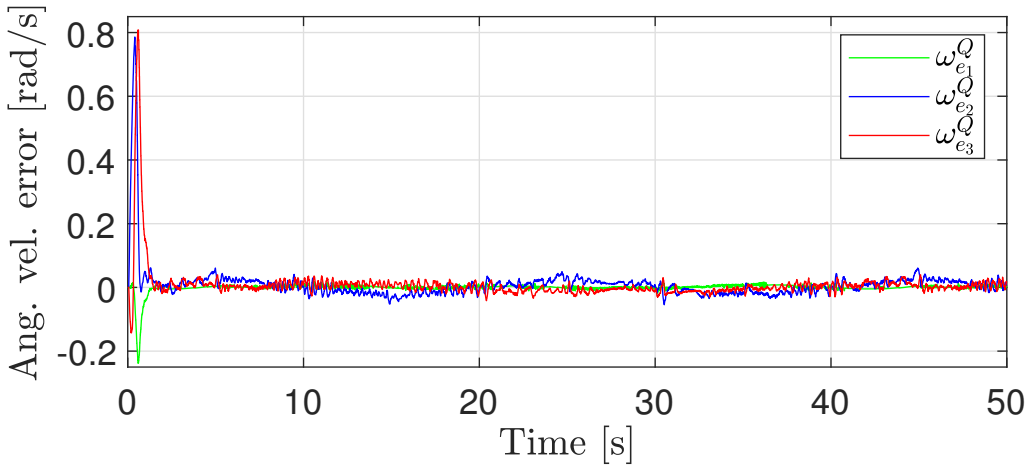

Figure F.9: Angular velocity error $\boldsymbol{\omega}_e^Q$ from experiment with quantization.

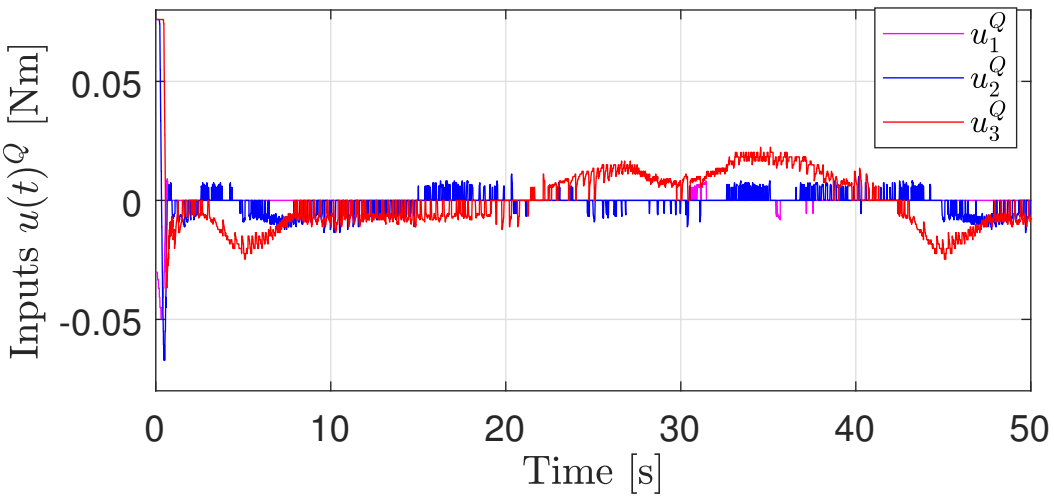

Figure F.10: Inputs $\boldsymbol{u}^Q$ from experiment with quantization.

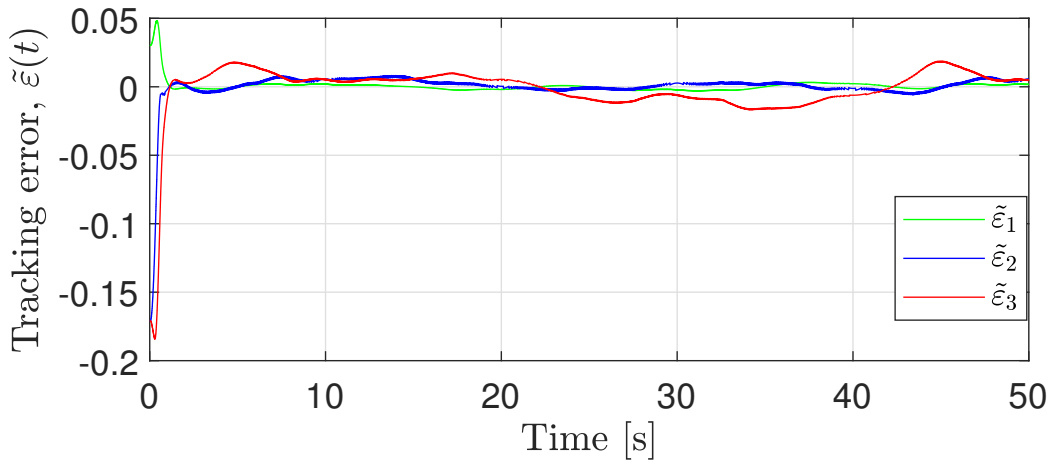

Figure F.11: Tracking error $\tilde{\boldsymbol{\varepsilon}}$ from experiment without quantization.

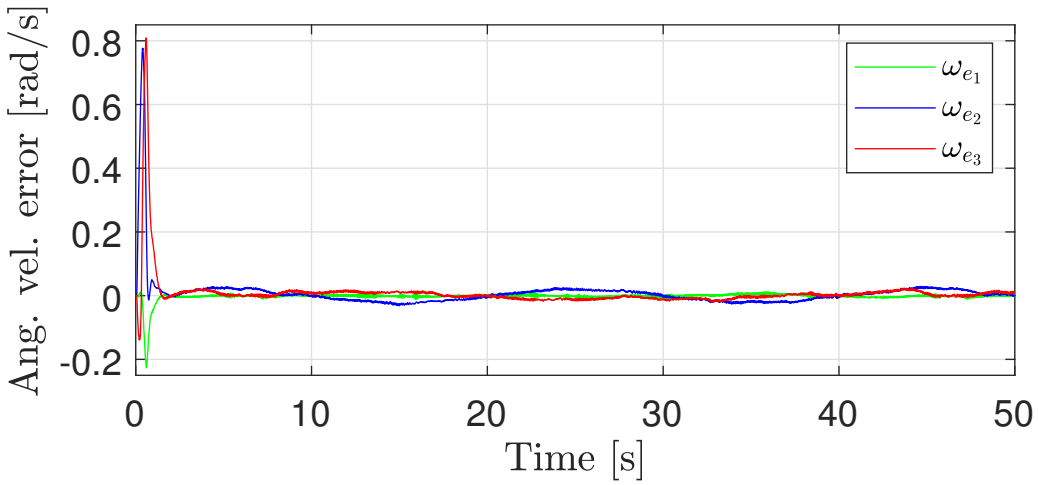

Figure F.12: Angular velocity error $\boldsymbol{\omega}_e$ from experiment without quantization.

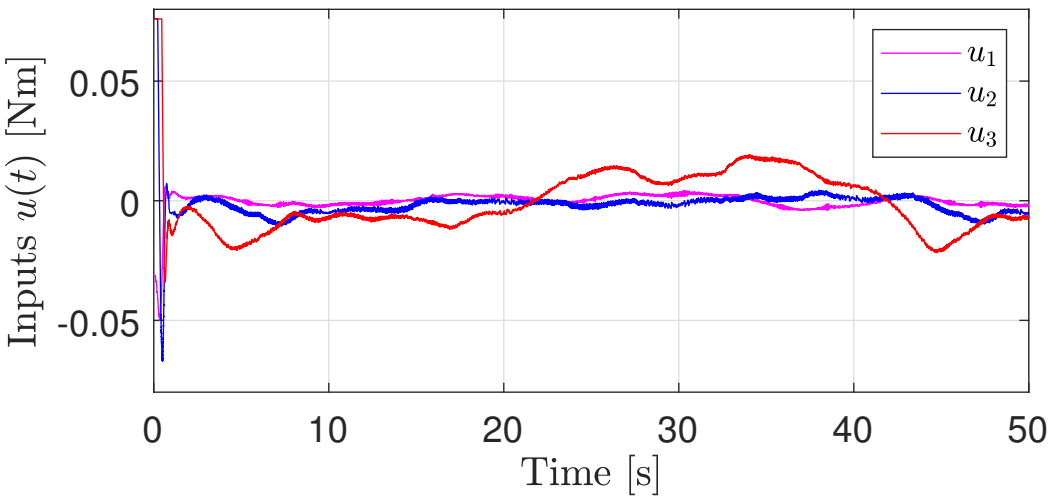

Figure F.13: Inputs $\boldsymbol{u}$ from experiment without quantization.

Table F.2: Tracking error with and without quantization.

z_{track} $\times 10^{-4}$		**State**	
		Continuous	Quantized
Input	Continuous	311	315
	Quantized	318	320

For both cases, the inputs and the states are shown to be bounded, and tracking is achieved with a bounded tracking error. The total tracking error was defined as

$$z_{\text{track}} = \int_{t_0}^{t_f} (\tilde{\boldsymbol{\varepsilon}}^Q)^\top \tilde{\boldsymbol{\varepsilon}}^Q d\tau, \tag{F.101}$$

where t_0 and t_f define start and end of experiment, respectively. The experiments were run for 50 s and results are provided in Table F.2, and is an average of three runs for each case. The tracking error is increased by introducing quantization as expected. As the results show, a good performance can be maintained by introducing quantization, while at the same time the communication burden over a network can be decreased.

F.6 Conclusion

An adaptive backstepping control design has been developed for attitude tracking of rigid body systems with uncertain parameters and with quantization of both inputs and states. Since there exist two equilibria using unit quaternions, a target equilibrium point is chosen before starting the maneuver, and thus one is regulated to the closest equilibrium point. This will avoid the problem of unwinding. A class of sector bounded quantizers has been considered, which introduce quantization errors that are linearly dependent on the inputs to the quantizers. All signals in the closed loop system are shown to be uniformly bounded and tracking of a given reference signal is achieved. The tracking performance is also established and can be improved by appropriately adjusting design parameters. The choice of quantization parameters directly affects the size of the equilibrium set, and this relationship is shown in the analysis. Experiments on a 2-DOF helicopter system illustrate the proposed control scheme.

Appendix A. Proof of Lemma 1

From (F.24) we have

$$\|\boldsymbol{\alpha}\| \leq \lambda_{\max}(\boldsymbol{C}_1)\|\tilde{\boldsymbol{\varepsilon}}\| \ \leq \lambda_{\max}(\boldsymbol{C}_1), \tag{F.102}$$

where $\|\tilde{\boldsymbol{\varepsilon}}\| \leq 1$. From (F.20), (F.23) and Assumption 1, the angular velocity error and angular velocity satisfy

$$\|\boldsymbol{\omega}_e\| \leq \|\boldsymbol{z}_2 + \boldsymbol{\alpha}\| \leq \lambda_{\max}(\boldsymbol{C}_1) + \|\boldsymbol{z}\|, \tag{F.103}$$

$$\|\boldsymbol{\omega}\| \leq \|\boldsymbol{\omega}_e + \boldsymbol{R}_i^b \boldsymbol{\omega}_d\| \leq \lambda_{\max}(\boldsymbol{C}_1) + k_{\omega_d} + \|\boldsymbol{z}\| \triangleq k_\omega + \|\boldsymbol{z}\|, \tag{F.104}$$

where $\boldsymbol{z} = [\boldsymbol{z}_1^\top, \boldsymbol{z}_2^\top]^\top$. □

Appendix B. Proof of Lemma 2

By using (F.34) and (F.47) and the property of (F.5) and (F.6), we have

$$\begin{aligned}\|\boldsymbol{R}_i^Q - \boldsymbol{R}_i^b\| &= \|\boldsymbol{R}_b^Q \boldsymbol{R}_i^b - \boldsymbol{R}_i^b\| = \|(\boldsymbol{R}_b^Q - \boldsymbol{I})\boldsymbol{R}_i^b\| \\ &\leq \|-2d_\eta \boldsymbol{S}(\boldsymbol{d}_{\tilde{\varepsilon}}) + 2\boldsymbol{S}^2(\boldsymbol{d}_{\tilde{\varepsilon}})^\top\| \, \|\boldsymbol{R}_i^b\| \\ &\leq \delta_\varepsilon \left(2k_\varepsilon + 2k_\varepsilon^2 \delta_\varepsilon\right) \triangleq \delta_\varepsilon k_R. \end{aligned} \tag{F.105}$$

From the definition in (F.36) and the fact that $\boldsymbol{G}\boldsymbol{z}_1 = \pm\tilde{\boldsymbol{\varepsilon}}$ and $\boldsymbol{G}^Q \boldsymbol{z}_1^Q = \pm\tilde{\boldsymbol{\varepsilon}}^Q$, it is shown that

$$\|\boldsymbol{G}^Q \boldsymbol{z}_1^Q - \boldsymbol{G}\boldsymbol{z}_1\| = \|(\pm\tilde{\boldsymbol{\varepsilon}}^Q) - (\pm\tilde{\boldsymbol{\varepsilon}})\| \leq \|\boldsymbol{d}_{\tilde{\varepsilon}}\| \leq \delta_\varepsilon k_\varepsilon. \tag{F.106}$$

From (F.24), (F.43) and (F.53) we have

$$\|\boldsymbol{\alpha}^Q - \boldsymbol{\alpha}\| = \|(-\boldsymbol{C}_1 \boldsymbol{G}^Q \boldsymbol{z}_1^Q) - (-\boldsymbol{C}_1 \boldsymbol{G}\boldsymbol{z}_1)\| \leq \lambda_{\max}(\boldsymbol{C}_1) k_\varepsilon \delta_\varepsilon \triangleq \delta_\varepsilon k_\alpha. \tag{F.107}$$

From (F.12) and (F.50) we have

$$\|\boldsymbol{\omega}^Q - \boldsymbol{\omega}\| \leq \delta_\omega \|\boldsymbol{\omega}\| + \omega_{\min} \leq \delta_\omega k_\omega + \omega_{\min} + \delta_\omega \|\boldsymbol{z}\|. \tag{F.108}$$

With the use of (F.46), (F.47) and (F.55) we have

$$\begin{aligned}\|\boldsymbol{\omega}_e^Q - \boldsymbol{\omega}_e\| &= \|\boldsymbol{\omega}^Q - \boldsymbol{R}_i^Q \boldsymbol{\omega}_d - (\boldsymbol{\omega} - \boldsymbol{R}_i^b \boldsymbol{\omega}_d)\| \\ &\leq \delta_\varepsilon k_R k_{\omega_d} + \delta_\omega k_\omega + \omega_{\min} + \delta_\omega \|\boldsymbol{z}\|. \end{aligned} \tag{F.109}$$

Using (F.23), (F.41), (F.54) and (F.56), we have

$$\begin{aligned}\|\boldsymbol{z}_2^Q - \boldsymbol{z}_2\| &\leq \|\boldsymbol{\omega}_e^Q - \boldsymbol{\alpha}^Q - (\boldsymbol{\omega}_e - \boldsymbol{\alpha})\| \\ &\leq \delta_\varepsilon (k_R k_{\omega_d} + k_\alpha) + \delta_\omega k_\omega + \omega_{\min} + \delta_\omega \|\boldsymbol{z}\| \\ &\triangleq \delta_\varepsilon k_{z_2} + \delta_\omega k_\omega + \omega_{\min} + \delta_\omega \|\boldsymbol{z}\|. \end{aligned} \tag{F.110}$$

By using (F.28), (F.45), (F.49) and (F.56), we have

$$\begin{aligned}\|\bar{\boldsymbol{\alpha}}^Q-\dot{\boldsymbol{\alpha}}\| &= \|\frac{1}{2}\boldsymbol{C}_1\left[\mp[\tilde{\eta}^Q\boldsymbol{I}+\boldsymbol{S}(\tilde{\boldsymbol{\varepsilon}}^Q)]\boldsymbol{\omega}_e^Q-[\mp[\tilde{\eta}\boldsymbol{I}+\boldsymbol{S}(\tilde{\boldsymbol{\varepsilon}})]]\boldsymbol{\omega}_e\right]\| \\ &\leq \frac{1}{2}\lambda_{\max}(\boldsymbol{C}_1)\left(2\|\boldsymbol{\omega}_e\|+\delta_\varepsilon k_R k_{\omega_d}+\delta_\omega k_\omega+\omega_{\min}+\delta_\omega\|\boldsymbol{z}\|\right) \\ &\triangleq \delta_\varepsilon k_{\bar{\alpha}_1}+\delta_\omega k_{\bar{\alpha}_2}+\omega_{\min}k_{\bar{\alpha}_3}+\lambda_{\max}(\boldsymbol{C}_1)^2+(\lambda_{\max}(\boldsymbol{C}_1)+\delta_\omega)\|\boldsymbol{z}\|. \quad \text{(F.111)}\end{aligned}$$

From Assumption 3, the unity property of unit quaternion and from (F.55) we have

$$\begin{aligned}\|\boldsymbol{\Phi}^Q-\boldsymbol{\Phi}\| &\leq L_1\|\boldsymbol{\varepsilon}^Q-\boldsymbol{\varepsilon}\|+L_2\|\boldsymbol{\omega}^Q-\boldsymbol{\omega}\| \\ &\leq \delta_\varepsilon L_1+\delta_\omega L_2 k_\omega+\omega_{\min}L_2+\delta_\omega L_2\|\boldsymbol{z}\|. \quad \text{(F.112)}\end{aligned}$$

□

Appendix C. Proof of Lemma 3

The norm of the control input $\boldsymbol{u}$ in (F.38) satisfies the following inequality

$$\begin{aligned}\|\boldsymbol{u}\| =& \|-\boldsymbol{G}^Q\boldsymbol{z}_1^Q-\boldsymbol{C}_2\boldsymbol{z}_2^Q-(\boldsymbol{\Phi}^Q)^\top\hat{\boldsymbol{\theta}}+\boldsymbol{S}(\boldsymbol{R}_i^Q\boldsymbol{\omega}_d)(\boldsymbol{J}\boldsymbol{\omega}^Q) \\ &+\boldsymbol{S}(\boldsymbol{\alpha}^Q)(\boldsymbol{J}\boldsymbol{\omega}^Q)-\boldsymbol{J}\left(\boldsymbol{S}(\boldsymbol{\omega}^Q)\boldsymbol{R}_i^Q\boldsymbol{\omega}_d-\boldsymbol{R}_i^Q\dot{\boldsymbol{\omega}}_d-\bar{\boldsymbol{\alpha}}^Q\right)\| \\ \leq& 1+\delta_\varepsilon k_\varepsilon+\lambda_{\max}(\boldsymbol{C}_2)\left(\delta_\varepsilon k_{z_2}+\delta_\omega k_\omega+\omega_{\min}+\delta_\omega\|\boldsymbol{z}\|+\|\boldsymbol{z}_2\|\right) \\ &+k_\theta\left(\delta_\varepsilon L_1+\delta_\omega L_2 k_\omega+\omega_{\min}L_2+\delta_\omega L_2\|\boldsymbol{z}\|+\|\boldsymbol{\varepsilon}\|+\|\boldsymbol{\omega}\|\right) \\ &+\lambda_{\max}(\boldsymbol{J})\left(2k_{\omega_d}+\|\boldsymbol{\alpha}\|+\delta_\varepsilon k_\alpha\right)\|\boldsymbol{\omega}^Q\|+\lambda_{\max}(\boldsymbol{J})\left(k_{\dot{\omega}_d}+\|\bar{\boldsymbol{\alpha}}^Q\|\right) \\ \triangleq& \delta_\varepsilon k_{u_1}+\delta_\omega k_{u_2}+\omega_{\min}k_{u_3}+k_{u_4}+\delta_\varepsilon k_{u_5}\|\boldsymbol{z}\|+\delta_\omega k_{u_6}\|\boldsymbol{z}\|+k_{u_7}\|\boldsymbol{z}\|, \quad \text{(F.113)}\end{aligned}$$

where we have used the properties from Lemmas 1 and 2. Then

$$\begin{aligned}\|\boldsymbol{u}^Q-\boldsymbol{u}\| &\leq \delta_u\|\boldsymbol{u}\|+u_{\min} \\ &\leq \delta_u\left(\delta_\varepsilon k_{u_1}+\delta_\omega k_{u_2}+\omega_{\min}k_{u_3}+k_{u_4}\right)+u_{\min} \\ &\quad+\delta_u\left(\delta_\varepsilon k_{u_5}+\delta_\omega k_{u_6}+k_{u_7}\right)\|\boldsymbol{z}\|. \quad \text{(F.114)}\end{aligned}$$

□

Appendix D. Proof of Lemma 4

We use the property

$$0 \leq (1 \mp \tilde{\eta})^2 \leq (1 - \tilde{\eta})(1 + \tilde{\eta}) = \tilde{\boldsymbol{\varepsilon}}^\top \tilde{\boldsymbol{\varepsilon}}, \tag{F.115}$$

that holds by Assumption 4. Then

$$(1 \mp \tilde{\eta})^2 + \tilde{\boldsymbol{\varepsilon}}^\top \tilde{\boldsymbol{\varepsilon}} \leq 2\tilde{\boldsymbol{\varepsilon}}^\top \tilde{\boldsymbol{\varepsilon}} \tag{F.116}$$

$$\frac{1}{2}\boldsymbol{z}_1^\top \boldsymbol{z}_1 \leq \tilde{\boldsymbol{\varepsilon}}^\top \tilde{\boldsymbol{\varepsilon}} \tag{F.117}$$

$$\frac{1}{2}\lambda_{\min}(\boldsymbol{C}_1)\boldsymbol{z}_1^\top \boldsymbol{z}_1 \leq \tilde{\boldsymbol{\varepsilon}}^\top \boldsymbol{C}_1 \tilde{\boldsymbol{\varepsilon}} = \boldsymbol{z}_1^\top \boldsymbol{G}^\top \boldsymbol{C}_1 \boldsymbol{G} \boldsymbol{z}_1. \tag{F.118}$$

□

References – Paper F

[1] N. Elia, S. K. Mitter, Stabilization of linear systems with limited information, IEEE Transactions on Automatic Control 46 (9) (2001) 1384–1400. doi:10.1109/9.948466.

[2] R. W. Brockett, D. Liberzon, Quantized feedback stabilization of linear systems, IEEE Transactions on Automatic Control 45 (7) (2000) 1279–1289. doi:10.1109/9.867021.

[3] C.-Y. Kao, S. R. Venkatesh, Stabilization of linear systems with limited information multiple input case, in: Proceedings of the 2002 American Control Conference (IEEE Cat. No.CH37301), IEEE, 2002. doi:10.1109/acc.2002.1024003.

[4] E. Fridman, M. Dambrine, Control under quantization, saturation and delay: An LMI approach, Automatica 45 (10) (2009) 2258–2264. doi:10.1016/j.automatica.2009.05.020.

[5] J. Liu, N. Elia, Quantized feedback stabilization of non-linear affine systems, International Journal of Control 77 (3) (2004) 239–249. doi:10.1080/00207170310001655336.

[6] T. Hayakawa, H. Ishii, K. Tsumaru, Adaptive quantized control for nonlinear uncertain systems, Systems & Control Letters 58 (9) (2009) 625–632. doi:10.1016/j.sysconle.2008.12.007.

[7] J. Zhou, C. Wen, Adaptive backstepping control of uncertain nonlinear systems with input quantization, in: IEEE Conference on Decision and Control, 2013, pp. 5571–5576. doi:10.1109/CDC.2013.6760767.

[8] C. D. Persis, Robust stabilization of nonlinear systems by quantized and ternary control, Systems & Control Letters 58 (8) (2009) 602–608. doi:10.1016/j.sysconle.2009.04.003.

[9] J. Zhou, C. Wen, G. Yang, Adaptive backstepping stabilization of nonlinear uncertain systems with quantized input signal, in: IEEE Transactions on Automatic Control, Vol. 59, 2014, pp. 460–464. doi:10.1109/TAC.2013.2270870.

[10] L. Xing, C. Wen, Y. Zhu, H. Su, Z. Liu, Output feedback control for uncertain nonlinear systems with input quantization, Automatica 65 (2015) 191–202. doi:10.1016/j.automatica.2015.11.028.

[11] J. Zhou, W. Wang, Adaptive control of quantized uncertain nonlinear systems, IFAC PapersOnLine 50 (1) (2017) 10425–10430. doi:10.1016/j.ifacol.2017.08.1970.

[12] Y. Li, G. Yang, Adaptive asymptotic tracking control of uncertain nonlinear systems with input quantization and actuator faults, Automatica 72 (2016) 177–185. doi:10.1016/j.automatica.2016.06.008.

[13] L. Xing, C. Wen, H. Su, Z. Liu, J. Cai, Robust control for a class of uncertain nonlinear systems with input quantization, International journal of robust and nonlinear control 26 (8) (2015) 1585–1596. doi:10.1002/rnc.3367.

[14] Y. Wang, L. He, C. Huang, Adaptive time-varying formation tracking control of unmanned aerial vehicles with quantized input, ISA Transactions 85 (2019) 76–83. doi:10.1016/j.isatra.2018.09.013.

[15] B. Huang, B. Zhou, S. Zhang, C. Zhu, Adaptive prescribed performance tracking control for underactuated autonomous underwater vehicles with input quantization, Ocean Engineering 221 (2021). doi:10.1016/j.oceaneng.2020.108549.

[16] S. M. Schlanbusch, J. Zhou, Adaptive backstepping control of a 2-DOF helicopter system with uniform quantized inputs, in: IECON 2020 The 46th Annual Conference of the IEEE Industrial Electronics Society, 2020, pp. 88–94. doi:10.1109/iecon43393.2020.9254497.

[17] A. Selivanov, A. Fradkov, D. Liberzon, Adaptive control of passifiable linear systems with quantized measurements and bounded disturbances, Systems and Control Letters 88 (2016) 62–67. doi:10.1016/j.sysconle.2015.12.001.

[18] A. Margun, I. Furtat, A. Kremlev, Robust control of twin rotor MIMO system with quantized output, IFAC-PapersOnLine 50 (1) (2017) 4849–4854. doi:10.1016/j.ifacol.2017.08.973.

[19] J. Zhou, C. Wen, W. Wang, F. Yang, Adaptive backstepping control of nonlinear uncertain systems with quantized states, IEEE Transactions on Automatic Control 64 (11) (2019) 4756–4763. doi:10.1109/TAC.2019.2906931.

[20] S. M. Schlanbusch, J. Zhou, R. Schlanbusch, Adaptive backstepping attitude control of a rigid body with state quantization, in: Proceedings of 60th IEEE

Conference on Decision and Control, 2021, pp. 372–377. doi:10.1109/CDC45484.2021.9683579.

[21] D. F. Coutinho, M. Fu, C. E. de Souza, Input and output quantized feedback linear systems, IEEE Transactions on Automatic Control 55 (3) (2010) 761–766. doi:10.1109/tac.2010.2040497.

[22] Y. Yan, S. Yu, Sliding mode tracking control of autonomous underwater vehicles with the effect of quantization, Ocean Engineering 151 (2018) 322–328. doi:10.1016/j.oceaneng.2018.01.034.

[23] Y. Yan, S. Yu, C. Sun, Quantization-based event-triggered sliding mode tracking control of mechanical systems, Information Sciences 523 (2020) 296–306. doi:10.1016/j.ins.2020.03.023.

[24] S. J. Yoo, B. S. Park, Quantized-states-based adaptive control against unknown slippage effects of uncertain mobile robots with input and state quantization, Nonlinear Analysis: Hybrid Systems 42 (2021) 1–17, article 101077. doi:10.1016/j.nahs.2021.101077.

[25] B. M. Kim, S. J. Yoo, Approximation-based quantized state feedback tracking of uncertain input-saturated MIMO nonlinear systems with application to 2-DOF helicopter, Mathematics 9 (9) (2021). doi:10.3390/math9091062.

[26] S. M. Schlanbusch, J. Zhou, R. Schlanbusch, Adaptive attitude control of a rigid body with input and output quantization, IEEE Transactions on Industrial Electronics (2021). doi:10.1109/tie.2021.3105999.

[27] W. Wang, J. Zhou, C. Wen, J. Long, Adaptive backstepping control of uncertain nonlinear systems with input and state quantization, IEEE Transactions on Automatic Control (2021). doi:10.1109/tac.2021.3131958.

[28] J. C. K. Chou, Quaternion kinematic and dynamic differential equations, IEEE Transactions on Robotics and Automation 8 (1) (1992) 53–64. doi:10.1109/70.127239.

[29] T. I. Fossen, Marine Control Systems: Guidance, Navigation, and Control of Ships, Rigs and Underwater Vehicles, Marine Cybernetics AS, Trondheim, Norway, 2002.

[30] O. Egeland, J. T. Gravdahl, Modeling and Simulation for Automatic Control, Marine Cybernetics AS, 2003.

[31] C. G. Mayhew, R. G. Sanfelice, A. R. Teel, Quaternion-based hybrid control for robust global attitude tracking, IEEE Transactions on Automatic Control 56 (11) (2011) 2555–2566. doi:10.1109/tac.2011.2108490.

[32] J. Zhou, L. Xing, C. Wen, Adaptive Control of Dynamic Systems with Uncertainty and Quantization, CRC Press, 2021. doi:10.1201/9781003176626.

[33] J. Zhou, C. Wen, W. Wang, Adaptive control of uncertain nonlinear systems with quantized input signal, Automatica 95 (2018) 152–162. doi:10.1016/j.automatica.2018.05.014.

[34] C. D. Persis, F. Mazenc, Stability of quantized time-delay nonlinear systems: a lyapunov–krasowskii-functional approach, Mathematics of Control, Signals and Systems 21 (4) (2010) 337–370. doi:10.1007/s00498-010-0048-1.

[35] M. Malcangi, Introduction - digital audio, Online, accessed: January 2023 (1995).
URL https://www.lim.di.unimi.it/IEEE/MALCANGI/B/INTRO.HTM

[36] Q. Shen, C. Yue, C. H. Goh, B. Wu, D. Wang, Rigid-body attitude tracking control under actuator faults and angular velocity constraints, IEEE/ASME Transactions on Mechatronics 23 (3) (2018) 1338–1349. doi:10.1109/tmech.2018.2812871.

[37] L.-J. Liu, J. Zhou, C. Wen, X. Zhao, Robust adaptive tracking control of uncertain systems with time-varying input delays, International Journal of Systems Science 48 (16) (2017) 3440–3449. doi:10.1080/00207721.2017.1382604.

[38] A. Benallegue, Y. Chitour, A. Tayebi, Adaptive attitude tracking control of rigid body systems with unknown inertia and gyro-bias, IEEE Transactions on Automatic Control 63 (11) (2018) 3986–3993. doi:10.1109/tac.2018.2808443.

[39] M. Krstić, I. Kanellakopoulos, P. Kokotović, Nonlinear and Adaptive Control Design, John Wiley & Sons, Inc., 1995.

[40] R. Schlanbusch, A. Loria, P. J. Nicklasson, On the stability and stabilization of quaternion equilibria of rigid bodies, Automatica 48 (12) (2012) 3135–3141. doi:10.1016/j.automatica.2012.08.012.